

The Decomposition of Alcohols Over Rutile

Gordon George Ferrier, B.Sc.

Ph.D.

University of Edinburgh

1980



ABSTRACT

The decomposition of alcohols over titanium dioxide (rutile) via dehydration and, to a lesser extent, dehydrogenation has been studied using a static and flow system with the same preparation of rutile throughout.

An examination of the decomposition of a number of substituted alcohols over rutile has suggested that the mechanism of the dehydration reaction has an E1 character and also that the final alkene product distribution is partly formed from the subsequent isomerisation of the initially formed species. The activity of the catalyst towards dehydration, but not dehydrogenation, was observed to increase with repeated use and it is suggested that this was due to migration of impurities from the bulk to the surface of the catalyst strengthening the surface acid sites. The activation of the dehydration of 2-methylpropan-2-ol following the adsorption of hydrogen chloride or chlorine confirmed that this was possible and poisoning of the catalyst by water, ammonia and trimethylamine suggested that Lewis acid/base pairs were probably active during the dehydration of this alcohol. Similar poisoning and activation studies revealed the situation to be more complex with propan-1-ol which was partly due to the higher temperatures necessary for the reaction of this alcohol to proceed. The dehydrogenation of propan-1-ol to propanal is followed by coupling and the formation of C₆ compounds and the effect of water, ammonia etc. on these reactions is discussed. The participation of Brønsted (protonic)

acid sites following the adsorption of water, ammonia and hydrogen chloride was also indicated and the existence of such sites was confirmed from studies of the isomerisation of deuterium-labelled alkenes over rutile in the presence of D_2O and pentan-1-ol.

Finally, experiments which varied the mode of catalyst pretreatment have suggested that O_2^- radical anions are the active sites during the dehydrogenation of an alcohol over rutile.

Foreword

The studies described in this thesis were undertaken by myself in the Chemistry Department of the University of Edinburgh between October 1975 and October 1978. Part of this work has been published in the Journal of the Chemical Society, Chemical Communications (see inside back cover).

Of the many people who have helped to make this thesis possible, I am particularly grateful to my academic supervisor Dr. H.F. Leach. I would also like to extend my gratitude to Professor C. Kemball, FRS, for the provision of laboratory facilities, to Dr. D. Taylor, Professor D.A. Dowden, Dr. D.A. Whan and other members of the catalytic research group for many helpful suggestions, to Mrs. Marie Manson for typing this work, to the technical staff of the Chemistry Department, in particular Mr. A. Anderson and Mr. J. Broom, to Tioxide International Ltd. who provided a studentship and to Dr. D. Urwin of that organisation. Also, I am especially indebted to Dr. C.S. John for his advice during the studies with labelled molecules.

Finally, I would like to thank my wife, Susan, and my parents for their patience and encouragement.

In the course of this work I attended the following seminars and lecture courses:-

1. Catalytic Group Seminars (1975-78)
2. Chemistry Department Seminars (1975-78)
3. The Optical Properties of Transition
Metal Complexes (1976)
4. An Introduction to Fortran Computing (1977)
5. The Encouragement and Exploitation of
Inventiveness in the Oil Industry (1977)
6. From Crawford to Kemball; 260 years-
a-growing (1977)
7. High Speed Liquid Chromatography (1977)
8. Chemistry at its most Colourful (1978)

The Decomposition of Alcohols over Rutile

Contents

	Page	
Chapter 1	An Introduction to the Properties of Titanium Dioxide	1
1.1	Titanium Dioxide: Commercial Importance	1
1.2	Crystal Structure	1
1.3	Surface Structure	2
1.4	Adsorption Studies on Titanium Dioxide	3
1.4.1	The Adsorption of Water on Rutile	4
1.4.2	The Adsorption of Acids and Bases on Rutile	11
1.4.3	Chlorine	16
1.4.4	The Adsorption of Organic Molecules on Rutile	17
1.5	Catalytic Studies on Titanium Dioxide	25
1.5.1	Alkene Isomerisation Reactions	25
1.5.2	Exchange Reactions	30
1.5.3	The Reactions of Ketones over Rutile	32
1.5.4	The Reactions of Dienes, Alkynes and Alkanes	33
1.5.5	Other Surface Studies on Rutile	38
Chapter 2	Experimental Procedure and Treatment of Results	39
2.1	The Source and Purity of Rutile Used in this Investigation	39

	Page	
2.2	The Source and Purity of Chemicals Used in this Investigation	39
2.3	Apparatus	40
2.3.1	Gas-Line I (Fig. 2.1) Static System with G.C. Analysis	43
2.3.2	Gas-Line II (Fig. 2.2) Flow System with G.C. Analysis	44
2.3.3	Gas-Line III (Fig. 2.3) Static System with Mass Spectrometric Analysis	47
2.4	Experimental Procedure	48
2.4.1	Static Systems	48
2.4.1.1	Reaction Procedure	48
2.4.1.2	Poisoning Studies	49
2.4.2	Flow System: Reaction Procedure	52
2.5	Analytical Techniques	54
2.5.1	Gas Chromatography	54
2.5.2	Mass Spectrometry	57
2.5.3	Microwave Spectroscopy	58
2.6	Treatment of Results	59
2.6.1	Static System	59
2.6.1.1	Gas Chromatography Data	59
2.6.1.2	Poisoning Studies	60
2.6.2	Flow System Data	60
2.6.3	Mass Spectrometric Data	64
Chapter 3	The Catalytic Decomposition of Alcohols	65
3.1	General Introduction	65

	Page	
3.2	Dehydration	66
3.2.1	Elimination Reaction Mechanisms	66
3.2.2	The Catalytic Dehydration of Alcohols	69
3.3	Dehydrogenation	74
3.4	Dehydration v Dehydrogenation: Selectivity	78
3.5	Linear Free Energy Relationship (L.F.E.R.)	83
3.6	The Decomposition of Alcohols over Titanium Dioxide	87
3.7	The Purpose of the Present Investigation	94
Chapter 4	The Reactions of Alcohols over Rutile; (Flow System)	97
4.1	Introduction	97
4.2	The Reaction of Pentan-1-ol	98
4.3	The Reaction of 4-Methylpentan-2-ol	100
4.4	The Reaction of 2,2-Dimethylpropan-1-ol	104
4.5	Reproducibility of Experimental Results Obtained on the Flow System	108
4.6	Discussion	117
4.7	Conclusions	136
Chapter 5	The Decomposition of Alcohols over Rutile; (Static System)	138
5.1	Introduction	138
5.2	The Effect of the Presence of Certain Species in the Reaction System on the Decomposition of 2-Methylpropan-2-ol	139

	Page	
5.2.1	Introduction	139
5.2.2	Water	140
5.2.3	Ammonia	141
5.2.4	Trimethylamine (T.M.A.)	142
5.2.5	Triethylamine (T.E.A.)	143
5.2.6	Hydrogen Chloride	143
5.2.7	Chlorine	144
5.3	The Reaction of Propan-1-ol over Rutile	145
5.3.1	Introduction	145
5.3.2	The Effect of the Presence of Certain Species in the Reaction System on the Decomposition of Propan-1-ol over Rutile	148
5.3.2.1	Introduction	148
5.3.2.2	Water	149
5.3.2.3	Ammonia	150
5.3.2.4	Trimethylamine (T.M.A.)	151
5.3.2.5	Hydrogen Chloride	152
5.3.3	The Decomposition of Propan-1-ol; Related Studies	154
5.3.3.1	Introduction	154
5.3.3.2	The Reaction of Propanal	154
5.3.3.3	The Reaction of Other Aldehydes and Ketones	155
5.3.3.4	Excess Propan-1-ol	156
5.3.3.5	Propene	157
5.3.3.6	The Reaction of Alkyl Halides: Dehydrohalogenation	157
5.4	Discussion	158
5.4.1	2-Methylpropan-2-ol	158
5.4.2	Propan-1-ol	163

	Page	
5.4.2.1	Dehydration	165
5.4.2.2	Dehydrogenation and the Formation of C ₆ compounds	171
5.4.3	Conclusion	175
Chapter 6	The Development of Brønsted Acidity on Rutile	179
6.1	Introduction	179
6.2	Results and Discussion	182
Chapter 7	The Influence of the Mode of Catalyst Pretreatment on the Dehydration/ Dehydrogenation Properties of Rutile	188
7.1	Introduction	188
7.2	Experimental	189
7.3	Results and Discussion	191
References		198

CHAPTER 1

An Introduction to the Properties of Titanium Dioxide

1.1 Titanium Dioxide: Commercial Importance

Commercially, the prime use of titanium dioxide is as an opacifying pigment in the manufacture of paints and dyes where its high refractive index, relatively low density and non-toxicity give it a superiority over other pigments such as white lead, zinc oxide and zinc sulphide. One of its disadvantages, however, is that it tends to absorb ultraviolet light, the energy of which when dissipated, promotes the degradation of the paint and other surface media. Therefore from this viewpoint alone, a knowledge of its surface chemical properties is of more than academic interest.

As a catalyst, titanium dioxide is of rather limited industrial importance. The study of its catalytic properties is, however, considered to be important as the results obtained are believed to provide useful information about the properties of oxide catalysts in general. One fascinating aspect of the surface chemistry of titanium dioxide has been the recent speculation that it may be active as an oxidation catalyst on the surface of the planet Mars¹.

1.2 Crystal Structure

There are three naturally occurring crystalline modifications of titanium dioxide; rutile, anatase and brookite. Thermochemical data shows that anatase is

12 kJ mol⁻¹ more stable than rutile; the common occurrence of rutile and the tendency for other modifications to take on a rutile structure at temperatures of approximately 1100 K has, however, brought about the general assumption that rutile is the more stable form.

In all the forms of titanium dioxide, each Ti⁴⁺ ion is surrounded by six O²⁻ ions and each O²⁻ ion has three Ti⁴⁺ ion neighbours although in anatase and brookite the arrangement of the O²⁻ ions about the Ti⁴⁺ ion forms a very distorted octahedra. The unit cell of rutile^{2,3} contains two TiO₂ units (see Fig. 1.1).

As is found with most metal oxides, the rutile modification is generally thought of as being ionic although some authors believe that it is an intermediate type of structure possessing both ionic and covalent character. The degree of covalency is not entirely settled; Grant², using a similar formula to that of Hannay and Smyth⁵ calculated 43% ionic character, whereas Boehm⁶, using Pauling's electronegativity values calculated 63% ionic character.

1.3 Surface Structure

Munuera and co-workers⁷ have worked out, on the basis of adsorption and spectroscopic data, the surface structures of anatase and rutile to be as shown in Fig. 1.2. On rutile, exposed Ti⁴⁺ ions are in a five-fold (C_{4v}) coordination whereas on anatase, they are in a four-fold (C_{2v}) coordination. This model, the authors claimed, is also supported by E.P.R. studies on slightly reduced TiO₂ surfaces⁸. They did not indicate to which surfaces of

rutile or anatase this model applied.

On the massive scale, rutile is reported to crystallise such that 98% of the surface is made up of three planes:- the (110), (101) and (100); there being approximately 60% of the (110) plane and roughly equal proportions of the (101) and (100) planes⁹. The other low index plane, the (111), is believed to make up the remainder of the surface but it is generally considered to be unimportant¹⁰.

As has been pointed out¹¹, it is not possible to predict the exact proportions of these surface planes on rutile powders but it is believed that the relative proportions of each plane do not vary to any large extent between different samples of rutile powders. Jones and Hockey¹¹, working with hydroxylated rutile, have described the three surface planes as in Fig. 1.3. The (110) plane has two rows of titanium ions; A and B (see Fig. 1.3(a)). Those in row A are five-fold coordinate with respect to lattice oxide ions whereas those in row B are four-fold coordinate. The dimensions of this plane are such that the distance A-A = B-B = 0.296 nm and A-B = 0.36 nm. There are equal numbers of A and B ions giving 10.2 Ti ions per nm². The Ti ions in both the (101) and (100) surface planes are coplanar and five-fold coordinate with respect to oxide ions (see Fig. 1.3(b) and 1.3(c)).

1.4 Adsorption Studies on Titanium Dioxide

There are numerous references in the chemical literature to adsorption studies on TiO₂. The following

section therefore will deal only with the most relevant aspects of this literature to the main body of the work presented in this thesis. Since it has become clear that the surface of metal oxides is usually covered with hydroxyl groups, a large amount of the adsorption studies on both rutile and anatase has been concerned with the adsorbability of water.

1.4.1 The Adsorption of Water on Rutile

The early studies of the adsorption of water on titanium dioxide revealed little more than the actual presence of hydroxyl groups and molecularly adsorbed water. More recent work however, has gone into more detail concerning the sites and modes of water adsorption. Detailed infra-red spectroscopic studies of the adsorption of water on rutile have been made by Jones and Hockey^{11,12}, Parfitt and co-workers^{13,14}, Primet et al¹⁵ and more recently Griffiths and Rochester¹⁶. The results of these investigations are summarised in Table 1.1. As can be seen from Table 1.1, the conclusions reached by the various research groups are by no means similar.

Primet and co-workers¹⁵ regarded the (110) modification as being representative of the rutile surface and considered that all the hydroxyl groups were adsorbed on this plane (see Fig. 1.4). They assigned the three OH frequencies (see Table 1.1) by putting all the hydroxyl groups in the place of the oxygen atom labelled 1 of Fig. 1.4 and, depending on the degree of dehydroxylation on outgassing the surface, the OH groups in that position

TABLE 1.1

THE IDENTIFICATION OF SURFACE SPECIES ON RUTILE BY I.R. SPECTROSCOPY

Author and reference	Sample area and major impurity	Outgassing temperature (K) ⁻¹	Absorption bands (cm ⁻¹) ⁻¹	Identification by the authors
Lewis and Parfitt (13)	28 m ² g ⁻¹ Chloride (0.08 %)	473 473 473 473 673 673	3660 3350 1440 & 1400 1270 3740 3690 & 3660 1270	Possibly surface carbonate νOH (later identified as SiOH) Geminal OH on the (100) and/or (101) planes Unidentified
Jackson and Parfitt (14)	24 m ² g ⁻¹	373-573 " " " " " " " " " " " " " " " "	3730 3700 3690 3670 3615 3530 3420 & 3350 1620 1324, 1240 and 1190	Si-OH νOH, bridged νOH, bridged and hydrogen bonded νOH, terminal H ₂ O H ₂ O νOH, terminal and hydrogen bonded H ₂ O δOH

CONTINUATION OF TABLE 1.1

Author and reference	Sample area and major impurity	Outgassing temperature (K) ⁻¹	Absorption bands (cm ⁻¹) ⁻¹	Identification by the authors
Primet, Pichat and Mathieu (15)	-	Peaks removed at: 673 623 473 - 523 373	3685 3655 3410 3630	νOH, terminal and isolated νOH, terminal and hydrogen bonded νOH, terminal and hydrogen bonded H ₂ O
Jones and Hockey (11)(12)	7 m ² g ⁻¹ SiO ₂ (500 ppm)	320 - 673	3680 3650 3610 3550 3410 1610	H ₂ O on (101) plane νOH, terminal on row A of (110) plane H ₂ O on (101) plane H ₂ O on (100) plane νOH, bridged on row B of (110) plane H ₂ O on (100) plane

ν = stretching mode δ = bending mode

CONTINUATION OF TABLE 1.1

Author and reference	Sample area and major impurity	Outgassing temperature (K) ⁻¹	Absorption bands (cm ⁻¹) ⁻¹	Identification by the authors
Griffiths and Rochester (16)	30.3 m ² g ⁻¹ Chloride (0.13 %)	318 - 663 Desorption depending upon pre-calcination temperature	3725 3700 3655 3410 3680 3610 3520 3400 1620	vOH, SiOH vOH, isolated, terminal, not necessarily on (110) plane on apex, edge or steps vOH, isolated, terminal above row A Ti ⁴⁺ ions on (110) plane vOH, isolated, and bridged between row B Ti ⁴⁺ ions on (110) plane vOH groups possibly perturbed by interactions of physisorbed water H ₂ O probably held on (100) and (101) planes

would occur in either a configuration in which they are on adjacent sites and are hydrogen bonded to one another, (3410 cm^{-1} and 3655 cm^{-1}), or one in which the OH groups are isolated from each other; (3685 cm^{-1}). As shown in Fig. 1.5, when dehydroxylation occurs the adjacent hydrogen bonded OH groups are removed first to produce sites (I) which include a bridging oxygen species and at higher temperatures, proton migration allows the removal of the isolated OH groups to form sites (II) which include incompletely coordinated titanium atoms. Site (I), the authors believed, could re-adsorb water, site (II) however was irreversibly dehydroxylated and could only adsorb coordinatively bonded water molecules which would be easily removed at 423 K. These results explained why only partial re-hydroxylation took place after the initial dehydroxylation.

Lewis and Parfitt¹³ considered that absorption bands at 3660 cm^{-1} , 3690 cm^{-1} and 3740 cm^{-1} represented different hydroxyl species and suggested that two hydroxyl groups could occur on a surface titanium atom, i.e. they proposed the existence of geminal sites which were present on both the (100) and (101) planes. At this time the existence of such sites was not established and it was later conceded¹⁴ that the band at 3740 cm^{-1} was due to the presence of SiOH.

Jackson and Parfitt¹⁴, who, like Primet¹⁵, considered the rutile surface solely in terms of the (110) plane, assigned sharp bands at 3700 cm^{-1} and 3670 cm^{-1} to isolated OH groups both bridged, 3700 cm^{-1} , and terminal, 3670 cm^{-1} ; the bridged species arising due to migration of a proton to a lattice oxygen atom after dissociation of

molecularly adsorbed water as in Fig. 1.6.

Jones and Hockey^{11,12} used their previously described model of the rutile surface, (see Fig. 1.3), to explain their water adsorption studies and took into account all of the main surface planes. They concluded that absorptions at 3680 cm^{-1} and 3610 cm^{-1} corresponded to H_2O on the (101) plane, 3550 cm^{-1} and 1610 cm^{-1} represented H_2O on the (100) plane, 3650 cm^{-1} represented the stretching mode of terminal hydroxyl species on the (110) plane and 3410 cm^{-1} represented the stretching mode of hydroxyl species formed from proton migration to the bridging oxide species on the row B of the (110) plane. Subsequent to this adsorption they postulated that the hydroxyl groups then re-aligned to positions directly above the surface Ti ions. Arrayed in this way, the OH^- ions in row A are above Ti ions that are five-fold coordinate with respect to lattice oxide ions whilst those in row B are above cations that are otherwise only four-fold coordinate. Steric factors led the authors to the conclusion that dissociative adsorption was not possible on the (100) and (101) planes and therefore adsorption on these planes must take place by a water molecule adsorbing as a σ -bonded ligand. Differences in energy between the hydrated and dehydrated states on the (100) and (101) planes allowed the assignment of certain absorption bands to the appropriate water molecules.

On the (110) surface plane, using similar principles to those of Peri¹⁷ who worked on alumina, Jones and Hockey proposed that the 3410 cm^{-1} band was due to the fundamental stretching frequency of the row B hydroxyl species and that at 3650 cm^{-1} was due to that on row A (see Fig. 1.3). They

proposed that on a fully hydroxylated rutile surface, since the hydroxyl groups on the same row were closer than those on adjacent rows, dehydroxylation would take place between OH^- ions within the same row and therefore original lattice oxide ions would desorb. As this form of desorption would leave the oxide ions in row B sited between Ti^{4+} ions that would otherwise be four-fold coordinate, whereas for row A this process leaves the oxide ion to be shared between Ti^{4+} ions that are five-fold coordinate with respect to lattice oxygen ions, the row B OH^- ions are more readily lost than those on row A and by such reasoning the infra-red bands were assigned as the temperature was raised.

The most recent and most detailed work on the adsorption of H_2O on rutile has been carried out by Griffiths and Rochester¹⁶ who offered new assignments for the various adsorption bands. They also compared various rutile samples pre-calcined at different temperatures and examined H_2O adsorption on rutile which had been partially reduced in hydrogen. They agreed with Jones and Hockey¹¹ concerning the band at 3655 cm^{-1} and assigned it to isolated hydroxyl groups completing the octahedral coordination of the row A Ti^{4+} ions; (using the nomenclature of Jones and Hockey¹¹; (Fig. 1.3)). However they disagreed with earlier workers^{14,15} about the band at 3410 cm^{-1} , originally attributed to hydroxyl groups involved in lateral hydrogen-bonded interactions, because the bands were too narrow for such species. They also disagreed with Jones and Hockey¹¹ about the assignment of this band and suggested that it was due

to isolated hydroxide ions bridged between adjacent Ti^{4+} ions in row B of the (110) surface plane. They referred to calculations by Jaycock and Waldsax¹⁸ to support this view.

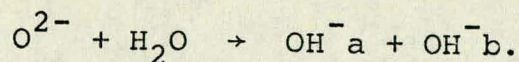
The band at 3700 cm^{-1} which had previously been assigned¹⁴ to bridging hydroxyl groups was assigned by Griffiths and Rochester to terminal OH groups, not necessarily on the (110) plane but perhaps on apex, edge or step surface sites. The adsorption of water molecules liganded to vacant Ti^{4+} ion sites on the (100) and (101) planes resulted in the bands at 3400 cm^{-1} and 1620 cm^{-1} . Calculations by Jaycock and Waldsax¹⁸ suggested that dissociative adsorption on the (100) plane was also possible and Griffiths and Rochester agree with this by assigning bands at 3680 cm^{-1} , 3610 cm^{-1} and 3520 cm^{-1} to this mode of adsorption which may be perturbed by physically adsorbed water molecules. However, concerning this point, the authors admitted to a degree of uncertainty. Griffiths and Rochester¹⁶ disagreed with the mode of H_2O desorption on heating rutile, which had been suggested by Jones and Hockey¹¹, as during desorption, the bands at 3655 cm^{-1} and 3410 cm^{-1} were observed to diminish at similar rates, which suggested that desorption occurred between hydroxyl groups on adjacent Ti^{4+} ions across the rows A and B; (as opposed to the desorption occurring between hydroxyl groups on the same row).

Clearly the interpretations of Jones and Hockey and Griffiths and Rochester should carry the most weight since all three surface planes were considered. However, one flaw in all the above discussion is that since different types of hydroxyl groups have been proposed, they ought to

have differing chemical properties. Exchange of deuterium with surface hydroxyl groups^{14,15} results in a decrease in the intensity of bands associated with surface hydroxyl groups and an increase in those associated with deuterioxyl groups. However this variation in the intensity of the absorption bands was observed to be similar throughout the spectrum of the bands which suggested that all the hydroxyl groups were chemically similar and it was for this reason that Primet¹⁵ rejected the possible existence of bridged hydroxyl species during his investigations.

In contrast to the infra-red work previously described, temperature programmed desorption (T.P.D.) studies by Munuera and Stone¹⁹ give a relatively simple interpretation of the surface environment of water pre-adsorbed on a rutile surface; the T.P.D. trace is displayed in Fig. 1.7.

The two modes of adsorption, molecular and dissociative, are characterised by the T.P.D. peaks at 643 K and 523 K and by comparing infra-red data and the temperatures at which a certain infra-red band disappeared, they concluded that the weak adsorption, T.P.D. peak at 523 K, was due to molecular water while the T.P.D. peak at 643 K was due to dissociative adsorption with proton transfer to a surface oxide ion as follows:-



This generates two distinguishable surface hydroxyl groups.

The examination of adsorption isotherms showed that the molecular adsorption could be divided between weakly adsorbed water, removable at room temperature, and strongly

adsorbed water which could only be removed at temperatures ≈ 523 K and corresponds to the 523 K peak in the T.P.D. experiment. The authors only considered the (110) plane of rutile in their discussion and concluded, from the results of the T.P.D. experiments and the surface densities of the five-fold coordinate Ti^{4+} ions, that no more than half of the surface becomes hydroxylated during the dissociative adsorption; i.e. one molecule dissociates on every other Ti^{4+} ion. The subsequent adsorption of water then takes place in a molecular fashion with H_2O molecules coordinating to the remaining exposed Ti^{4+} ions. The weak molecular adsorption, the authors proposed, could be due to adsorption at the surface O^{2-} ions or to the onset of multilayer adsorption.

Jones and Hockey¹¹ criticised the proposal of Munuera and Stone¹⁹ that only 50% of the (110) surface plane is hydroxylated as they (Jones and Hockey) referred to the fact that only 60% of the rutile surface is made up of the (110) plane and that therefore half of the total amount of water desorbed, which corresponds to that on the T.P.D. trace at 643 K (see Fig. 1.7), could be due to desorption from a fully hydroxylated (110) plane. They also disagreed with Munuera and Stone¹⁹ in that they (Jones and Hockey) believed there was an overlap between the end of dissociative adsorption and the start of molecular adsorption.

Therefore, in the light of all the differing explanations, it is difficult to form conclusions which may be granted a high degree of validity. However, the following general conclusions are reasonable:-

1. Water adsorbs on the rutile surface, both dissociatively to form OH species and molecularly as a coordinately bonded ligand.
2. The desorption of the molecularly adsorbed water, which probably resides on the (100) and (101) planes, requires temperatures in the region of 373-523 K.
3. Dissociative adsorption occurs probably on the (110) plane and dehydroxylation requires temperatures in excess of 600 K. (Dissociative adsorption may also occur on the (100) plane).
4. Excess water adsorption may occur which results in the formation of multilayers. This form of adsorption may interact with certain hydroxyl species, perhaps through hydrogen bonding.

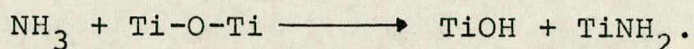
1.4.2 The Adsorption of Acids and Bases on Rutile

Infra-red spectroscopic studies of the adsorption of acids and bases onto oxide surfaces is known to provide useful information about the nature of the chemically active sites on catalyst surfaces. Ammonia, pyridine or some other species may react as a Brønsted base with surface hydroxyl groups and/or as a Lewis base with surface electron acceptor sites. Thus the early work of Parry²⁰ with pyridine, for example, indicated that on silica, pyridine is adsorbed via surface hydrogen bonds only, alumina displays Lewis but not Brønsted acidity and a cracking catalyst possesses both forms of surface acid site. Similarly, Primet²¹ and co-workers tried to identify the acidic or basic sites on rutile and anatase by adsorbing acids (CH_3COOH , $\text{C}_6\text{H}_5\text{OH}$, CO_2) and

bases (NH_3 , $\text{C}_5\text{H}_5\text{N}$, $(\text{CH}_3)_3\text{N}$) onto the oxide surfaces. Their studies of the adsorption of ammonia, pyridine and trimethylamine indicated the presence of two types of Lewis acid site on both anatase and rutile, the weaker of which was generated by the removal of molecular water at ≈ 423 K and the stronger by the removal of isolated hydroxyl groups at ≈ 673 K. It was also found that some OH groups of anatase have sufficient acidic character to protonate trimethylamine but this was not observed for the OH groups on rutile. They also assigned a broad band at 3250 cm^{-1} to the existence of hydrogen bonding between surface hydroxyl groups and the adsorbed bases. This was disputed by Jones and Hockey²² who claimed, from pyridine adsorption studies, that there was no evidence of OH.....N hydrogen bonds. Jones and Hockey²² did believe, like Primet et al²¹, that surface hydroxyl groups on rutile had no acidic character and that Lewis acid sites were generated by the displacement of water or hydroxyl species from the surface.

A series of papers by Parfitt, Ramsbotham and Rochester, describes infra-red studies of the adsorption of NH_3 ²³, pyridine²⁴ and HCl ²⁵ onto rutile surfaces. Prior to the adsorption studies, an infra-red examination of a dry rutile surface revealed a band at 3700 cm^{-1} which was assigned to the stretching vibrations of a hydroxyl group remaining on the surface. The admission of a small amount of ammonia (up to 133 Pa) caused this band to disappear which the authors attributed to the formation of hydrogen bonds between the ammonia and the surface

hydroxyl groups. Treatment of the surface with excess ammonia, 133 Pa - 400 Pa , followed by evacuation at 318 K, led to an increase in the intensity of a band at 3660 cm^{-1} which had been previously assigned to surface OH species. This was believed to be due to the dissociative adsorption of ammonia on rutile which partially re-hydroxylated the surface as follows:-



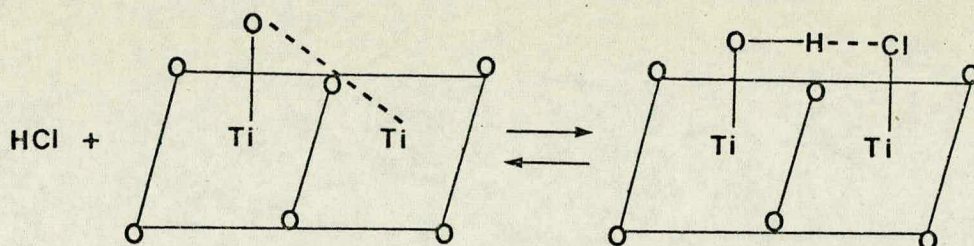
Bands which appeared at 3400 cm^{-1} and 3350 cm^{-1} were partly ascribed to the formation of NH_2 groups. Four major N-H stretching vibrations, ($3200, 3250, 3350, 3400\text{ cm}^{-1}$), were observed when ammonia was adsorbed on a dry rutile surface and, since only two such bands were expected, these were believed to be due to ammonia molecules adsorbed onto two distinct Lewis acid sites.

The spectra of an adsorbed NH_4^+ ion was established by the adsorption of ammonia onto a rutile sample which had been pretreated with HCl. This spectra was not observed when ammonia was adsorbed on dry or water pretreated rutile samples which led the authors to suggest that Brønsted acid sites were not formed on rutile surfaces.

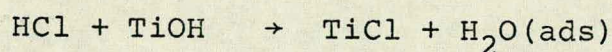
As pyridine is a weaker Lewis base than ammonia, Parfitt et al²⁴ considered that it would be more selective in its reactions with surface sites. The results, however, were similar to those obtained with NH_3 . A band at 3400 cm^{-1} was assigned to pyridine molecules hydrogen-bonded to surface hydroxyl groups, bands at 1225, 1440, 1487, 1575 and 1605 cm^{-1} were believed to

be due to the adsorption of pyridine on Lewis acid sites and a band at 1525 cm^{-1} was attributed to pyridine possibly adsorbed on a different type of Lewis site. As with ammonia, the adsorption of pyridine on a water pretreated rutile did not result in the formation of pyridinium ions although they were formed when pyridine was adsorbed on an HCl pretreated surface.

The adsorption of HCl on anatase was studied by Primet et al²⁶ and resulted in a sharp infra-red band at 3540 cm^{-1} which the authors attributed to the dissociative adsorption of HCl and the formation of hydroxyl groups as follows:-



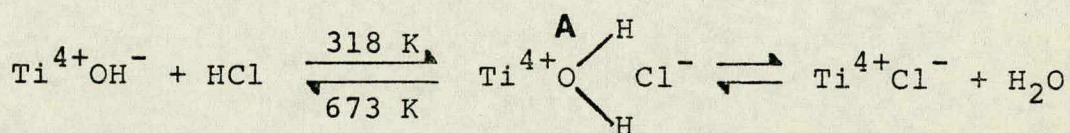
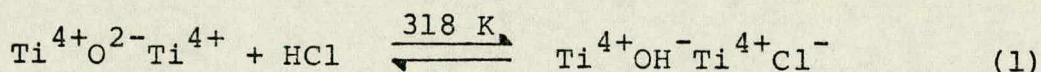
Further heating of the system then liberated the HCl which then reacted with the OH groups, i.e.



Parfitt et al²⁵ came to similar conclusions about the adsorption of HCl on rutile. Initial small doses of HCl onto dry rutile samples resulted in a sharp band at 3660 cm^{-1} which was attributed to the formation of hydroxyl groups and the perturbation of the normally present band at 3700 cm^{-1} to a shoulder at 3690 cm^{-1} coupled with intensity increases in absorption bands at 1600 cm^{-1} and 3400 cm^{-1} suggested that some water had been formed. The ultimate

disappearance of the band at 3690 cm^{-1} after further HCl adsorption suggested that a chemical reaction had taken place between these hydroxyl species and HCl. When excess HCl was added to the system ($>133\text{ Pa}$) followed by evacuation, the band at 3660 cm^{-1} diminished in intensity which suggested that a similar chemical reaction had taken place between these hydroxyl species and HCl. The presence of HCl also led to the appearance of bands at 1565 cm^{-1} and 3360 cm^{-1} which suggested that another species giving both H-O-H bending and O-H stretching vibrations was formed. This species was removed at $\approx 673\text{ K}$.

The following reaction schemes were proposed to explain the above observations:



The species A contains a water molecule and gave rise to the bands at 1565 cm^{-1} and 3360 cm^{-1} .

Experiments with reduced rutile indicated that the oxide ions removed by the reduction in hydrogen were those which, on the oxidised surface, interacted with HCl to form the hydroxyl groups. As stated previously^{23,24}, the adsorption of NH_3 or pyridine onto HCl pretreated rutile indicated the presence of Brønsted acid sites as shown by the formation of ammonium or pyridinium ions and there was evidence that species A was responsible in part for this form of acidity.

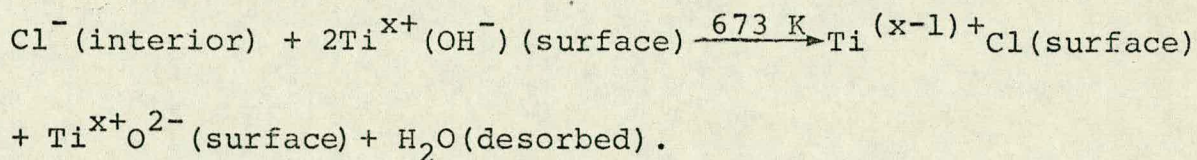
In conclusion therefore, the work of Parfitt et al^{23,24,25} revealed that;

- (a) Both HCl and NH₃ could adsorb in a dissociative manner, with the production of hydroxyl species.
- (b) The molecular adsorption of NH₃ and pyridine was onto two distinct types of Lewis acid site.
- (c) Dry or water pretreated rutile does not have any Brønsted acid character but HCl pretreated rutile does contain Brønsted acid surface sites.

Little emphasis was placed however on the possible differences in activity of the three main surface planes.

1.4.3 Chlorine

According to the literature, the adsorption of chlorine onto rutile has received little attention; presumably because of the difficulties involved when working with chlorine gas. More interest has been focussed on the effect of chlorine impurities in rutile on its surface properties and it is known^{14,22} that such species produce marked changes in adsorption and infra-red spectroscopic characteristics. Jones and Hockey²² compared a rutile sample made from the hydrolysis of TiCl₄ which had a significant surface concentration of chloride ions with rutile made from Ti(isoPrO)₄ which had a negligible chloride content. It was found that the sample with the higher chloride content lost surface OH species at a lower temperature than the other rutile sample and it was suggested that this was due to bulk chloride ion migration to the surface which encouraged the desorption of surface OH⁻ species as water; i.e.

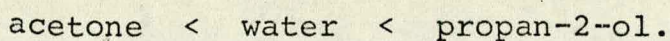


These results were in broad agreement with similar work by Jackson and Parfitt¹⁴.

1.4.4 The Adsorption of Organic Molecules on Rutile

Early work by Shchekochikhin et al²⁷ included the use of infra-red spectroscopy to study the adsorption and catalytic decomposition of MeOH, MeOD, EtOH, nPrOH, isoPrOH and C₂H₄ on TiO₂(anatase) outgassed at 623 K. Strong adsorption was found between 293 K and 573 K and the spectra of all the alcohols were similar. They all had intense bands at 1140 cm⁻¹ and 1060 cm⁻¹ which disappeared only above 623 K and were believed to be due to the formation of two types of surface ester which were thought to be intermediates formed during the catalytic decomposition of the alcohols.

Munuera and Stone¹⁹ examined the adsorption of water, propan-2-ol and acetone at 273 K on hydroxylated rutile and by preadsorbing one species onto the sample followed by dosing with a second, the relative adsorption strengths were obtained. All six combinations between water, propan-2-ol and acetone were investigated and they found that acetone was displaced by both propan-2-ol and water, water was not displaced by acetone and only slightly by propan-2-ol and propan-2-ol was not displaced by either acetone or water which suggested that the relative strengths of adsorption were:-



The authors believed that both propan-2-ol and acetone adsorbed in an associative manner such that the limiting coverages at 273 K was ≈ 2 molecules nm^{-2} . Since they also considered that the surface density of the Ti^{4+} ions was $\approx 3 \times 10^{18}$ ions nm^{-2} and that 50% of the surface was hydroxylated, this suggested to the authors that adsorption occurred at isolated Ti^{4+} ions as in (a) or (b) in Fig. 1.8; or, in the case of propan-2-ol, a Ti-O surface pair may be involved as in (c). The modes of adsorption (d) and (e) in Fig. 1.8, involving OH-OH pairs or OH-O pairs were also possible but considered less likely.

Day and co-workers²⁸ studied the adsorption of nitrogen, water, ethanol and n-pentane on various rutile samples which had been pretreated with water, ethanol, hexan-1-ol or hexan-1,6-diol. They concluded, among other things, that ethanol rapidly displaced water from the surface of hydroxylated rutile which is in agreement with the work of Jackson and Parfitt²⁹ who found infra-red evidence for surface ethoxide species after exposure of ethanol to "dry" and water pretreated rutile. Jackson and Parfitt³⁰ continued their adsorption studies on rutile and selected ethanol, butan-1-ol and hexan-1-ol as adsorbates but only considered the (110) crystal plane. Their conclusions differed from those of Munuera and Stone¹⁹, who believed that only associative adsorption took place, and they found that adsorption of the alcohols occurs dissociatively to produce alkoxide and OH groups on the rutile surface. All three alcohols were found to adsorb equally on both hydroxylated and non-hydroxylated surfaces and increasing the temperature to 573 K resulted

in the rapid decomposition of the alkoxides to the alk-1-ene and water as is shown in Table 1.2.

Table 1.2

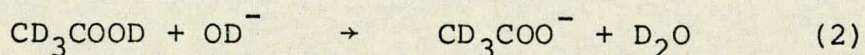
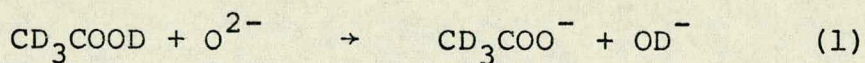
Infra-red Analysis Of The Thermal Desorption And Decomposition Products Of Alcohols Chemisorbed On Rutile, (After Jackson And Parfitt³⁰)

Alcohol	Temperature		
	373 K	473 K	573 K
ethanol	water	water	water
	ethanol	ethanol	ethylene
		ethylene	
butan-1-ol	water	water	water
	butan-1-ol	butan-1-ol	butan-1-ol
hexan-1-ol	water	water	water
	hexan-1-ol	hex-1-ene	hex-1-ene

Although they did not go into great detail, the suggested decomposition mechanism at 573 K of the alkoxide involved proton extraction from the β methylene group (methyl in the case of ethoxide) and rupture of the carbon-oxygen bond to produce the alk-1-ene and a surface OH species which then condensed to form water and leaves the surface hydroxylated to the extent normally associated with the reaction temperature. No ethers or other oxygenated compounds were identified.

Recent work on the adsorption of organic compounds on rutile has been carried out by Griffiths and Rochester who worked with acetic acid³¹, hexafluoroacetone³² and acetone³³.

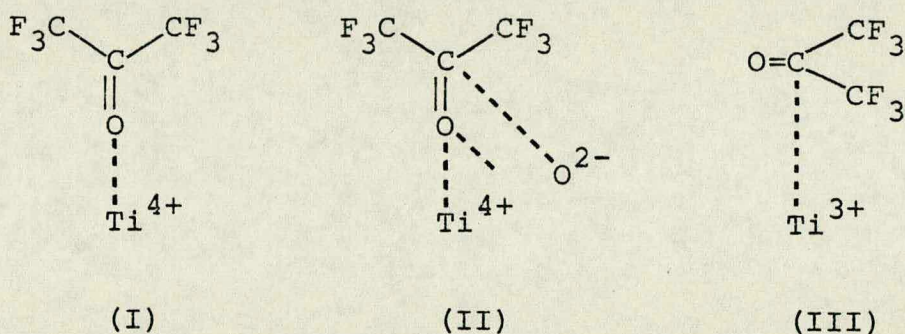
The adsorption of [$^2\text{H}_4$] acetic acid took place on samples of rutile which had been either heated in oxygen, heated in oxygen followed by exposure to D_2O or reduced in hydrogen. Bands at 1670 and 1685 cm^{-1} which were observed after adsorption of small doses of [$^2\text{H}_4$] acetic acid onto a sample of rutile preheated in O_2 were assigned to adsorbate molecules which were strongly coordinatively liganded to Ti^{4+} ion sites and, since such species could not displace D_2O from the Lewis acid sites, were believed to exist on the (100) and (101) surface planes. Reduced rutile was unable to adsorb [$^2\text{H}_4$] acetic acid through coordinative interactions and this was thought to be due to a decline in the surface Lewis acidity due to the removal of O^{2-} ions and the conversion of Ti^{4+} ions to Ti^{3+} ions. The production of [$^2\text{H}_4$] acetic acid dimers, which had been observed on O_2 pretreated rutile, was also diminished after reduction in hydrogen which suggested that Ti^{4+} ions were involved in their formation also. The admission of larger doses of [$^2\text{H}_4$] acetic acid onto rutile displaced the coordinatively bound adsorbate molecules and the resulting bands between 1400 and 1600 cm^{-1} were attributed to the formation of acetate species and bands between 2500 and 2700 cm^{-1} to the simultaneous formation of deuteroyl and/or D_2O species as follows:-



The reduction of rutile in hydrogen and the presence of adsorbed D_2O hindered the dissociative adsorption of [$^2\text{H}_4$] acetic acid. Evidence was also found for deuterium

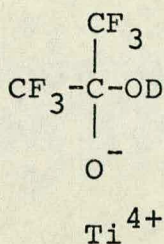
bonding interactions between OD groups and adsorbed [$^2\text{H}_4$] acetic acid species. Using the terminology of Jones and Hockey¹¹, row A deuteroyl groups reacted with [$^2\text{H}_4$] acetic acid to give acetate and D_2O as in (1) above but row B OD groups were less reactive.

Similar work with hexafluoroacetone³² (HFA) produced information about the activity of surface species other than Ti^{4+} ions; (e.g. deuteroyl groups and D_2O molecules, Ti^{3+} and O^{2-} ions), on rutile. Bands between 1600 and 1800 cm^{-1} were assigned to species (I), (II) and (III) below:-

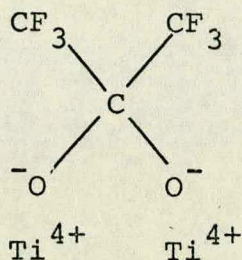


Formation of species (I), hexafluoroacetone adsorbed onto Lewis acidic Ti^{4+} ion sites, was hindered by (a) preadsorption of molecular water as hexafluoroacetone is a weak base and (b) reduction of rutile in hydrogen. The authors proposed that when H.F.A. adsorbed on rutile, as electron donation of the ketone to the Ti^{4+} ion took place, there was simultaneous nucleophilic attack of the carbonyl carbon atom by O^{2-} ions with the formation of species (II) above and eventually (V) below - a precursor to the formation of acetate ions. Bands at 1705 and 1742 cm^{-1} , absent with unreduced rutile, were assigned to species (III) above where Ti^{3+} ions in reduced rutile could act as electron

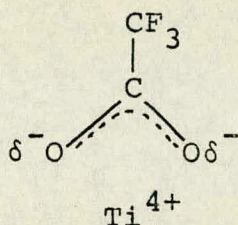
donors. The reaction of H.F.A. with deuteroxyl groups led to the formation of trifluoroacetate species with absorption bands at around 1600 cm^{-1} via (IV) below. The final acetate species could be chelating (VI) or bridging (VII) as shown below:-



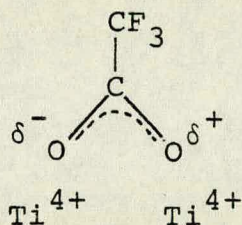
(IV)



(V)



(VI)



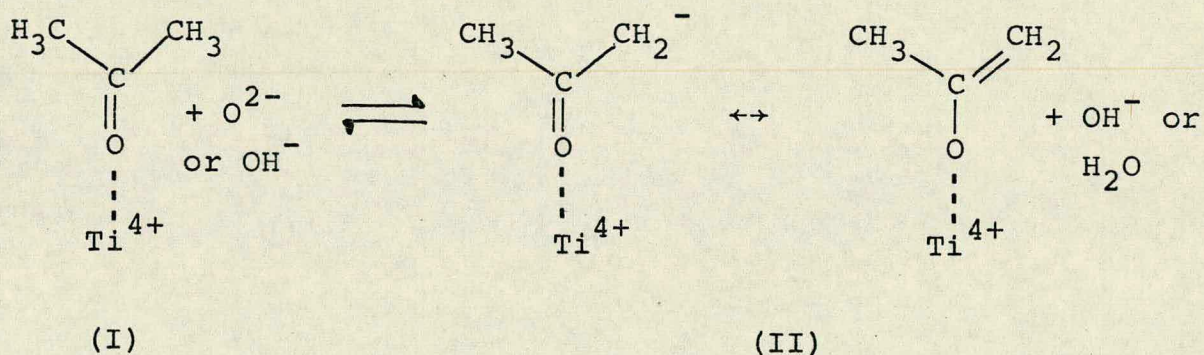
(VII)

Unlike other dissociative adsorptions, the formation of trifluoroacetate species was believed to occur on the (100) and (101) planes as the OD groups at $\approx 2690\text{ cm}^{-1}$ on row A of the (110) plane only formed weak deuterium bonds with adsorbed H.F.A. and displayed no nucleophilic character. Also the OD groups on row B at 2536 cm^{-1} did not interact in any way with H.F.A.

Finally the adsorption of acetone and $[^2\text{H}_6]$ acetone, both stronger bases than H.F.A., was studied since it was thought to be less susceptible to nucleophilic attack and,

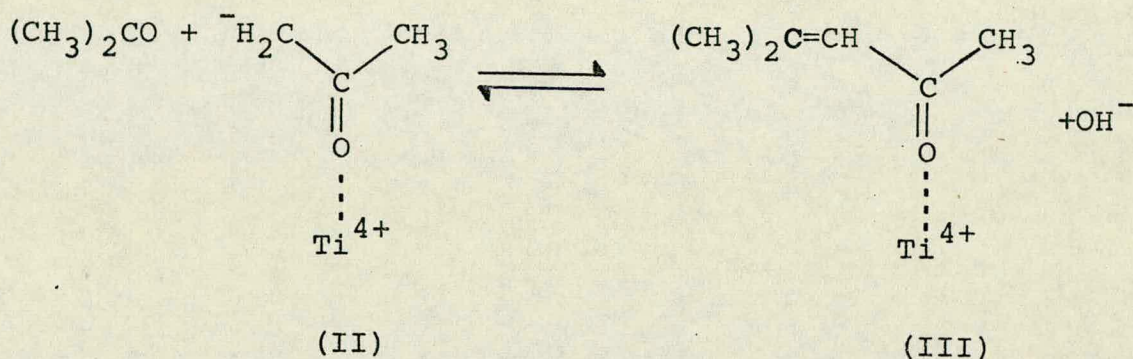
as with the H.F.A. and [$^2\text{H}_4$] acetic acid studies, the rutile samples were examined at various conditions of dehydration and reduction. Low coverage adsorption of acetone produced a band at 1680 cm^{-1} which was attributed to molecular acetone coordinately bound to Ti^{4+} Lewis acid sites and, as with [$^2\text{H}_4$] acetic acid and H.F.A., acetone could not displace molecular water from the Ti^{4+} Lewis acid sites.

The isotopic exchange of hydrogen atoms between deuteroyl groups and adsorbed acetone was examined and the authors concluded that this reaction was base catalysed since there was no evidence for Brønsted acid sites on a rutile surface^{21,23,24}. Furthermore the basic character of the surface hydroxyl and O^{2-} groups had been established from their work with [$^2\text{H}_4$] acetic³¹ acid and hexafluoroacetone³². The authors thus proposed that the mechanism for this exchange reaction involved the formation of an enolate anion (assigned to a band at 1545 cm^{-1}), as follows:-



Since it had already been established that the row B O^{2-} ions on the (110) plane readily accept protons to form bridged^{11,16} OH^- ions such species were suggested as a possible site for the exchange reaction.

Bands at 1655 and 1595 cm^{-1} were assigned to the (CO) and (C=C) stretching vibrations respectively of mesityl oxide coordinatively liganded to Lewis acid Ti^{4+} ion sites on the oxide surface. This compound was thought to be formed via the reaction of an acetone molecule and the enolate complex (II):-



The formation of acetone following the adsorption of mesityl oxide led the authors to suggest that this reaction was reversible. The reaction was also hindered by preadsorption of water onto rutile and this was thought to be due to the O^{2-} ions which, being protonated, could not catalyse the formation of the enolate ions.

Therefore the results obtained with acetone differed from those found with hexafluoroacetone (H.F.A.) in that the interaction of H.F.A. with rutile favoured nucleophilic attack by O^{2-} and/or OH^- ions accompanied by the fission of C-C bonds to form acetate species whereas the lability of hydrogen atoms in acetone resulted in the ready formation of enolate species to form mesityl oxide and compounds of higher molecular weight. As with H.F.A., the prereluction of rutile in hydrogen increased the nucleophilic as well as the basic character of surface O^{2-} and OH^- ions resulting in the production of acetate species.

Thus although most of the adsorption studies on rutile tend to focus on the activity of the Lewis acidic Ti^{4+} ions, there is evidence also that O^{2-} ions, hydroxyl species and Ti^{3+} ions are also important in the surface reactivity of this oxide.

The majority of the studies tend to suggest that hydroxyl groups on rutile are non-acidic. Boehm³⁴ however, working with a number of oxides which included rutile and anatase, was of the opinion that two types of OH group exist on the surface of these oxides; approximately 50% of which were acidic in character and approximately 50% were basic. The formation of methoxy groups from the reaction of hydroxylated rutile with a solution of diazomethane in diethyl ether is an example of Boehm's evidence for the presence of acidic surface hydroxyl groups. There was also some evidence for the production of NH_4^+ species following the adsorption of ammonia from the gas phase although infrared studies did not unambiguously support such an assignment.

(In the review above, the term for the hydroxyl group has been given as OH or OH^- depending upon the description and arguments used by the original authors).

1.5 Catalytic Studies on Titanium Dioxide

1.5.1 Alkene Isomerisation Reactions

The isomerisation of alkenes over rutile has been studied by Shannon et al^{35,36} and by Brookes³⁷.

By examining the initial rates and product ratios of the reactions of but-1-ene and cis-but-2-ene over

rutile, Shannon and co-workers^{35,36} found that at temperatures above 373 K, all six interconnecting reaction paths of the n-butenes exist as shown below and, by using a theoretical equation which had been put forward by Haag and Pines³⁸, the relative rate constants were derived.

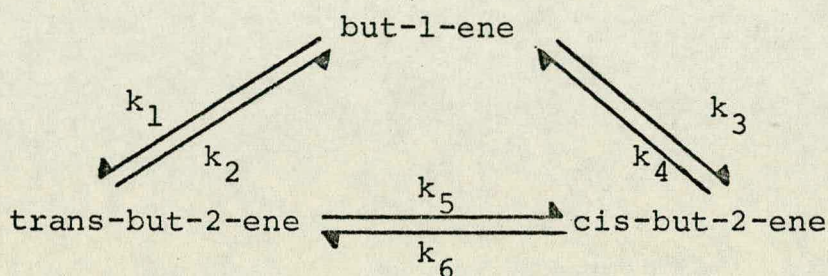


Table 1.3

Relative Rate Constants For The Isomerisation Of The
Butenes At 411 K

k_1	k_2	k_3	k_4	k_5	k_6
6.90	1.00	40.1	12.0	0.92	1.91

It is seen that although trans-but-2-ene is thermodynamically the more stable,¹⁰⁸ the kinetically favoured processes were initially the formation of cis-but-2-ene from but-1-ene and the opposite reaction when cis-but-2-ene was used as a starting material. At later stages of the reactions, the equilibrium % of the trans isomer was produced.

The double bond migration reaction was explained in terms of a mechanism involving basic sites on the rutile surface, (although such sites were not identified).

Removal of a proton from the butene reactant resulted in the formation of cis or trans allylic carbanions and such species could not interconvert due to restricted rotation about the allylic carbon-carbon bond. Since Bank et al³⁹ proposed that a cis-allylic anion is thermodynamically more stable than the trans form, this explained the preferential formation of cis rather than trans-but-2-ene from but-1-ene. It also explained the preference for double bond migration as opposed to cis/trans interconversion during the reaction of cis-but-2-ene over rutile. Another mechanism, and consequently another site, was necessary to account for the direct cis/trans isomerisation and the authors proposed that this could take place via 2-butyl radical or 2-butyl carbonium ion intermediates. Their observations that the presence of D₂ in the reaction system barely affected the isomerisation but the presence of D₂O, although a poison for the reaction, resulted in the incorporation of deuterium in the products suggested the intermediates were of ionic character. D₂ would be expected to dissociate homolytically whereas D₂O dissociates heterolytically to form ionic species. Co-isomerisation experiments with light and heavy cis-but-2-ene did not produce conclusive results but the authors thought that a common mechanism existed for both isomerisation and the exchange reaction between the light and heavy alkenes.

Poisoning studies by Brookes³⁷ suggested that the active site on rutile is a Ti⁴⁺ which acts as a Lewis acid.

The preadsorption of nucleophilic molecules such as H_2O , NH_3 , pyridine and ethylene diamine all poisoned the isomerisation of but-1-ene to cis/trans-but-2-ene but there was little effect on the final cis/trans ratio. It was therefore concluded that there could only be one active site for alkene isomerisation and not two as Shannon^{35,36} had previously suggested. Brookes also quoted the then (1972) recent spectroscopic work of Jones et al^{11,12,13}, Primet et al^{15,21,26} and Parfitt et al^{13,14,23,24,25} which had shown no evidence for the existence of Brønsted acid surface sites on rutile. The consideration that full activity of rutile was only achieved after outgassing the catalyst at 423 K, (after which temperature all the surface molecular water was expected to be removed), and also the effects of the preadsorption of NH_3 and other nucleophiles, led to the belief that the active site was the Ti^{4+} ion, and that the isomerisation proceeded via nucleophilic attack by the carbon-carbon double bond as in Fig. 1.9 which resulted in a σ -bonded carbonium ion intermediate.

The geometry of the surface is such that this mechanism would lead to the C_4 atom being attracted to a neighbouring Ti^{4+} ion which would favour the anti-conformation of the molecule and so account for the preference of cis- over trans-but-2-ene production. Only with high coverages of HCN, HCl and H_2O was the cis-preference lost and this could be accounted for by adsorption on the neighbouring Ti^{4+} ion sites. Brookes³⁷ also studied the isomerisation reactions of alkylcyclopropanes and dimethylbutenes and found the order of

reactivity for the two series to be:-

(a) 1,1-dimethylcyclopropane > 1,2-dimethylcyclopropane
> methylcyclopropane > cyclopropane

(b) 2,3-dimethylbut-1-ene > 3,3-dimethylbut-1-ene >
but-1-ene.

The above series could be accounted for by the relative stabilities of the carbonium ion intermediates.

Work by Hattori et al^{40,41} has shown that the isomerisation of butenes over rutile is remarkably dependent upon the mode of preparation and pretreatment of the catalyst. Their interpretation of the results were rather different to that of Brookes³⁷. An increase in the evacuation temperature of the catalyst was found to decrease the activity of the TiO₂ for the but-1-ene isomerisation but to increase the cis/trans ratio from 4:1 to 4:6.5. This the authors interpreted as signifying that the reaction proceeds via Brønsted acid sites and carbonium ion intermediates with catalyst samples evacuated below 673 K and with Ti³⁺ electron donating sites and π-allyl carbanion intermediates with catalysts evacuated above this temperature due to the reduction of the Ti⁴⁺ ions to Ti³⁺ ions. The authors conceded that this interpretation could only apply to certain types of TiO₂ as other samples made in a different manner gave different results and a mixed oxide TiO₂-SiO₂ sample also reacted differently. These results were supported by co-isomerisation experiments with light and per-deuterated cis-but-2-ene and with catalysts pretreated with D₂O. With catalysts evacuated at 523 K, isomerisation

was found to proceed via an intermolecular mechanism which suggested carbonium ion intermediates on Brønsted acid sites whereas with catalysts evacuated at 873 K, the results suggested an intramolecular reaction mechanism proceeding via carbanionic intermediates.

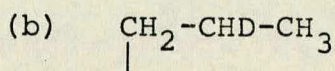
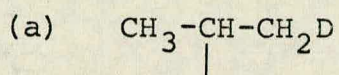
Recent work on anatase⁴² revealed that it also behaves in a complex manner. Using [2,3-²H₂]-cis-but-2-ene and [1,4-²H₆]-cis-but-2-ene and following the isomerisation to but-1-ene and trans-but-2-ene with or without exchange of the allylic or vinylic hydrogens, it was found that depending upon the pretreatment temperature, the isomerisation of the butenes could take place by three different mechanisms involving Brønsted acid sites, Lewis acid sites or basic sites.

1.5.2 Exchange Reactions

Exchange and addition reactions of ethene, propene and isobutene with deuterium over rutile have been examined by Lake and Kemball⁴³ in the temperature range of 523 K to 723 K. It was observed that the hydrogen atoms of the molecules can be grouped according to their rate of exchange. Thus all the hydrogens of isobutene and five of the six in propene exchanged approximately 100 times faster than the sixth hydrogen in propene and all the hydrogens in ethene. The grouping led the authors to believe that the rapid hydrogen atom exchange could be linked to the reversible dissociative adsorption of the alkene, with the formation of an allyl radical on the surface. The terminal hydrogen atoms on propene and all

those on isobutene can be regarded as chemically equivalent in such a mechanism which explained the similarity for the rate of their exchange. The authors also pointed out that the formation of an allyl carbanion intermediate would also be consistent with the results.

The second group of hydrogens (which exchanged at a slower rate) were believed to react via an associative mechanism leading to the formation of an alkyl species on the surface. With propene, the propyl species could take either the form (a) or (b) below:-



Species (a) would, like an allyl intermediate, lead to exchange of the terminal hydrogen atoms and (b) would give the exchange of the hydrogen atom on the central carbon atom. Thus if species (a) was formed more readily than (b) the results with the faster hydrogens could be explained but the authors preferred to explain the ready exchange of this group in terms of the allyl intermediate. Since addition occurred at rates similar to the exchange of the second group, alkyl intermediates were believed to be involved with this group also.

Later Kemball⁴⁴ pointed out that the molecule used to supply the labelling isotope, i.e. D_2 or D_2O , probably affects the reaction. Thus with isobutene, the presence of D_2 probably resulted in an allyl intermediate whereas a carbonium intermediate was probably formed when D_2O was used in the exchange reaction.

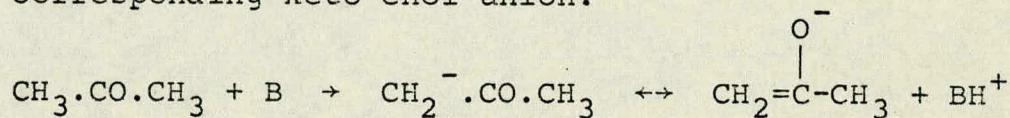
Lake and Kemball⁴³ also examined the exchange of benzene, toluene and m-xylene with deuterium on rutile in the temperature range 523-723 K, as this reaction offered an insight into the nature of the interaction of rutile with different types of carbon-hydrogen bond. The main feature of such reactions was the apparent lack of selectivity of rutile for the activation of the hydrogen atoms in the side groups or in the different ring positions. There was no difference in activity between the two groups during exchange of D₂ with toluene, and with m-xylene the ring hydrogens were only more active by a factor of four. These results were thought to be fairly inconclusive as they were similar to that observed with homogeneous base, homogeneous acid and metal catalysts and therefore none of the various alternative mechanisms and intermediates could be excluded. The low selectivity was however indicative of radical intermediates.

1.5.3 The Reactions of Ketones over Rutile

Shannon, Lake and Kemball³⁶ confirmed their suspicions that water was easily activated by rutile for exchange when they found that D₂O readily exchanged at temperatures of only 320 K with a series of ketones; acetone, methyl ethyl ketone, methyl isopropyl ketone, mesityl oxide and cyclopentanone. No exchange occurred between acetone and D₂ at such temperatures and above 340 K this reaction was complicated by condensation of the acetone to form mesityl oxide and mesitylene and also

by the loss of material to the surface.

With each ketone, exchange with D₂O was limited to the number of enolizable hydrogen atoms, i.e. those on the carbon atoms α to the keto group and those in the methyl groups in mesityl oxide, (CH₃)₂.C=CH.CO.CH₃ . The mechanism proposed for the exchange reaction was one in which the rutile surface could act as both an acid and as a base. Interaction with basic sites on rutile, which the authors did not specify, produces a carbanion which could be resonance stabilised by the corresponding keto-enol anion.



The catalyst would then act as an acid by supplying a proton or deuteron to effect the exchange. This explains the preference of the catalyst to exchange the enolisable hydrogen atoms. The authors also appreciated that a more complex mechanism, involving a concerted acid-base, could also explain the results. No explanation was offered as to why this reaction proceeded so rapidly at ambient temperatures.

1.5.4 The Reactions of Dienes, Alkynes and Alkanes

Halliday et al^{45,46} have recently studied the interaction of dienes and alkynes with rutile.

The purpose of the investigation was to ascertain why the hydrogenation of alkenes to alkanes over rutile requires reaction temperatures >630 K⁴³ whereas brief investigations by Shannon^{35,36} and

Brookes³⁷ had shown that lower temperatures of approximately 450 K were sufficient for the hydrogenation of buta-1,3-diene to butenes. The authors also hoped to clarify whether the hydrogenation was a self-hydrogenation or if gaseous hydrogen was incorporated into the reacting diene.

Loss of material from the gas phase was found to be the main reaction with all the reactants, although this occurred to a greater extent with alkynes than with dienes. A residue was formed on the surface which the authors suggested was oligomeric in nature. This was subsequently confirmed by pyrolysis and temperature-programmed-desorption experiments which revealed the formation of aromatic and long-chain carbon compounds.

The formation of but-1-ene and cis/trans-but-2-ene from buta-1,3-diene accompanied the loss of material to the surface and mass spectrometric experiments with mixtures containing deuterium produced evidence that the reaction was a self-hydrogenation process which did not require the presence of hydrogen or deuterium. In the presence of D₂O, the main reaction between 473 and 523 K was found to be exchange of the diene with the formation of a [²H₁] butadiene species.

The presence of water during the reaction of buta-1,3-diene was found to inhibit both the loss of material to the surface and the formation of alkenes but preadsorption of ethanol selectively hindered the self-hydrogenation. Above 400 K, the presence of HCl increased the loss of buta-1,3-diene to the surface by

a factor of 180 but had little effect on the self-hydrogenation process.

At temperatures below 400 K, propadiene was found to isomerise to propyne in a reversible fashion but above this temperature, the reaction was complicated, as with buta-1,3-diene, by loss of material to the surface and self-hydrogenation. Exchange reactions with D_2O were similarly complicated.

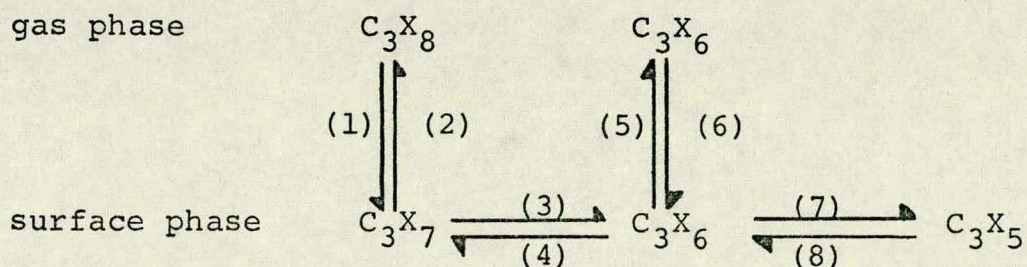
The manner by which water, deuterium oxide, ethanol and HCl affected the rate of material loss and the production of the alkenes suggested that the two reactions occurred on different sites. The authors proposed that (a) material loss occurred on Ti^{4+} Lewis acid sites, (the activity of which is known to be readily altered by water, ethanol and HCl^{14,37}), and, (b) $Ti^{4+}.O^{2-}$ acid-base pairs were the sites for alkene production. No detailed mechanisms were suggested for either material loss or self-hydrogenation. The isomerisation of propadiene to propyne was also thought to involve $Ti^{4+}.O^{2-}$ surface pairs; (Fig. 1.10).

The observation that the alkene production resulted from a self-hydrogenation process explained why lower temperatures than those required for H_2/D_2 exchange⁴³ were sufficient as the diene hydrogenation reaction did not require the activation of gaseous hydrogen - unlike the hydrogenation of alkenes to alkanes. The general conclusion, comparing the work of the authors with that of

others on ZnO and CoO, was that rutile was an inefficient catalyst for the hydrogenation of alkynes and dienes.

Working mainly with propane, isobutane and cyclopentane, and using a gas chromatograph linked to a rapid-scanning mass spectrometer, the exchange of alkanes with D₂ and D₂O has been observed^{45,47} at temperatures above 700 K and the reactivity pattern of the hydrocarbon molecules indicated that in this case, rutile behaves in a similar manner to that of a metal catalyst in promoting homolytic fission of C-H bonds. The exchange was accompanied by dehydrogenation to alkenes. Initially the rate of dehydrogenation was similar to the rate of exchange but eventually it decreased as the composition of the mixture approached the hydrogenation equilibrium.

The majority of the results with all the alkanes were rationalized in terms of the following reaction scheme with reference to propane as the reactant, and where X is either hydrogen or deuterium.



The exchange of alkane was envisaged to occur through the reversible formation of the alkyl species

by steps (1) and (2) and since exchange and dehydrogenation occurred at similar rates, this implied that steps (2) and (3) had similar rates. Stepwise exchange was believed to occur as reaction (4) is slow under initial conditions. Steps (7) and (8) were fast compared to step (5) and consequently most of the propene molecules underwent several reversible dissociations to the C_3X_5 species before leaving the surface which explained the formation of alkene species containing several deuterium atoms. Once gaseous propene was formed, steps (6) and (4) become more important resulting in more highly exchanged propenes and the formation of highly exchanged propanes. The results were similar to that of Lake and Kemball⁴³ in that, of the alkenes formed from the dehydrogenation reaction, only five of the six hydrogens of propene and all of those in isobutene were exchanged readily. This therefore suggested that the C_3X_5 species was an allyl species which was either neutral or carbanionic in character.

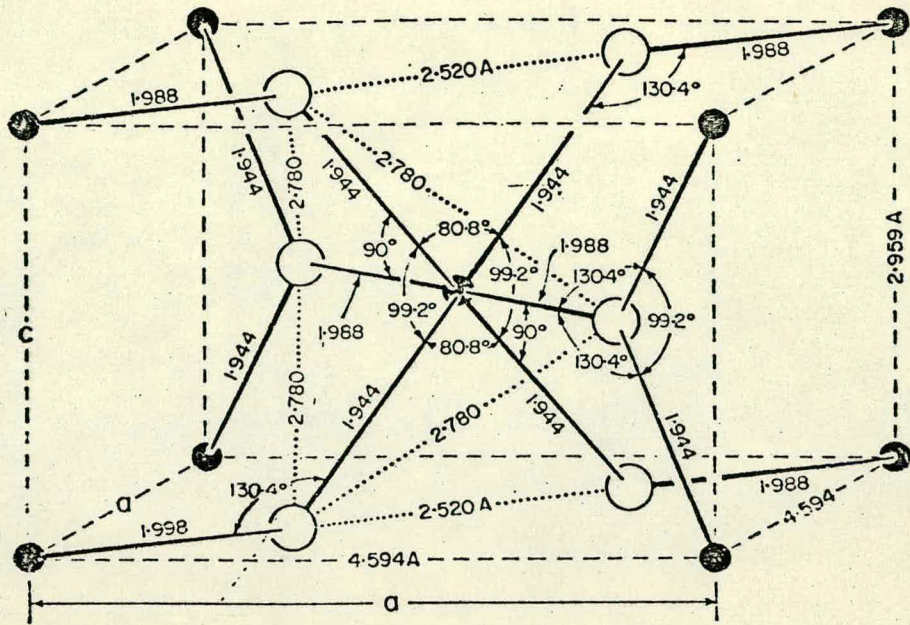
The dehydrogenation and exchange of cyclopentane resulted in the production of significant amounts of d_0 , d_1 , d_2 and d_3 compounds which suggested that the adsorbed species were oriented with the ring parallel to the surface and that it did not readily turn over.

The facts that (i) the results suggested that rutile was acting like a metal in promoting homolytic dissociation of C-H bonds during the reaction of alkanes, (ii) the presence of hydrogen or deuterium, and (iii) the high temperature necessary for this

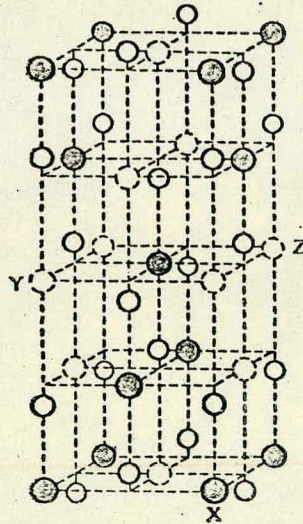
reaction would certainly promote reduction of the catalyst, prompted Halliday⁴⁵ to suggest that the active centres involved could be Ti^{3+} ions acting as electron donors. Fig.1.11 shows a possible reaction scheme for the formation of radical species from alkanes.

1.5.5 Other Surface Studies on Rutile

The preceding review has summarised those aspects of the chemistry of TiO_2 which are considered to be the most relevant to the work described later in this thesis. The other area in which TiO_2 has been investigated as a catalyst is the field of alcohol decomposition and this aspect of the surface properties of TiO_2 will be discussed in Chapter 3 which deals with the catalytic decomposition of alcohols in general. A number of photocatalytic studies have been made on TiO_2 but these will also be discussed at more appropriate points in this thesis.



(a)



(b)

figure 1.1, (a) unit cell of rutile, after von Hippel³ et al. (The large circles represent oxygen atoms, small circles titanium atoms).

(b) unit cell of anatase, after Wells⁴. (Shaded circles represent titanium atoms, open are oxygen and dotted are metal atoms removed from the NaCl structure).

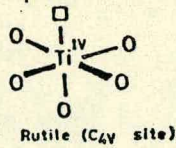
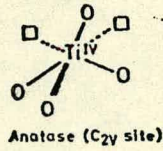


figure 1.2, atomic models for anatase and rutile surfaces after Munuera et al.⁷ (O represent anions and □ represent anionic vacancies).

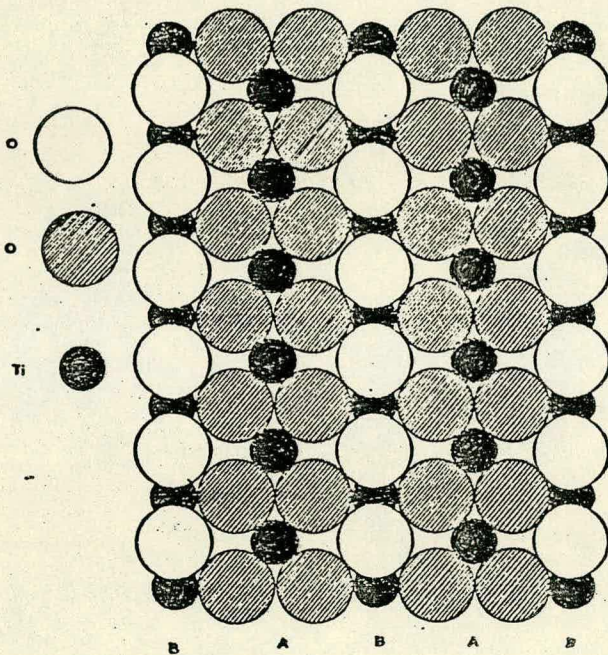


figure 1.3, (a) - a plan view of the (110) plane of rutile after Jones and Hockey.¹¹ There are 10.2 Ti ions
 -2
 nm.

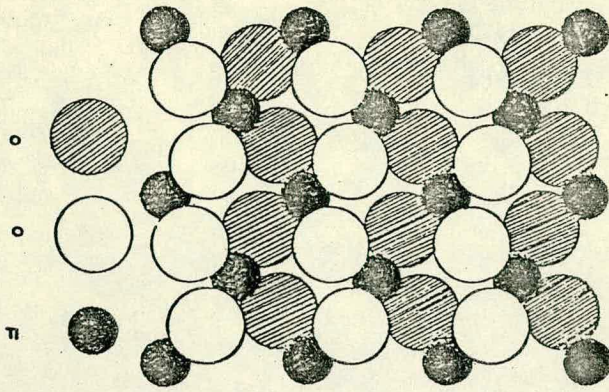


figure 1.3, (b) - a plan view of the (101) plane of rutile after Jones and Hockey.¹¹ There are 7.9 Ti ions nm.⁻²

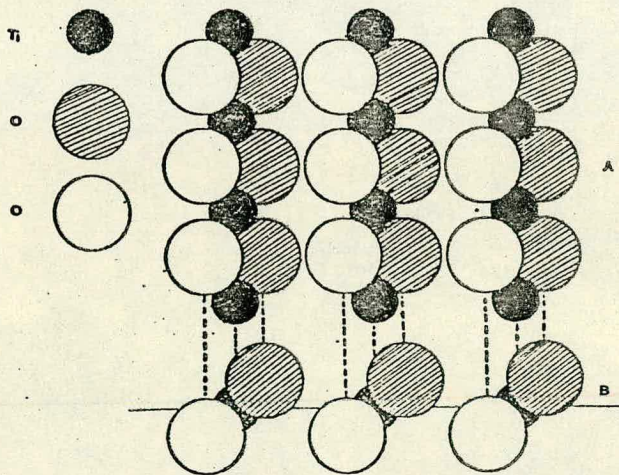


figure 1.3, (c) - (A) a plan view of the (100) cleavage plane of rutile after Jones and Hockey.¹¹ There are 7.4 Ti ions nm.⁻² (B) an elevation looking along the C-axis of the (100) plane.

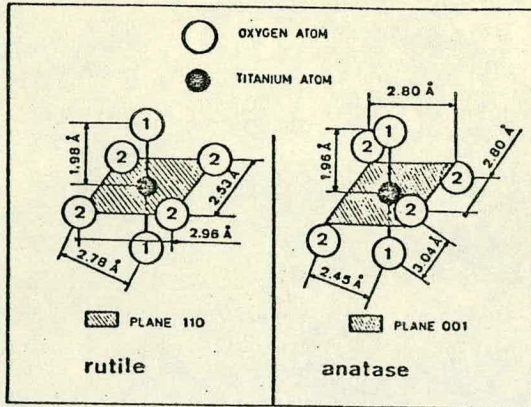


figure 1.4, interatomic distances in rutile and anatase after Primet et al.¹⁵

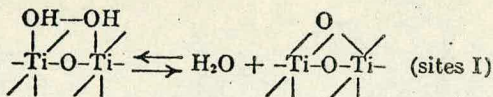


figure 1.5, (a) condensation of adjacent terminal hydroxyl groups to yield sites I; after Primet et al.¹⁵

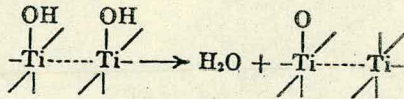


figure 1.5, (b) condensation of isolated terminal hydroxyl groups to yield incompletely co-ordinated titanium atoms (sites II) after Primet et al.¹⁵

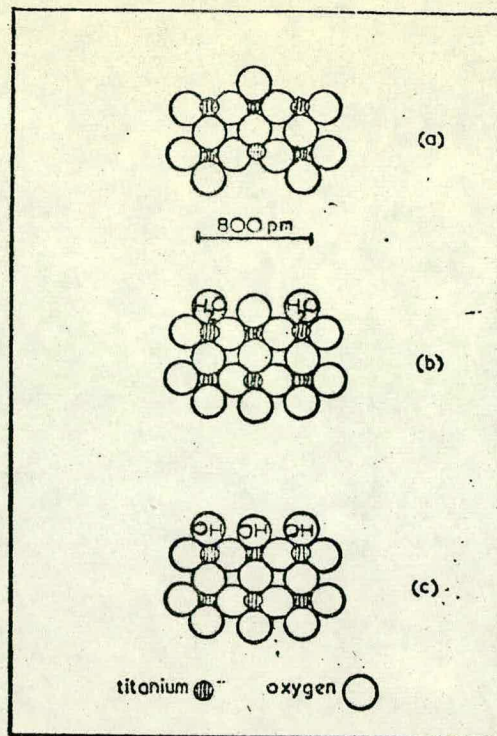


figure 1.6, cross-section of rutile crystal showing the (110) plane (a), after water molecules adsorbed (b), and after dissociation to form hydroxyl groups (c), after Jackson and Parfitt.¹⁴

—Temperature programmed desorption (TPD) of water. TPD from TiO_2 outgassed at 400°C and on which increasing amounts (b→e) had been re-adsorbed. Amount of water re-adsorbed: (a), none (residual water after outgassing at 400°C); (b), $0.08 \times 10^{-6} \text{ m}^3 \text{ g}^{-1}$; (c), $0.15 \times 10^{-6} \text{ m}^3 \text{ g}^{-1}$; (d), $0.25 \times 10^{-6} \text{ m}^3 \text{ g}^{-1}$; (e) $0.52 \times 10^{-6} \text{ m}^3 \text{ g}^{-1}$. TPD heating rate $\beta = 14.5 \text{ K min}^{-1}$.

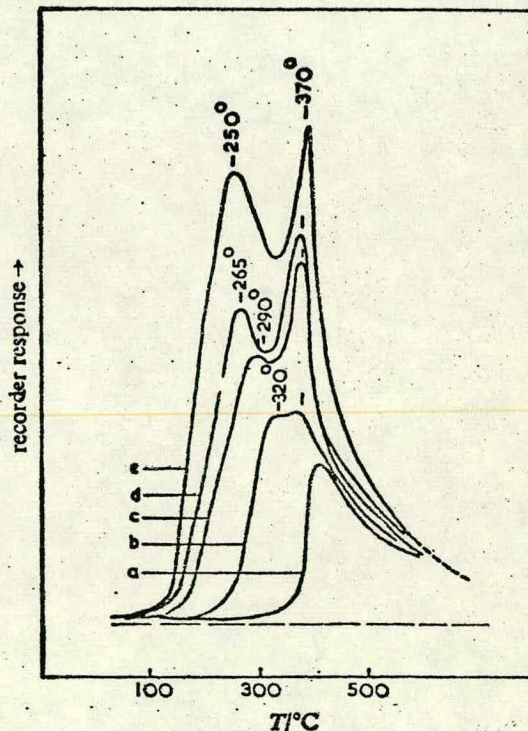


figure 1.7, Temperature-programmed-desorption of water after Munuera and Stone.¹⁹

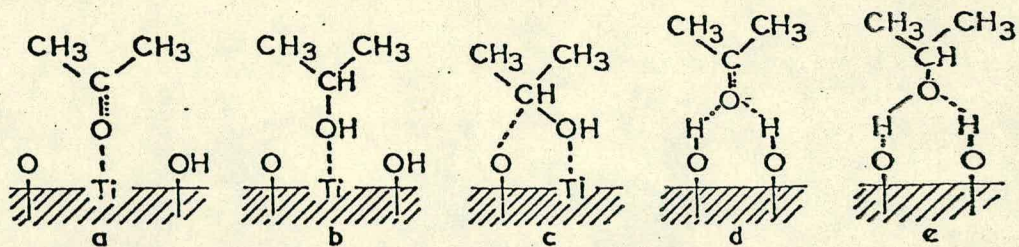


figure 1.8, sites for the adsorption of propan-2-ol and acetone on rutile, after Munuera and Stone.¹⁹

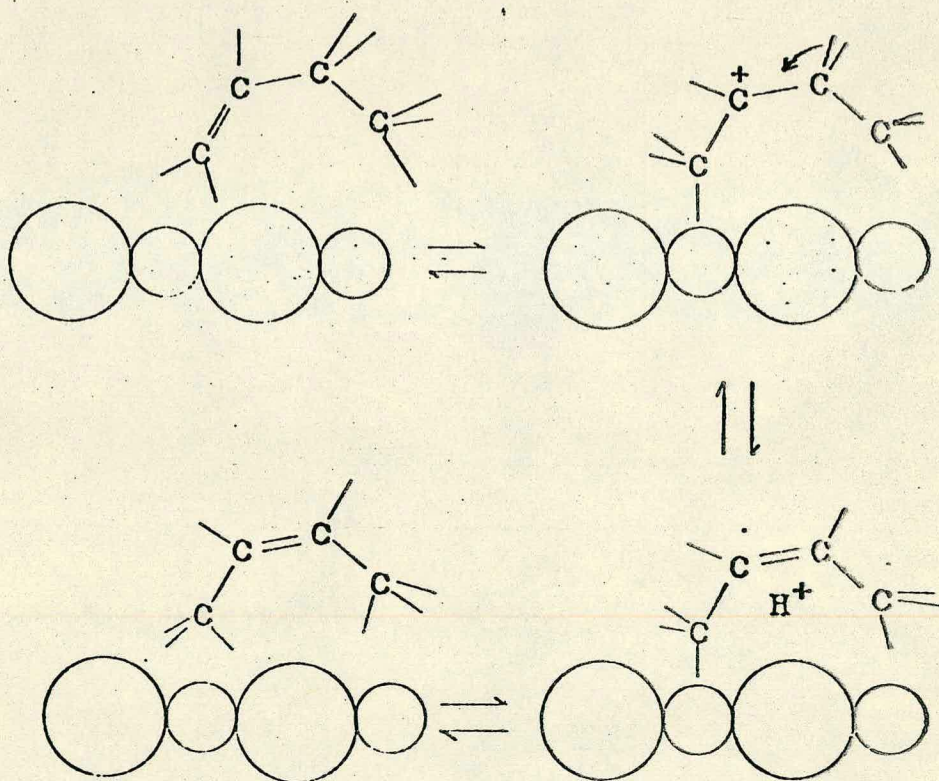


figure 1.9, the interconversion of but-1-ene and cis but-2-ene after Brookes;³⁷ large circles represent oxygen ions and small circles represent titanium ions.

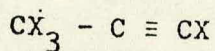
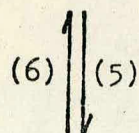
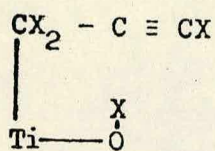
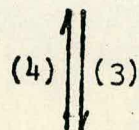
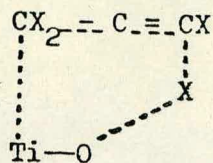
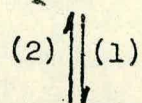
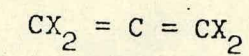


figure 1.10, reaction scheme for the isomerisation and exchange of propadiene on rutile after Halliday,⁴⁵ X=H or D.

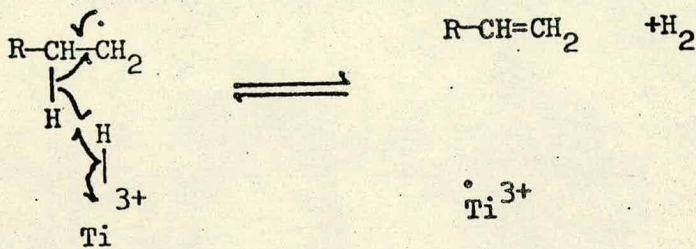
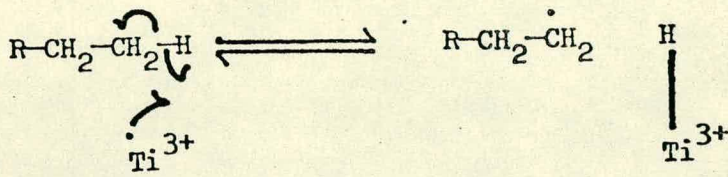


figure 1.11, reaction scheme for the production of neutral species from alkene molecules using paramagnetic centres on the surface of rutile after Halliday.⁴⁵

CHAPTER 2

Experimental Procedure and Treatment of Results

2.1 The Source and Purity of Rutile Used in this Investigation

All samples of catalyst used in this work were of the rutile modification of TiO_2 and were from batch code number: CL/D412 which was supplied by Tioxide International Ltd. The catalyst was prepared by hydrolysis of titanium tetrachloride, washed and then calcined at 698 K. The major impurities are as described below in Table 2.1

Table 2.1 CL/D412: Major Impurities

Cl.	0.3%
Fe, Pb, Nb_2O_5 , ZrO_2	<10 p.p.m.
CuO, K_2O , Sb_2O_3 , ZnO	<20 p.p.m.
Al, Si, P_2O_5 , SO_3	<100 p.p.m.

The surface area as determined by B.E.T. adsorption of nitrogen was found to be $25 \pm 1 \text{ m}^2 \text{ g}^{-1}$.

2.2 The Source and Purity of Chemicals Used in this Investigation

A description of the source and purity of the more important chemicals used in this investigation is summarised in Table 2.2: the majority were claimed to be >99% pure according to the manufacturers'

specification. The purity was checked by gas chromatography before use and only 4-methylpentan-2-ol was found to contain a major impurity which could be detected on the G.C. attenuation range used in catalytic runs. The 4-methylpentan-2-ol was purified using a spinning band rotary evaporator after which, G.C. analysis revealed it to be 100% pure. The reactants were either stored as received or in tap-ampoules, and were always degassed and further purified by freeze-pump-thaw cycles before a reaction was carried out. Two reactants, 1-chloropropane and 2-chloropropane were prepared in the laboratory by the halogenation of the respective alcohols and their purity which was checked by both infra-red spectroscopy and G.C. analysis, was found to be >99%.

2.3 Apparatus

The majority of the work described in this thesis was carried out with gas-lines I and II (Figs. 2.1 and 2.2), which were static and flow-systems respectively: both were coupled to gas-chromatography apparatus to monitor the reactions. The work with labelled molecules was undertaken on a static system, referred to as gas-line III, Fig. 2.3, which was very similar to gas-line I and which was coupled to a mass spectrometer. This system also had separate G.C. facilities and has been described by Moller⁴⁸. Another system, again similar in design to gas-line I, was linked to a combined gas chromatograph/mass spectrometer. In all systems, reactors were surrounded by furnaces operated by Eurotherm temperature control units.

Table 2.2

The Source And Purity Of Chemicals Used In This Investigation

ALCOHOLS

<u>Chemical</u>	<u>Manufacturer's name</u>	<u>Manufacturer</u>	<u>Claimed Purity</u>
pentan-1-ol	same	B.D.H.	98%+
4-methyl-pentan-2-ol	same	Aldrich	98%+
2,2-dimethyl-propan-1-ol	neopentanol	Ralph N. Emanuel	99%
propan-1-ol	propylalkohol	Fluka	puriss
propan-2-ol	same	Analar	99%+
2,3-dimethyl-butan-2-ol	same	Aldrich	99%+
2-methyl-propan-2-ol	tert-butanol	Ralph N. Emanuel	-

ALDEHYDES, KETONES AND ETHERS

pentanal	valeraldehyde	Aldrich	99%
4-methyl-pentan-2-one	methyl isobutyl ketone	Cambrian	-
2,2-dimethyl-propanal	trimethyl-acetaldehyde	Aldrich	99%+
propanal	propionaldehyde	Koch-Light	Pure
acetone	acetone	Fisons	AR
n-propyl ether	same	B.D.H.	contains 12% n-propanol

cont/d....

Table 2.2 cont/d....

<u>Chemical</u>	<u>Manufacturer's</u> <u>name</u>	<u>Manufacturer</u>	<u>Claimed</u> <u>Purity</u>
<u>ALKENES</u>			
pent-1-ene	same	Koch-Light	puriss
cis-pent-2-ene	same	Fluka	puriss
trans-pent-2-ene	same	Koch-Light	puriss
methylpentenes	-	Aldrich	99%+
methylbutenes	-	Koch-Light	puriss
[² H ₂] propene	-	Merck, Sharp & Dohme	98%
[² H ₂] isobutene	-	Merck, Sharp & Dohme	98%

2.3.1 Gas-Line I (Fig. 2.1) Static System with G.C. Analysis

The studies of the decomposition of those reactants with suitable vapour pressures at ambient temperature ⁴⁹ were carried out on gas-line I. Preadsorption, poisoning and related studies were also undertaken on this apparatus.

The powdered catalyst was placed in reaction vessels A and B, (Fig. 2.1), which were connected via a water-cooled joint to give total reaction volumes of $1.31 \times 10^{-4} \text{ m}^3$ and $1.45 \times 10^{-4} \text{ m}^3$ for A and B respectively. A glass-wool plug was placed in the neck of each vessel before connection to the rest of the system in order to prevent scatter of the catalyst throughout the line during evacuation and a cold-finger, $2.5 \times 10^{-2} \text{ m}$ in length, was sealed into the bottom of each reaction vessel so that $1.5 \times 10^{-2} \text{ m}$ of the open end protruded inside the vessel. Thus when the external part of the cold-finger was surrounded by liquid nitrogen, it was possible to freeze a reactant mixture into the vessel with minimal contact onto the catalyst surface. The reaction vessels were connected through three-way glass stopcocks to a Perkin-Elmer F.11 sampling valve with a sample loop volume of $2.5 \times 10^{-7} \text{ m}^3$ and thence to a gas chromatograph. The sampling valve was later replaced by a Carle Instruments mini sampling valve which had a sample loop volume of $2 \times 10^{-7} \text{ m}^3$.

Three pumping systems were used on the line. The gas-handling system and the outgassing system each had a three-stage mercury diffusion pump backed by an oil rotary pump. A third rotary pump was used to evacuate the atmospheric chambers of the McLeod gauges. The outgassing

system was connected to the reaction vessels and the main McLeod gauge, and was essentially used for outgassing catalysts. After outgassing, the pressure in the gas-line as registered by the McLeod gauge was 1.33×10^{-4} Pa. (1×10^{-6} τ).

In addition to the McLeod gauge already described, this line was also equipped with another McLeod gauge, connected through a glass-mercury cut off and a glass stopcock to sections D and F, (see Fig. 2.1). This gauge had been calibrated previously³⁷ and allowed measurement of pressures in the region 0-2.22 kPa. It was employed in the preadsorption studies.

Gases in frequent use were stored in bulbs attached to section G, (Fig. 2.1), which also had a number of taps and cone-joints through which other gases could be admitted. During the admission of gases into the line via points N and P, use was made of two mercury-filled lutes which acted to prevent the build-up of excessive pressures in the line. All gases were subjected to several freeze-pump-thaw cycles by use of cold traps C, H and I before being finally admitted into the storage bulbs on the reaction vessel. Palladium thimbles J and K and bulbs L and M were available for the purification and storage of hydrogen.

2.3.2 Gas-Line II (Fig. 2.2)

Flow System with G.C. Analysis

The very low vapour pressure of some alcohols at room temperature resulted in the employment of the flow system, previously described in Halliday's thesis⁴⁵.

Reactants such as pentan-1-ol with vapour pressures ≈ 133.3 Pa (1 τ) at room temperature⁴⁹, do not readily diffuse through the apparatus and tend to condense at any cool-position, e.g. water-cooled joints. Consequently it is extremely difficult to study their catalytic decomposition if a static system is employed. The flow system, all of which could be heated electrically to prevent condensation, is shown in Fig. 2.2.

The carrier gas used with "white spot" nitrogen which passed from a cylinder fitted with a pressure regulator, through a Negretti and Zambra precision regulator, a Napro needle valve and a G.E.C. Elliot "Rotameter 1100" flowmeter which gave gas flow rates in the range $(3.3-11.6) \times 10^{-7} \text{ m}^3 \text{ s}^{-1}$. Later, this flowmeter was replaced by a similar make of flowmeter which allowed measurement of flow rates between $(0.83-25) \times 10^{-7} \text{ m}^3 \text{ s}^{-1}$. Later, this flowmeter was replaced by a similar make of flowmeter which allowed measurement of flow rates between $(0.83-25) \times 10^{-7} \text{ m}^3 \text{ s}^{-1}$. The carrier gas then passed through a glass saturator containing the appropriate reactant. The saturator was positioned in a water bath and was heated to the desired temperature by a Shandon circotherm. The saturator was made from three glass tubes in series, each containing the liquid reactant supported by a Pyrex-2 sintered disc through which the nitrogen carrier gas bubbled and became saturated with the reactant. From the saturator, the carrier gas plus reactant vapour passed through a Carle Instruments mini-sampling valve which enabled the gas stream to be diverted into the reactor or directly into the G.C. to allow for the examination of the reactants prior to contact with the catalyst. After flowing

through the reactor, which was constructed from a glass tube incorporating a Pyrex-2 sintered disc on which the rutile was placed, (Fig. 2.4), the samples for analysis were directed to the G.C. by another Carle mini-sampling-valve. The arrangement of the two valves is shown in Fig. 2.5.

In order to prevent condensation of the reactants, electrically heated steel tubing was used and any glass tubing was warmed with heating tape. The temperature of the reactor was measured by either a digital voltmeter or a digital thermometer using a Chromel-Alumel thermocouple positioned by heat-resistant tape around the reactor so that the end of the thermocouple was situated at the same level as the catalyst in the reactor. The temperature of the reactor was stabilised by surrounding the glass tube with asbestos string and also by immersing the reactor within the furnace as completely as possible. After stabilisation, the temperature remained constant to ± 0.5 K throughout a typical experiment.

The reactor was connected via the Carle mini-valves to a gas-handling system connected to a mercury diffusion pump backed by a rotary pump. Bulbs attached to this part of the line were used for storing gases in frequent use. This part of the line also contained a rank of stopcocks and cone-joints through which other gases could be admitted to the line and was also used for G.C. calibration studies of the reactants and products. Correct manipulation of the Carle-valves was necessary to ensure that the catalyst was not scattered throughout

the system. Admission or evacuation of gases was always carried out in such a manner that the flow was against the catalyst's pyrex support.

2.3.3 Gas-Line III (Fig. 2.3)

Static System with Mass Spectrometric Analysis

The basic design of gas-line III was essentially similar to that of gas-line I except that a reaction mixture could be studied using both mass spectrometry and gas chromatography. A fine capillary leak 0.27m in length allowed about 4% of the gas in the reaction vessel to flow into the mass spectrometer during a two hour reaction thus the reaction could be readily monitored without excessive loss of reactant.

An A.E.I. M.S.10 mass spectrometer equipped with a permanent magnet was used and the accelerating voltage was varied, manually or automatically, to allow the scanning of masses between 36 and 70 a.m.u.

An Edwards high vacuum rotary pump in series with an oil diffusion pump equipped with a liquid nitrogen trap produced the required vacuum within the mass spectrometer. This vacuum, measured with an insertion ionisation gauge, was considered satisfactory if it was less than 1.3×10^{-2} Pa; (10^{-4} Torr).

Various protection circuits were built into the apparatus to minimise any damage which might occur due to vacuum failure and before any experiment, the mass spectrometer was baked out overnight at 473 K to remove any adsorbed species on the internal surfaces of the mass spectrometer.

2.4 Experimental Procedure

2.4.1 Static Systems

2.4.1.1 Reaction Procedure

Before any experimental work was carried out on gas-lines I and II, the catalyst samples were pretreated as follows; with reference mainly to gas-line I:-

The samples were first placed in the reaction vessel and outgassed overnight at 723 K resulting in a partial reduction of the catalyst samples which caused them to take on a grey/blue appearance and also removed any water molecules, hydroxyl species or other undesirable surface species present. Following this overnight treatment, and prior to a catalytic run, a first dose of approximately 1×10^{20} molecules of oxygen was admitted into the reaction vessel for 5 minutes at 723 K, the reaction vessel was then evacuated for 2 minutes at this temperature and then a further dose of approximately 1×10^{20} molecules of oxygen was admitted. After 15 minutes at 723 K the sample was allowed to cool to room temperature and finally outgassed for 20 minutes. The oxygen treatment re-oxidised the surface of the rutile, restored the initial white appearance, and also removed by oxidation any carbonaceous residue which may have formed on the catalyst by reaction with the stop-cock grease.

Reactants were admitted into the dosing volume E, (Fig. 2.1) to the appropriate pressure (measured on mercury manometer) and then were either frozen or expanded into reaction vessels A or B. A mixing bulb

of volume $5.49 \times 10^{-4} \text{ m}^3$ was available for rapid mixing of two or more species, and was also used as an expansion volume when it was necessary to admit very small doses of gases into the reaction vessel.

As soon as the reactants had been admitted to the reaction vessel, a furnace, previously set at the required temperature, was raised around the reaction vessel and after a few minutes the first gas phase sample was taken. Samples of the reaction mixture were taken at intervals until the reaction had gone to completion or until sufficient data had been collected to allow calculation of the reaction rates.

The amount of alcohol used in the catalytic experiments on gas-line I was normally $\approx 0.4 \times 10^{20}$ molecules, and those experiments with labelled alkenes on gas-line III used 1×10^{20} molecules of reactant. 0.1 g of catalyst was used during the alcohol decomposition studies whereas with the reactions of the labelled alkenes a 1 g sample of catalyst was used. Any variations to the above standard procedures are discussed at the appropriate points in the thesis.

2.4.1.2 Poisoning Studies

Although strictly speaking a poison is a species which slows down or halts a catalytic reaction, in this section explanation is simplified if it is understood that the term "poison" refers to a species which causes perturbation of the "normal" reaction pattern or rate.

Three variations in experimental technique were employed in the poisoning studies.

Method (I)

If quantitative information was required concerning the surface coverage of species adsorbed prior to a catalytic run, use was made of the small, calibrated McLeod gauge on gas-line I, (Fig. 2.1) but, unlike previous work³⁷, alterations were made to this gas-line in order that use could be made of reaction vessels A and B for the poisoning studies. It was known from previous work³⁷ with this sample of rutile (CL/D 412), that for small molecules such as H₂O or NH₃, at temperatures <423 K, total adsorption of the measured dose only occurred when the resulting surface coverage was <2 molecules nm⁻². Thus, using this as a guide-line, it was planned to achieve surface coverages in the range 0-2 molecules nm⁻².

Approximately $(1.3-2.6) \times 10^2$ Pa, (1-2τ), of adsorbate vapour was expanded into the dosing volume E and then expanded into a larger volume which included the mixing bulb and the small McLeod gauge to make a total volume of 7.55×10^{-4} m³. This volume could be divided into smaller amounts by suitable manipulation of appropriate taps on the line. The pressure in the system was then measured using the small McLeod gauge, and the desired coverage was obtained by allowing the necessary volume of gas to adsorb onto the catalyst for approximately 30 minutes at room temperature. The catalyst was then heated to the desired reaction

temperature for 30 minutes. Any residual pressure was measured and taken care of in the calculation of the resulting surface coverage of adsorbed species at the reaction temperature. Subsequent to the preadsorption, the catalyst was cooled to room temperature where it was expected that no adsorbate would remain in the gas phase, and the reactant was then expanded or frozen into the reaction vessel.

The small McLeod gauge was operated by first raising the mercury within to a fixed mark just below the opening of the McLeod gauge bulb - this fixed the volume of the quantity of gas being measured. The mercury was then raised in the closed limb to one of five calibration levels which determine the range and sensitivity of the pressure scale. The pressure was found by noting the scale reading of the mercury in the evacuated limb and using the calibration graph appropriate to the chosen calibration level. The pressure ranges, scale readings and calibration levels are listed in Table 2.3.

Table 2.3

Distance of calibration level from top of closed limb (10^{-2} m)	Scale reading on evacuated limb (10^{-2} m)	Pressure range kPa
0.3	24.5 - 51.0	0 - 0.017
0.7	24.1 - 51.0	0 - 0.033
3.4	21.4 - 51.0	0 - 0.185
6.8	18.0 - 51.0	0 - 0.466
24.8	0.0 - 51.0	0 - 2.22



Care had to be taken when using the McLeod gauge to measure the pressure of condensable gases such as H₂O or trimethylamine to ensure that the experimental conditions were such as to allow the vapour to exhibit essentially ideal behaviour.

Methods (II) and (III)

Three situations arose where the above could be replaced by a simplified procedure:-

(i) The interest was focussed primarily on the qualitative rather than the quantitative aspects of the effects of adsorption.

(ii) The effect of such small doses as described above could not lead to any significant conclusions.

In these situations method (II) was employed in which amounts of poison, which were either equivalent to or in excess of the amount of reactant, were frozen into the reaction vessel with the reactant and so "competed" with the reacting molecules for catalytic sites.

(iii) If maximum adsorption onto the surface was all that was required, the catalyst was exposed, prior to admission of the reactant, to an equivalent amount of poison for approximately 10 minutes at room temperature and then the poison was pumped off for another 10 minutes. This was method III for poisoning the catalyst.

2.4.2 Flow System: Reaction Procedure

Prior to catalyst evaluation, samples of catalyst were outgassed overnight and oxygen pretreated as with the static system (section 2.4.1.1). To prevent

the scatter of catalyst powder throughout the system, oxygen or other gases were always admitted to the reactor through tap B (Fig. 2.2) with valve 1 in position 1 (Fig. 2.5) and sample evacuation always proceeded through tap A (Fig. 2.2) with valve 1 (Fig. 2.5) in position 2, the nitrogen blocked off and valve 2 in position 1. Once the catalyst was under vacuum, it was considered safe to place valve 1 in position 1 which resulted in the catalyst being outgassed through tap B. The by-pass system could then be brought to atmospheric pressure by opening tap A to the vent and with valve 2 in position 1. Thus the saturator could then be connected to the reactor via the inlet to valve 1.

The temperature of the water bath was such that the vapour pressure above the liquid reactant in the saturator was between 1.333-2.666 kPa (10-20 τ). The pressure regulator and flow meter were then adjusted to give the required flow of gases through the by-pass system. At this point in the procedure, samples of the unreacted gases could be directed to the G.C. to check their purity.

A furnace, previously set at the appropriate reaction temperature was then placed around the reactor and by placing valve 1 in position 2, the gas stream was then passed over the catalyst sample and, with valve 2 in position 1, out through the vent. The gases were allowed to flow for approximately 2 hours in order that the system might reach a steady state. G.C. analysis of the reactants and products was obtained by placing

valve 2 to position 2 for 10 seconds, which diverted the flow into the G.C. column, and then returning it to position 1.

Experiments were mainly carried out by either (a) varying the reaction temperature and keeping the flow rate constant or (b) varying the flow rate and keeping the reaction temperature constant. The saturator temperature normally remained constant but on occasion, both flow rate and reaction temperature were fixed and the water bath temperature was varied. Whenever reaction conditions were altered, a period of fifteen minutes was allowed to elapse so that stability would return to the system. Once stability had been achieved, at least four samples were directed to the G.C. for analysis and an average conversion was then obtained.

2.5 Analytical Techniques

2.5.1 Gas Chromatography

Gas chromatography was the main analytical technique used in this investigation and was employed on all the gas-lines. Perkin-Elmer F.11 gas chromatographs equipped with flame ionisation detectors (F.I.D.) were used.

Reactant/product mixtures were allowed to expand into the G.C. sample loop for 10 seconds and this mixture was then swept, using nitrogen as carrier gas, into the G.C. column. About 3% of the total gas phase reaction mixture was removed from a static system reactor each time a sample was taken. The electrical signals obtained from the F.I.D. were then amplified and recorded

on a Servoscribe R.E. 541 potentiometric pen-recorder and a Hewlett-Packard 3373B integrator.

A 2 m column of Porapak S was used to separate the reactant alcohols from aldehyde, ketone, alkene, ether or other products, and the operating condition required for each alcohol is given in Table 2.4. G.C. traces and individual retention times are described in Chapters 4 and 5. The Porapak S column was sometimes unable to completely separate the alkene products when more than one alkene was obtained during a reaction. In such cases, therefore, duplicate experiments had to be carried out using a 2 m column of propylene carbonate on Chromosorb P which was able to separate both pentenes and methylbutenes from each other at room temperature. This column was cooled to 258 K in an ethanol-ice bath for the analysis of methylpentenes but even at such low temperatures, separation was only partially successful.

G.C. sensitivity factors, listed in Table 2.4, were calculated relative to the reactant using the equation

$$S = \frac{P/Pr}{A/Ar}$$

where P and Pr are the vapour pressures of the product and reactant respectively and A and Ar are the corresponding areas of the respective peaks on the G.C. traces.

In the static system, sensitivity factors were established by the repeated G.C. examination of known reactant/product mixtures. The low vapour pressure of the reactants used on the flow system resulted in a

Table 2.4

Operating Conditions For 2m Porapak S Column

Alcohol	Column Temp/K	Pressure carrier gas/kPa	Approximate alcohol retention time/S	Approximate alkene retention time/S	Sensitivity factor
Propan-1-ol	448	207	270	60	0.95
Propan-2-ol	423	207	180	60	1.03
2-methyl- propan-2-ol	453	207	240	73	1.20
Pentan-1-ol	488	207	520	120	1.33
2,2-dimethyl- propan-1-ol	473	207	436	120	0.87
4-methyl- pentan-2-ol	488	207	515	147	0.71
2,3-dimethyl- butan-2-ol	503	207	360	102	1.07

different technique being employed. Variation of the temperature of the saturator (Fig. 2.2) resulted in a variation of the vapour pressure of the alcohol, and thus linear graphs of integrator response versus alcohol vapour pressure could be constructed. Use was made of the gas-handling part of the flow system to establish similar graphs for the products of the reaction and comparison of the gradients of the graphs for the reactants and products allowed the calculation of the sensitivity factors. Fig. 2.6 shows typical graphs of integrator response versus vapour pressure for pentan-1-ol and pent-1-ene.

Care had to be taken when working with some alkenes e.g. pentenes and methylpentenes, as they attacked the Apiezon L grease in the taps and joints of the apparatus. This problem was diminished by storing such compounds at liquid nitrogen temperatures on all occasions when they were not in use.

2.5.2 Mass Spectrometry (Gas-Line III)

The experimental procedure employed with gas-line III was essentially the same as that with gas-line I; (see section 2.4.1.1).

The mass spectrometer was used to follow the reactions of certain alkenes over rutile in the presence of D₂O or pentan-1-ol and allowed the production of certain species to be monitored by fast scanning in the mass range 30-50 a.m.u. When such species were considered to have been produced in sufficient quantities, as revealed by the mass spectrum of the reaction mixture,

the reaction was stopped and the reactants and products frozen into a suitable container and then removed for further analysis.

The mass spectrum of the reaction mixture was recorded on a Servoscribe potentiometric recorder and the peak heights were then measured.

2.5.3 Microwave Spectroscopy

Microwave spectroscopy was used to distinguish certain labelled molecules which could not be separately identified by mass spectroscopy as they differed only by their principal moments of inertia.

The form of molecular energy utilised in microwave studies is rotational energy which, like all other forms of molecular energy, is quantized. Thus a particular molecule can exist in a variety of rotational energy levels and can move from one level to another, only by a sudden jump involving a specific amount of energy; the permitted values of the energy levels are dependent upon the principal moments of inertia and therefore the distribution of mass within the molecule. The condition for a certain molecule to be microwave active is that it has a permanent electric dipole moment and fluctuation of this dipole moment measured in a particular direction occurs on rotation of the molecule. The fluctuating electric field produced by microwave radiation is exactly similar in form to that generated by a rotating molecule and therefore interaction occurs between the two and absorption of energy takes place.

The microwave spectroscopic measurements were kindly carried out by the staff in the Chemistry Department of the University of Glasgow.

2.6 Treatment of Results

2.6.1 Static System

2.6.1.1 Gas Chromatography Data

The results obtained from experimental work on the static system, (gas-line I), were plotted as percentage composition versus time graphs and initial reaction rates were calculated from the gradients of such graphs. During the investigation with 2-methylpropan-2-ol (section 5.2), it was observed that plots of \log_{10} (percentage composition) versus time were found to be linear for the decomposition of the alcohol which suggested that this reaction followed first order kinetics as described by the equation;

$$\log_{10} [\% A] = \frac{-kt}{2.303} + 2$$

where % A is the percentage concentration of the reactant at time t and k is the rate constant for the reaction. In such cases it was therefore considered more practical to use the rate constant k to describe the kinetics of the decomposition instead of the initial absolute rate.

When excessive material loss to the surface took place, this loss was measured by a comparison of the total area under the peaks on the G.C. trace at time t with the area under the reactant peak at zero time. Allowance was made for loss of material from the gas

phase arising from the actual analysis procedure.

2.6.1.2 Poisoning Studies (see also section 2.4.1.2)

The estimation of the extent of adsorption of a species onto the surface of a sample was determined by following the procedure as described in section 2.4.1.2.

At the pressures under study, it was considered that the adsorbates would have properties which approximated to those of an ideal gas. The number of molecules in the gas phase therefore was calculated by using the ideal gas equation, i.e.

$$PV = nRT$$

where P, V and T are the pressure, volume and temperature of the adsorbate gases respectively, n is the number of moles of the gas and R is the universal gas constant. Thus, by the use of Avogadro's number, the number of adsorbate molecules in the gas phase before and after adsorption could be calculated. The difference, when divided by the surface area of the sample, allowed the adsorption to be expressed in molecules nm^{-2} which facilitated comparison with previous poisoning studies on rutile³⁷.

2.6.2 Flow System Data

The initial raw data obtained from the flow system were first converted to percentage conversion data from which reaction rates were calculated on the assumption that there was plug flow through the reactor.

Plug flow⁵⁰ is regarded as an idealised state of flow where through any cross-section normal to the direction

of the fluid motion, the mass flow rate and the fluid properties (pressure, temperature and composition) are uniform and diffusion relative to the bulk flow is negligible. It follows from these assumptions that, in each element of fluid which passes through the reactor, reaction will occur to the same degree.

The method of calculation of the performance of the reactor is explained with the help of Fig. 2.7 where the reactor is assumed to contain no solid catalyst or any sort of packing.

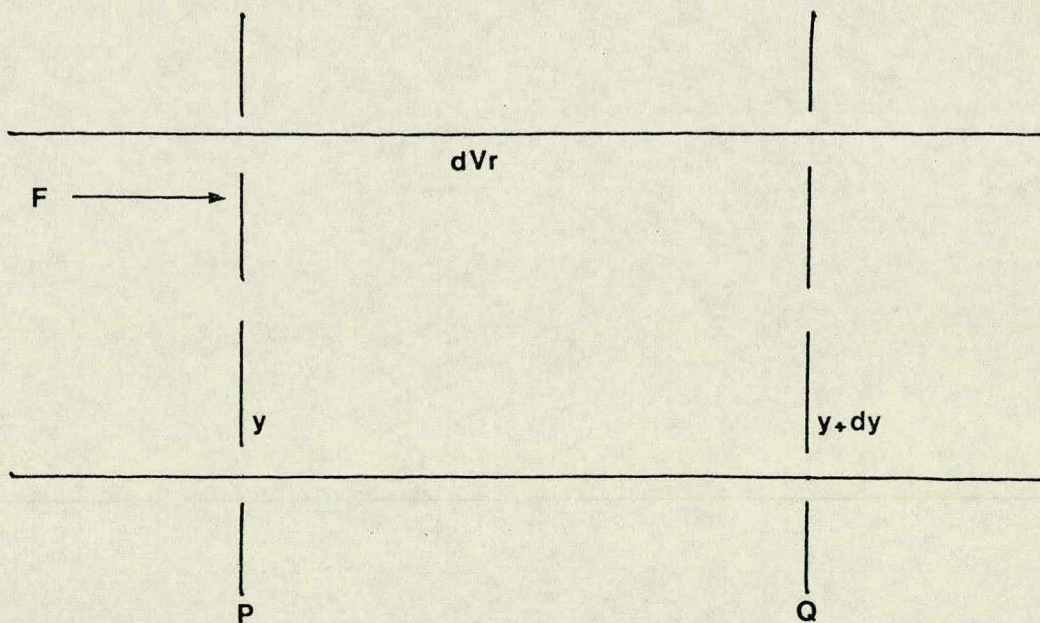


Fig. 2.7 Volume Element of a Tubular Reactor

In Fig. 2.7, P and Q are two planes which enclose between them an infinitesimal part, dV_r , of the total reactor volume V_r . F is the mass flow rate across either of these planes and y and $y+dy$ are the number of moles of a given product per unit mass of the fluid at planes P and Q respectively.

Considering this diagram and assuming plug flow, it can be shown⁵⁰ that

$$V_r = F \int_{y_i}^{y_e} \frac{dy}{r} \quad (I)$$

where V_r is the total reactor volume, y_i and y_e are the inlet and exit concentrations of the product respectively and r is the reaction rate expressed as moles of product per unit time and volume. Assuming $y_i=0$, a similar equation can be derived for application to reactors containing particles of solid catalyst i.e. -

$$W_r = F \int_0^{y_e} \frac{dy}{r'} \quad (II)$$

where r' is the reaction rate per unit mass of catalyst and W_r is the total mass of catalyst necessary to bring the exit concentration of product up to the value y_e .

Integrating gives

$$W_r = \frac{F \cdot y_e}{r'} \quad \rightarrow \quad r' = \frac{F \cdot y_e}{W_r} \quad (III)$$

and if the surface area rather than the mass of the catalyst is considered, equation (III) becomes

$$r'' = \frac{F \cdot y_e}{S} \quad (IV)$$

where r'' is the reaction rate per unit surface area of the catalyst.

In the present work, the following modified version of equation (IV) was used:-

$$\text{rate} = \frac{n \text{ alc.} X}{S} \quad (\text{V})$$

where $n \text{ alc}$ is the number of alcohol molecules flowing per unit time, X is the fractional conversion of the alcohol and S is the surface area of the catalyst. Thus $n \text{ alc.} X$ is equivalent to $F.ye$.

Equation (V) gives the rate expressed as the number of alcohol molecules converted per a particular flow rate and is all that is required when comparing reaction rates at a fixed flow rate of carrier gas. Differing rates of flow were accounted for by dividing by m the residence time (that is, the time a molecule took to pass through a catalyst bed). The term $n \text{ alc}$ was obtained from the ideal gas equations and the partial pressures of the alcohols at the saturator temperatures⁴⁹. Variation of the reaction temperature at a fixed flow rate allowed the calculation of Arrhenius parameters by the use of the equation

$$\log_{10} \text{ rate} = \log_{10} A - \frac{E_a}{2.303 RT} \quad (\text{VI})$$

where T is the temperature of the reaction and R , A and E_a correspond to the gas constant, the frequency factor and the activation energy respectively.

Alternatively, experiments were also carried out at a constant temperature whilst varying the flow rate. As the flow rate is inversely proportional to the residence time, such experiments were equivalent to % conversion versus time experiments on a static system.

2.6.3 Mass Spectrometric Data

The raw data were collected by monitoring over a mass range of interest and measuring the heights of all the peaks in the range. A computer program was used to correct for each of the following:- background in the mass spectrometer; naturally occurring isotopes; and fragmentation of the molecules inside the mass spectrometer. Graphs of the progress of exchange and isomerisation reactions were plotted from the processed information. As the mass spectrometer was only used to estimate when a satisfactory amount of product had been obtained for microwave analysis, it was not considered necessary to apply a rigorous kinetic treatment of the results.

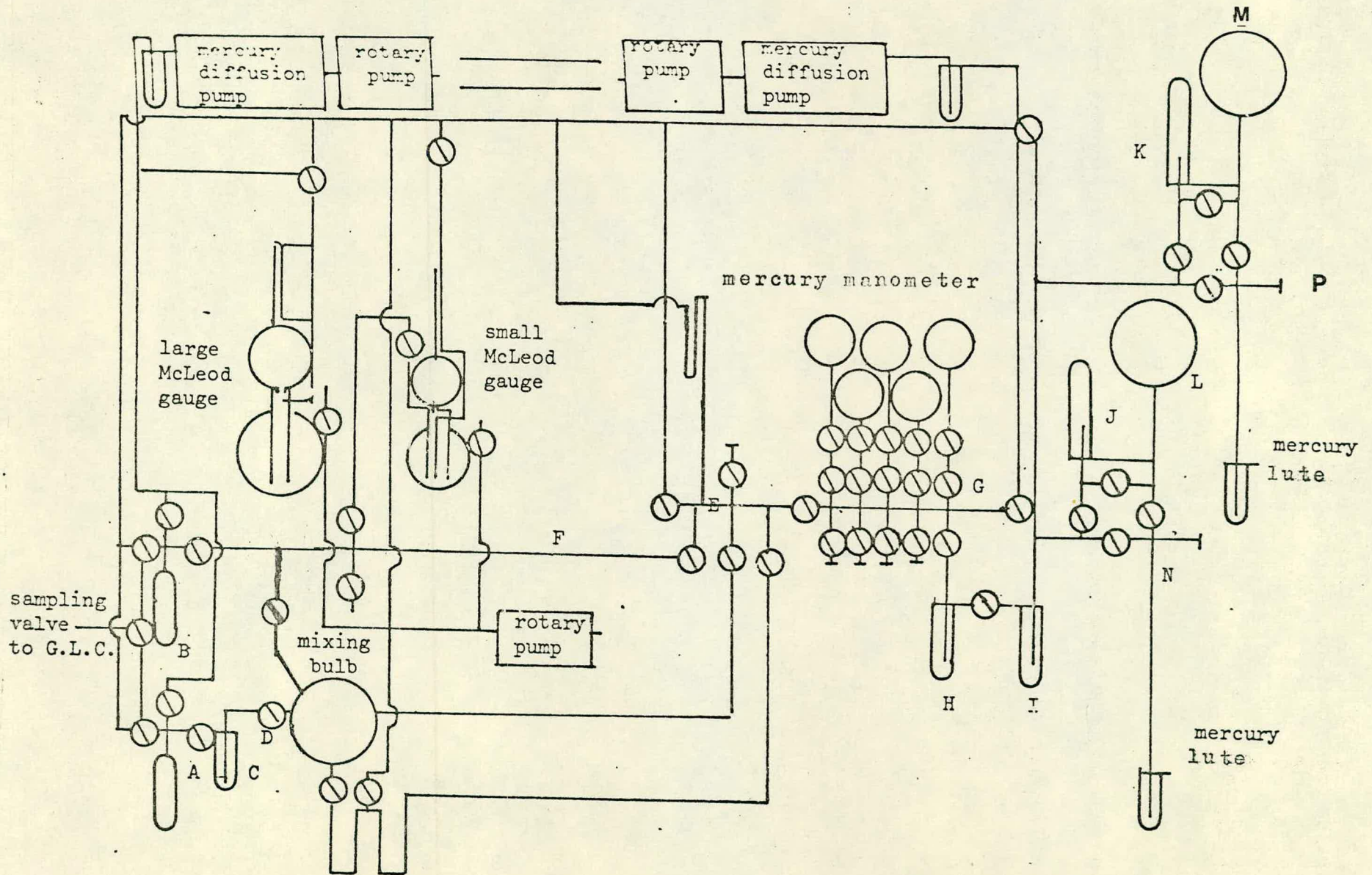


figure 2.1, gas-line I : static system linked to a gas-chromatograph

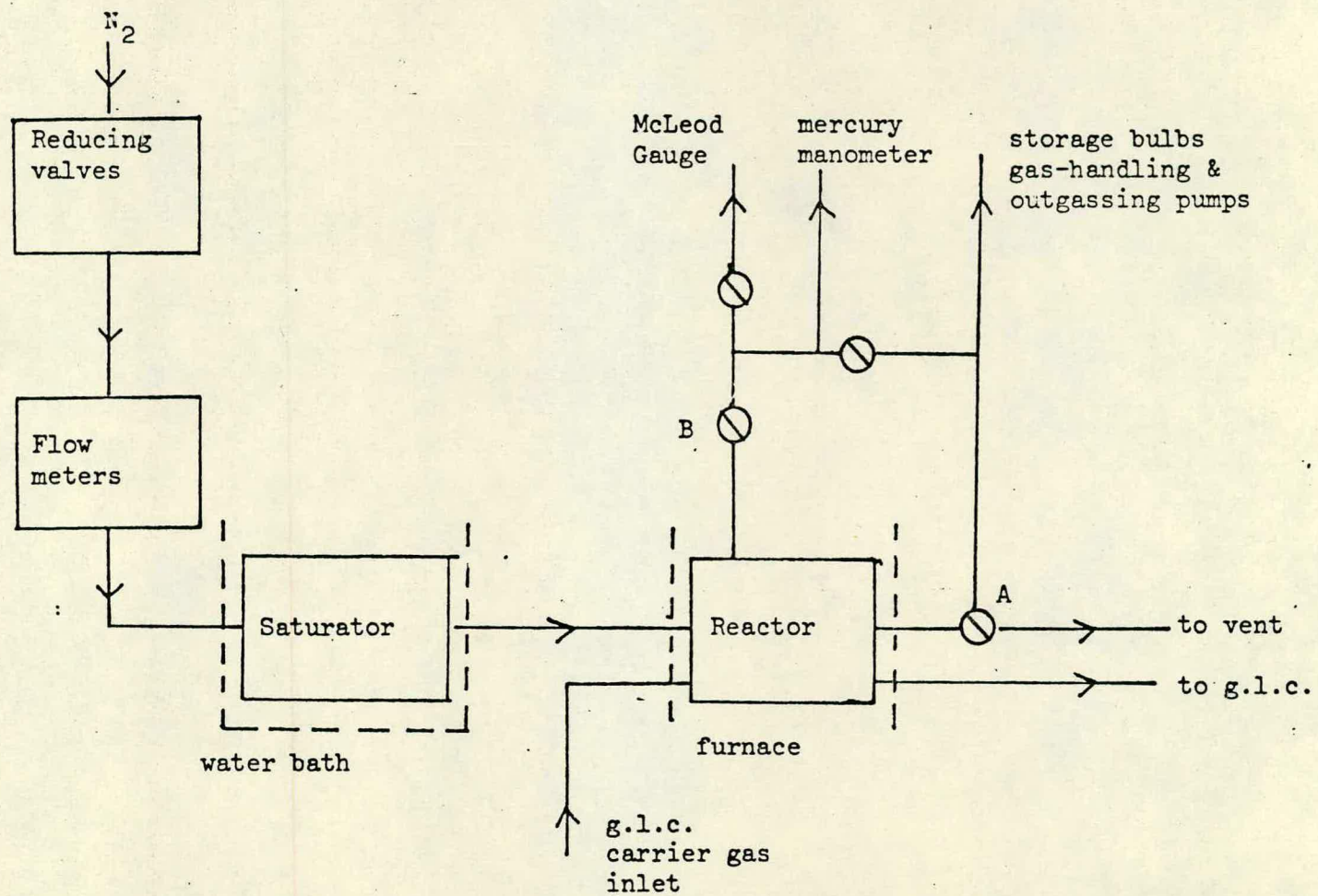
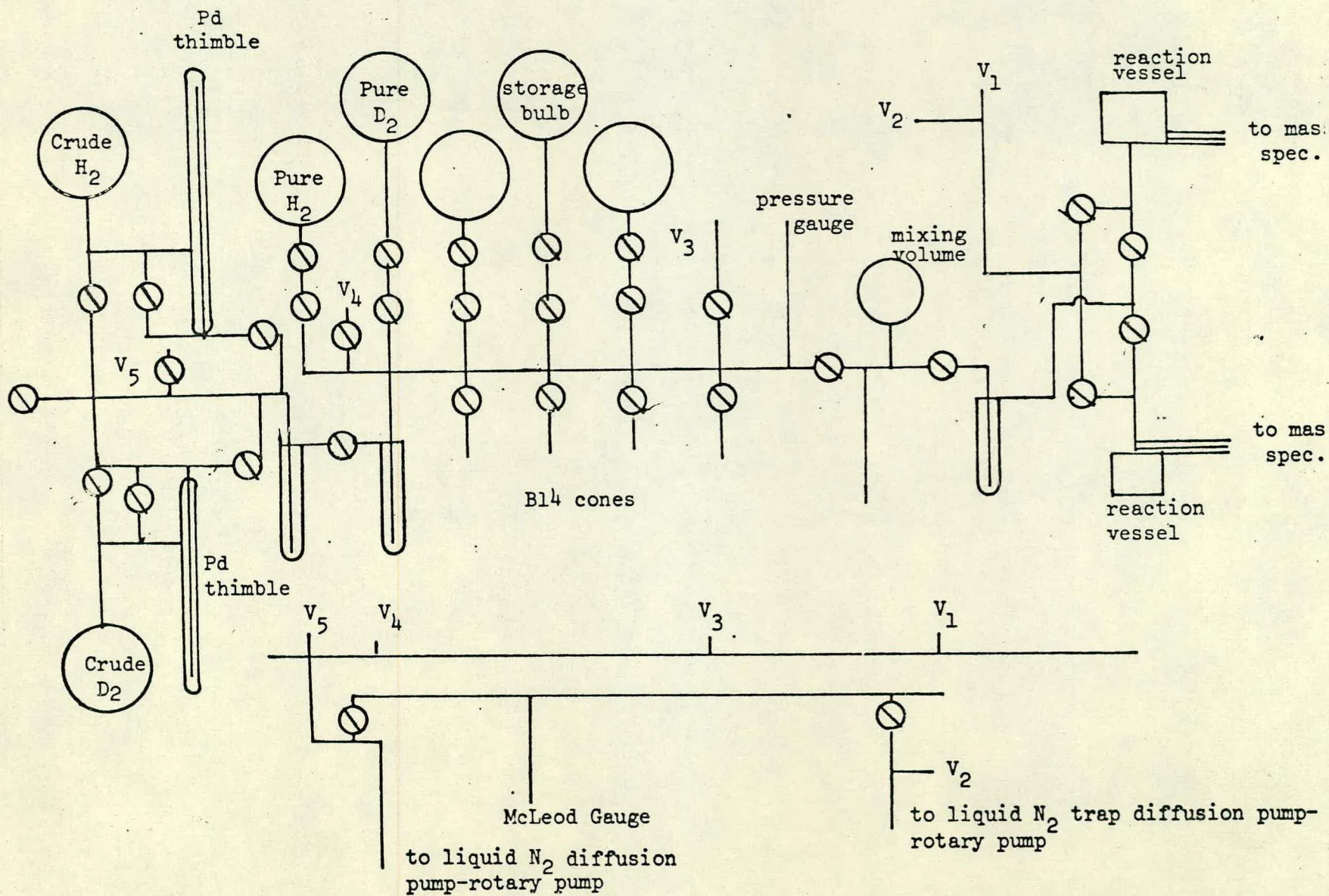


figure 2.2, gas-line II: flow system linked to a gas-chromatograph.

figure 2.3, gas-line III: static system linked to a mass-spectrometer



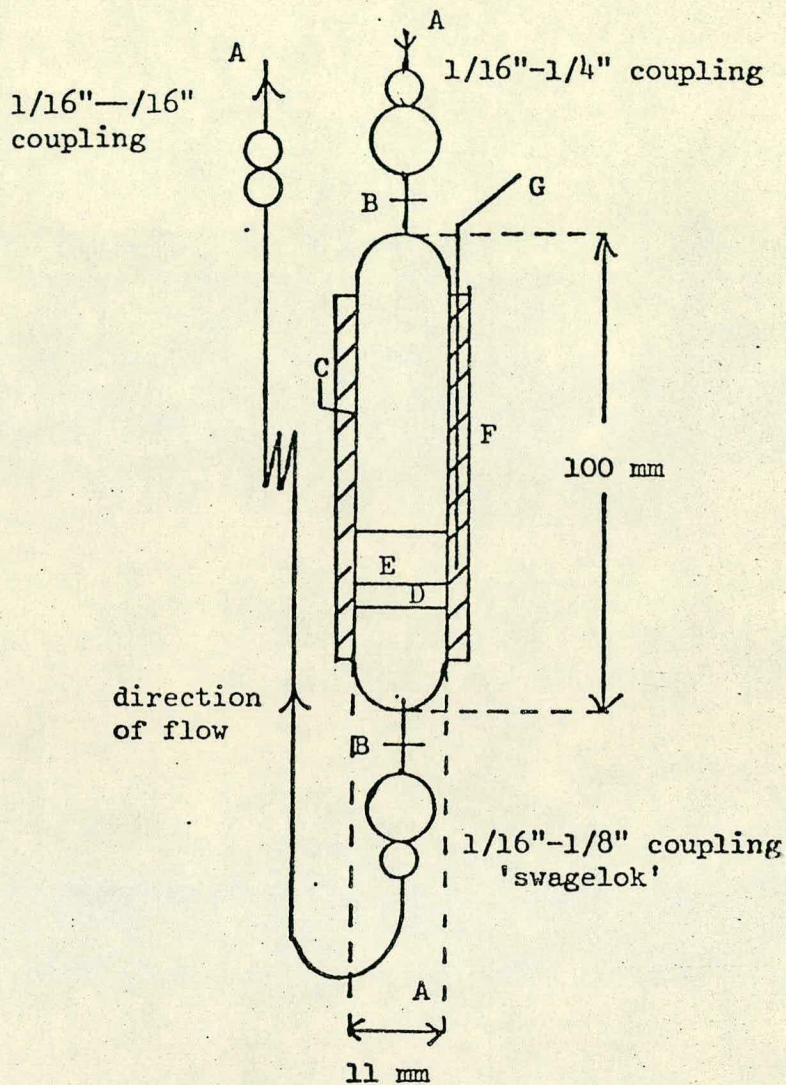
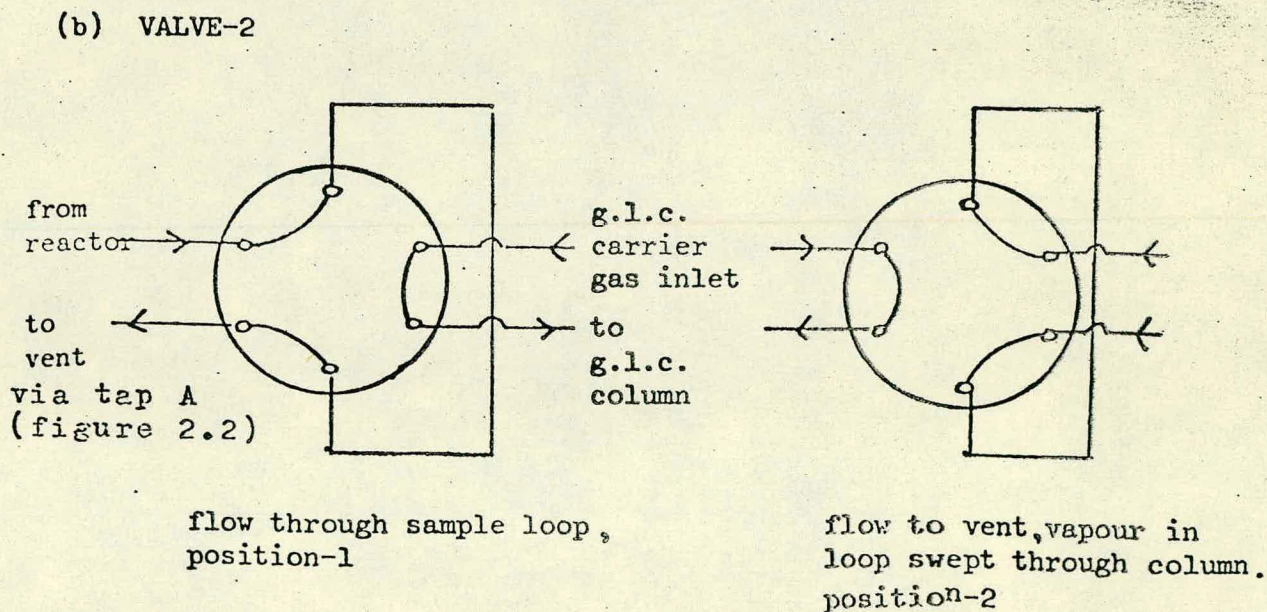
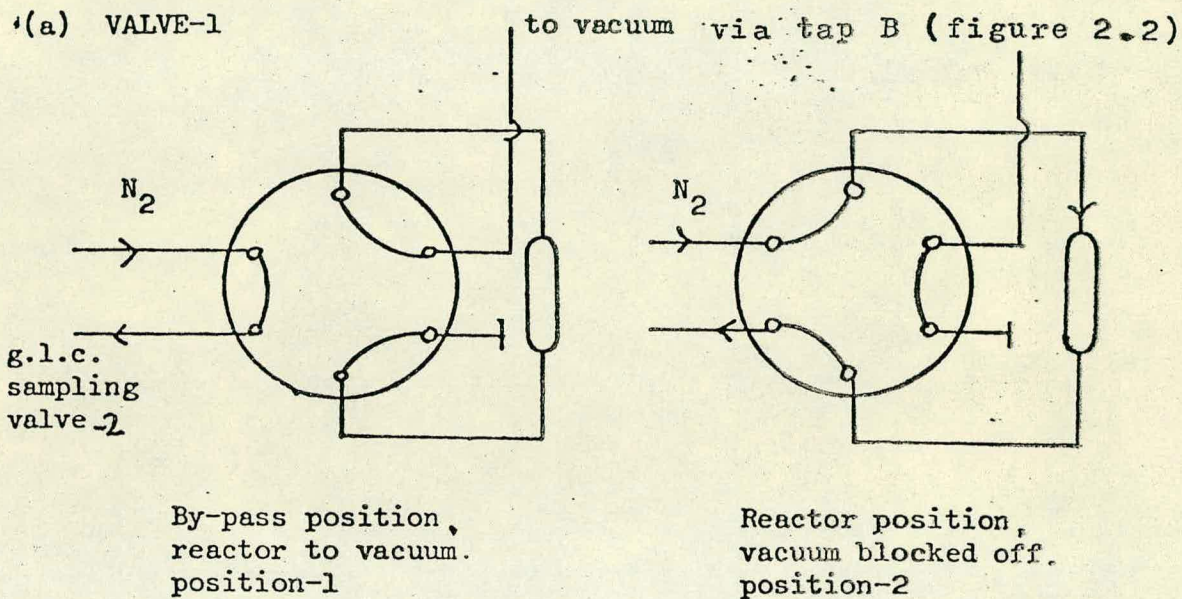


figure 2.4, reactor for gas-line II:

- A, 1/16" steel tubing
- B, glass-metal seal
- C, glass reaction vessel
- D, Pyrex-2 sintered disc
- E, catalyst bed
- F, asbestos string surrounding the glass vessel
- G, Chromel-Alumel thermocouple connected to a digital voltmeter or thermometer.

figure 2.5, sampling valve arrangement for gas-line II



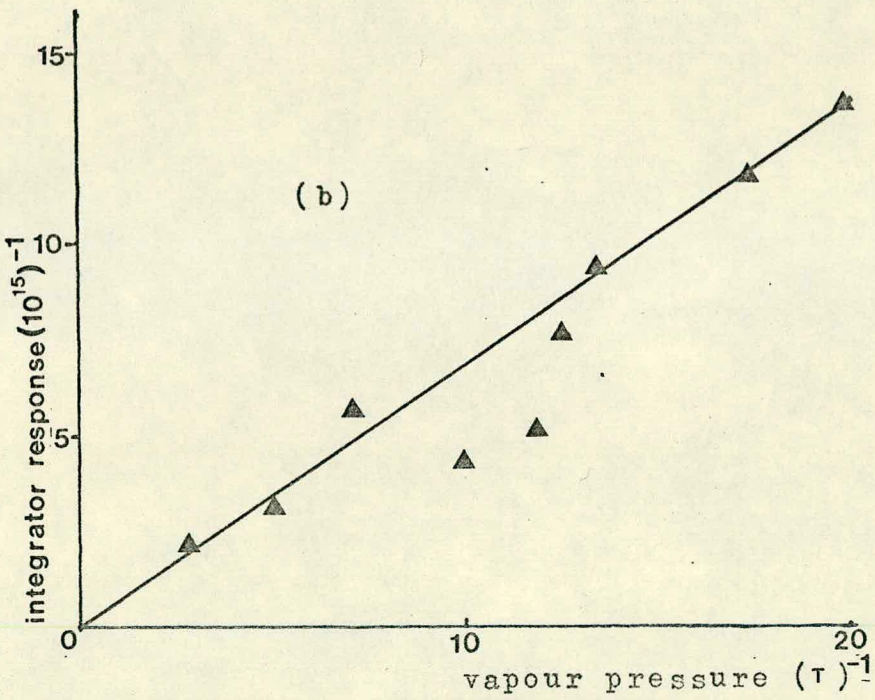
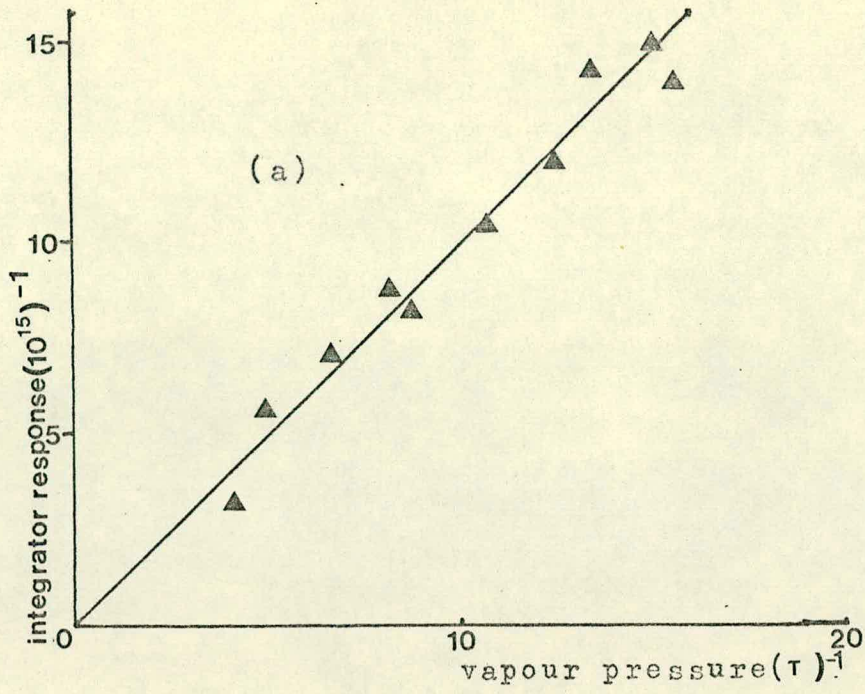


figure 2.6, calculation of G.C. sensitivity factors: integrator response v vapour pressure for (a) pentan-1-ol (b) pent-1-ene

CHAPTER 3

The Catalytic Decomposition of Alcohols

3.1 General Introduction

The decomposition of alcohols over solid surfaces is one of the most widely studied chemical reactions and the interaction of alcohols with virtually all forms of catalyst, e.g. metals, metal oxides, sulphides, zeolites, etc., has been reported somewhere in the chemical literature⁵¹.

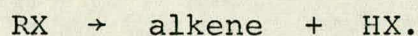
The two basic modes of alcohol decomposition over a solid catalyst are (a) dehydrogenation to an aldehyde (in the case of a primary alcohol) or a ketone (in the case of a secondary alcohol) and (b) dehydration to an alkene or an ether.

With metals, the predominant reaction is usually dehydrogenation although some alcohols which cannot undergo this process without re-arrangement of the carbon skeletal structure, e.g. tertiary alcohols, are also known to dehydrate over metals⁵². Concerning non-metals, dehydration is generally a more important reaction and countless studies have been made of this process; particularly with oxides and zeolites⁵¹. Zeolites are known to be very selective dehydration catalysts although dehydrogenation has also been reported. Studies with oxides have shown that their selectivity towards dehydration or dehydrogenation varies widely and depends upon which oxide is under study, its mode of preparation and its treatment prior to catalytic evaluation. Both forms of decomposition are important with such catalysts.

3.2 Dehydration

3.2.1 Elimination Reaction Mechanisms

The dehydration of alcohols to alkenes is a particular example of a larger group known as elimination reactions which are generally of the form



An intense study of elimination reactions by Hughes, Ingold⁵³, and other workers, which lasted over a twenty year period, resulted in the publication of numerous papers on this subject and the conclusions and basic concepts arising from this work are briefly summarised here.

When a proton and a hydroxyl group are lost from two bonded carbon atoms in the following manner,

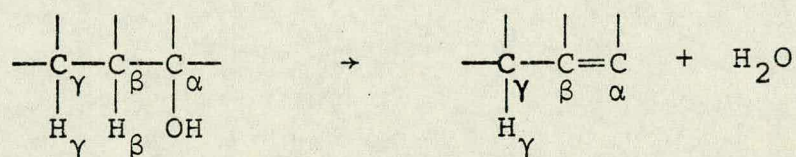


(Fig. 3.1)

the process is known as a β -elimination and there are a number of mechanisms by which this reaction can occur:-

(a) The E1 Mechanism (Elimination, Unimolecular)

This mechanism involves first the loss of a hydroxyl group to form a carbonium ion followed by the loss of a proton to form the alkene. The first step is rate-determining and consequently the reaction exhibits first order kinetics, (in substrate).

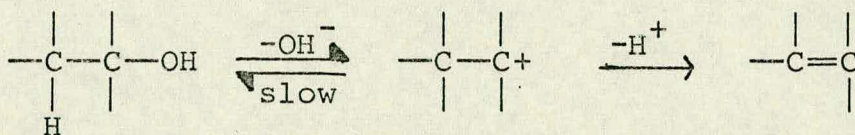


(Fig. 3.2)

This type of elimination is favoured by the formation of stable carbonium ion intermediates, e.g. tertiary carbonium ions, and has been established for a number of organic reactions.

(b) The E2 Mechanism (Elimination, Bimolecular)

In this mechanism, the hydroxyl and protonic groups depart simultaneously, the proton being abstracted by a base:-

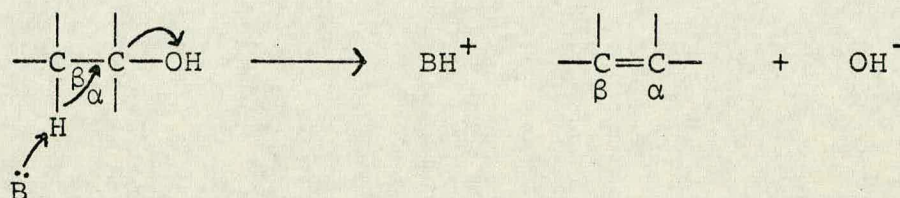


(Fig. 3.3)

This mechanism follows overall second order kinetics, first order in both substrate and base and has also been established for a number of organic reactions.

(c) The E1cB Mechanism (Elimination Unimolecular Conjugate Base)

In this mechanism the proton is first abstracted by a base to form a carbanionic intermediate and, after a finite period of time, this is followed by departure of

the hydroxyl group:-

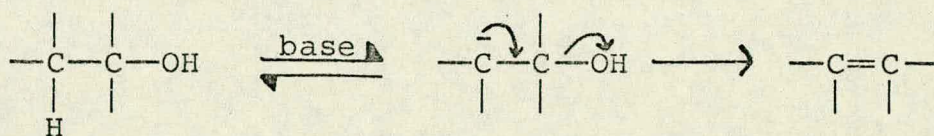


(Fig. 3.4)

This mechanism is described as E1cB as it is the conjugate base of the substrate which gives up the leaving group and as it involves both the base and the substrate in the rate determining step, it is thus a second order mechanism. The existence of such a mechanism is much less firmly established than the E1 or E2 mechanisms.

As far as the three mechanisms so far discussed are concerned, it is now generally accepted that there probably exists a range of mechanisms varying from the pure E1, through E2, to the pure E1cB.

Eliminations where γ as opposed to β hydrogens are removed and which consequently result in a double bond shift are also known. This form of elimination depends to a certain degree on the structure of the substrate and the probability of its occurrence is enhanced by anchimeric assistance, from neighbouring groups, which itself is promoted when certain groups on the reaction intermediate become bonded to the reaction centre for a finite period of time during the reaction.

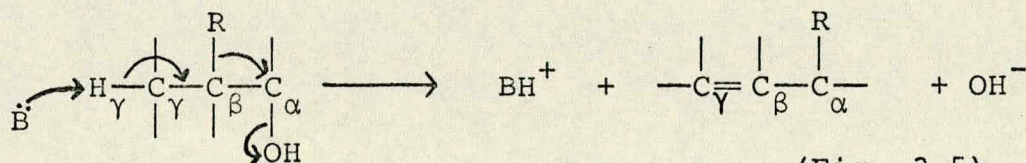
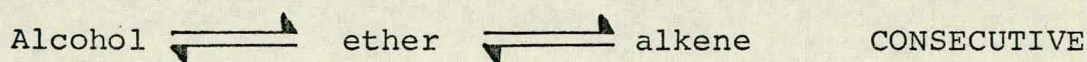


(Fig. 3.5)

3.2.2 The Catalytic Dehydration of Alcohols

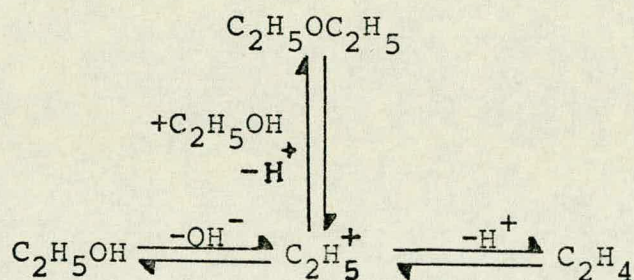
Although the ability of oxides to dehydrate alcohols was first reported in the late eighteenth century, the first systematic study of this reaction was carried out in the early twentieth century by Ipatiew⁵⁴ who concluded his work by proposing the use of this reaction as a general method for the production of alkenes. As vast quantities of alkenes subsequently become far more readily available from petroleum, the incentive to study catalytic dehydration was lost and today it is mainly of academic interest. The Lebedev synthesis of buta-1,3-diene is one of the few large scale industrial processes involving alcohols because of the importance of the product in the manufacture of synthetic rubber⁴⁵.

Metal oxides can either dehydrate alcohols to alkenes or bimolecularly to ethers and the initial studies, which were mainly concerned with the ethanol/alumina system, resulted in some controversy as to whether the two forms of dehydration occurred via consecutive, parallel or simultaneous schemes as below:-



The "simultaneous" or "parallel-consecutive" scheme is now generally accepted and has been proved by kinetic analysis and by studies with ^{14}C -labelled ethanol⁵¹.

In the 1930's and 1940's, the concept of carbonium ion intermediates became firmly established⁵⁵ and consequently Brey and Krieger⁵⁶ proposed the dehydration equilibria below which, when considering the ethanol/alumina system, has the carbonium ion C_2H_5^+ as the intermediate to both the ether and the alkene; i.e.



The contemporary postulate was that the carbonium ion resulted from oxonium ions produced by proton-donation from the surface of the catalyst to the alcohol^{55,56,57,58}.

Although ionic mechanisms are the most widely accepted, it is reported⁵¹ that other mechanisms have been proposed which include covalently bonded intermediates, radical intermediates and mechanisms involving the electronic theory of heterogeneous catalysis. There is however, very little experimental evidence to support such theories and catalytic alcohol dehydration reactions are now usually thought of in terms of OH group removal by acidic surface sites coupled with proton loss due possibly to the activity of basic surface sites; (see Fig. 3.6).

Extensive research has been carried out to try to identify the specific sites responsible for dehydration

on the surface of oxide catalysts; particularly alumina. A complete, unequivocal, understanding of the surface reactions has not yet been achieved. The dehydration of alcohols over alumina has been extensively studied by both Pines and co-workers⁵⁹ and by Knozinger and co-workers⁵¹. It is known that under the necessary conditions for catalytic dehydration to proceed, alumina is at least partially hydrated¹⁷ therefore, overall, the possible active sites on alumina for this reaction must be; oxygen ions which may act as basic sites, hydroxyl groups which are possible Brønsted acid sites, and incompletely co-ordinated aluminium ions which may act as Lewis acid centres.

A high degree of isomerisation of the primary formed alkene products is often found to accompany the dehydration of alcohols over alumina^{51,59,60} and this secondary reaction was inhibited by the presence of bases such as ammonia, pyridine and piperidine which indicated that strong Lewis acid sites were responsible for the isomerisation^{59,61,62,63}. The dehydration itself was not affected by the presence of such bases^{51,69} and this indicated that such sites do not take part as active centres in the alkene formation from alcohols. Pines and Haag^{60,65} however, found that a high purity alumina, when impregnated with sodium hydroxide, simultaneously lost its activity for butan-1-ol dehydration and for the skeletal isomerisation of cyclohexene and 3,3-dimethylbut-1-ene which indicated that similar "acid" sites were active for the two forms of reaction. This seemingly contradictory situation can be explained if it is considered that the

surface of alumina is of a heterogeneous nature and acid sites of varying strength are present. Thus reactions which require strong acid sites (i.e. alkene isomerisation reactions) are readily poisoned whereas dehydration, which is catalysed by weaker acid sites, is not. A certain level of sodium hydroxide can therefore poison both reactions. The comparative acid/base strengths of all the components in such experiments is therefore important.

The necessity of both acidic and basic sites on a catalyst surface for dehydration to take place has been postulated by Pines and co-workers^{59,61} and the participation of basic sites, i.e. the oxygen ions, in such reactions on alumina and silica/alumina has been proved by poisoning experiments with tetracyano ethylene⁶⁶.

Knozinger⁵¹ has postulated the general necessity of the presence of H-bond donors and acceptors as active sites on all dehydration catalysts although the activity of hydroxyl species on the surface of oxide catalysts is not yet fully understood. It has been reported that the presence of species derived from water can improve the activity of alumina as a dehydration catalyst⁵⁶. Aluminium trihydroxide⁵¹, however, which exposes only hydroxyl groups on the surface is completely inactive as a dehydration catalyst. Therefore it seems unlikely that acidic hydroxyl groups alone on an oxide surface are responsible for its dehydration activity. Hydroxyl groups on alumina are known to display very weak Brønsted acidity and therefore seem unlikely to be potential proton donors in a catalytic dehydration⁵⁹.

A problem arises however in that spectroscopic studies employed to establish the presence of Brønsted acid sites on a catalyst surface are not usually carried out at the elevated temperatures necessary for catalytic reactions. Also, many of the methods used to determine the surface acidity of a catalyst cannot distinguish between Brønsted and Lewis acid sites. Detailed surface catalytic mechanisms of alcohol dehydration reactions have not therefore been established.

The production of ethers from alcohols is suspected to be catalysed by Lewis acid sites as their formation is inhibited by the presence of bases⁵¹ and surface alkoxide species are suspected as intermediates⁶⁷. Poisoning studies by Jain and Pillai⁶⁸ also indicated that on alumina, dehydration to an alkene and dehydration to an ether require different types of active site. Alkene/ether selectivity is, however, considered to be of less interest than the mechanism of alkene formation as ether formation usually only occurs with simple, non-bulky alcohols.

The exhaustive study by Pines and co-workers⁵⁹ of the dehydration of alcohols over alumina should be further mentioned because this has covered the reactions of primary, secondary and tertiary aliphatic alcohols, aromatic alcohols, cyclic alcohols and diols over this catalyst. A consideration of the product distribution of the alkenes formed during the alcohol decomposition led the authors to propose that tertiary alcohols are dehydrated via free carbonium ions (i.e.

an E1 elimination; see Fig. 3.2); secondary via an E2 mechanism (see Fig. 3.3) containing an ionic or partially ionic intermediate and primary alcohols are dehydrated via a purely concerted E2 mechanism in which both acidic and basic surface sites participate. The close similarity between dehydration reactions in solution and on alumina surfaces led Pines et al⁵⁹ to conclude that such catalysts seem to act as solvating agents and therefore may be considered as "pseudo solvents" for this reaction. Knozinger⁵¹ supported this view and suggested that it may be applied to dehydrating catalysts in general.

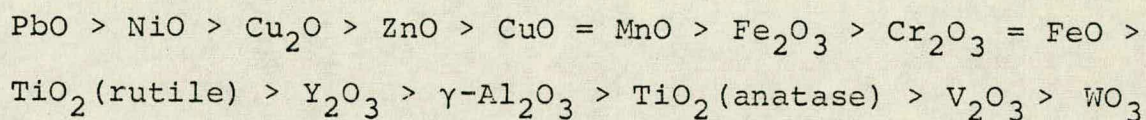
The general conclusion is that more work must be carried out to obtain absolute clarification of this surface reaction, alcohol dehydration, over alumina and that over other oxide catalysts, the mechanisms remain highly speculative. It can be said, that when considering alcohol dehydration, all or any of the available sites may be active, any mechanism may be occurring and that, at the present state of the art, nothing can be discounted to explain a particular reaction over a particular catalyst.

3.3 Dehydrogenation

The dehydrogenation of alcohols by oxides or other polar catalysts has not been subjected to such an intense study as dehydration and, as with dehydration, no general conclusions concerning the mechanism of this reaction can, as yet, be formulated.

A survey of the published work on alcohol dehydrogenation by metal oxides has been made by Krylov⁶⁹ who reviewed a

number of conclusions, based on the various theories of catalysis, for catalyst selection in alcohol decomposition. Considering the published literature on propan-2-ol decomposition, a statistical weight was assigned to a particular piece of work depending upon the standard of the work and this allowed the construction of a table of the relative catalytic activity of various binary compounds towards dehydration and dehydrogenation. An activity series for dehydrogenation taken from this table is as follows:-



To a certain extent, this table is reversed when alcohol dehydration is considered. Krylov⁶⁹ also attempted to correlate catalytic activity towards dehydrogenation with other known properties of oxide catalysts such as the spacing between the metal and oxide ions or the work function of a catalyst. A very wide scatter of the data was obtained in such analyses and the main conclusion arrived at by the author was very general; i.e. that the activity of binary catalysts towards the dehydrogenation of propan-2-ol was a function of not one but several properties of the solid.

Eucken⁷⁰ and Wicke⁷¹, in the late 1940's suggested that alcohol dehydrogenation took place on metal oxygen pairs. More recently, expressing metal oxygen pairs as acid-base pairs, Kibby and Hall⁷² have suggested that such sites on the surface of hydroxy-apatite catalysts may be active during alcohol

dehydrogenation reactions in addition to being active during dehydration reactions (see section 3.2). A correlation of the rates of dehydrogenation of the secondary alcohols propan-2-ol, butan-2-ol, pentan-2-ol, 3-methyl butan-2-ol and pentan-3-ol over such catalysts at 668 K in the co-ordinates of the Taft equation (section 3.5) suggested that a negatively charged transition state was involved in the process. The authors suggested a mechanism whereby the alcoholic proton was discharged to a basic site and the α hydrogen to the acid site; (see Fig. 3.7). In a later paper, Kibby and Hall⁷³ considered a connection between alcohol dehydrogenation and hydrogen transfer reactions. Working again with hydroxyapatite catalysts, they found that those catalysts which were most active for the dehydrogenation of butan-2-ol were also the most active for hydrogen transfer from this alcohol to pentan-3-one and from this they concluded that both reactions must occur on the same sites and involve similar intermediates which they suggested were alkoxide species. Heterolytic cleavage of the alcohol to form the alkoxide was thought to be the initial step in both processes. Subsequent transfer of the α hydrogen (as H^-) to a closely situated adsorbed ketone would complete the hydrogen transfer reaction or transfer of this hydrogen to a calcium cation to form a calcium hydride would result in the overall dehydrogenation of the alcohol. Another alkoxide species would then be created by reaction of the hydride with another alcohol molecule to produce H_2 , (see Fig. 3.8). The authors conceded

that a mechanism very similar to this had already been proposed by Noto et al⁷⁴ for the dehydrogenation of formic acid over ZnO.

Jacobs and Uytterhoeven⁷⁵, working with alkali cation - and lanthanum - exchanged X and Y zeolites found close similarities in the activity of the catalysts for both propan-2-ol dehydrogenation and H₂-D₂ exchange which led to the conclusion that the rate-determining step for both reactions was similar. The catalytic activity for both reactions was observed to be closely related to the iron impurity content of the catalyst and since the associative desorption of H₂ had been previously found⁷⁶ to determine the rate of the H₂-D₂ exchange reaction, the mechanism for the dehydrogenation of propan-2-ol was established; (see Fig. 3.9).

Nondek and Sedlacek⁷⁷ considered the dehydrogenation of alcohols on chromia to occur on active centres formed by groupings of surface Cr³⁺ and O²⁻ species because a decrease in the activity of the catalyst for this reaction was observed after the adsorption of species such as water, pyridine or acetic acid which are known to adsorb on the Cr³⁺ surface ions. Oxidation of the catalyst by heat treatment in oxygen at 623 K also resulted in a loss of catalyst activity. A kinetic isotope effect was observed after the substitution of the α hydrogen with deuterium which indicated that the splitting of the C- α H bond was part of the rate determining step and this, combined with quantum mechanical calculations, suggested an overall reaction

pathway as in Fig. 3.10. This also included alkoxide and negatively charged intermediates.

3.4 Dehydration v Dehydrogenation: Selectivity

The dehydration and dehydrogenation of alcohols over solid surfaces very commonly take place simultaneously and the selectivity for one or the other of the processes varies widely from catalyst to catalyst. This phenomenon, which has probably been known since alcohol decomposition reactions were first studied, is considered important yet it remains largely unexplained.

Sabatier⁷⁸, in an early study on catalysis in organic chemistry, thought that the selectivity was an intrinsic property of a catalyst. Later studies, however, disclosed the situation to be more complex.

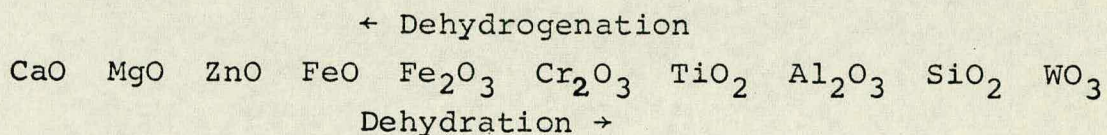
Eucken⁷⁰ and Wicke⁷¹ explained the selectivity factor

$$(s = \frac{[H_2]}{[H_2] + [H_2O]})$$

by geometrical considerations. On zinc oxide, two surface structures were proposed and that which allowed exposure of the metal ion was believed to be the site for dehydrogenation whereas that which allowed exposure of surface oxide only, acted as a dehydration site (Fig. 3.11). On the wurtzite structure of zinc oxide, equal numbers of metal and oxide ions are exposed which would imply a value of $s=0.5$. Experimentally however, it was found that this form of zinc oxide behaved like a metal by favouring almost 100% dehydrogenation. This discrepancy was explained by the suggestion that the dehydration sites were readily poisoned by water.

Hauffe⁷⁹ did not believe that the surface position of the anions and cations on a catalyst had an appreciable influence upon selectivity and proposed an explanation based on semi-conductor theory. Thus lowering the Fermi-level of a catalyst would enhance dehydrogenation and reduce dehydration activity. This suggestion was in contrast to that of Vol'kenshtein⁸⁰ who believed that the relative variation of the Fermi-levels would produce the opposite effects.

A different explanation was offered by Szabo and co-workers⁸¹ who suggested that the character of the metal oxide bond influenced a catalyst's selectivity towards alcohol dehydration or dehydrogenation. An increase in the ionic character of the bond would increase the dehydrogenation properties and conversely, the dehydration properties increase with an increase in covalent bond character. Thus the following sequence of catalysts was presented:-



Knozinger⁵¹ has pointed out that the situation is more complex as zinc oxide, ferric oxide and chromia all exhibit the same ionic character as calculated by means of Pauling's formula⁸². Zinc oxide is, however, mainly a dehydrogenation catalyst whereas ferric oxide and chromia mainly catalyse dehydration.

Niiyama and Echigoya⁸³ tackled the problem of selectivity by using alkaline earth silicates which are acid-base bifunctional catalysts. CaO-SiO₂ was

observed to catalyse both the dehydration and the dehydrogenation of butan-1-ol and poisoning studies revealed that pyridine retarded dehydration and activated dehydrogenation whereas phenol had no effect on dehydration but retarded dehydrogenation. Thus the authors concluded that dehydration took place on acidic sites while dehydrogenation took place on basic sites. The validity of this conclusion was strengthened by applying the Taft equation (see section 3.5) to their results which indicated that positively charged intermediates were formed during dehydration and negatively charged intermediates were formed during dehydrogenation. Simple poisoning experiments such as this do not usually provide such simple conclusions about catalyst selectivity and often, all that can be inferred from such experiments is that the sites responsible for dehydration are not the same as those responsible for dehydrogenation^{72,73}.

It has been known for some time that the mode of preparation of a catalyst can greatly influence the catalyst's selectivity properties. Schwab and Schwab-Agallidis⁸⁴ examined the decomposition of ethanol over a number of oxides (including rutile) and found that those modes of preparation which increase crystal size and reduce the surface area, such as excessive heat treatment, tend to change the selectivity of a catalyst in favour of dehydrogenation. Thus the authors concluded that dehydrogenation takes place mainly on the flat surfaces of catalyst particles and that dehydration occurs in the interior of pores, cracks or channels of molecular

dimensions within the catalyst. The authors proposed a simple mechanism for the two processes based on Balandin's^{51,85} duplet hypothesis for catalytic reactions, (i.e. dehydrogenation and dehydration are thought to proceed on an active surface unit consisting of two neighbouring surface atoms, i.e. a duplet. The reaction for which the duplet has the proper spacing will be favoured. see Fig. 3.12).

The influence of the preparative mode and the pretreatment on the selectivity properties of a catalyst have been studied more recently by Davis and co-workers and the oxides chosen for study have included thoria (ThO_2)⁸⁶, alumina (Al_2O_3)⁸⁷, yttria (Y_2O_3)⁸⁸, india (In_2O_3)⁸⁹ and others⁹⁰. No conclusions concerning oxides in general were possible from this work as experiments showed that the alteration of selectivity properties with pretreatment in oxygen or hydrogen varied from oxide to oxide. Alumina⁸⁷, which is usually thought of as a dehydration catalyst, was found to display considerable dehydrogenating activity if it was pretreated with oxygen at 873 K and alumina⁸⁷ and thoria⁸⁶ were both found to increase their selectivity towards dehydration when oxygen pretreatment was replaced by hydrogen pretreatment. This the authors at first attributed to an increased exposure of the cation after pretreatment of the oxide in hydrogen and vice versa after pretreatment with oxygen; (the authors believing that the cation provided the dehydration site). Later studies⁹⁰ however revealed that gallia (Ga_2O_3) remained a very selective dehydration catalyst even

after O_2 pretreatment and many oxides after O_2 or H_2 pretreatment acted in an opposite manner to alumina or thoria e.g. ZnO , La_2O_3 and ZrO_2 . Zirconium oxide was particularly complex in that catalysts prepared by various procedures varied widely in both their selectivity properties and in the way they responded to O_2 or H_2 pretreatment. A consideration of only one group in the periodic table did not clarify the situation as alumina, gallia and india all varied widely in their properties and the increase in cation size on going down this group did not result in an increase in selectivity towards dehydration which upset their hypothesis. Some catalysts varied their selectivity properties with the length of time which they were exposed to the alcohol; notably Y_2O_3 and In_2O_3 .

Thus the situation is very complex and the influence of impurities on the selectivity properties of a catalyst is probably very important. Indeed the problem of dehydration-dehydrogenation selectivity may prove to be a problem of reproducible catalyst preparations.

To summarise this section, it is difficult to definitely ascribe a geometric or electronic effect of the catalyst on the dehydration and dehydrogenation reactions of alcohols, although work by Szabo⁸¹ on covalent versus ionic bonding in the catalyst could be ascribed to a type of electronic effect and work by Schwab⁸⁴ on crystallite size effects could indicate a geometric property. It is interesting to note that

treatment in oxygen or hydrogen will give varying effects and the formation of non-stoichiometric oxides may be important, particularly when selectivity varies with time.

3.5 Linear Free Energy Relationship (L.F.E.R.)

Studies of the relationship between substrate structure and reactivity are known to provide useful information on reaction pathways and this approach has often been used in homogeneous organic chemistry and, to a lesser degree, in heterogeneous catalysis.

The early work in this field included that of Hammett⁹¹ who found that relative rates or equilibrium constants of meta and para-substituted benzene derivatives can be correlated by the equation:

$$\log K \text{ relative} = \rho \sigma$$

which subsequently became known as the Hammett equation. ρ is a proportionality factor characterising the reaction and the catalyst if the reaction is catalytic and σ is a constant characterising a substituent in the meta or para positions. The values of the σ constants were derived from dissociation constants of substituted benzoic acids for which the value of ρ was taken as unity. Taft⁹² later proposed a similar relationship correlating the reactivity of aliphatic compounds:-

$$\log K \text{ relative} = \rho^* \sigma^*$$

and this became known as the Taft equation. The reference compounds were an unsubstituted benzene

derivative in the case of the Hammett equation (i.e. $\sigma_H=0$) and a methylated derivative in the case of the Taft equation (i.e. $\sigma^*CH_3=0$).

The term "linear free energy relationship (L.F.E.R.)" arose because it is known from thermodynamics that the equilibrium constant of a chemical reaction is related to the Gibbs Free Energy change by the equation:

$$\Delta G = -RT \ln K$$

and from transition state theory a rate constant is related to the activation free energy by the equation

$$\Delta G^\ddagger = \text{const} -RT \ln k$$

Thus if the rate or equilibrium constants of a given reaction are related to those of the standard reaction by a Hammett or Taft-type equation, the free energies of the two processes are being related by a linear relationship.

Other, more complicated, versions of the above equations have been derived, of which several reviews have been written^{93,94,95}, and it has been shown that such equations can also be used to describe the effects of structure on the spectral properties of organic molecules and the effects of media on reaction kinetics and equilibria.

The applicability of linear free energy relationships to heterogeneous catalysis has been reviewed by Kraus⁹⁶ who pointed out that the presence of a solid catalyst introduces certain limitations to the use of the simple two parameter Hammett and Taft equations as they are only valid if the solid catalyst introduces no

independent type of interaction between the substrate and the catalyst and it behaves as a constant factor with respect to all reacting compounds of a series. This condition is generally assumed in catalytic studies but some authors⁹⁷ have taken into account the fact that the interaction between a catalyst and a substrate is mutual and that differing substrates may, after covering a part of the surface, modify the overall activity of a solid catalyst to a differing degree. The steric arrangement of a reacting molecule on a solid catalyst has been found⁹⁸ to have a more pronounced influence on the reaction than that which occurs during the homogeneous reactions for which the Taft and Hammett equations were originally designed. Thus good correlation analysis may not be obtained when dealing with heterogeneous catalytic reactions involving bulky substituents. Considering further the fundamental differences between heterogeneous and homogeneous reactions, Kraus⁹⁶ also remarked that even the simplest reaction over a solid surface consists of a series of diffusional, adsorption, surface reaction and desorption steps and if the rate was determined by say diffusional or desorption steps, surface structure would have relatively little relevance to the overall reaction rate and correlation analysis would become meaningless. Also, since the σ and σ^* constants were determined by experimentation at ambient temperatures, the use of such constants at the high temperatures associated with many catalytic reactions may not be entirely valid. This point was

recently referred to by Carrizosa and Munuera⁹⁹ who studied alcohol decomposition over anatase.

In catalytic studies, correlation analysis is often used to obtain a value of ρ^* for a particular catalyst and from its sign and magnitude it is possible to draw conclusions about the reaction mechanism. The accepted explanation of a negative value for ρ^* is that a positively charged transition state is formed during the reaction⁹⁶. This, of course, implies a carbonium ion type mechanism, i.e. in the range E1→E2, for elimination reactions and a more negative value means a mechanism closer to E1 with a more polar transition state being formed. Kochloefl and co-workers¹⁰⁰, for example, found the Taft equation to be valid for the dehydration of a number of alcohols on four different catalysts (SiO_2 ; TiO_2 ; ZrO_2 , Al_2O_3) and the values of ρ^* associated with each catalyst were found to decrease in the order $\text{Al}_2\text{O}_3 > \text{ZrO}_2 > \text{TiO}_2 > \text{SiO}_2$ (see Fig. 3.13). This suggested a change in the mechanism from an E2 to an E1 elimination across the series of catalysts.

Carrizosa and Munuera⁹⁹ have recently criticised the use of correlation analysis in catalytic studies. Studies of the dehydration of alcohols over anatase revealed that although the Taft equation held at 473 K, at 573 K no correlation was observed (see Fig. 3.14). Also, the value of ρ^* at 473 K was found to be -10.7 which suggested a more highly polar mechanism than was indicated by other experimental data. They also quoted the work of Criado¹⁰¹ who has shown that the value of ρ^* depends on the temperature and therefore, changes in the

ρ^* value can be expected without changes in the mechanism. Therefore Carrizosa and Munuera⁹⁹ concluded that much correlation analysis in heterogeneous catalysis may be merely fortuitous and mechanistic conclusions from such studies may be of doubtful value.

3.6 The Decomposition of Alcohols over Titanium Dioxide

The early work^{78,102} on the decomposition of alcohols over TiO_2 was mainly confined to studies with ethanol in which the TiO_2 was found to catalyse both dehydration and dehydrogenation at temperatures above 593K. The selectivity towards dehydrogenation increased at higher reaction temperatures as did the overall reaction rate and the authors of this early work also reported that hydrogen and water hindered dehydrogenation and dehydration respectively. Rudisill and Engelder¹⁰³ later found that the properties of TiO_2 catalysts depended on their mode of preparation. Overall, those catalysts made by re-precipitation from a sulphate solution were slightly more active than those made from a chloride solution. Also the optimum temperature for drying the catalyst preparations was 623K with higher drying temperatures decreasing the activity of the catalyst. This early work was also used to support the idea that the surface area, as opposed to the mass of a catalyst was an important factor in catalytic activity.

Kemball et al¹⁰⁴ examined the desorption and decomposition of ethanol, propan-2-ol, 2-methylpropan-2-ol and butan-1-ol over a number of oxides, which included

anatase and rutile, at temperatures below those normally required for catalytic reactions to take place and found that the two forms of titania showed relatively little tendency to decompose the alcohols. An interesting result from these studies was that the total oxygen content of the products from the decomposition of butan-1-ol over anatase was greater than expected which suggested that oxygen from the catalyst was combining with the reacting material. Thermodynamic calculation, however, did not support this. It was also found that propan-2-ol could displace ethanol from anatase at a faster rate than that which occurs with the desorption of ethanol alone.

The electronic theory of catalysis whereby it is believed that the collective electronic properties of solids are related to their catalytic activity was invoked by Keier et al¹⁰⁵ to explain the decomposition of propan-2-ol over pure and doped samples of TiO_2 . The introduction of WO_3 into samples of rutile shifted the activity and selectivity of the observed reaction towards dehydration and the introduction of Fe_2O_3 into the TiO_2 lattice decreased both the activity and the selectivity for dehydration. Samples doped with equimolar quantities of Fe_2O_3 and WO_3 acted in a similar manner to pure rutile. These observations, together with measurements of semi-conductivity, changes in work function and the influence of applied electrostatic fields were taken as evidence for electron transfer mechanisms for both dehydration and dehydrogenation; e.g. for dehydration.

Stage 1 Rapid chemisorption of alcohol



Stage 2 Addition of an electron to the adsorbed intermediate complex and desorption of the reaction products



The effect of doping rutile with Cr_2O_3 , Fe_2O_3 , NiO , Nb_2O_5 and WO_3 has more recently been examined by Gentry, Rudham and Wagstaff¹⁰⁶ and it was observed that the selectivity for dehydration was increased by dopant ions of valency less than four. These findings therefore suggested that the electronic properties of rutile are important in determining the catalytic properties. Exposure of the rutile samples to both pyridine and/or tetracyanoethylene however, resulted in the poisoning of the dehydration reaction and since pyridine and tetracyanoethylene are highly unlikely to be adsorbed by electron transfer in the same direction, this convinced the authors that the dehydration reaction proceeded via an acid-base mechanism (see section 3.2) rather than via an electron transfer mechanism. Thus it was concluded that the effects of dopants were simply due to an alteration of the geometry of the rutile surface; the metal-oxygen octahedra of the dopants influencing the orientation of the surface titanium-oxygen octahedra as well as providing different surface metal-oxygen octahedra themselves. Dehydrogenation was affected by the presence of dopants and was promoted by adsorbed tetracyanoethylene. These effects could not be correlated with the activity of the

pure dopants for this reaction or with electronic or geometric factors. Thus the conclusion drawn was solely that the "active centres" responsible for ~~dehydrogenation~~ were not those responsible for dehydration.

Carrizosa and Munuera^{99,107} have recently studied the interaction of alcohols with anatase by examination of adsorption isotherms, infra-red and temperature-programmed-decomposition studies and by the use of a flow system. The adsorption studies with ethanol, propan-2-ol and 2-methylpropan-2-ol revealed that adsorption could take place in a reversible and in an irreversible fashion and the latter mode, on heating, was responsible for the decomposition of the alcohols to alkenes and water. The alcohols adsorbed in such a way as to complete the co-ordination of the Ti^{4+} ions on the surface. Infra-red studies revealed that on anatase water is easily displaced by alcohol molecules in the gas phase and water itself readily desorbs from the surface at 543 K. Also, temperature-programmed-decomposition (T.P.D.) experiments showed that when ethanol and propan-2-ol decompose in the range 573-627 K the water formed immediately desorbs from the surface. Thus during the decomposition of ethanol and propan-2-ol, the desorption of water was not thought to be the rate controlling step. The T.P.D. experiments revealed that isobutene desorbs at 453 K from a surface previously treated with 2-methylpropan-2-ol and the water formed still remains until temperatures \approx 543 K were attained. The authors tended to believe, however, that in this case also, the nucleophilicity of the 2-methylpropan-2-ol molecule weakens the strength of the bond of the adsorbed water

making the displacement easier than the decomposition of the alcohol itself. Thus it was thought that with all alcohols, the overall kinetics of the reaction were controlled by the surface reaction step (see Fig. 3.15). Concerted E2 eliminations were preferred, as opposed to E1 or E1cB, as temperature-programmed-decomposition of butan-1-ol, butan-2-ol and 2-methylbutan-2-ol revealed a product distribution of alkenes far removed from thermodynamic equilibrium which would be attained if an E1 mechanism via carbonium ions was acting. The decomposition of butan-2-ol resulted in the formation predominantly of but-1-ene and, at higher temperatures, cis-but-2-ene (see Fig. 3.16). But-1-ene formation was explained in terms of cis-elimination after the initial adsorption of the alcohol with the CH₃ group oriented with preference towards the most exposed O²⁻ ions while the bulky CH₃-CH₂ group was directed away from the surface (see Fig. 3.16(a)). Cis-but-2-ene formation occurred following rotation of (a) through 180° around the C-O bond of the alcohol and abstraction of H_β from the methylenic group in an anti-periplanar position relative to the OH group (see Fig. 3.16(b)).

Temperature-programmed-decomposition of methanol over anatase and rutile was also studied by Munuera and co-workers⁷ and the products of this reaction were dimethylether, ethane, and, to a lesser extent, methane, CO and CO₂. Alkanes were formed, it was thought, via an oligomerisation of Ti-CH₃ species formed on the surface. The decomposition of methanol over anatase or rutile in

a flow system resulted in the formation of similar products although these experiments were hindered by surface carbonization which poisoned the reactions. Fig. 3.17 illustrates the proposed mechanism for ether formation on anatase which includes removal of lattice oxygen during the desorption of water from the surface, followed by attack of the remaining alkyl group by a nucleophilic oxygen on a neighbouring alcoholate species. It is surprising to note that Munuera and co-workers^{7,99,107} never mentioned the possible decomposition of the alcohols into aldehydes or ketones, particularly since it is known that such species can condense to form compounds of higher molecular weight.

In order to minimise the influence of methods of catalyst preparation and pretreatment on experimental data, Halliday⁴⁵ has studied the decomposition of a number of aliphatic alcohols over one preparation of rutile catalyst and this preliminary examination formed the basis of the work presented in this thesis. A summary of this work is described in Table 3.1 and it is seen that primary, secondary and tertiary alcohols were used in this study varying from ethanol to the more complex dimethylbutanols.

Although the work of Halliday⁴⁵ is described in more detail elsewhere in this thesis, it is appropriate to note the main features of this work at this point. The predominant reaction of alcohols over rutile was found to be the decomposition by loss of water to form the corresponding alkene(s). The dehydrogenation of alcohols to the corresponding aldehyde or ketone also occurred but to a much lesser extent. The application of the Taft

Table 3.1 The Decomposition Of Alcohols Over Rutile After Halliday⁴⁵

No.	Alcohol	Flow (F) or Static (S) System	Reaction Temperature Range/K	Products
1	Ethanol	S	568-613	Ethene, Diethyl ether, Ethanal, Butenes
2	Propan-1-ol	F,S	578-615	Propene, Propanal, n-Propyl ether, Hexene, Benzene
3	Propan-2-ol	F,S	524-553	Propene, Acetone
4	Butan-1-ol	F	538-576	Butenes, Butane, Butanal
5	Butan-2-ol	F,S	438-526	Butenes, Methyl ethyl ketone
6	2-Methylpropan-1-ol	F,S	540-596	Butenes, 2-Methylpropane, Methylcyclopropane
7	2-Methylpropan-2-ol	F,S	403-423	2-Methylpropene
8	Pentan-2-ol	F	476-506	Pentenes, Pentan-2-one
9	2-Methylbutan-2-ol	F	419-438	2-Methylbut-1-ene, 2-Methylbut-2-ene
10	2,3-Dimethylbutan-2-ol	F	398-419	2,3-Dimethylbut-1-ene, 2,3-Dimethylbut-2-ene
11	3,3-Dimethylbutan-2-ol	F	498-423	2,3- and 3,3-Dimethylbut-1-ene, 2,3-Dimethylbut-2-ene, Traces Ketone

equation (see section 3.5) to the results revealed the existence of a linear free energy relationship which indicated that a transition state with a positive (or at least partially positive) charge was formed during the dehydration reaction. Ti-O acid/base pairs were considered to be the active sites involved with the dehydration reaction and the studies with dimethylbutanols were particularly interesting in that Arrhenius parameters and product distributions suggested that γ -eliminations are preferred when this form of elimination is possible. The decompositions of ethanol and propan-1-ol were unique in that coupling reactions also took place with the formation of hydrocarbons of higher carbon number than the original alcohol and it was believed that the initial dehydrogenation products played an important role in this reaction.

3.7 The Purpose of the Present Investigation

The survey in this chapter and chapter 1 reveals that, in comparison to other catalysts such as alumina, relatively little has been written about rutile as a catalyst; particularly when alcohol decomposition is the reaction under study. This, as has often been stated, is probably because rutile is relatively inactive as a catalyst in areas of chemistry which are of industrial importance. However, as it does display some activity for a large number of reactions, results obtained with rutile do provide information on the catalytic activity of oxides in general.

The work of Halliday⁴⁵ has shown that a study of the decomposition of higher alcohols over rutile can provide useful information on the possible reaction

mechanisms and led to the postulate that the sites responsible for dehydration were $\text{Ti}^{4+}\text{O}^{2-}$ acid/base pairs. A continuation of this study, using the same preparation of catalyst, with other specially selected substituted alcohols would therefore confirm previous postulates and provide more information on reactions of this type. It was also considered important to find out the reproducibility of the results obtained with this preparation of rutile.

Brookes³⁷, again using the same preparation of rutile, had previously proposed from poisoning studies that the Ti^{4+} ion, acting as a Lewis acid, was the active site in double bond migration reactions. Alcohol dehydration, although also an acid catalysed reaction, is considerably more complex therefore it was considered desirable to compare directly, by carrying out similar poisoning studies, the catalytic decomposition of alcohols with the isomerisation of alkenes. It was also considered of interest to find out how such treatment of rutile would affect the other alcohol decomposition reactions such as dehydrogenation and coupling of which little information has been gathered in terms of active sites and reaction mechanisms.

The work on rutile presented in this thesis therefore, falls into two main sections - the study of the decomposition of substituted alcohols on a flow system and an examination, on a static system, of the effect of certain molecules on the reactivity of the catalyst

towards the decomposition of propan-1-ol and 2-methylpropan-2-ol. The results obtained from the main body of the work necessitated supporting experiments with labelled molecules which is described in a separate section and the final part covers how a variation of the method of oxygen pretreatment alters the dehydration/dehydrogenation properties of the catalyst.

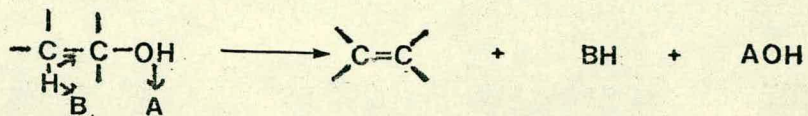


figure 3.6, acid/base dehydration of alcohol over solid catalyst.

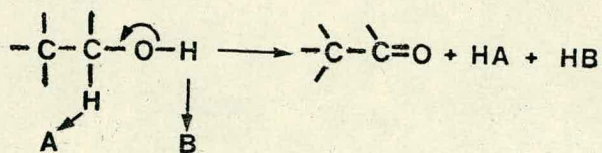
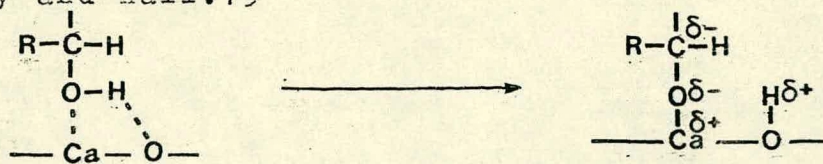
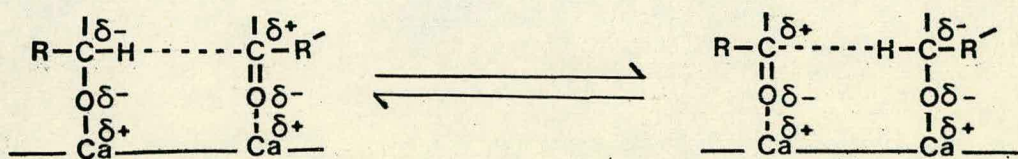


figure 3.7, dehydrogenation of alcohols over hydroxyapatite catalysts after Kibby and Hall.⁷²

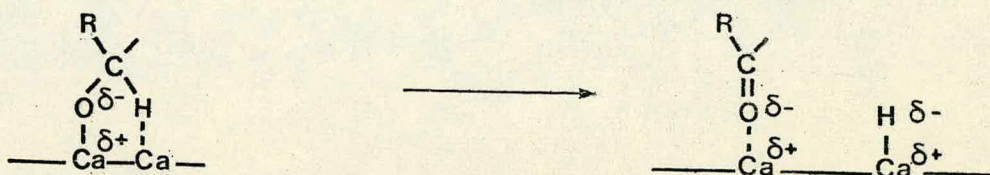
figure 3.8, mechanism of alcohol dehydrogenation and hydrogen transfer over hydroxyapatite catalysts after Kibby and Hall.73



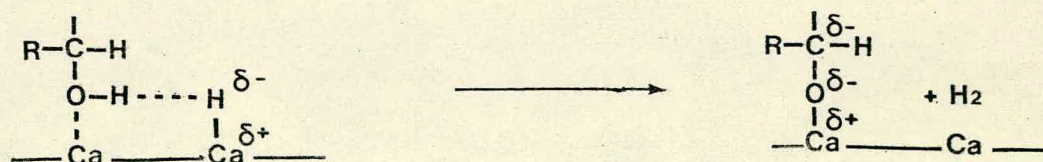
initial step: formation of alkoxide species.



hydrogen transfer to an adsorbed ketone.



formation of both calcium hydride species and ketone product.



regeneration of alkoxide and formation of hydrogen.

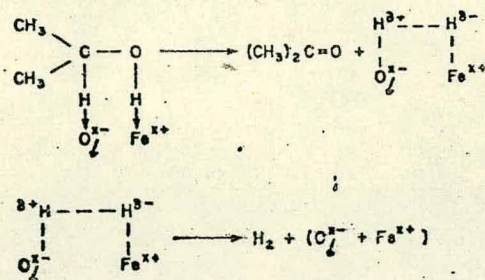


figure 3.9, mechanism of alcohol dehydrogenation over lattice oxygen and iron impurities on alkali cation-exchanged X and Y zeolites after Jacobs and Uytterhoeven.⁷⁵

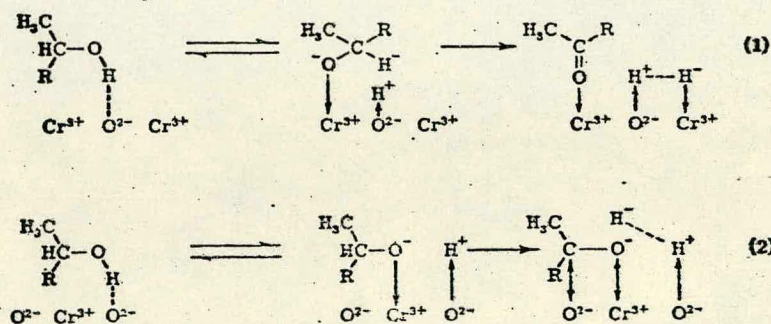


figure 3.10, mechanism of alcohol dehydrogenation over chromia after Nondek and Sedláček.⁷⁷

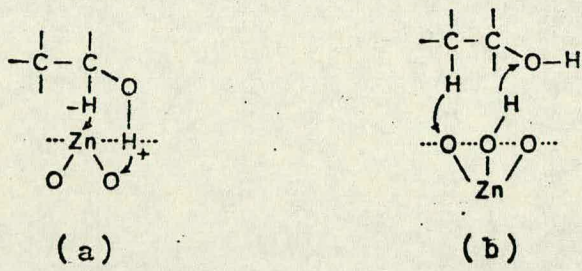


figure 3.11, dehydrogenation (a) and dehydration (b) over ZnO after Eucken and Wicke.^{51, 70, 71}

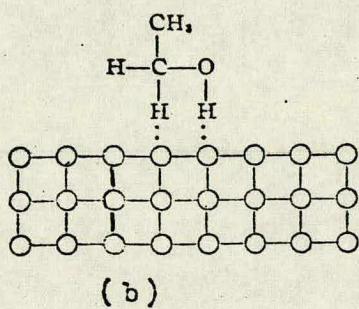
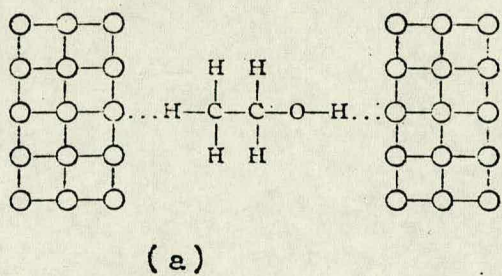


figure 3.12, dehydration (a) and dehydrogenation (b) after Schwab and Schwab-Agallidis⁸⁴ based on Balandin's duplet theory for catalysis.^{51, 85}

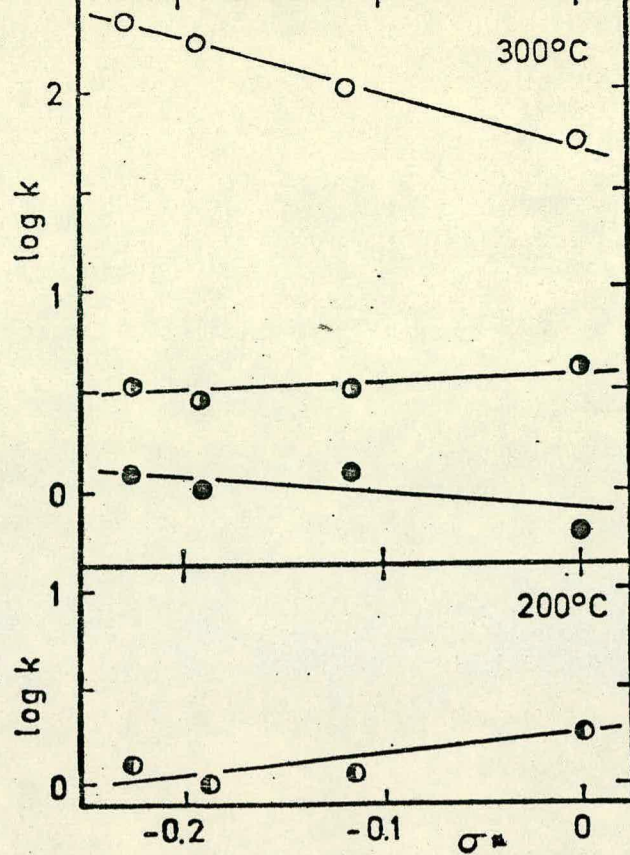


figure 3.13, correlation of reaction rate constants of the dehydration of secondary alcohols in the co-ordinates of the Taft equation: ○ SiO₂; ● ZrO₂; ◐ TiO₂; ◑ Al₂O₃; after Koechloefl et al.(100)

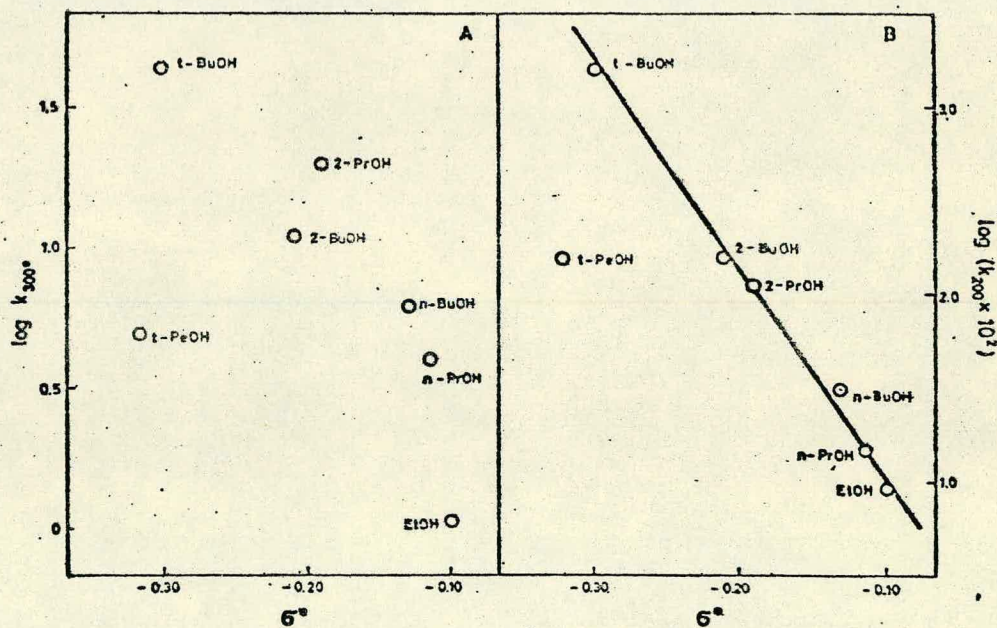


figure 3.14, Taft representation for aliphatic alcohol dehydration over anatase at (A) 300 and (B) 200°C after Carrizosa and Munuera.(99)

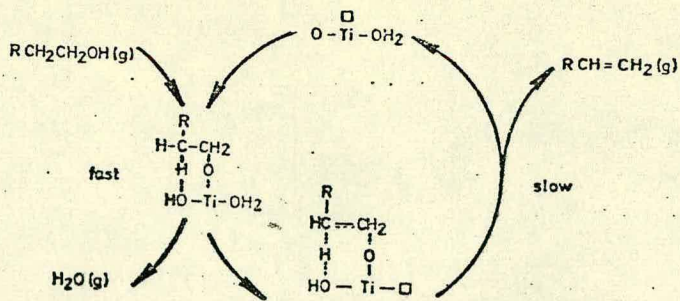


figure 3.15, mechanism of the dehydration of alcohols over anatase after Carrizosa and Munuera.¹⁰¹

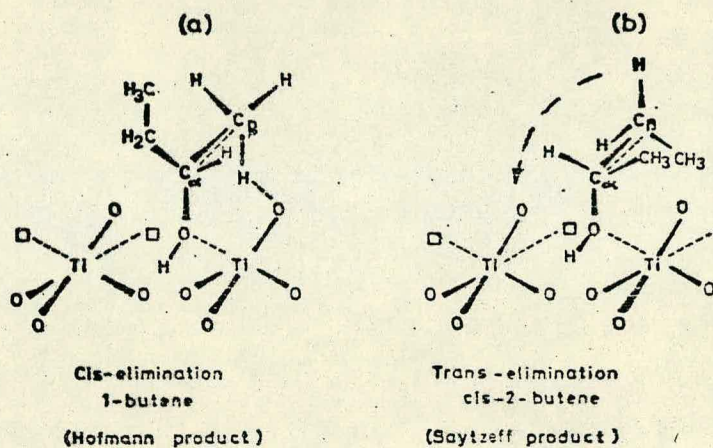


figure 3.16, formation of but-1-ene and cis but-2-ene from butan-2-ol over anatase after Carrizosa and Munuera.⁹⁹

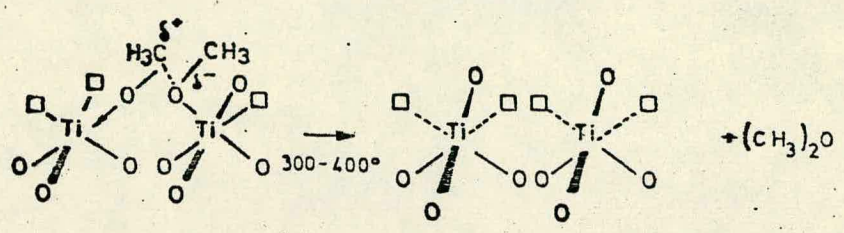
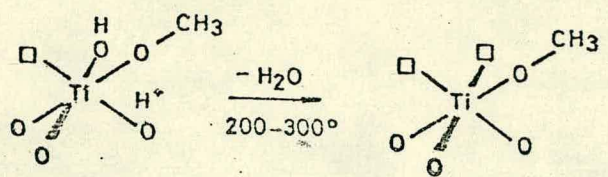


figure 3.17, formation of di-methyl ether from methanol over anatase after Carrizosa, Munuera and Castanar.⁷

CHAPTER 4

The Reactions of Alcohols over Rutile; (Flow System)

4.1 Introduction

The work on the flow system was initially intended to be a direct continuation of previous work on the reactions of alcohols over rutile⁴⁵. As has been previously stated in Chapter 2, the design of the flow system is such that it allows the study of those alcohols which have a vapour pressure that is too low at room temperature to be employed in a static apparatus.

The alcohols chosen for study on the flow system were propan-2-ol, 2,3-dimethylbutan-2-ol, pentan-1-ol, 4-methylpentan-2-ol and 2,2-dimethylpropan-1-ol (neopentanol). The main reaction of these alcohols over rutile was dehydration to an alkene which was usually accompanied by some dehydrogenation to an aldehyde or ketone. Under the experimental conditions used, there was no evidence of the formation of any ether as a dehydration product.

Propan-2-ol was used to test the stability of the flow system over a period of time comparable to that of a typical experiment. The temperature and the flow rate were kept constant and the conversion of propan-2-ol to propene and acetone was monitored for approximately four hours, (see Fig. 4.1). The initial sample, taken one minute after the flow had been diverted through the reactor, showed that approximately 7% of the alcohol had been converted to propene and approximately 7% to acetone. However all subsequent samples showed that although the conversion to

propene remained effectively constant for the period of the experiment (between 7.2% and 7.8%) the conversion to acetone had dropped to less than 0.5%. A comparison of the integrator response for the initial sample with those taken later suggested that some 30% of the reactant is lost from the gas phase in the early stages of the reaction.

2,3-Dimethylbutan-2-ol was studied for direct comparison with previous work⁴⁵ to ensure that reproducible data were being obtained. Subsequently the study on pentan-1-ol, 4-methylpentan-2-ol and 2,2-dimethylpropan-1-ol was initiated.

Standard experiments investigated the effect on reaction rate and product distribution of changing (a) the reaction temperature and (b) the flow rate. Frequently repeat experiments were performed to establish that the activity of the catalyst samples was reproducible.

4.2 The Reaction of Pentan-1-ol

The decomposition of pentan-1-ol over rutile was followed over the temperature range 490 to 570 K. This alcohol had a particularly low vapour pressure at room temperature (≈ 0.2 kPa)⁴⁹ and the saturator (see Chapter 2) had to be heated to 321 K in order to obtain a more convenient working pressure of 1.62 ± 0.1 kPa. The saturator temperature was kept constant for the majority of the experiments. In one experiment, however, the results of which are described in the table below and in Fig. 4.2, the reaction temperature and the flow rate remained constant at 550 K and $5 \times 10^{-7} \text{ m}^3 \text{ s}^{-1}$ respectively and the saturator temperature varied. Such an experiment provided data re the effect of changing the reactant concentration in the

gas flow and hence an indication of the order of the reaction with respect to the alcohol.

Saturator Temperature/K	Vapour Pressure pentan-1-ol/kPa	Rate of decomposition to pentenes/molecules $s^{-1} m^{-2}$
333	3.349	3.078×10^{15}
326	2.188	2.746×10^{15}
321	1.621	2.411×10^{15}
317.5	1.294	2.268×10^{15}
309	0.741	1.389×10^{15}
298	0.340	0.643×10^{15}

Fig. 4.2 shows that at low vapour pressures the overall rate of the decomposition to pentene was dependent upon the pentanol vapour pressure, but as the alcohol vapour pressure increased, the order of the reaction with respect to pentan-1-ol tended to zero. Thus at the operating pressure for most experiments, an assumption of zero order, though not entirely correct, is a reasonable estimate.

The G.C. traces (see Figs. 4.3(a) and 4.3(b)) of the product distribution obtained with the two G.C. columns (see Chapter 2) show that the main products of this reaction were pent-1-ene, cis-pent-2-ene, trans-pent-2-ene, n-pentane and pentanal (valeraldehyde). These products accounted for at least 99.5% of the alcohol conversion although the gas chromatographic traces indicated the presence of other minor products. Attempts to identify these materials established that they were not the following:-
2-methylbut-1-ene, 2-methylbut-2-ene, 3-methylbut-1-ene, 1,4-pentadiene, cyclopentene, cyclopentanone or trans-5-decene. (The final three were considered as certain

alcohols are known to react over rutile to form species of higher carbon number⁴⁵).

At the lower end of the temperature range examined, dehydration to pentenes and dehydrogenation to pentanal occurred at comparable rates (see Fig. 4.4) but at higher temperatures dehydration became the predominant reaction. At these higher temperatures there was also significant decomposition of any pentanal that was formed. Table 4.1 gives the rates of formation of the main products and Arrhenius data are presented in Figs. 4.5 and 4.6.

Fig. 4.7 shows how with decreasing contact time, as the flow rate increases, the % conversion of the alcohol decreases. The product ratios described in Table 4.2 and Fig. 4.8, which is of the variation of the relative proportions of the dehydration products with temperature, show that pent-2-ene and pentane production became more important as the temperature was increased and this was also observed when the contact time of the alcohol vapour was increased (Fig. 4.9). The ratio of cis/trans-pent-2-ene also decreased with temperature.

4.3 The Reaction of 4-Methylpentan-2-ol

The decomposition of 4-methylpentan-2-ol was investigated over the temperature range 470-520 K with the saturator at a temperature of 308 K which resulted in an alcohol vapour pressure of 1.33 ± 0.1 kPa.

The major reaction was dehydration of the alcohol to a mixture of alkenes and this was accompanied by dehydrogenation which produced small amounts of 4-methylpentan-2-one (methyl isobutyl ketone). The rate of production of the ketone varied between 4% - 7%

Table 4.1 Decomposition Of Pentan-1-ol

$$\text{Flow rate} = 5.0 \times 10^{-7} \text{ m}^3 \text{ s}^{-1}$$

$$\text{Rate of formation} / 10^{14} \text{ molecules s}^{-1} \text{ m}^{-2}$$

Temp /K	Total Pentenest+ Pentane+ Unknown	Pent-1-ene	Cis-Pent-2-ene	Trans-Pent-2-ene	Pentane	Pentanal
492	0.44	0.24	0.02	0.01	0.05	0.55
495	0.52	0.33	0.02	0.01	0.07	0.50
501	0.94	0.57	0.07	0.04	0.14	0.66
505	0.99	0.57	0.07	0.04	0.14	1.05
515	2.78	1.55	0.28	0.20	0.49	1.10
521	4.35	2.29	0.49	0.33	0.72	1.33
533	7.31	3.85	0.88	0.66	1.44	2.15
541	12.97	6.62	1.82	1.33	2.71	3.37
555	26.77	12.76	4.09	3.20	6.13	6.02
564	66.36	30.44	10.55	8.23	16.18	2.87

(The unknown, minor products, are not listed).

Table 4.2 The Variation Of The Relative Proportions Of Alkene And Alkane Products With Temperature And Flow Rate

Constant Flow Rate = $5 \times 10^7 \text{ m}^3 \text{ s}^{-1}$				Constant Temperature = 550 K			
Temp /K	Ratio			Flow Rate / $10^{-7} \text{ m}^3 \text{ s}^{-1} \propto \left(\frac{1}{\text{Contact time}} \right)$	Ratio		
	Pent-1-ene /Pent-2-ene	Cis/Trans- Pent-2-ene	Pentene /Pentane		Pent-1-ene /Pent-2-ene	Cis/Trans- Pent-2-ene	Pentene /Pentane
492	8.00	2.00	5.40				
495	11.00	2.00	5.14				
501	5.18	1.75	4.86	11.67	2.71	1.41	3.30
505	5.18	1.75	4.86	10.00	2.60	1.40	3.20
515	3.23	1.40	4.14	8.33	2.64	1.40	3.25
521	2.79	1.48	4.32	6.67	2.17	1.44	3.30
533	2.50	1.33	3.74	5.00	2.01	1.45	3.11
541	2.10	1.36	3.60	3.33	1.83	1.53	3.25
555	1.75	1.28	3.27	Equilibrium ¹⁰⁸	0.18	0.56	0.06
564	1.62	1.28	3.04				

of the rate of production of the alkene.

The G.C. traces (Fig. 4.10) also revealed the presence of two other products which from their G.C. retention times were believed to be species resulting from certain molecules fragmenting over the catalyst. They were considered unimportant as they only accounted for approximately 1% of the total alcohol decomposition.

The variation of the rate of formation of alkenes with the vapour pressure of the alcohol (Fig. 4.11) again indicated that, as with pentan-1-ol, the reaction could reasonably be considered as being of zero order with respect to the alcohol under the reaction conditions employed during the experiments described in this section.

The G.C. column packed with propylene carbonate on Chromosorb P was not as efficient a separator of the dehydration products as it had been when used to study the decomposition of pentan-1-ol. However, if operated at reduced temperature (268 K), at least partial separation of the dehydration products into two peaks was achieved. The products were identified as 4-methylpent-1-ene and 4-methylpent-2-ene; cis and trans isomers of the latter remaining indistinguishable. The incomplete separation of the gas chromatographic peaks prevented a detailed quantitative analysis of the reaction but throughout the temperature range studied there appeared to be a slight predominance of the pent-2-ene over the pent-1-ene species.

Table 4.3 gives the rates of formation of the main products and Arrhenius data are given in Fig. 4.12. The variation of % conversion with temperature is shown in Fig. 4.13 and the variation of % conversion with the rate of flow is illustrated in Fig. 4.14.

Table 4.3 Decomposition Of 4-Methylpentan-2-ol

$$\text{Flow Rate} = 5 \times 10^{-7} \text{ m}^3 \text{ s}^{-1}$$

Temp/K	Rate of Formation/ 10^{14} molecules $\text{s}^{-1} \text{ m}^{-2}$	
	Total Alkenes	4-Methylpentan-2-one
471	9.76	0.71
484	17.36	1.17
486	18.44	1.64
491	23.76	2.16
499	38.77	3.46
508	69.44	4.60
515	76.91	3.28
521	69.53	4.19

4.4 The Reaction of 2,2-dimethylpropan-1-ol (neopentanol)

2,2-Dimethylpropan-1-ol is a solid at ambient temperatures and the saturator was heated at 291 K to obtain a vapour pressure of approximately 1.6 ± 0.1 kPa. As with the previous alcohols, experiments which varied the vapour pressure of the alcohol revealed that a zero order for the reaction could be assumed.

The decomposition of 2,2-dimethylpropan-1-ol was investigated over the temperature range 465-532 K. The G.C. traces, Figs. 4.15 a and b, show that the products of the decomposition were 2-methylbut-1-ene,

2-methylbut-2-ene, 2,2-dimethylpropanal (trimethylacetaldehyde) and traces ($\leq 0.5\%$) of a compound which could be either 3-methylbut-1-ene or 1,1-dimethylcyclopropane. The variation of the % conversion with temperature of this alcohol to these products is illustrated in Fig. 4.16.

The rates of formation of the main products are given in Table 4.4 and the Arrhenius data are presented in Fig. 4.17. Arrhenius data for dehydrogenation to the aldehyde were not calculated as conversions to this product were small.

Fig. 4.16 and Table 4.5 reveal that at low temperatures the % conversion to the two alkenes was similar but that at higher temperatures, conversion to 2-methylbut-2-ene became more important. This variation of the ratio of the alkene products with temperature is more strikingly revealed in Fig. 4.18.

Figs. 4.19 and 4.20 show how the product distribution varies with the carrier gas flow rate, with longer contact times favouring the production of 2-methylbut-2-ene.

The stability of the flow system was checked with 2,2-dimethylpropan-1-ol as previously described with propan-2-ol (section 4.1), and with similar results (Fig. 4.21). The first sample taken after 5 minutes also showed that much of the reactant is lost to the surface at the start of the experiment and also at this point in time the catalyst displayed an abnormally large activity for dehydrogenation. It can be concluded, however, that after a period of time, the stability of the flow-system was satisfactory.

Table 4.4 Decomposition Of 2,2-Dimethylpropan-1-ol (neopentanol)

$$\text{Flow Rate} = 5 \times 10^{-7} \text{ m}^3 \text{ s}^{-1}$$

Rate of Formation/ 10^{14} molecules $\text{s}^{-1} \text{ m}^{-2}$

Temp/K	Total Alkenes	2-Methyl- but-2-ene	2-Methyl- but-1-ene	Other Alkene	2,2-Dimethylpropanal
465	0.11	-	-	-	0.28
491	0.78	0.41	0.36	0.01	0.31
522	6.12	3.67	2.32	0.13	0.89
532	8.42	5.26	3.03	0.13	0.48
543	20.40	13.36	6.63	0.41	0.74
553	31.16	21.18	9.35	0.63	0.65

Table 4.5 The Variation Of The Ratio Of 2-Methylbut-1-ene/2-Methylbut-2-ene With Temperature and Flow Rate

Constant Flow Rate = $5 \times 10^{-7} \text{ m}^3 \text{ s}^{-1}$			Constant Temperature = 550 K	
Temp/K	Ratio 2-Methylbut-1-ene /2-Methylbut-2-ene	Equilibrium ¹⁰⁸ Ratio	Flow Rate/ $10^{-7} \text{ m}^3 \text{ s}^{-1}$	Ratio 2-Methylbut-1-ene /2-Methylbut-2-ene
465	-	0.323	1.67	0.40
491	0.88	0.345	3.33	0.50
522	0.63	0.383	6.67	0.62
532	0.58	0.398	13.33	0.80
543	0.50	0.409	16.67	0.88
553	0.44	0.421	21.67	0.99
			25.00	1.11
			Equilibrium ¹⁰⁸	0.39

4.5 Reproducibility of Experimental Results Obtained on the Flow System

Generally, it was found that the use of a fresh catalyst sample for each experiment resulted in satisfactory reproducibility of the experimental data. Fig. 4.22 and Table 4.6 show that on repeating the decomposition of pentan-1-ol with a fresh catalyst sample, the reaction is approximately three times slower than previously described although the activation energy for the total dehydration remains effectively constant at 160 kJ mol^{-1} . The product distribution was as described in section 4.2 and the variation with temperature and flow rate followed a similar trend.

Similarly Fig. 4.23, shows the results of a re-investigation of the decomposition of 2,2-dimethylpropan-1-ol over a fresh catalyst sample. Again the trend towards an increasing ratio of 2-methylbut-1-ene to 2-methylbut-2-ene with higher flow rates (and shorter contact times) is apparent. However, this variation in product ratio is not exactly as before (compare Fig. 4.20); possibly a consequence of the new catalyst sample being less active. Examination of the gas chromatographic traces suggests that the overall rate of dehydration was approximately half that described in section 4.4. Thus the lower catalyst activity probably also accounts for the relative concentrations of the dehydration products being further from their equilibrium values than was found in section 4.4.

It is apparent that the reproducibility of the experimental data obtained using the flow system is not entirely satisfactory and this might well be one of the

Table 4.6 Repeat Of Decomposition Of Pentan-1-ol Over Rutile

$$\text{Flow Rate} = 5 \times 10^{-7} \text{ m}^3 \text{ s}^{-1}$$

Temperature/K	Rate of formation/ 10^{14} molecules $\text{s}^{-1} \text{ m}^{-2}$	
	Total Pentenes + Pentane	Pentanal
472	0.03	1.14
518	0.70	0.82
523	1.01	1.55
526	1.55	0.85
529	2.48	1.56
538	3.07	0.87
541	3.62	1.78
552	10.33	2.46
565	18.72	3.60

reasons why the L.F.E.R. plot, Fig. 4.38, is less well defined than was previously thought⁴⁵. Rather more satisfactory reproducibility of the experimental results was obtained if fresh catalyst samples were used for each experiment instead of repeated use of one catalyst sample. The fragility of the flow system reactor, however, limited the frequency of the replacement of the catalyst samples which consequently led to their repeated use and it was found that gradually the samples became more active for dehydration, though not for dehydrogenation, when used repeatedly in alcohol decomposition experiments.

The variation in activity with repeated use of a catalyst is illustrated by a re-examination of the decomposition of 4-methylpentan-2-ol as shown in Figs. 4.24 and 4.25. Comparing Fig. 4.24 with Fig. 4.13, it is seen that at similar temperatures, the conversion to alkenes is much greater than was found previously although the ketone production remains similar to that observed before. The previously chosen reaction temperature of 489 K (Fig. 4.14) had to be lowered to 473 K in order to obtain similar conversions, to alkene with flow rate (Fig. 4.25), to those obtained when the catalyst was initially used. Fig. 4.25 also shows that at low flow rates with high contact times and consequently high conversions to alkene, ketone production decreases with temperature which confirms previously held suspicions (Fig. 4.4) that once the majority of the alcohol molecules have decomposed, the dehydrogenation products begin to decompose over rutile. This explains why Arrhenius plots

for the dehydrogenation of an alcohol over rutile are sometimes of poor quality. New rate data for the decomposition of 4-methylpentan-2-ol over the more active rutile sample is given in Table 4.7 (compare with Table 4.3).

Table 4.8 and Figs. 4.20, 4.23, 4.26, 4.27 and 4.28 illustrate the progressive increase in activity towards dehydration of a catalyst sample with repeated use. The decomposition of 2,2-dimethylpropan-1-ol was selected as a typical reaction. Although the absolute values of the areas under the gas chromatography peaks only offer an indication of the overall rate of decomposition to the alkenes, it is seen from Table 4.8 that those experiments in which the smaller variations in the ratio of 2-methylbut-1-ene/2-methylbut-2-ene occur, are those with the larger peak areas; i.e. greater overall conversion to alkenes took place in such experiments. It must be remembered that 2-methylbut-2-ene is the thermodynamically more stable of the two alkenes at these temperatures¹⁰⁸; therefore the smaller the value of the above ratio, the closer the system is to equilibrium.

In Table 4.8, the experiments are noted Day 1, Day 7, etc., which indicates the chronological order in which the experiments took place. Comparison of the results obtained on Day 1 and Day 8 has been discussed previously (see above). With the second catalyst sample, the results of the experiment on Day 9 show little differences to those on Day 8. However a comparison of the results of experiments on Day 1 and Day 7 and on

Table 4.7 Repeat Examination Of The Decomposition Of 4-Methylpentan-2-ol Over Rutile

$$\text{Flow Rate} = 5 \times 10^{-7} \text{ m}^3 \text{ s}^{-1}$$

Temperature/K	Rate of formation/ 10^{14} molecules $\text{s}^{-1} \text{ m}^{-2}$	
	All Alkenes	4-Methylpentan-2-one
457	14.77	-
461	19.56	-
465	23.91	-
471	36.17	0.21
476	47.62	0.33
481	50.63	0.48
488	60.21	1.18

Table 4.8 Activation Of Rutile For The Dehydration Of
2,2-Dimethylpropan-1-ol with repeated catalyst use

Variation of rates of formation of 2-methylbut-1-ene and
2-methylbut-2-ene with rates of flow

Reaction temperature = 533 K

<u>Catalyst Sample 1</u>		<u>Day 1</u>		<u>(Fig. 4.20)</u>		
Flow Rate/ $10^{-7} \text{ m}^3 \text{ s}^{-1}$	PKA	PKB	%A	%B	A/B	
1.67	169600	428800	27.4	69.3	0.40	
3.33	101000	201000	32.8	65.1	0.50	
6.67	64510	105000	37.5	60.8	0.62	
13.33	38570	48440	43.2	54.3	0.80	
16.67	31660	35840	46.0	52.4	0.88	
21.67	15170	14990	47.8	48.1	0.99	

<u>Catalyst Sample 1</u>		<u>Day 7</u>		<u>(Fig. 4.26)</u>		
Flow Rate/ $10^{-7} \text{ m}^3 \text{ s}^{-1}$	PKA	PKB	%A	%B	A/B	
1.67	290200	934800	23.2	74.9	0.31	
3.33	241400	744600	24.4	75.0	0.33	
6.67	169700	484200	25.7	73.4	0.35	
13.33	118800	299800	28.0	70.8	0.40	
16.67	97060	233200	29.3	70.3	0.42	
21.67	71360	163300	30.2	69.1	0.44	

<u>Catalyst Sample 2</u>		<u>Day 8</u>		<u>(Fig. 4.23)</u>		
Flow Rate/ $10^{-7} \text{ m}^3 \text{ s}^{-1}$	PKA	PKB	%A	%B	A/B	
1.67	107700	191900	35.3	62.1	0.57	
3.33	75480	94840	42.6	54.1	0.74	
6.67	41910	43560	47.7	48.5	0.98	
13.33	22430	20290	51.6	46.7	1.10	
16.67	-	-	-	-	-	
20.00	7715	5415	56.5	40.0	1.41	

<u>Catalyst Sample 2</u>		<u>Day 9</u>		<u>(Fig. 4.27)</u>		
Flow Rate/ $10^{-7} \text{ m}^3 \text{ s}^{-1}$	PKA	PKB	%A	%B	A/B	
1.67	106300	186800	35.4	62.2	0.57	
3.33	74310	98420	41.6	55.1	0.75	
6.67	41810	43620	46.1	48.1	0.96	
13.33	23690	21790	50.0	46.0	1.09	

continued ...

Table 4.8 continued ...

<u>Catalyst Sample 2</u>	<u>Day 20</u>		<u>(Fig. 4.28)</u>		
Flow Rate/ $10^{-7} \text{ m}^3 \text{ s}^{-1}$	PKA	PKB	%A	%B	A/B
1.67	291300	977300	22.7	76.5	0.30
3.33	235900	705300	24.8	74.7	0.33
6.67	150000	403600	26.8	72.0	0.37
13.33	78520	177700	30.2	69.1	0.44
18.33	55260	116000	32.0	67.5	0.47
23.33	25870	52280	33.2	66.6	0.50

Key to table

A = 2-Methylbut-1-ene

B = 2-Methylbut-2-ene

PKA = Area of Peak A (\propto Rate of formation of 2-methylbut-1-ene)

PKB = Area of Peak B (\propto Rate of formation of 2-methylbut-2-ene)

Areas expressed in arbitrary units.

Day 8 and on Day 20, with both catalyst samples 1 and 2, show that ageing of the catalyst results in an increase in its activity for dehydration. The experiment with 2,2-dimethylpropan-1-ol (Fig. 4.21) which tested the stability of the flow system revealed that this variation of activity of a catalyst sample did not take place during any one specific experiment.

One catalyst sample had considerably more activity for dehydration than any previously discussed samples. The decomposition of pentan-1-ol over this sample at the previous (section 4.2) temperature range of (490-570 K) resulted in the apparent total conversion of the reactant to alkenes, i.e. with no detectable reactant pentan-1-ol remaining and the temperature range for study had to be lowered by approximately 35 degrees to 465-518 K in order to obtain conveniently measurable rates of conversion. At such low temperatures for pentan-1-ol decomposition over rutile, dehydrogenation to pentanal was barely apparent (always less than 1% of the total alcohol decomposition).

Table 4.9 and Fig. 4.29 give rate and Arrhenius data for pentan-1-ol decomposition over this catalyst sample and it is noted that the activation energy is now approximately 110 kJ mol^{-1} instead of the previously reported (section 4.2) 180 kJ mol^{-1} . The rate data shows that for pentan-1-ol, this catalyst sample was approximately 28 times more active for dehydration than the original catalyst sample (Table 4.1).

Gas chromatographic analysis of the alkene product distribution was particularly revealing in that unlike

Table 4.9 Decomposition Of Pentan-1-ol Over Superactive Rutile Catalyst Sample

Temperature/K	Rate of formation/ 10^{14} molecules $s^{-1} m^{-2}$	
	All Alkenes	Pentanal
466	4.06	0.09
471	5.43	0.10
481	11.07	0.12
493	22.36	0.22
501	32.16	0.31
511	46.63	0.44
517	63.77	0.64

the previous decomposition of pentan-1-ol over rutile, (section 4.2) no pentane was observed (Fig. 4.30) which made a direct comparison with Fig. 4.4 rather difficult. However, Fig. 4.30 again shows that with pentan-1-ol decomposition, the formation of pent-2-ene becomes more important at higher temperatures.

4-Methylpentan-2-ol was also reacted over this catalyst sample and the temperature of the reaction had to be lowered by approximately 80 degrees in order to obtain similar conversions to those in section 4.3. Again no dehydrogenation product was observed.

4.6 Discussion

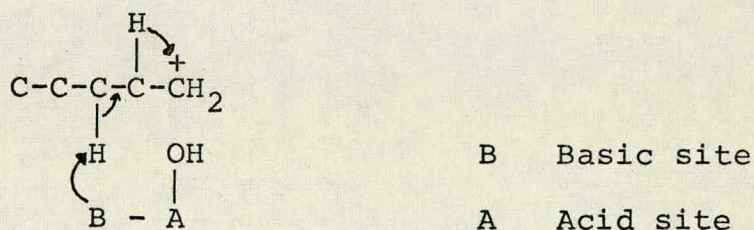
The above results confirm (i) that the main reaction of an alcohol over TiO_2 is dehydration to alkenes, (ii) that dehydrogenation to the corresponding aldehyde or ketone occurs to a much lesser extent and (iii) that there is no ether formation. It is also noted that dehydration of the secondary alcohol (4-methylpentan-2-ol) occurred more readily than that of the two primary alcohols (pentan-1-ol and 2,2-dimethylpropan-1-ol).

As has been previously discussed, the G.C. facilities available did not allow a complete examination of the product distribution resulting from the decomposition of 4-methylpentan-2-ol which could have been compared with that of other hexanols previously examined⁴⁵. The information obtained, however, suggesting the formation of approximately equal amounts of 4-methylpent-1-ene and 4-methylpent-2-ene is compatible with a scheme in which the removal of a proton from a 4-methyl-2-pentyl

carbonium ion occurs in a statistical manner (Fig. 4.31). The alkenes are certainly not formed in the relative equilibrium concentrations expected from thermodynamic considerations of the reaction at temperatures of approximately 500 K. Considering only a 1,2 double bond shift, if the system had gone to equilibrium the product distribution would have overwhelmingly consisted of the 4-methylpent-2-enes¹⁰⁸. (A product distribution similar to that described here was found by Davis¹⁰⁹ for the decomposition of 4-methylpentan-2-ol over tungsten oxides at similar reaction temperatures). If equilibrium concentrations had been observed, very little could have been understood about the mechanism of the dehydration. The fact that both 4-methylpent-1-ene and 4-methylpent-2-enes were both formed in similar quantities does not distinguish between a mechanism in which there occurs (a) a simultaneous dehydration to the two isomers or (b) the initial formation of 4-methylpent-1-ene (as statistically expected) with subsequent isomerisation to 4-methylpent-2-ene. However, since substantial amounts of 4-methylpent-1-ene were formed, it can be concluded that the situation is more complicated than that where the first complete step in the decomposition of the alcohol is a direct dehydration to the thermodynamically most stable isomers or to the equilibrium proportions of the isomers.

Studies of the reaction of 3,3-dimethylbutan-2-ol over rutile⁴⁵ revealed the removal of γ -hydrogens as being of importance during the decomposition of this alcohol. The decomposition of pentan-2-ol and butan-2-ol over the temperature range 476-520 K disclosed that the ratio of

alk-1-ene/alk-2-ene remained constant at about 0.50 but this did not signify any preference for a β or γ elimination as the alk-2-ene could be formed by both forms of elimination. The decomposition of butan-1-ol however showed a variation in the alk-1-ene/alk-2-ene ratio (which represents the relative rates of β to γ elimination) from 5.5 at 558 K to 3.9 at 583 K. A similar variation is observed here for the decomposition of pentan-1-ol with an alk-1-ene/alk-2-ene ratio of 11.0 at 495 K, dropping to 1.62 at 564 K. At all temperatures in the above range (495 to 564 K) the cis and trans-pent-2-enes are thermodynamically more stable than pent-1-ene therefore it is certain that although the situation is complicated by pentane production, on increasing the reaction temperature, the pentenes are moving towards their relative equilibrium concentrations. The reaction sequence leading to the final product distribution after pentan-1-ol decomposition, therefore, could take one of two forms:- (a) alk-2-ene production via a γ elimination, coupled with a 1,2 H shift, from the intermediate positively charged species formed after the initial removal of the hydroxyl groups i.e.



or (b) initial pent-1-ene formation which subsequently desorbs, re-adsorbs and isomerises to the pent-2-enes. But-1-ene is known³⁷ to isomerise over rutile at 423 K and it is expected that pent-1-ene isomerisation should

also occur at the reaction temperatures necessary for the dehydration of pentan-1-ol.

To test this hypothesis a short experiment was carried out by passing pent-1-ene vapour over rutile at a series of reaction temperatures on the flow system. (A static system could not be used as all the available apparatus was constructed with greased taps and joints and the pentenes were found to readily attack tap grease). The difficulties encountered when operating the flow system with pent-1-ene were the opposite to those with pentan-1-ol as pent-1-ene has a very high vapour pressure at room temperature (≈ 66.7 kPa) and therefore the saturator had to be cooled with an ethanol/liquid N_2 slush bath to 213 K to produce a vapour pressure in the saturator of approximately 0.67 kPa. It was impossible to maintain such low temperatures in the rest of the apparatus and because of this the G.C. peak areas did not show good reproducibility which consequently made the experiment more qualitative in nature rather than quantitative as initially planned.

The results which were obtained are summarised below:-

Table 4.10 Reaction Of Pent-1-ene Over Rutile

Temp/K	448	463	468	473	487	493
% Pent-1-ene	83.38	77.45	72.07	67.19	51.64	47.77
% Trans-Pent-2-ene	8.31	11.28	14.16	16.62	25.42	28.04
% Cis-Pent-2-ene	8.31	11.28	13.76	16.18	21.93	24.14
Ratio Cis/Trans	1	1	0.97	0.97	0.86	0.86
Eq Ratio Cis/Trans ¹⁰⁸	0.48	0.52	0.54	0.52	0.50	0.51
Ratio Cis/Trans						
Dehydration Expt	-	-	-	-	-	2.00

These results, obtained over a lower temperature range than those for the dehydration of pentan-1-ol, prove that the isomerisation of pent-1-ene does occur over rutile at the reaction temperatures under study, but it should be noted that in the alkene isomerisation studies, the ratios for the cis/trans-pent-2-enes lie closer to their equilibrium values, which indicates that the dehydration process interferes with any subsequent isomerisation if, indeed, a subsequent isomerisation is taking place.

Plots of the variation of the isomer composition of the alkenes, due to the variation of the flow rate, against the total alkene production, Fig. 4.32, and a plot of % composition of the dehydration products against (flow rate)⁻¹ (Fig. 4.33) both show that when extrapolated to zero alkene production, the initial product distribution includes substantial quantities of the pent-2-enes which indicates that γ eliminations do occur at low contact times to form the pent-2-enes directly. As the contact time increases, however, it is apparent that the proportions of the pent-2-enes increase at the expense of the pent-1-ene and the system moves towards its equilibrium composition. This strongly suggests that at the high contact times where greater overall dehydration is taking place, pent-1-ene isomerisation is occurring to form the cis and trans-pent-2-enes although perhaps not in exactly the same manner as when pent-1-ene isomerisation over rutile occurs unaccompanied by simultaneous dehydration of an alcohol. Therefore it is suggested that both mechanisms occur for the formation of pent-2-enes from the dehydration of pentan-1-ol over rutile. The pentane fraction of the

gas phase composition remains constant in Figs. 4.32 and 4.33 and does not parallel the variation in the % composition for either pent-1-ene or for the cis/trans-pent-2-enes. Such a result is compatible with a scheme in which pentane is produced from the hydrogenation of an alkene with the actual structure of the alkene being unimportant, i.e. pent-1-ene, cis or trans pent-2-ene all have an equal chance of being hydrogenated.

It is noted that for both the pentan-1-ol dehydration and to a lesser extent the pent-1-ene isomerisation, the pent-2-enes are not formed in their equilibrium concentrations but in a stereo-selective manner tending to favour the cis-isomer. This was also found for butan-1-ol decomposition over alumina⁶⁵ and for pentan-2-ol decomposition over rutile⁴⁵. Pines et al^{59,65,110} ascribed the cis preference to the formation of an intermediate proton-alkene complex over alumina and the greater stability of cis π -complexes compared to trans π -complexes.

This idea led Pines and co-workers to suggest that a cis preference indicated that a concerted E2, trans-elimination involving anchimeric assistance of hydrogen occurred during alcohol dehydration over alumina and it may be that similar results here allow similar conclusions to apply for reactions catalysed by rutile. The acceptance of such an explanation however is not general as results obtained by Davis¹¹¹ working on the decomposition of octan-2-ol over alumina can be explained by both a cis and a trans elimination and Krozinger¹¹² explained the cis preference in terms of steric restriction between certain groups of the adsorbed species and the catalyst

surface. A lateral inclination of the reactant on the surface, which was assumed, would be sterically less hindered when the most bulky groups are on the same sides of the carbon atom, i.e. in a cis position to each other. Noller and Kladnig¹¹³ pointed out that such an inclination effect would however affect a concerted mechanism more than a carbonium-ion mechanism which does suggest that Pines was originally correct when stating that cis-olefin preference was indicative of an E2 mechanism.

Early work by Whitmore¹¹⁴ showed that 2,2-dimethylpropan-1-ol (neopentanol) is very inactive to heat treatment, even at temperatures above 503 K, and in the presence of reagents such as I₂, K₂CO₃ or HCl. Decomposition over alumina is known to occur at approximately 620 K^{62,112}.

2,2-Dimethylpropan-1-ol is interesting in that it differs from other aliphatic alcohols, and indeed from other neopentyl-type alcohols such as 3,3-dimethylbutan-2-ol or 3,3-dimethylpentan-2-ol, in that dehydration is impossible without rearrangement of the carbon skeletal structure. This condition does not apply as far as dehydrogenation is concerned, and therefore there was a possibility that as a consequence the decomposition of this alcohol over rutile would lead to the formation of more aldehyde than alkene. An almost opposite situation was envisaged to that which occurs over metals where the usual reaction of an alcohol is a dehydrogenation except where skeletal restrictions, as with tertiary alcohols, make such a decomposition impossible and hence dehydration occurs⁵². Over alumina^{62,112}, dehydrogenation of an

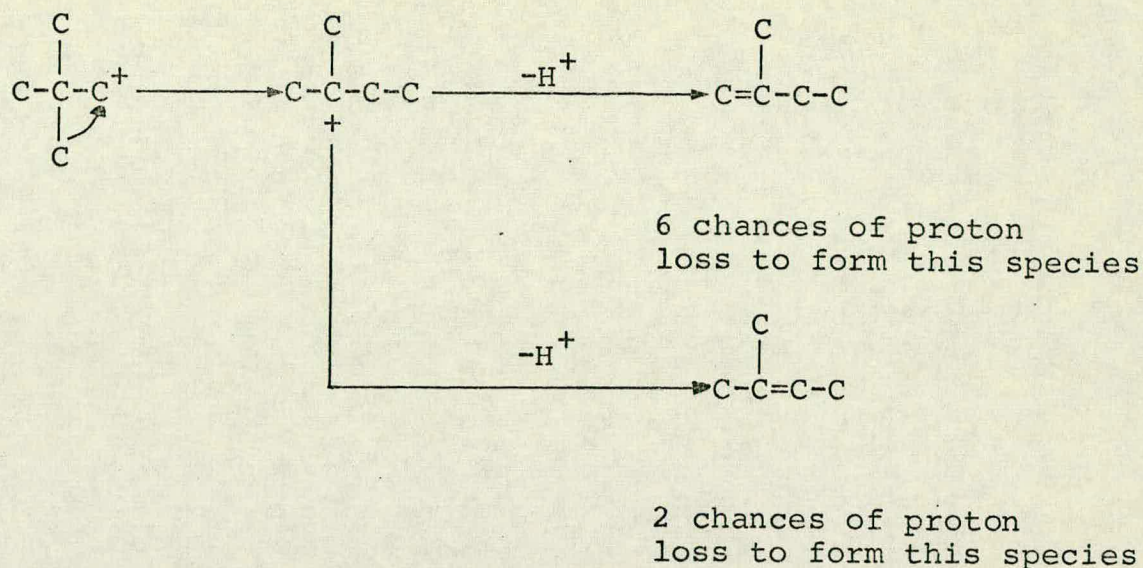
alcohol is not known to occur therefore this line of speculation did not arise.

The experimental results show, that carbon-skeleton rearrangement does not introduce any form of restriction towards dehydration. The products of the reaction are overwhelmingly the alkenes and their formation is accompanied by the usual small amount of dehydrogenation. This situation was also found by Pillai and Pines working with alumina⁶² where no dehydrogenation took place. It is pertinent to note that the dehydrogenation product was found to be 2,2-dimethylpropanal (trimethylacetaldehyde) and thus dehydrogenation does not involve any skeletal rearrangement; i.e. the mechanism for dehydrogenation is a direct process and does not involve subsequent oxidation of any initially formed alkenes.

Compared with pentan-1-ol, graphs of % composition v flowrate⁻¹ for 2,2-dimethylpropan-1-ol do not allow for a linear extrapolation to zero conversion and when an extrapolation is attempted, it can be shown (Fig. 4.34) that the initial product formed is solely 2-methylbut-1-ene, the less thermodynamically stable¹⁰⁸ of the alkene products. With increasing contact time, the trend is for the more thermodynamically stable 2-methylbut-2-ene to be preferentially formed which suggests a subsequent isomerisation of the 1-alkene is occurring.

Considering the reaction scheme statistically, 2-methylbut-1-ene formation is 3 times more likely than 2-methylbut-2-ene formation as shown below :-

Fig. 4.35



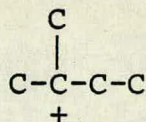
Formation of both species involves a common positively charged intermediate followed by a β hydrogen elimination. Thus extrapolation of Fig. 4.34 to an initial product distribution of 75% 2-methylbut-1-ene and 25% 2-methylbut-2-ene is more realistic than the previous extrapolation of 100% and 0% for the two alkenes. Therefore it is suggested that a statistical explanation of the initial product distribution is more valid with subsequent isomerisation occurring at higher temperatures and lower contact times (Tables 4.4 and 4.5).

Pines⁵⁹ explained the formation of 2-methylbut-1-ene from the decomposition of 2,2-dimethylpropan-1-ol over alumina by a concerted mechanism involving the removal of a proton from a γ carbon atom with migration of the methyl group and this also explained the formation of 1,1-dimethylcyclopropane (Fig. 4.36).

This reaction scheme may also be applicable over rutile as traces were found of another compound which had a retention time on the chromatographic column similar to that of 1,1-dimethylcyclopropane. However the difference between the mechanism suggested by Pines and that offered

here depends only upon whether the decomposition is a truly concerted elimination or if a positively charged intermediate exists. A L.F.E.R. plot for alcohol dehydration over rutile (Fig. 4.38) does suggest the existence of positively charged intermediates: thus it would seem that truly concerted eliminations do not take place. However with skeletal rearrangement, the classification of a particular carbon as being α, β or γ becomes more difficult and arguments distinguishing between the different forms of elimination become less precise.

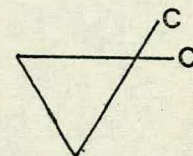
Pines et al^{59,62} also compared the product distributions from the decomposition of 2-methylbutan-2-ol and 2,2-dimethylpropan-1-ol over alumina. The ratio of 2-methylbut-1-ene to 2-methylbut-2-ene from 2,2-dimethylpropan-1-ol was found to be approximately 3 whereas that from 2-methylbutan-2-ol was only 1.4. (The equilibrium ratios being ≈ 0.5). The authors explained the decomposition of the tertiary alcohol as taking place via a carbonium ion mechanism. However, because of the differences in product distribution observed for the two alcohols, this type of mechanism was not adequate to explain the rearrangement taking place during the dehydration of 2,2-dimethylpropan-1-ol, in as much as the two alcohols would have had the same ionic intermediate: i.e.



A comparison of the decomposition of the two alcohols over rutile is described in Table 4.11. The results can be simply interpreted by considering that at the higher temperatures required for the decomposition of 2,2-

Table 4.11 Comparison Of The Dehydration Of 2,2-Dimethylpropan-1-ol And 2-Methylbutan-2-ol Over Rutile.

Temperature/K	Flow Rate/ $10^{-7} \text{ m}^3 \text{ s}^{-1}$	Dehydration (%)	%Composition of Product		
			$\begin{array}{c} \text{C}=\text{C}-\text{C}-\text{C} \\ \\ \text{C} \end{array}$	$\begin{array}{c} \text{C}-\text{C}=\text{C}-\text{C} \\ \\ \text{C} \end{array}$	
			2,2-dimethylpropan-1-ol		
530	3.33	12.3	32.5	65.0	0.99
530	6.66	6.0	37.5	60.5	0.53
530	10.00	4.5	40.5	57.5	-
530	Equilibrium ¹⁰⁸		28.5	71.5	-
			2-methylbutan2-ol (after Halliday ⁴⁵)		
435	3.33	20	49.0	51.0	-
435	6.66	9.8	51.0	48.9	-
435	10.00	7.0	51.3	48.7	-
435	Equilibrium ¹⁰⁸		22.2	77.8	-



dimethylpropan-1-ol secondary isomerisation of the initial alkene dehydration products will occur and consequently the final product distribution is more likely to be similar to the equilibrium predictions. These results differ from those found by Pines et al^{59,62} in that over alumina, the final product distribution from the primary alcohol was further from the respective equilibrium proportions than that obtained from the tertiary alcohol even though, as with the experiments described here, higher temperatures were required for the decomposition of the primary alcohol. In the present work with rutile, the similarity of the product distribution for the two alcohols (particularly if the temperature difference is taken into account) suggests that although classical carbonium ions may not be formed in the dehydration of the primary alcohols, the formation of positively charged, or at least partially positively charged species, may be occurring and that the truly concerted mechanism involving no net positively charged intermediates as suggested by Pines et al^{59,62} may be less applicable. The rupture of the C α -OH bond may progress more rapidly than the rupture of the C-H bond resulting in a partial positive charge on the α -carbon atom. The Linear Free Energy Relationship (Fig. 4.38) originally presented by Halliday⁴⁵ and which has been augmented by work presented in this thesis has a negative slope ($\rho^* = -4.3$) and this also suggests that the reaction intermediates involved in the dehydration reaction develop a whole or partial positive charge.

The present results over rutile are in agreement with the work of Kochoefl^{100,115} and co-workers who also found

that comparing alcohol dehydration over alumina with that over TiO_2 suggested a change in mechanism from an E2 to an E1 elimination.

The similarities between dehydration reactions in solution and those on alumina surfaces led Pines and Manassen⁵⁹ to conclude that alumina was a "pseudo-solvent" and acted as a solvating agent with dehydration occurring in pores or channels of molecular dimensions within the catalysts. They also assumed the acidic and basic sites to be located on opposite walls of such crevices (a suggestion which had been previously offered by Schwab and Schwab-Aqallidis⁸⁴). Pines and Manassen believed that this view could be of general applicability to all heterogeneous catalysts. The aluminas studied by Pines and co-workers⁶⁰ however had surface areas of approximately $150\text{-}300 \text{ m}^2 \text{ g}^{-1}$, values much larger than that of the rutile catalysts at present under examination i.e. $25\pm 1 \text{ m}^2 \text{ g}^{-1}$. The rutile thus has a much less porous structure than the alumina, and therefore the dehydration process must occur "on" rather than "within" its surface. The activation energies associated with the dehydration of pentan-1-ol, 4-methylpentan-2-ol and 2,2-dimethylpropan-1-ol over rutile were 160, 110 and 140 kJ mol^{-1} respectively which certainly indicates that the reactions were not diffusion controlled (reactions under diffusion or mass transfer control having activation energies very much less than these values.) If dehydration was occurring within sub-microscopical pores in the catalyst then it is much more likely that diffusion would become important,

although Knozinger¹¹² has pointed out that diffusion control has never been observed for the dehydration of alcohols over alumina.

Irreproducibility

The Linear Free Energy Relationship presented in Fig. 4.38 and the Tables 4.6, 4.7 and 4.8 all show how the activity of the catalyst towards dehydration is not particularly reproducible although generally, the reproducibility of the results improves if repeat experiments involve the use of fresh catalyst samples. This variation in activity is particularly noticeable when working with the flow system.

Brey and Krieger⁵⁶ attributed an increase with use in the dehydrating activity of some alumina catalysts to the existence of an optimum surface water content for the reaction which was present on some catalyst samples only after initial use. The variation of the dehydrating activity of rutile with surface water content is discussed elsewhere in this thesis and may partly explain the present results.

An increase in the surface area of the catalyst with use does not provide an explanation as B.E.T. studies of the more active catalysts did not indicate that this had taken place. Another explanation for this increase in activity may be related to the fact that the design of the flow system is such that it will not hold a vacuum greater than ≈ 1.33 Pa. Thus the overnight evacuation at 723 K of a catalyst sample may be better described as a heating of the catalyst under a small pressure of air.

The increase of a catalyst's activity for a certain reaction after heating in air is not unknown. V.H.J. de Beer and co-workers¹¹⁶ found that heating a $\text{CoO-MoO}_3-\gamma\text{Al}_2\text{O}_3$ catalyst in air at 323 K resulted in enhanced activity for thiophene desulphurization by as much as 36% which they explained as being due to oxygen ligands improving the specific catalytic properties of some Mo sites. Pillai and Pines¹¹⁷ observed that regeneration in air of an alumina catalyst gave a more active alcohol dehydration material. They only explained this by suggesting that this regeneration resulted in new strong acid sites being formed. It has also been observed¹¹⁸ that inadvertant overnight heating of an alumina catalyst in air caused an increase in its activity for alkene isomerisation although heating the catalyst in the separate constituents of air (O_2 , N_2 , etc.) had no such effect!

Furlong and Parfitt¹¹⁹, studying the electrophoretic mobility of colloidal dispersions of titanium dioxide in solutions of potassium nitrate of varying pH, found that ageing certain samples of rutile and anatase in air led to a decrease in the value of the iso-electric point, (the pH of the solution at which the colloidal particles have zero charge), which could then be increased again by subsequent soxhlet washing. This indicated that the ageing had resulted in an increase in the concentration of anionic impurities, such as chloride or sulphate species, on the particle surfaces as a consequence of diffusion of the impurities from the bulk of the particles. X-ray fluorescence studies by Jones and Hockey²² also revealed

that heating samples of rutile at 673 K caused an increase in the chlorine content of the surface layers. Therefore it is suggested that the variation in the catalytic activity of rutile reported in the present work could well be due to an increase in the surface concentration of certain bulk impurities which produces a resultant increase in the surface acidity of the catalyst.

Shibata et al¹²⁰ found that the addition of Fe_2O_3 caused a dramatic increase in the surface acidity of TiO_2 . However, since the major impurity in the samples of rutile used in the experiments described in this thesis was chlorine (0.3%), with iron impurities being less than 10 ppm, it is more likely that the effects described here are due to an increase in chloride concentration on the catalyst surface. Brookes³⁷ found that pre-adsorption of HCl or Cl_2 increased the activity of rutile for but-1-ene isomerisation and Halliday^{45,46} found that a similar pretreatment caused a 130-fold increase in the rate of loss of buta-1,3-diene from the gas phase to the surface of a rutile sample. Results described elsewhere in this thesis (Chapter 5) also show that HCl preadsorption increases the activity of rutile for alcohol dehydration. Calculations show that in a 1 g sample of rutile with a 0.3% Cl impurity, if all the Cl migrated to the surface there would be a surface concentration of $4.06 \text{ Cl ions nm}^{-2}$ or $2.03 \text{ Cl}_2 \text{ molecules nm}^{-2}$ which is close to the surface concentration of chlorine that Brookes³⁷ reported was necessary to produce a similar increase in the activity of rutile for but-1-ene isomerisation.

Other than the overall activation of the catalyst for dehydration, the effects of catalyst ageing/use on the

product distribution should also be noted. Dehydrogenation was not affected by the catalyst's activation towards dehydration and the higher temperatures required for aldehyde or ketone production over the unactivated catalysts had to be maintained for their production over the activated catalyst samples. This indicates therefore that the sites associated with dehydration are not the same as those associated with dehydrogenation. (The sites and mechanism involved with dehydrogenation are discussed later in this thesis).

The increase in activity for dehydration of 2,2-dimethylpropan-1-ol also displaces the alkene product distribution further towards its equilibrium value (Fig. 4.37). Fig. 4.37 and the table below show the results of extrapolating to zero a graph of % composition vs flow rate⁻¹ for the activated catalyst in order to obtain the initial product distribution for the reaction.

Temperature 533 K

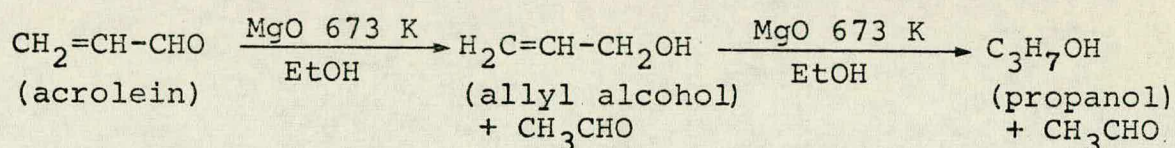
Catalyst Activity	Initial Product Distribution	
	% 2-Methylbut-1-ene	% 2-Methylbut-2-ene
Normal	75	25
Activated	40	60
Equilibrium	28	72

These results might imply that the catalyst has been activated for the direct formation of 2-methylbut-2-ene which may mean a change in the mechanism for the dehydration of the catalyst. However it is more likely that the subsequent isomerisation of 2-methylbut-1-ene is now occurring so quickly that the effect of the length of

alcohol residence time on the catalyst surface is much reduced. This is particularly the case since tertiary carbonium ions would be involved with the isomerisation of 2-methylbut-1-ene. The isomerisation of methylbutenes has not been investigated over rutile but the isomerisation of 2,3-dimethylbut-1-ene³⁷ and the migration of the double bond in the reactions of $\text{CD}_2\text{C}(\text{CH}_3)_2$ over rutile¹²¹ are believed to occur via tertiary carbonium ion intermediates and both take place at fast rates over a temperature range as low as 250-283 K.

It is interesting to note during the decomposition of pentan-1-ol over the very active rutile sample (Fig. 4.30) which occurred at temperatures approximately 50 K below those required for pentanal production, that no pentane was observed which implies a connection between the production of pentanal and pentane. Direct hydrogenation of the alkenes, however, using hydrogen released during the aldehyde production, is not likely since it has been found that a temperature of about 630 K is required for such a reaction⁴³. Balandin et al¹²² found that the formation of ethane from ethanol over TiO_2 between 623 K and 683 K occurred solely by hydrogenolysis of the alcohol and not by hydrogenation of ethene. These temperatures, however, are even higher than those required for direct hydrogenation and about 100 K higher than the temperatures required for pentan-1-ol decomposition as described in this thesis. Halliday et al⁴⁶ found that the hydrogenation of butadiene to butene over rutile occurred at 470 K and accompanied the loss of the hydrocarbon from the gas phase to the surface. On the surface, the diene formed an oligomeric residue which supplied the hydrogen

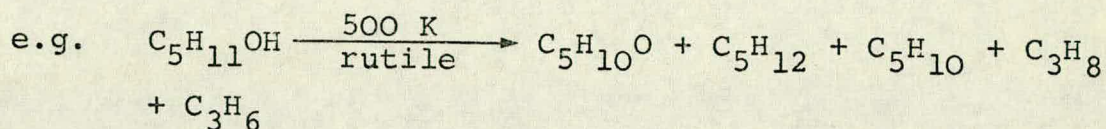
for the reaction to proceed. Aldehydes and ketones are also readily lost to a rutile surface (see reference 36 and Chapter 5) and thus may also be capable of providing a supply of hydrogen for pentane formation. A hydrogen transfer mechanism from the alcohol to the alkene during the formation of the aldehyde offers another possible explanation for the formation of pentane. Ballard, Finch and Winkler¹²³ have reported that acrolein can be hydrogenated to allyl alcohol with hydrogen transfer from ethanol over oxides which are inactive during direct hydrogenation reactions. Propanol was also identified as one of the products of the reaction as follows:-



The ability of alcohols to act as a source of hydrogen has also been noted by Kibby and Hall⁷³ who, working with hydroxy apatite catalysts, concluded that the catalytic sites which were active for alcohol dehydrogenation were also those associated with hydrogen transfer. This situation seems very similar to that reported here where if no pentanal is produced, no pentane appears among the final products.

To confirm that a hydrogen transfer reaction is occurring it is suggested that future work over rutile may include an experiment in which an alkene is inserted into the reaction mixture along with the reacting alcohol. The added compound should, when hydrogenated, form a compound which cannot be formed directly from the main

reacting alcohol. The detection of such a compound in the product mixture would therefore imply the existence of a hydrogen transfer mechanism.



The products after the insertion of gaseous deuterium into the reaction mixture would then exclude direct hydrogenation if no deuterium appeared in the hydrocarbon products.

4.7 Conclusions

The general conclusion is that the dehydration of primary and secondary alcohols over rutile involves partially positively charged intermediates i.e. the elimination has more of an E1 character than the truly concerted E2 elimination which is thought to occur over alumina. Experimental evidence suggests the participation of the hydrogen on the γ -carbon relative to the hydroxyl group in the formation of some alkene species in the product mixture although subsequent isomerisation of initially formed products to such species is also thought to occur.

Repeating certain experiments showed that (1) dehydrogenation of an alcohol does not occur on the same sites as dehydration and dehydrogenation always requires high temperatures, (2) although qualitatively the decomposition of the alcohols over rutile is experimentally reproducible, quantitative reproducibility of the results

on the flow system requires the use of fresh catalyst samples for each experiment as ageing/use of the rutile samples resulted in an increase in their activity for dehydration though not for dehydrogenation.

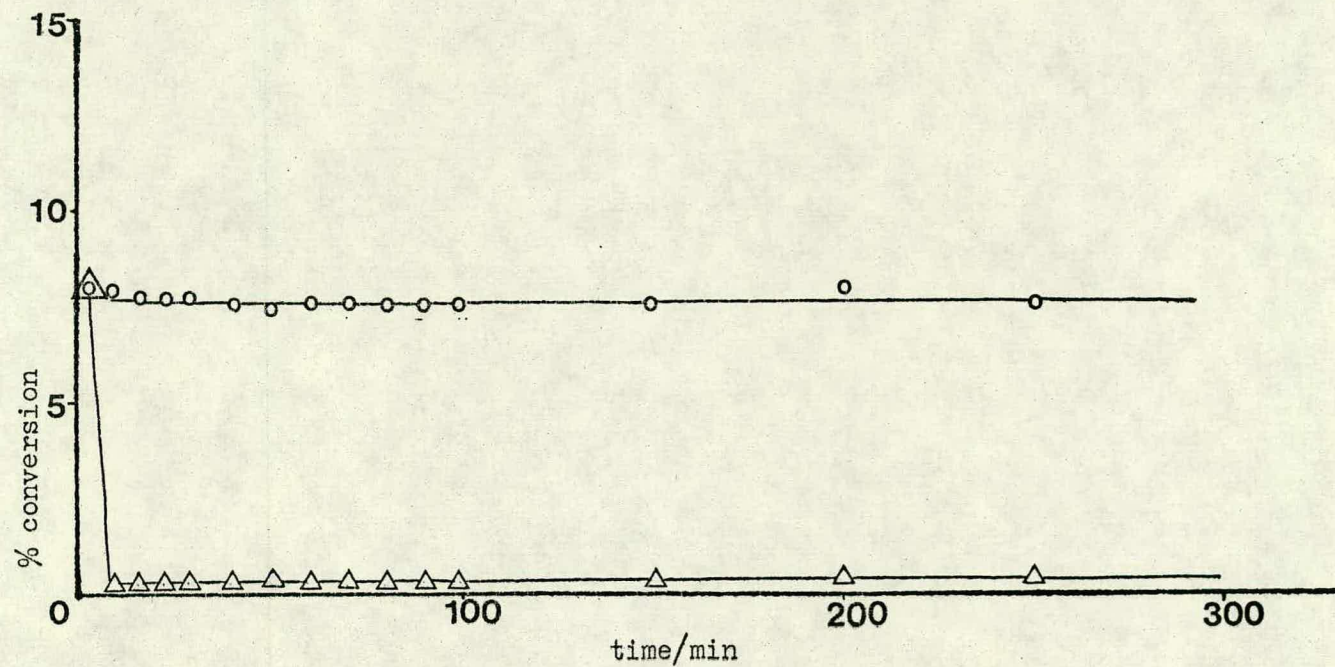


figure 4.1 decomposition of propan-2-ol on the flow system:
% conversion v time: propene o; acetone Δ.

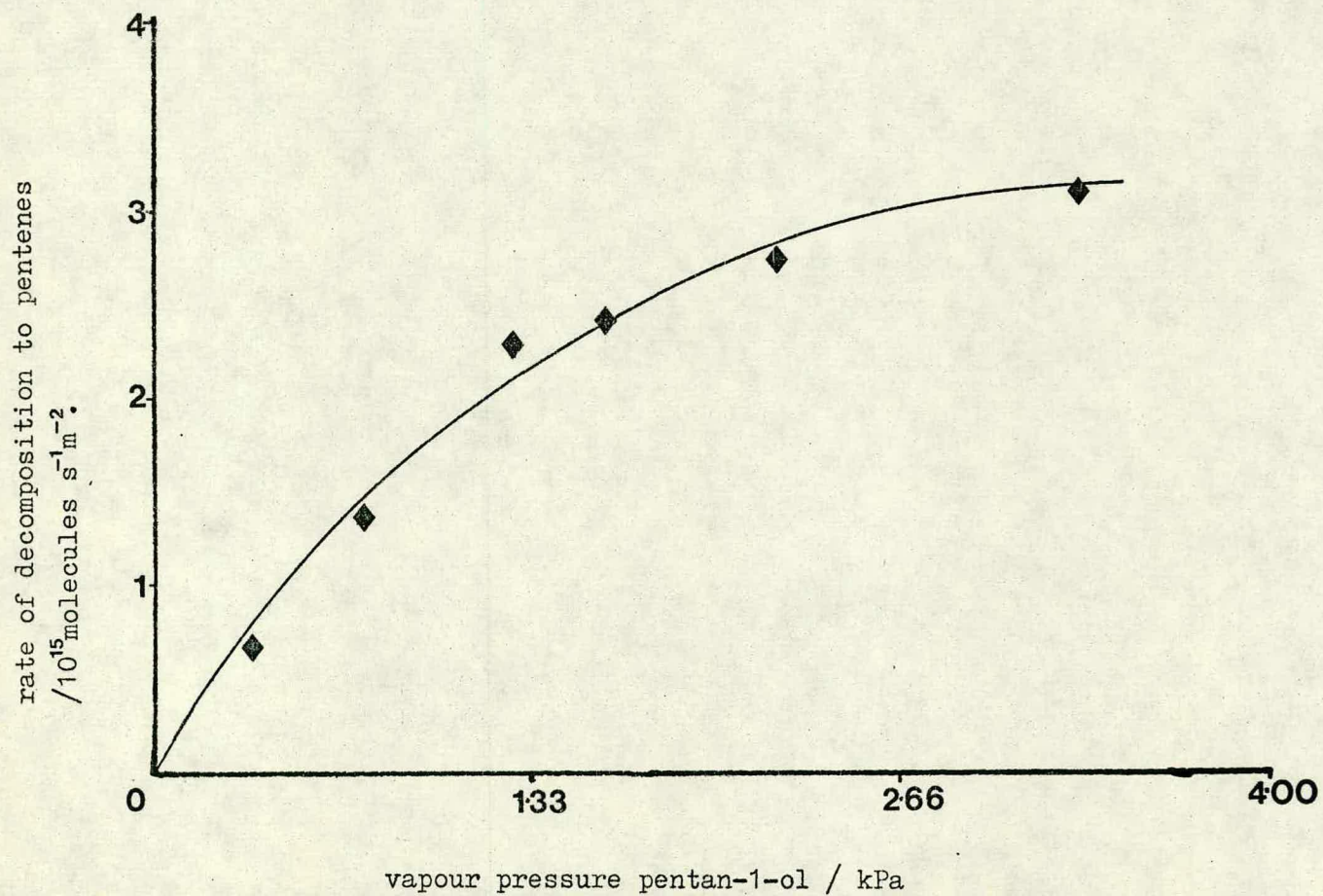
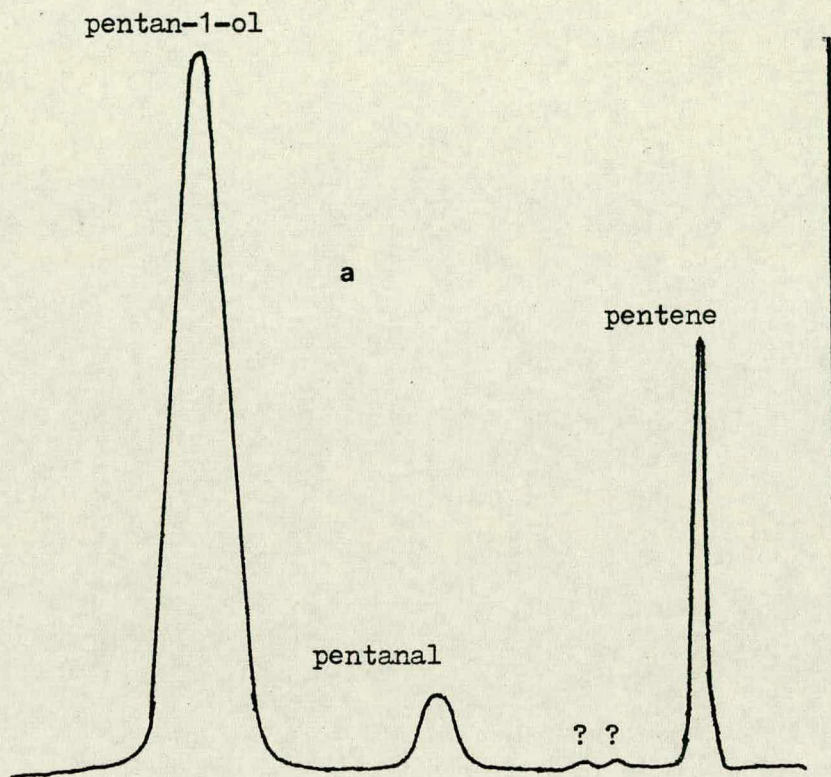


figure 4.2 variation of rate of dehydration of pentan-1-ol with vapour pressure of the alcohol.

reaction temperature=550K.



- 1 pentane
- 2 pent-1-ene
- 3 trans-pent-2-ene
- 4 cis-pent-2-ene
- 5 ?

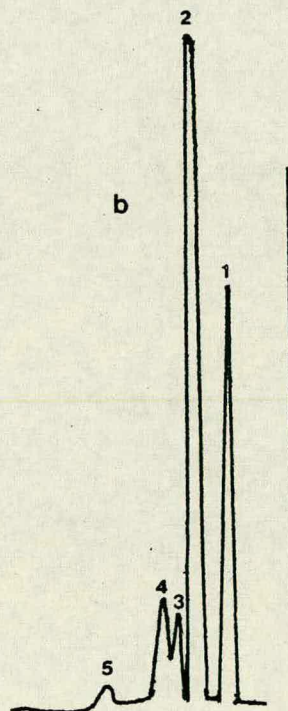
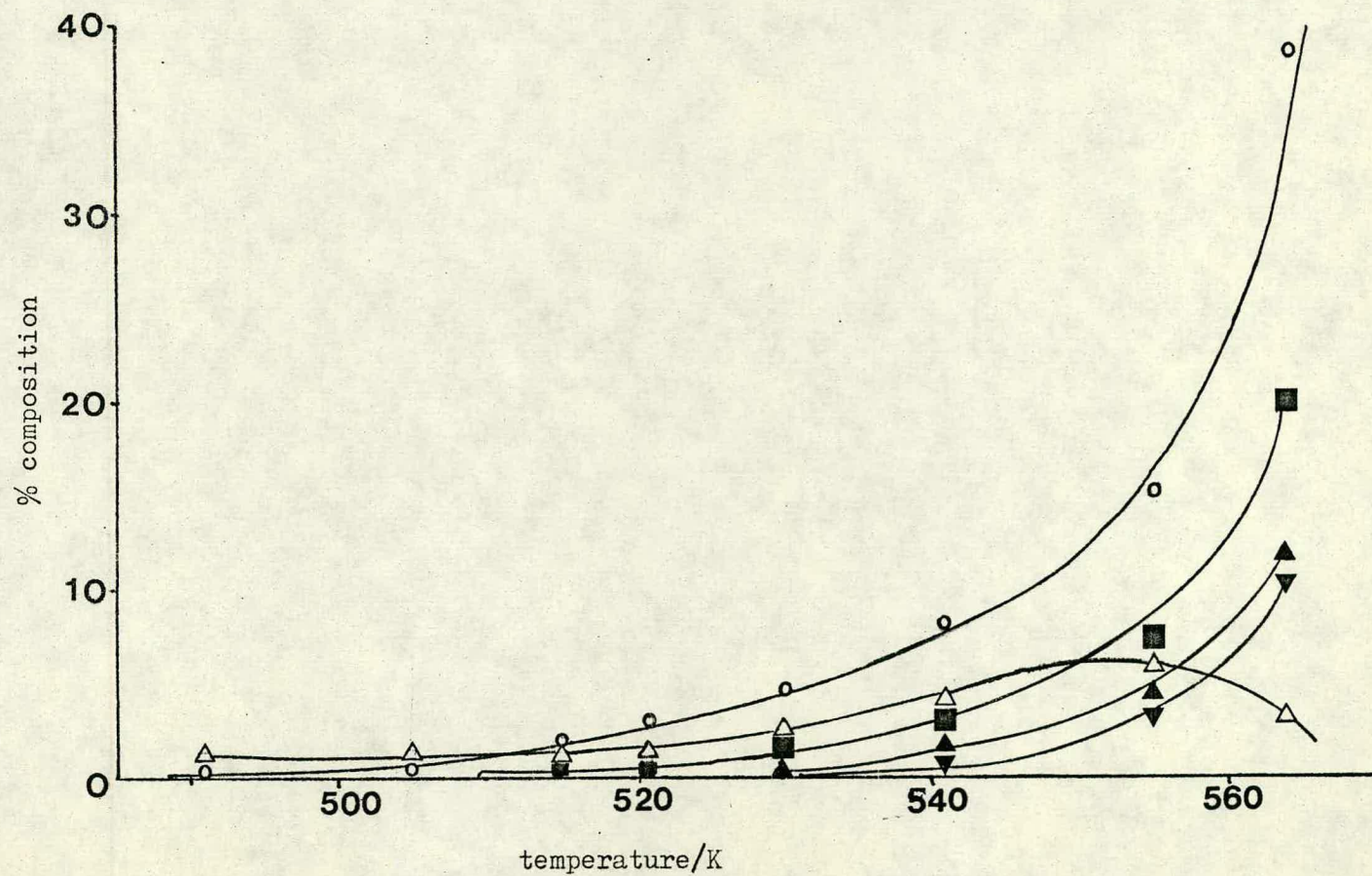


figure 4.3(a) G.C. trace of the decomposition of pentan-1-ol obtained with the Porapak S column.

figure 4.3(b) G.C. trace of the decomposition of pentan-1-ol obtained with the propylene carbonate on Chromasorb P column.

figure 4.4 decomposition of pentan-1-ol : variation of product distribution with temperature : pent-1-ene, \circ ; pentane, \blacksquare ; cis-pent-2-ene, \blacktriangle ; trans-pent-2-ene, \blacktriangledown ; pentanal, \triangle . (flow rate = $5 \times 10^{-7} \text{ m}^3 \text{ s}^{-1}$.)



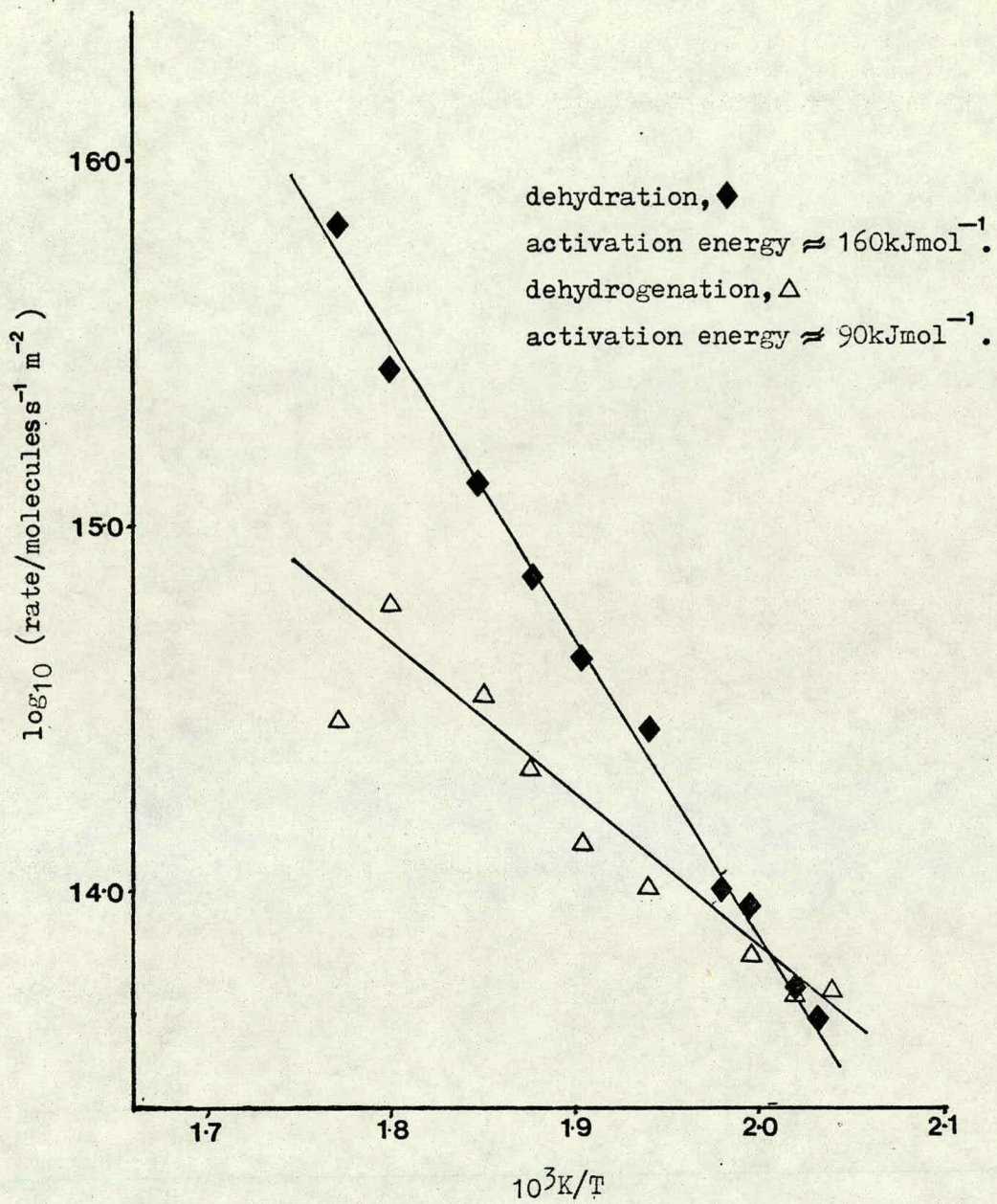
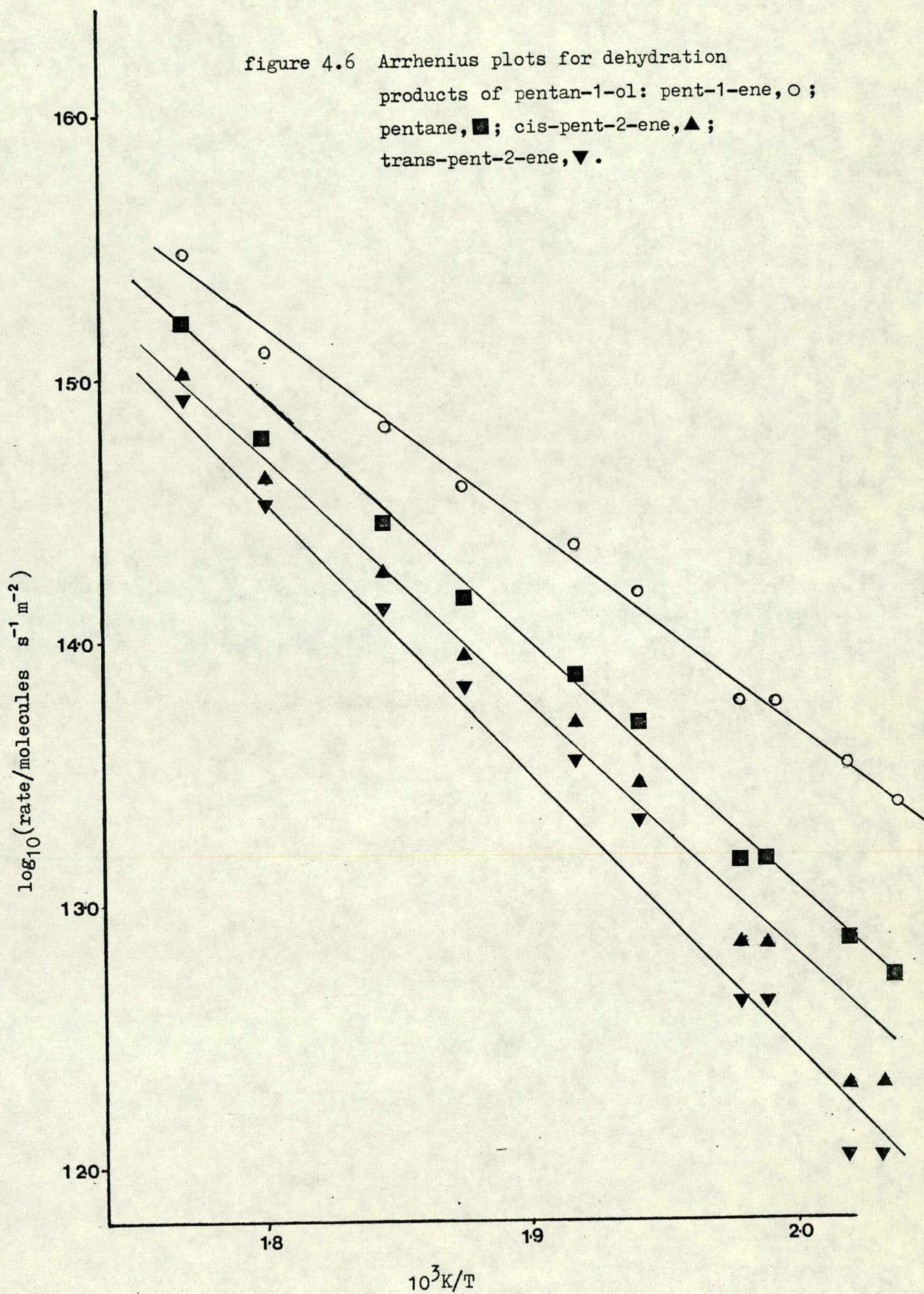


figure 4.5 Arrhenius plot for the overall dehydration of pentan-1-ol \blacklozenge and for the dehydrogenation of pentan-1-ol \triangle .

figure 4.6 Arrhenius plots for dehydration products of pentan-1-ol: pent-1-ene, \circ ; pentane, \blacksquare ; cis-pent-2-ene, \blacktriangle ; trans-pent-2-ene, \blacktriangledown .



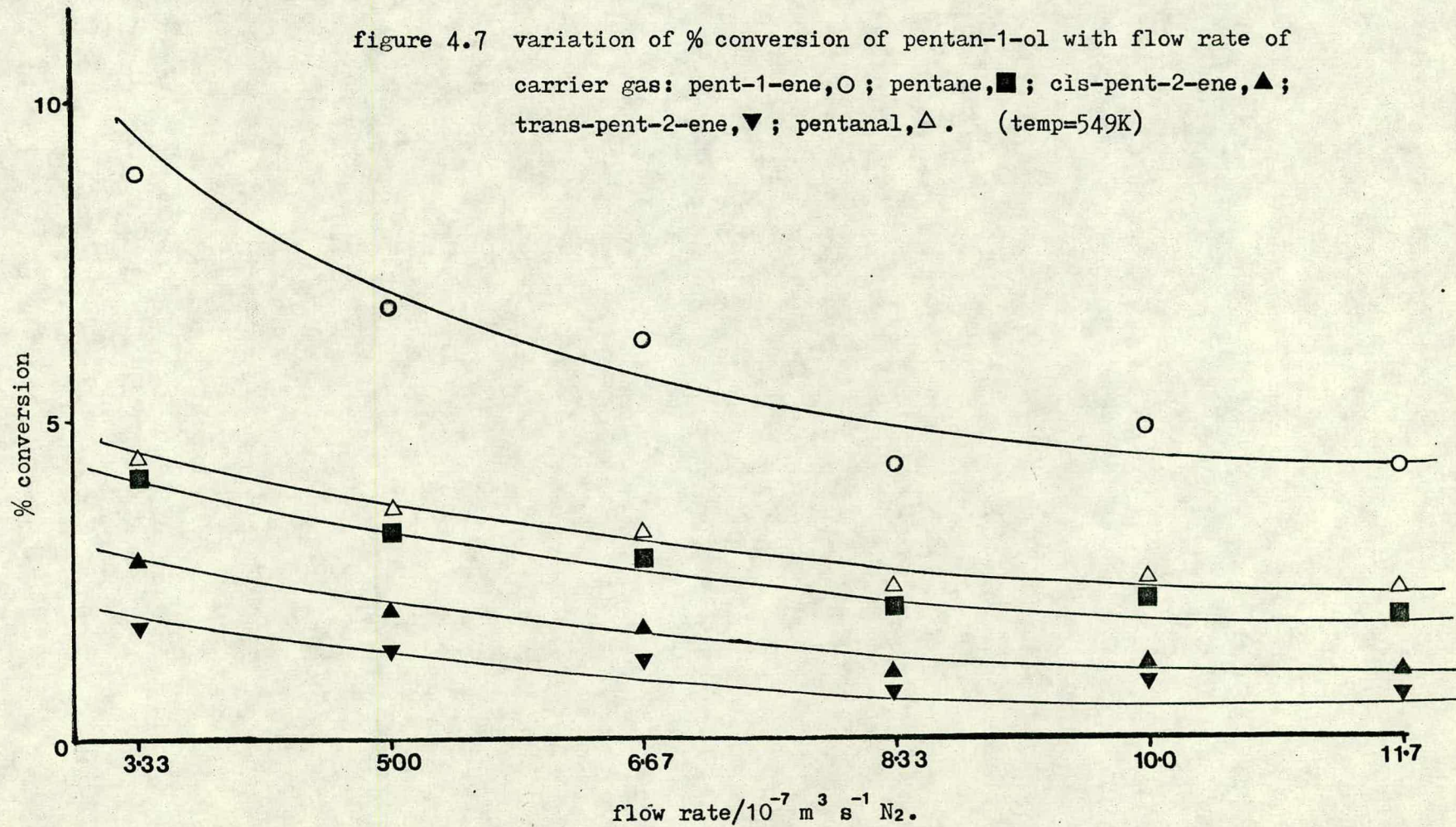
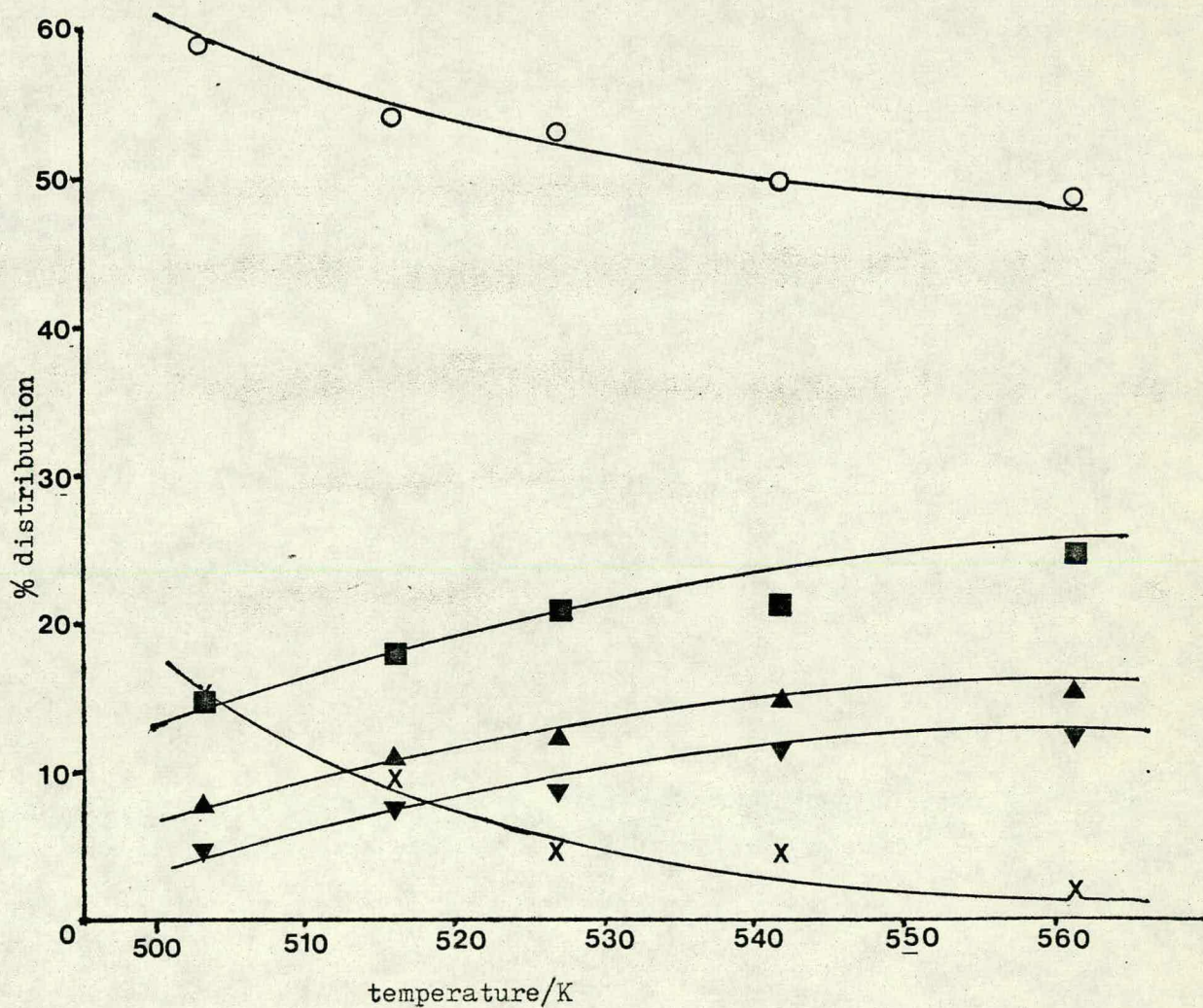


figure 4.8 variation of % distribution of dehydration products of pentan-1-ol decomposition with temperature: pent-1-ene, ○; pentane, ■; cis-pent-2-ene, ▲; trans-pent-2-ene, ▼; unknown, X.

(flow rate = $5 \times 10^{-7} \text{ m}^3 \text{ s}^{-1}$)



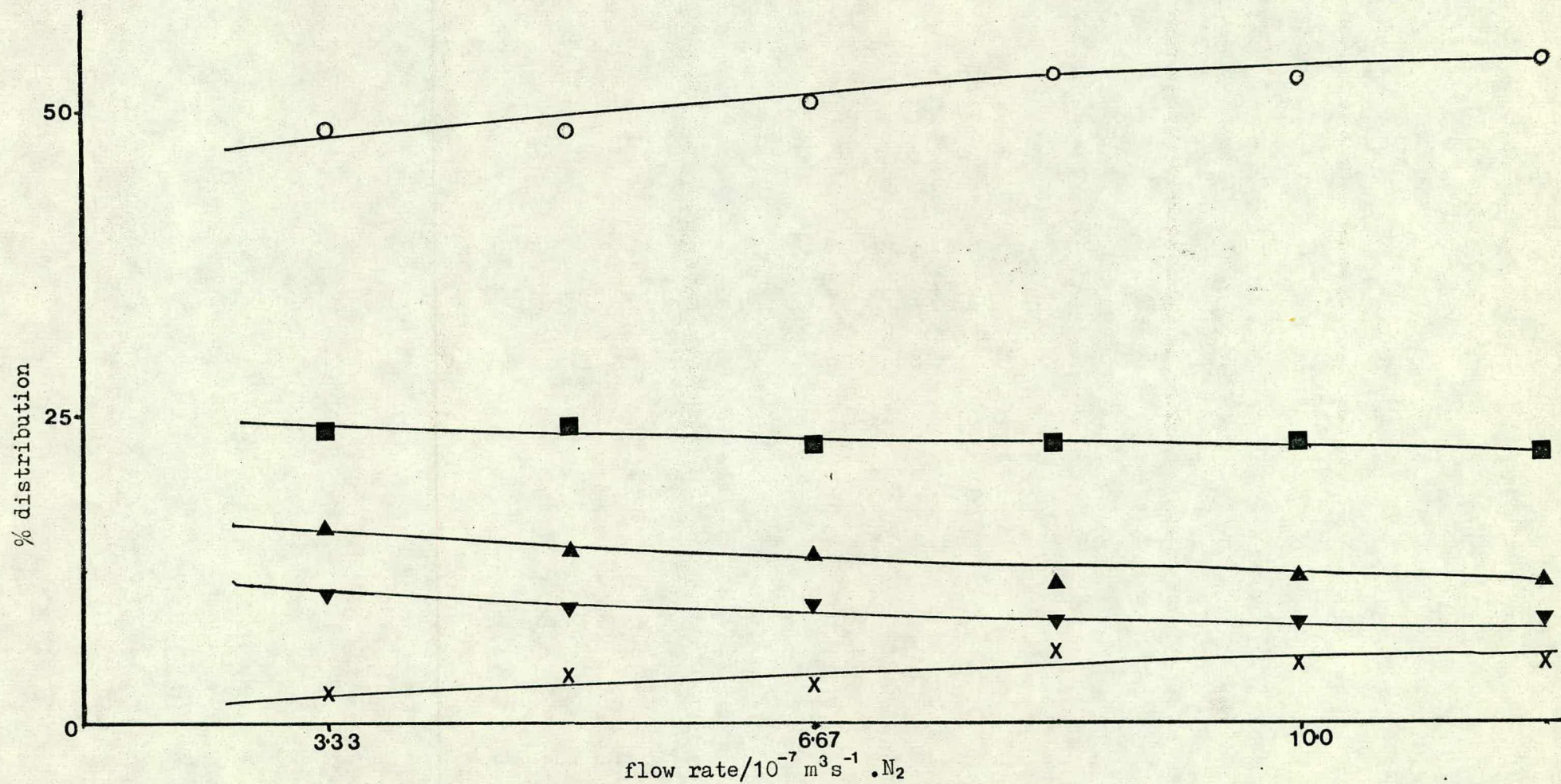


figure 4.9 variation of % distribution of dehydration products of pentan-1-ol decomposition with flow rate of carrier gas : pent-1-ene, O; pentane, ■; cis-pent-2-ene, ▲; trans-pent-2-ene, ▼; unknown, X. (temp = 549K)

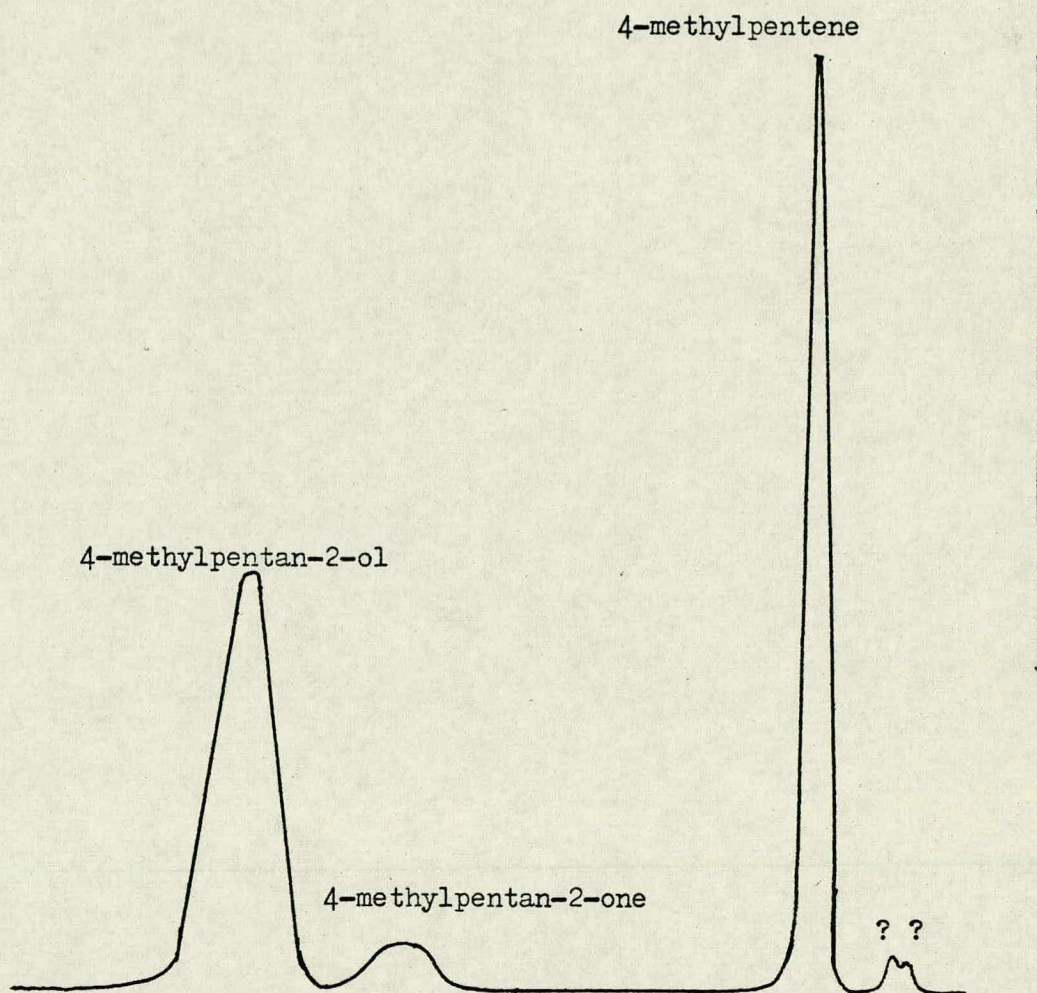
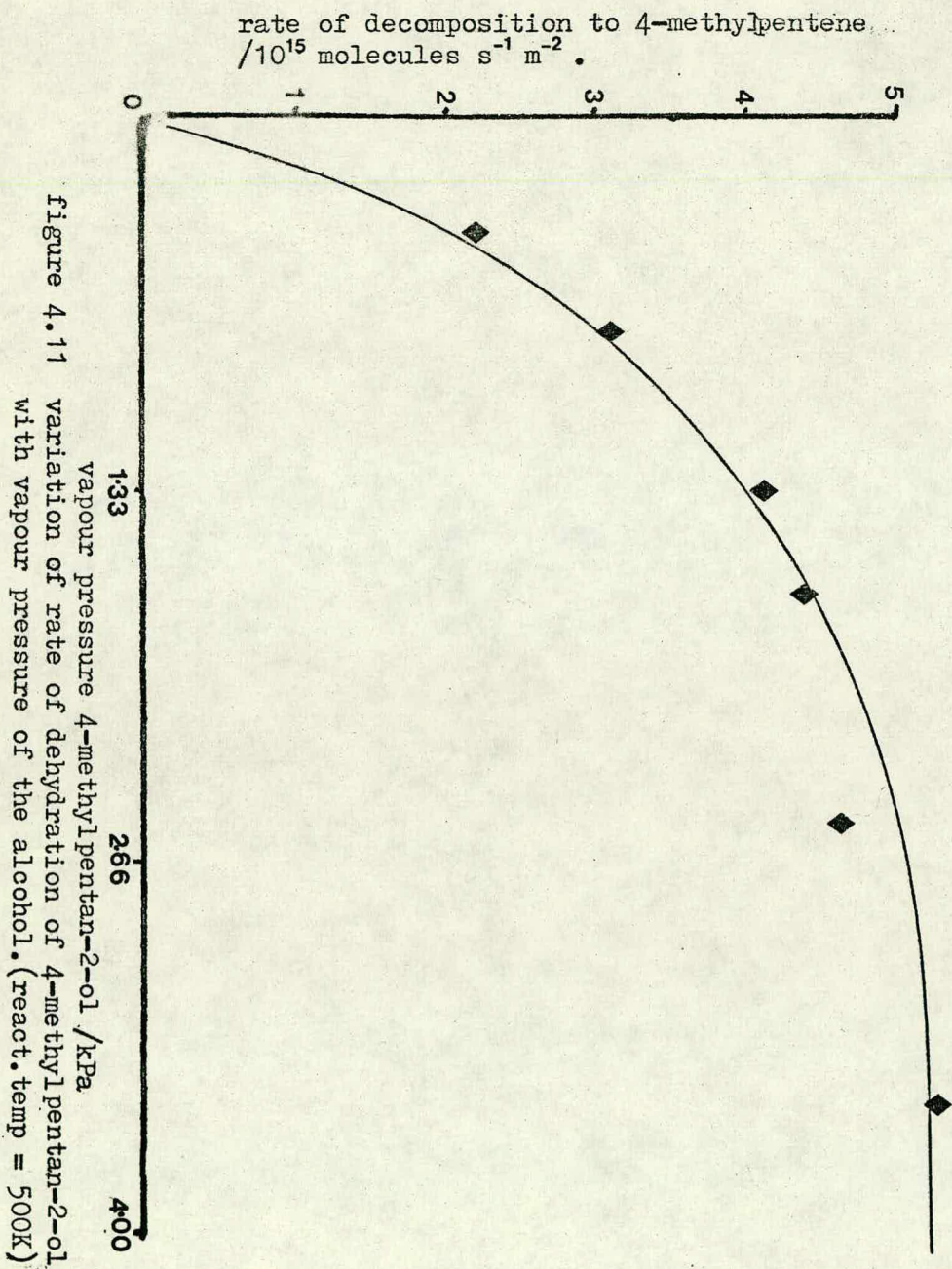


figure 4.10 G.C. trace of the decomposition of 4-methylpentan-2-ol
obtained with the Porapak S column.



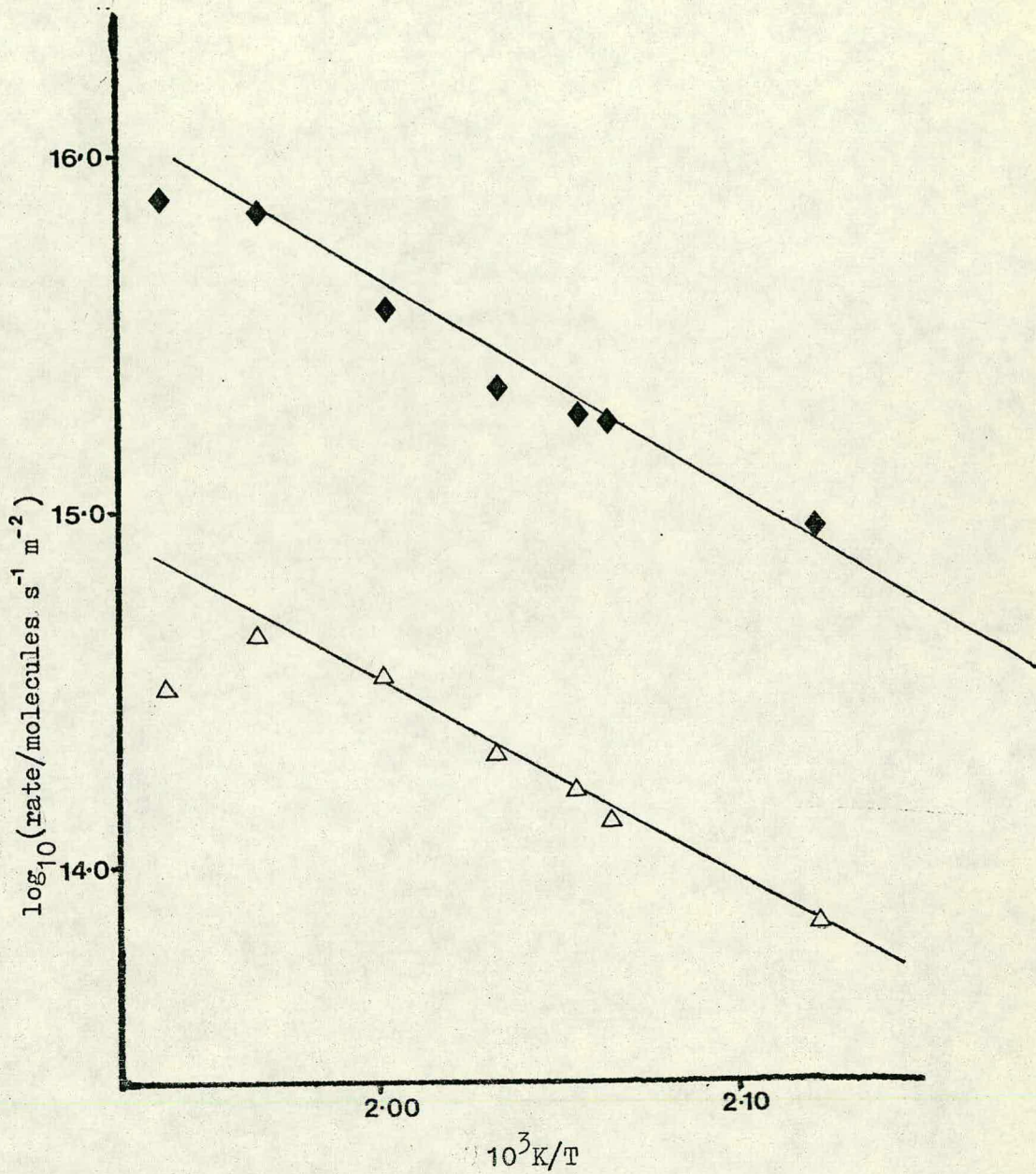


figure 4.12 Arrhenius plot for the decomposition of 4-methylpentan-2-ol
 dehydration, ◆; dehydrogenation, △;
 dehydration activation energy $\approx 110 \text{ kJmol}^{-1}$.
 dehydrogenation activation energy $\approx 100 \text{ kJmol}^{-1}$.

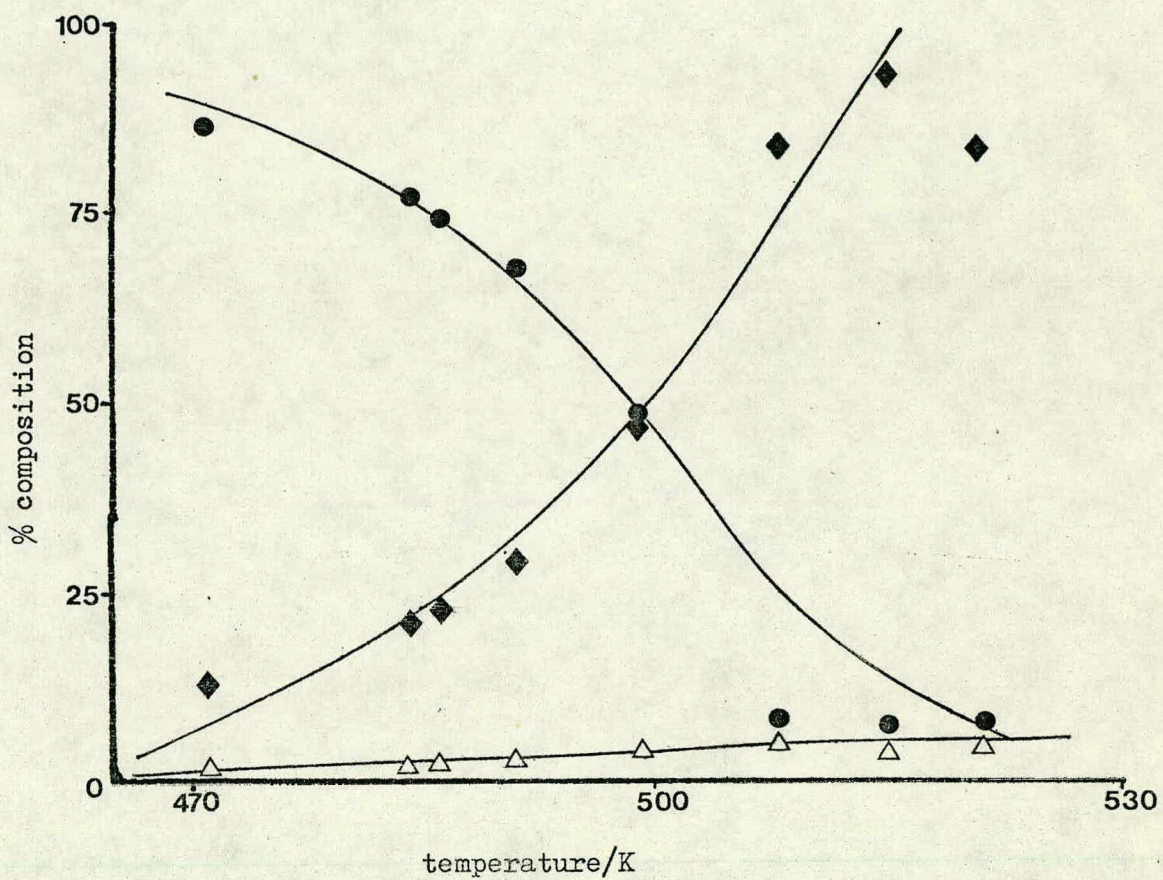


figure 4.13 decomposition of 4-methylpentan-2-ol: variation product distribution with temperature:
 4-methylpentene, \blacklozenge ; 4-methylpentan-2-one, \triangle .
 (flow rate = $5 \times 10^{-7} \text{ m}^3 \text{ s}^{-1}$.)

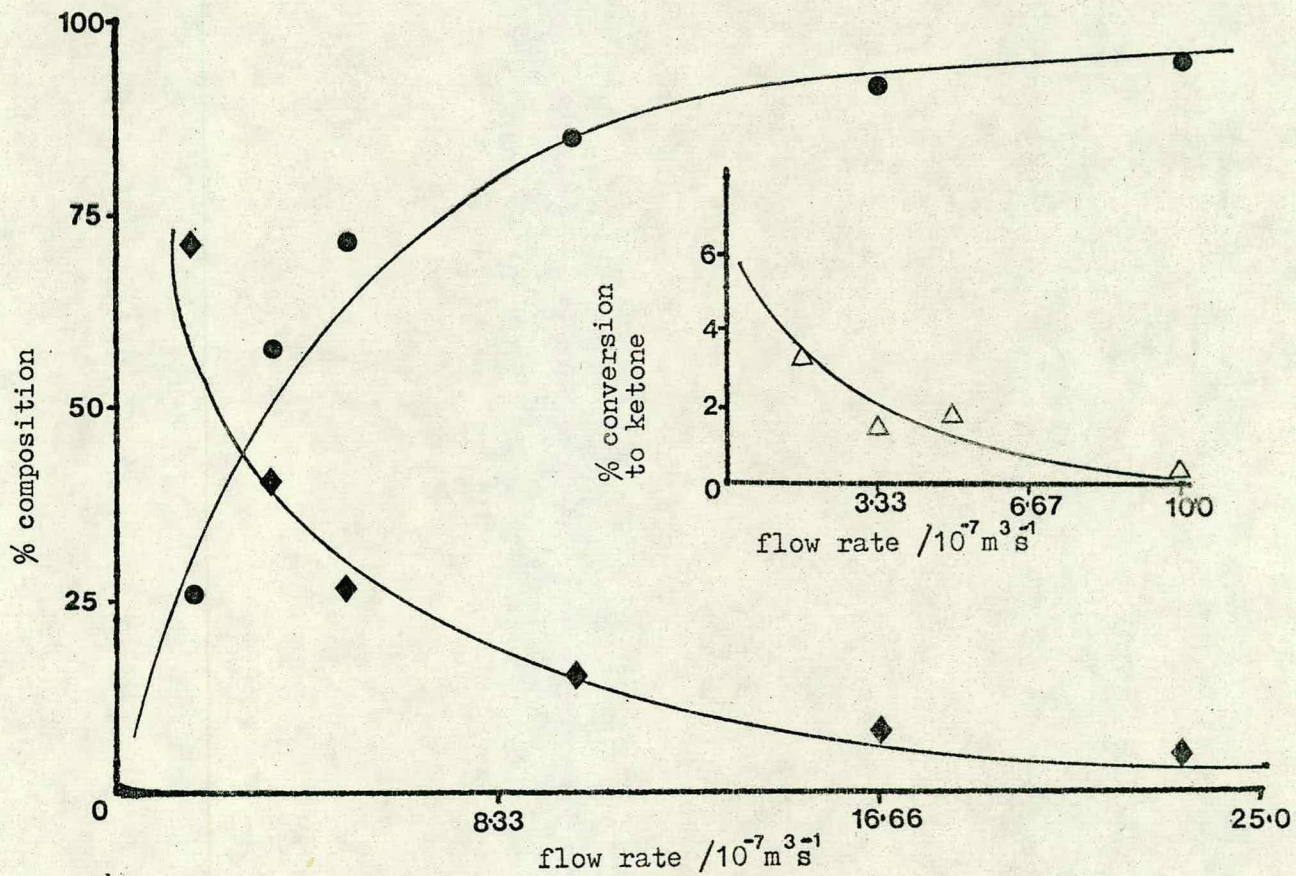
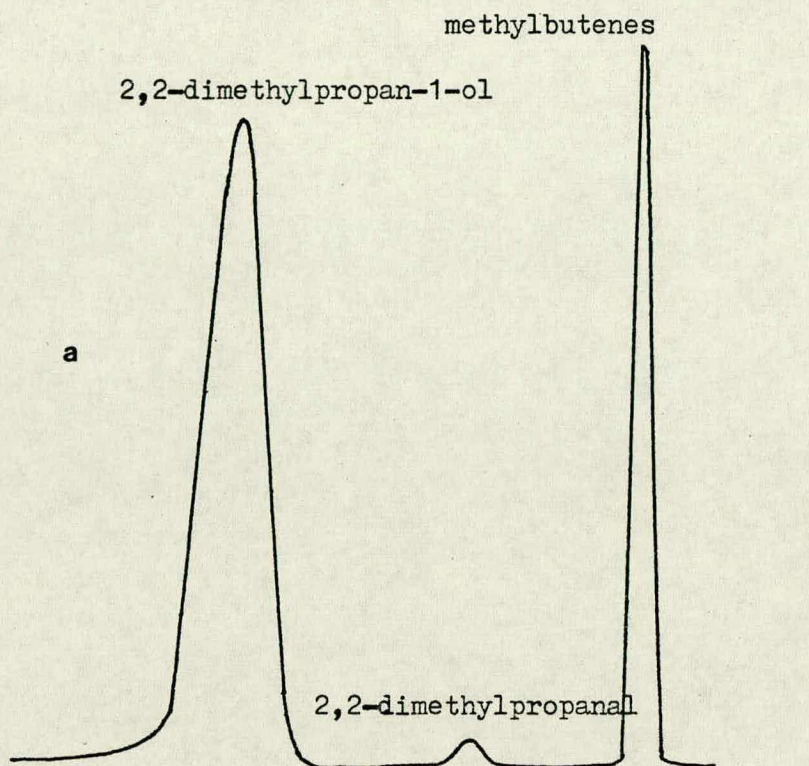


figure 4.14 decomposition of 4-methylpentan-2-ol: variation product distribution with rate of flow of carrier gas: 4-methylpentan-2-ol, ●; 4-methylpentene, ◆; 4-methylpentan-2-one, △. (react. temp. = 489K)



1,1-dimethylcyclopropane or
 13-methylbut-1-ene.
 22-methylbut-1-ene.
 32-methylbut-2-ene.

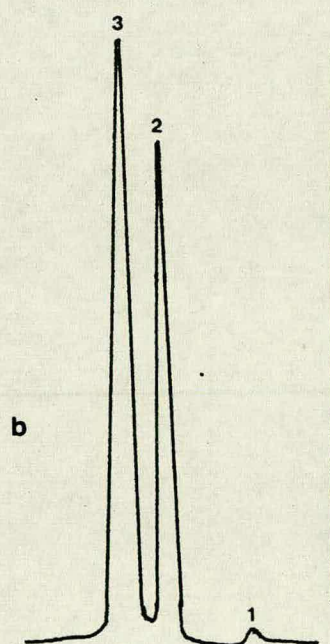


figure 4.15(a) G.C. trace of the decomposition of 2,2-dimethylpropan-1-ol obtained with the Porapak S column.

figure 4.15(b) G.C. trace of the decomposition of 2,2-dimethylpropan-1-ol obtained with the propylene carbonate on Chromasorb P column.

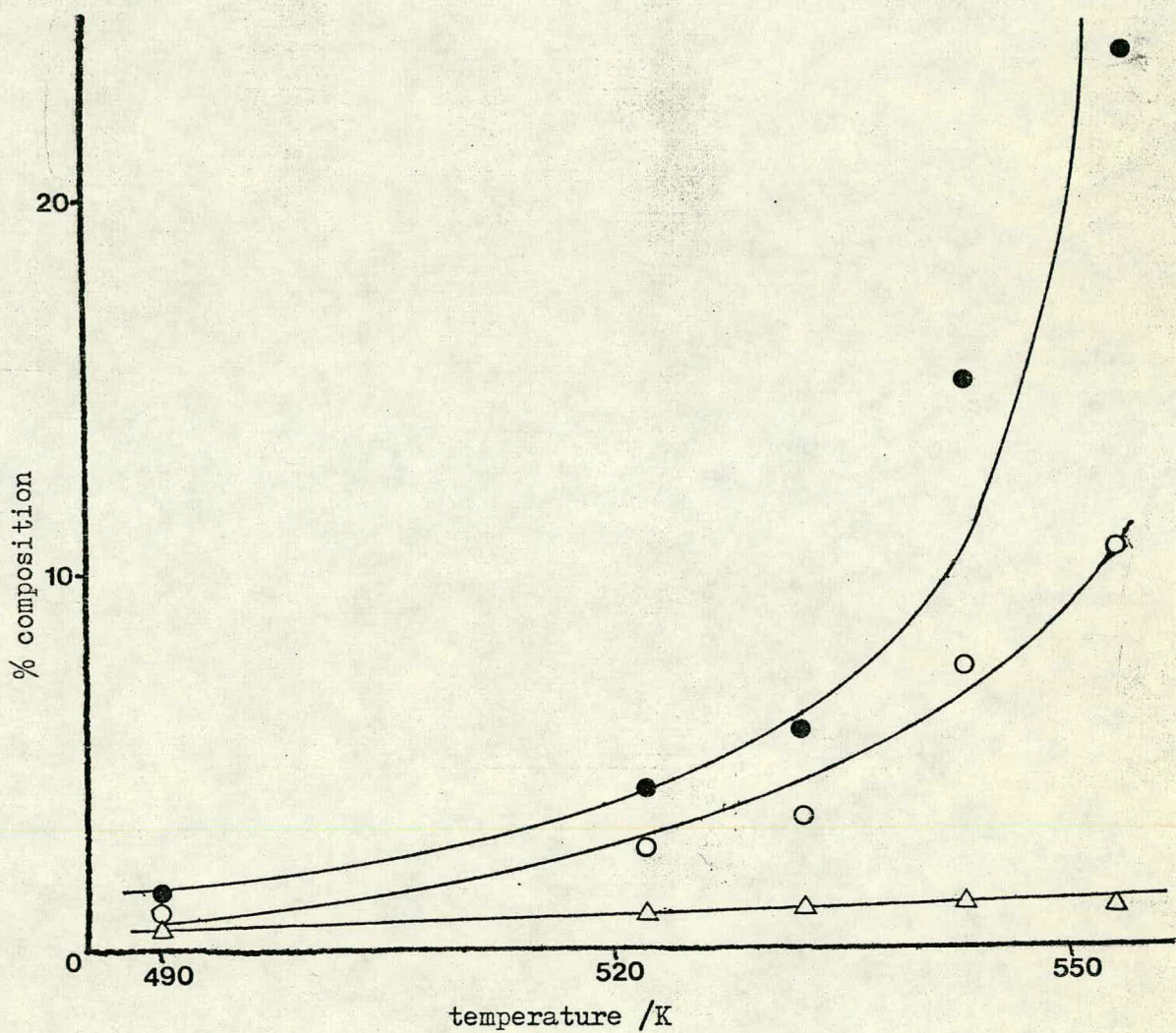
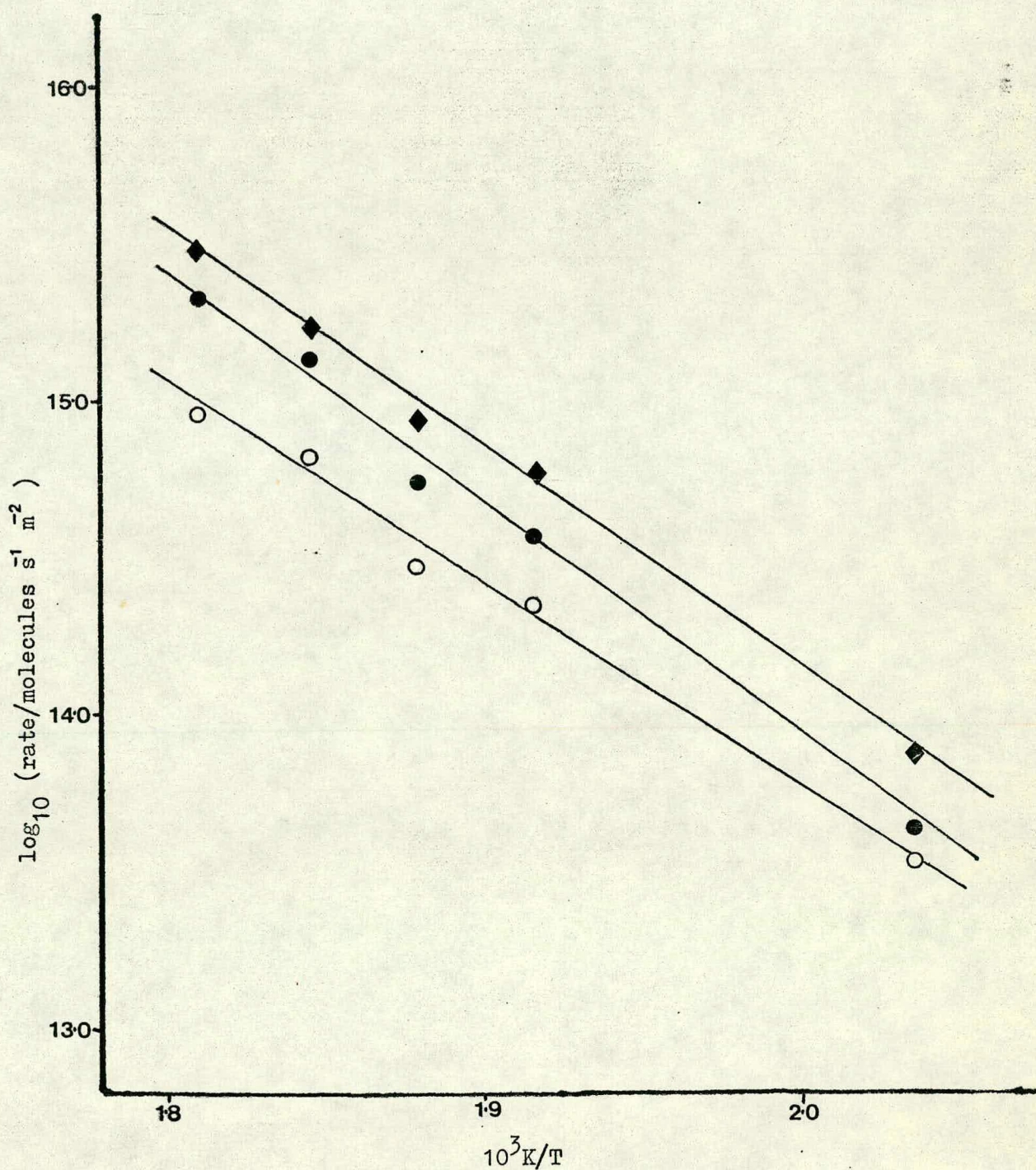


figure 4.16 decomposition of 2,2-dimethylpropan-1-ol:
 variation of product distribution with temperature:
 2-methylbut-2-ene, ●; 2-methylbut-1-ene, ○;
 2,2-dimethylpropanal, △.

flow rate = $5 \times 10^{-7} \text{ m}^3 \text{ s}^{-1}$.

figure 4.17 Arrhenius plots for the dehydration of
2,2-dimethylpropan-1-ol: total dehydration, \blacklozenge ;
2-methylbut-2-ene, \bullet ; 2-methylbut-1-ene, \circ .

activation energy overall decomposition
 $\approx 140 \text{ kJ mol}^{-1}$.



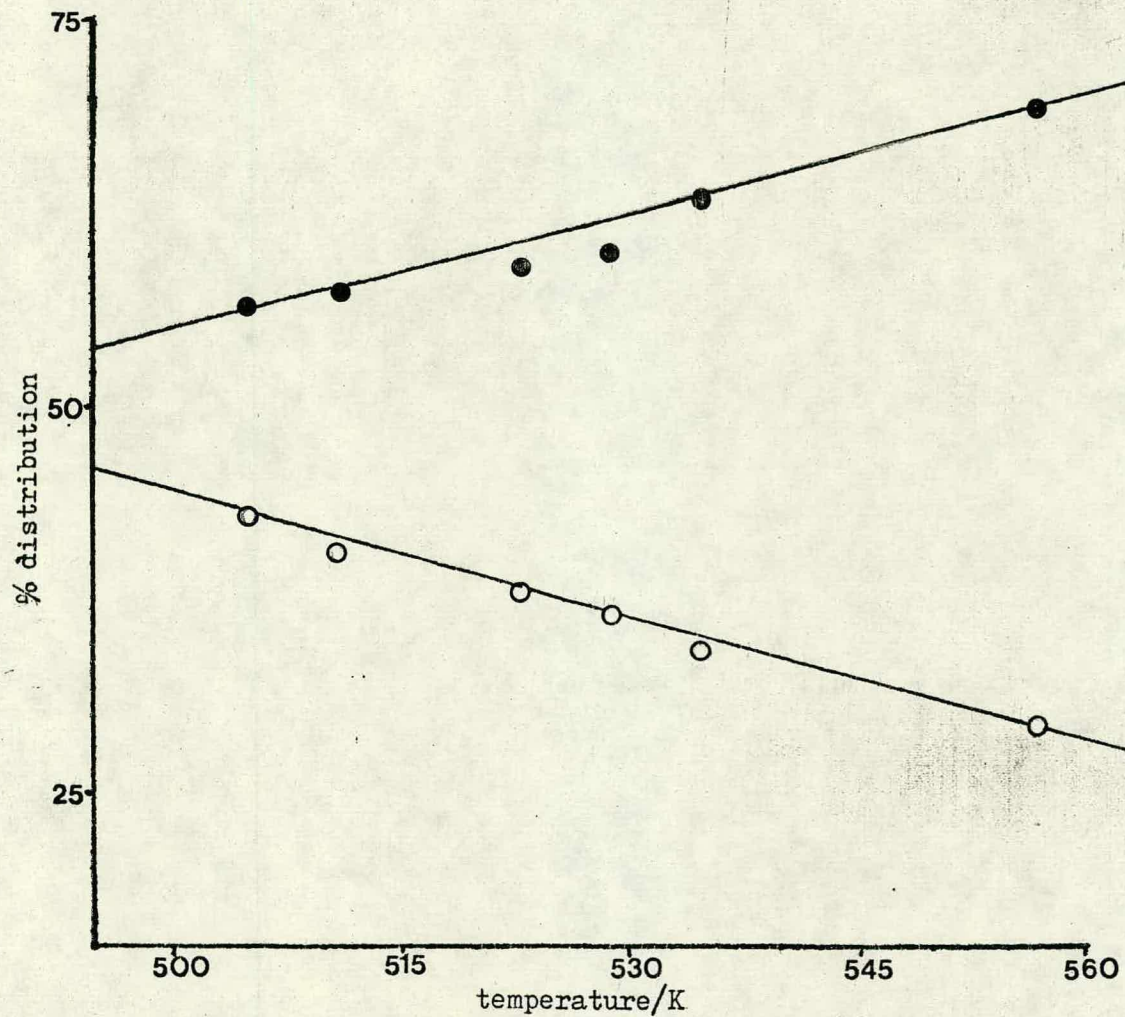


figure 4.18 variation of % distribution of dehydration products of decomposition of 2,2-dimethylpropan-1-ol with temperature: 2-methylbut-2-ene, ●; 2-methylbut-1-ene, ○. (flow rate = $5 \times 10^{-7} \text{ m}^3 \text{ s}^{-1}$)

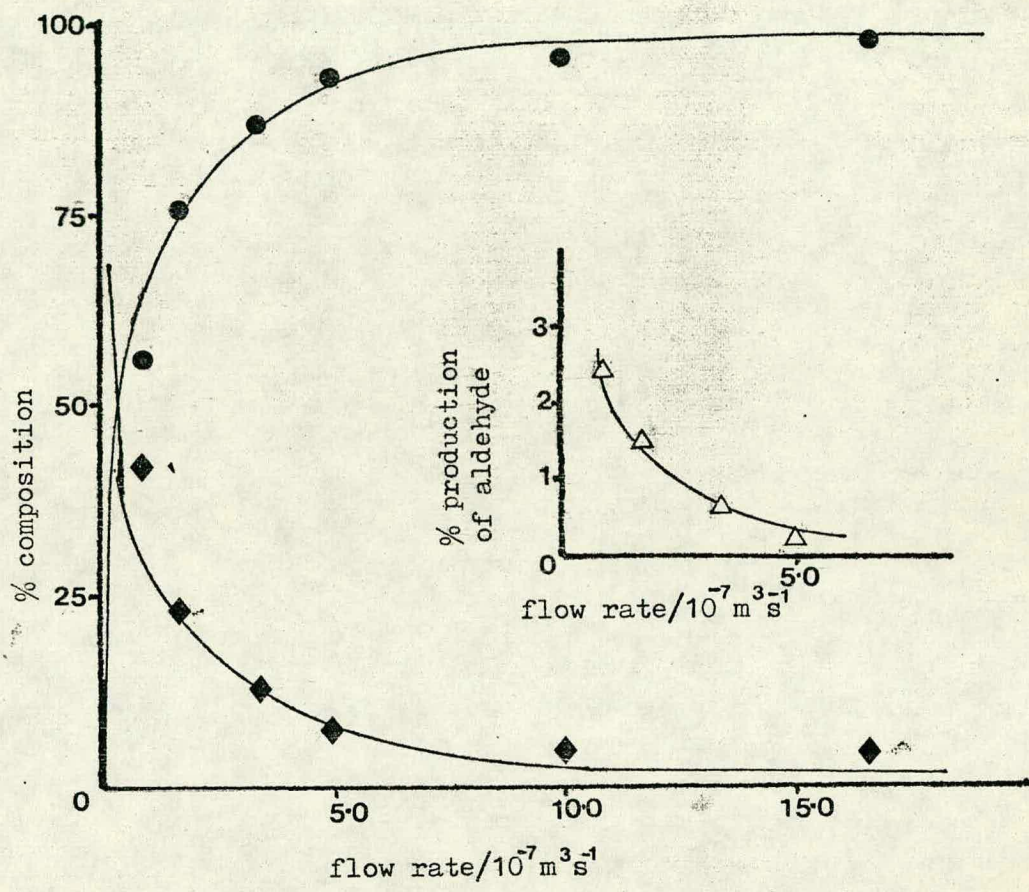
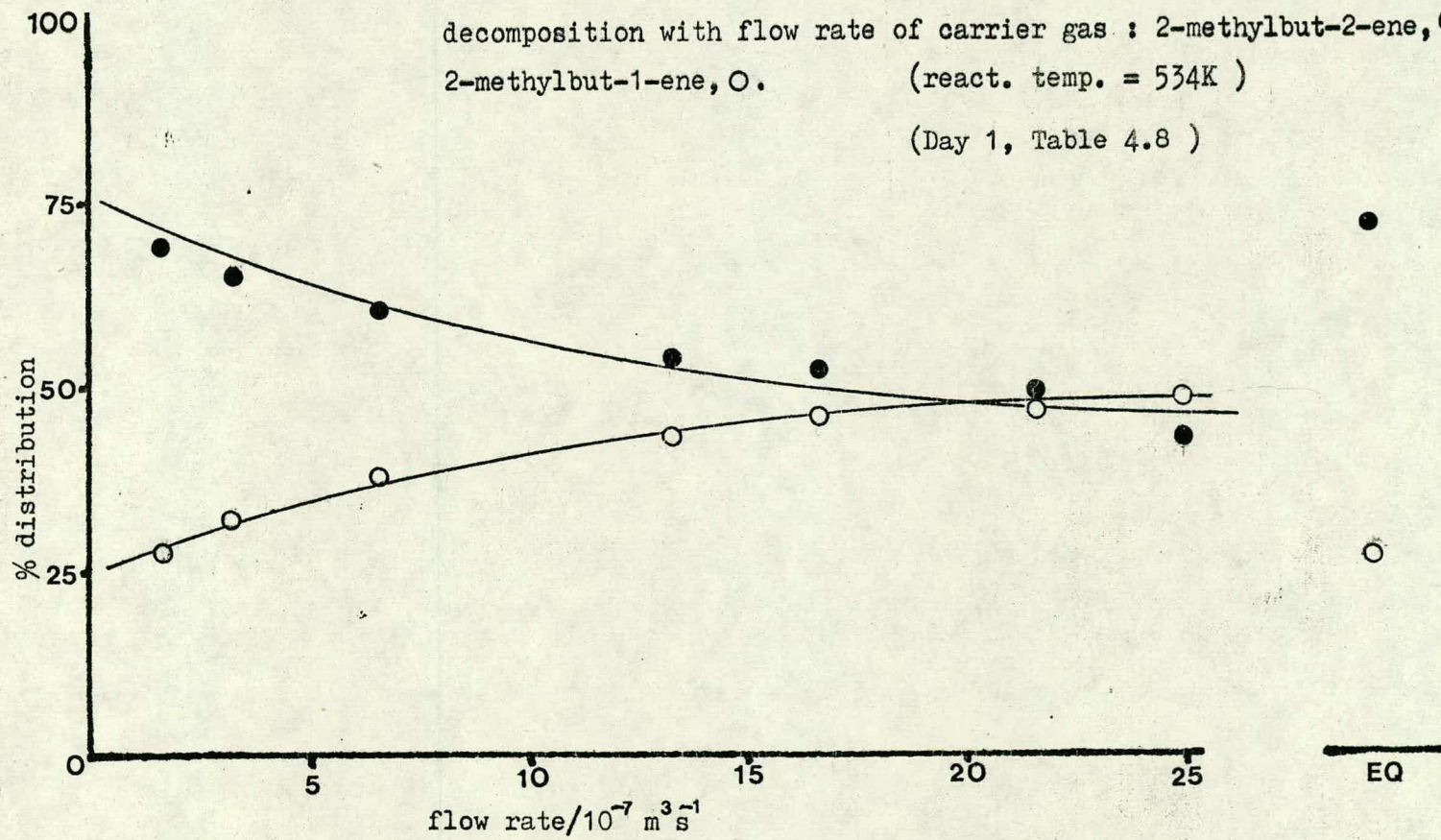


figure 4.19 decomposition of 2,2-dimethylpropan-1-ol:
 variation of product distribution with rate of
 flow of carrier gas:
 2,2-dimethylpropan-1-ol, ● ; methylbutenes, ◆;
 2,2-dimethylpropanal, △. (react. temp. = 522K)

figure 4.20 variation of % distribution of dehydration products of 2,2-dimethylpropan-1-ol decomposition with flow rate of carrier gas : 2-methylbut-2-ene, ●; 2-methylbut-1-ene, ○. (react. temp. = 534K) (Day 1, Table 4.8)



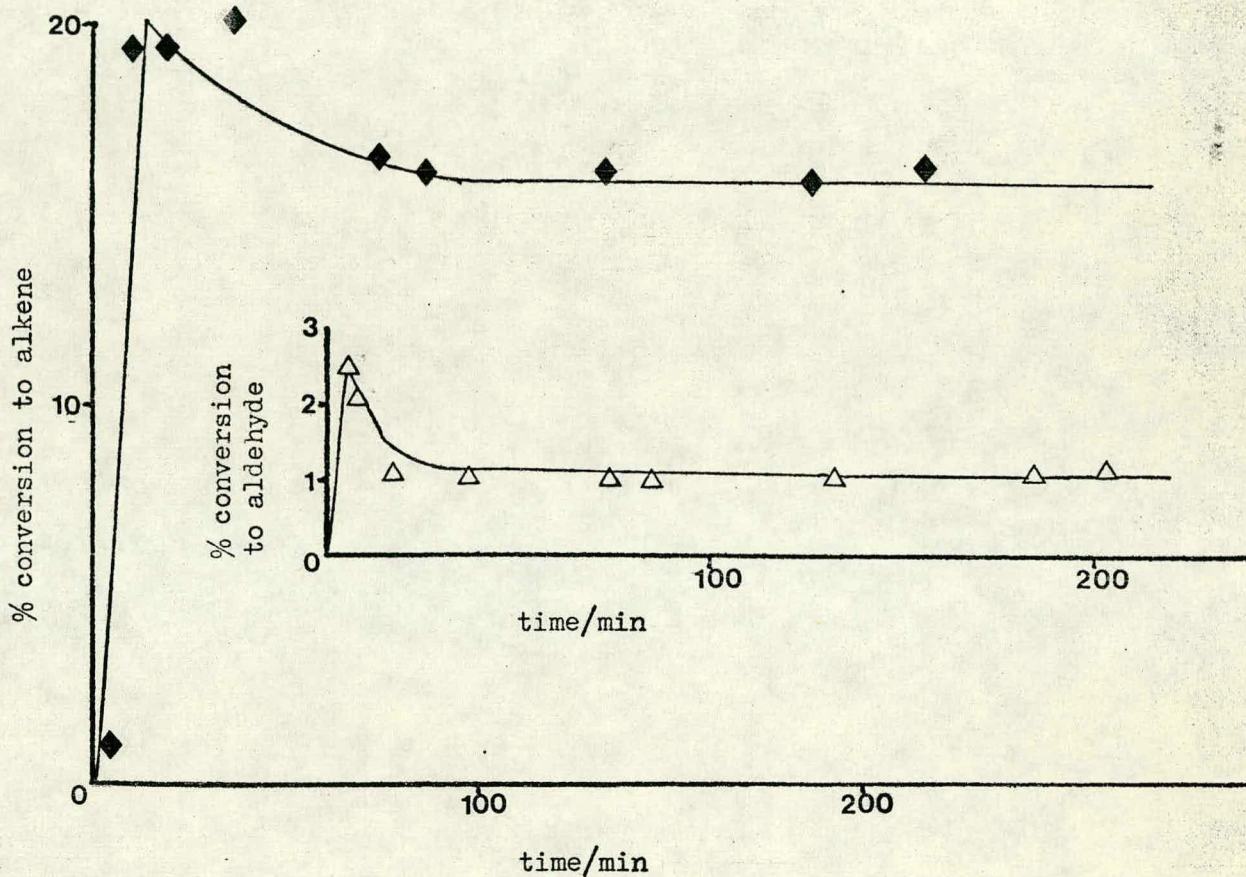


figure 4.21 decomposition of 2,2-dimethylpropan-1-ol:
 % conversion v time: conversion to alkene, ◆;
 conversion to 2,2-dimethylpropanal, △.

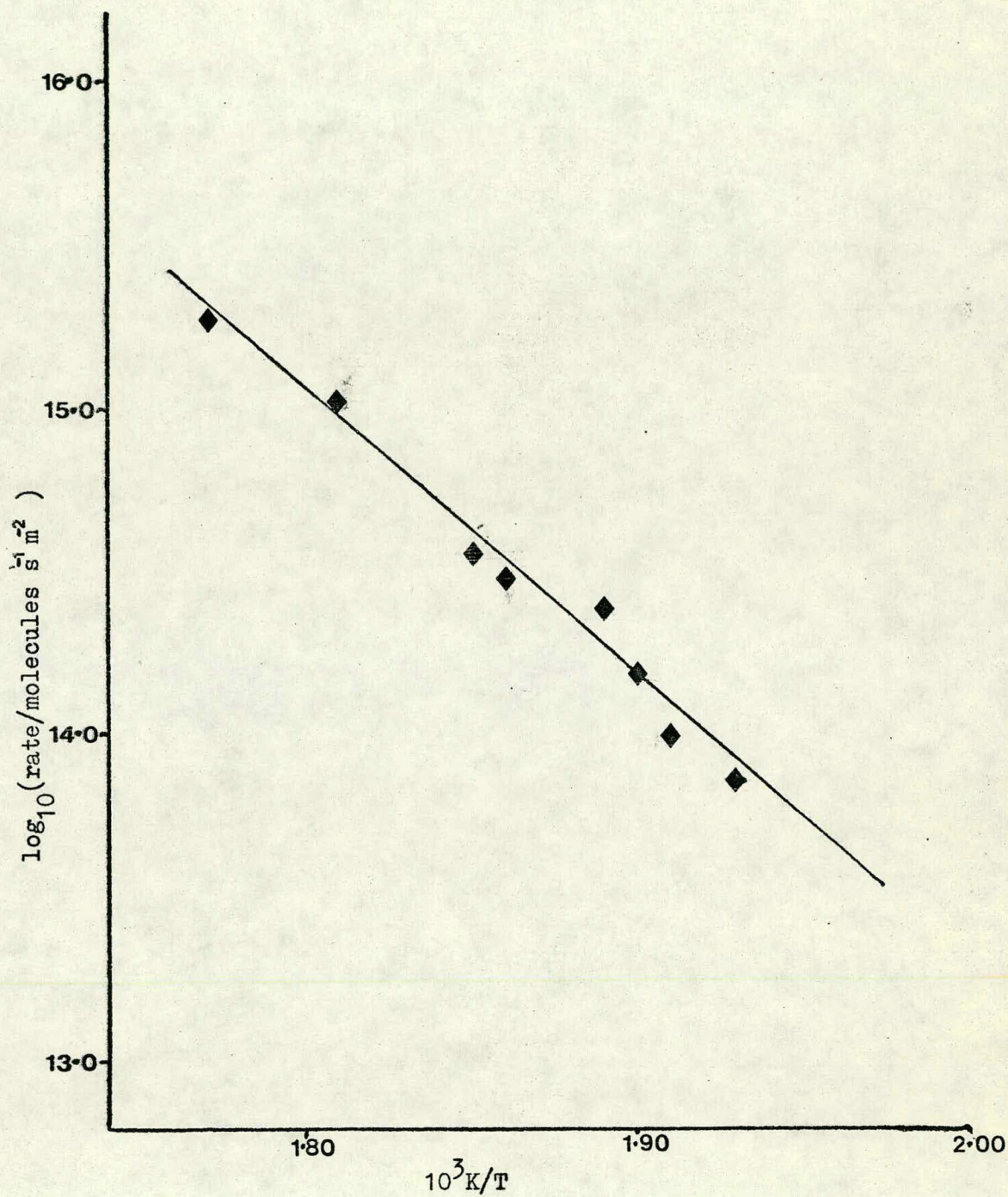


figure 4.22 Arrhenius plot for repeat dehydration of pentan-1-ol.

activation energy $\approx 160 \text{kJmol}^{-1}$.

figure 4.23 repeat of the variation of % distribution of dehydration products of 2,2-dimethylpropan-1-ol decomposition with flow rate of carrier gas: 2-methylbut-2-ene, ●; 2-methylbut-1-ene, ○. (react. temp. = 534K) (Day 8, Table 4.8)

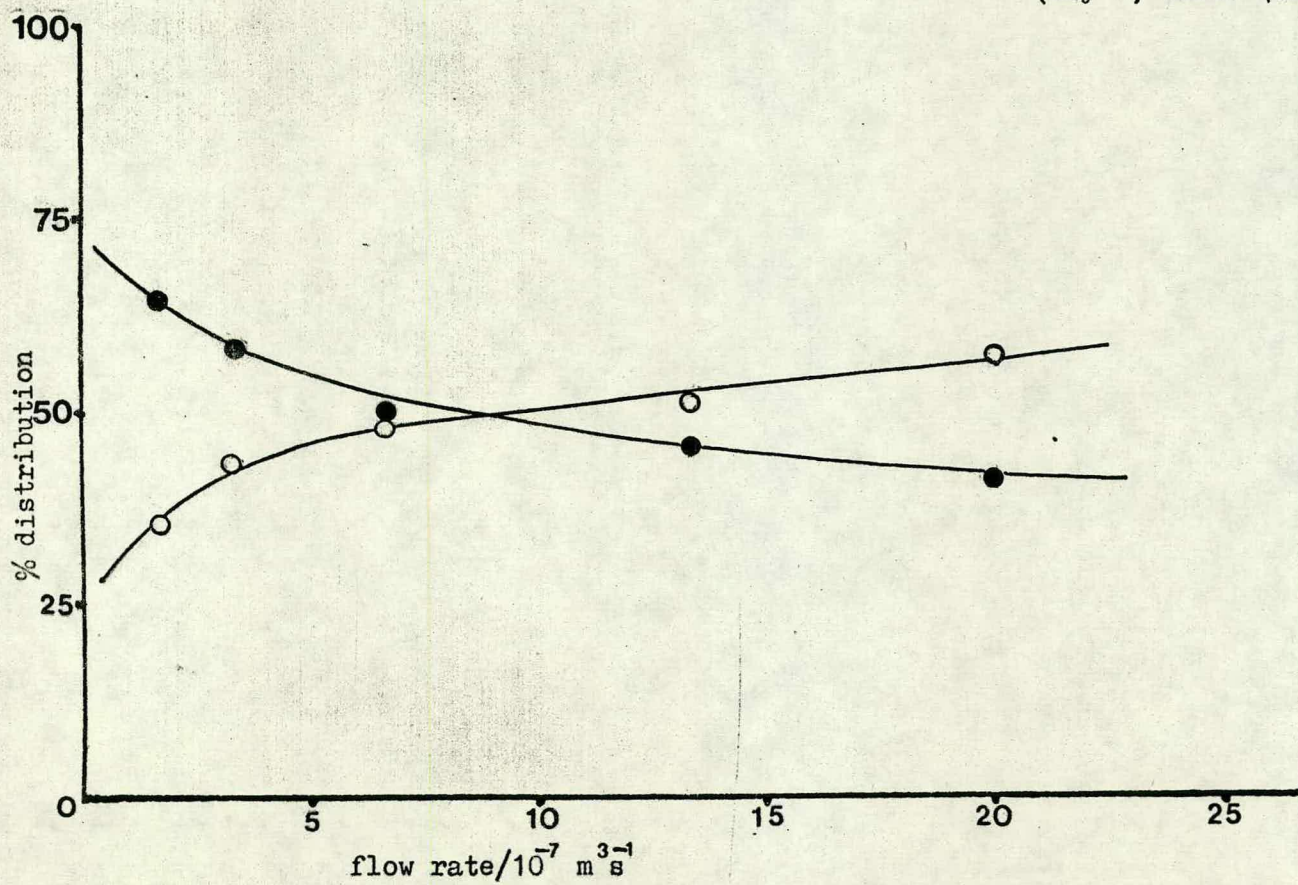


figure 4.24 repeat examination of the decomposition of
4-methylpentan-2-ol: variation product
distribution with temperature:

4-methylpentan-2-ol, ●; 4-methylpentene, ◆;
4-methylpentan-2-one, △.

(flow rate = $5 \times 10^{-7} \text{ m}^3 \text{ s}^{-1}$)

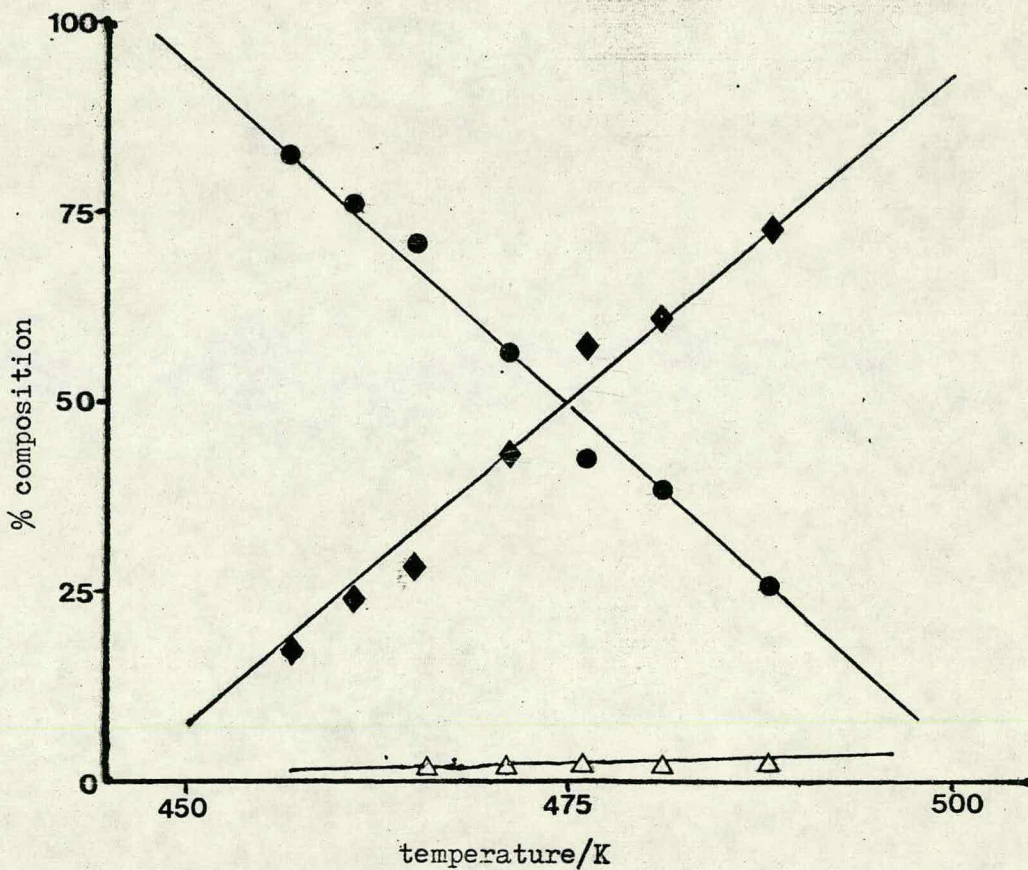
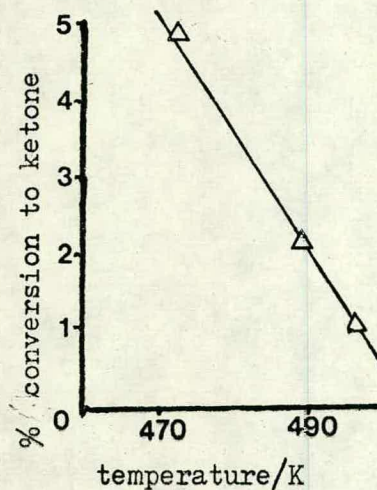
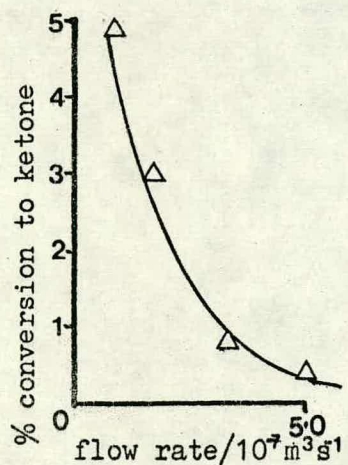
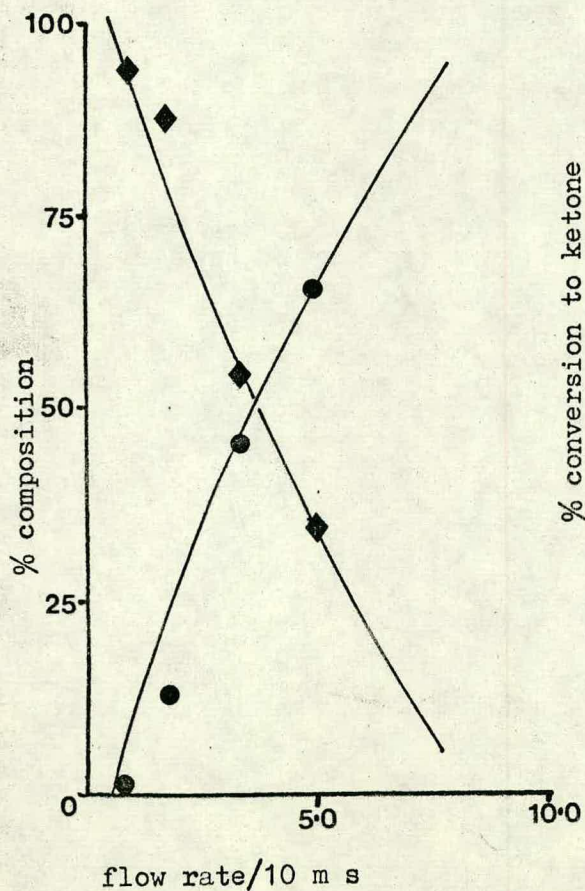


figure 4.25 repeat examination of the decomposition of 4-methylpentan-2-ol: variation product distribution with rate of flow of carrier gas: 4-methylpentan-2-ol, ●; 4-methylpentene, ◆; 4-methylpentan-2-one, △; (react. temp. = 473K)



variation of % production of ketone with temperature at $0.83 \times 10^{-7} \text{ m}^3 \text{ s}^{-1}$ (i.e. all alcohol converted)

figure 4.26 repeat of the variation of % distribution of dehydration products of
2,2-dimethylpropan-1-ol decomposition with flow rate of carrier gas:
2-methylbut-2-ene, ● ; 2-methylbut-1-ene, ○. (react.temp. = 534K)
(Day 7, Table 4.8)

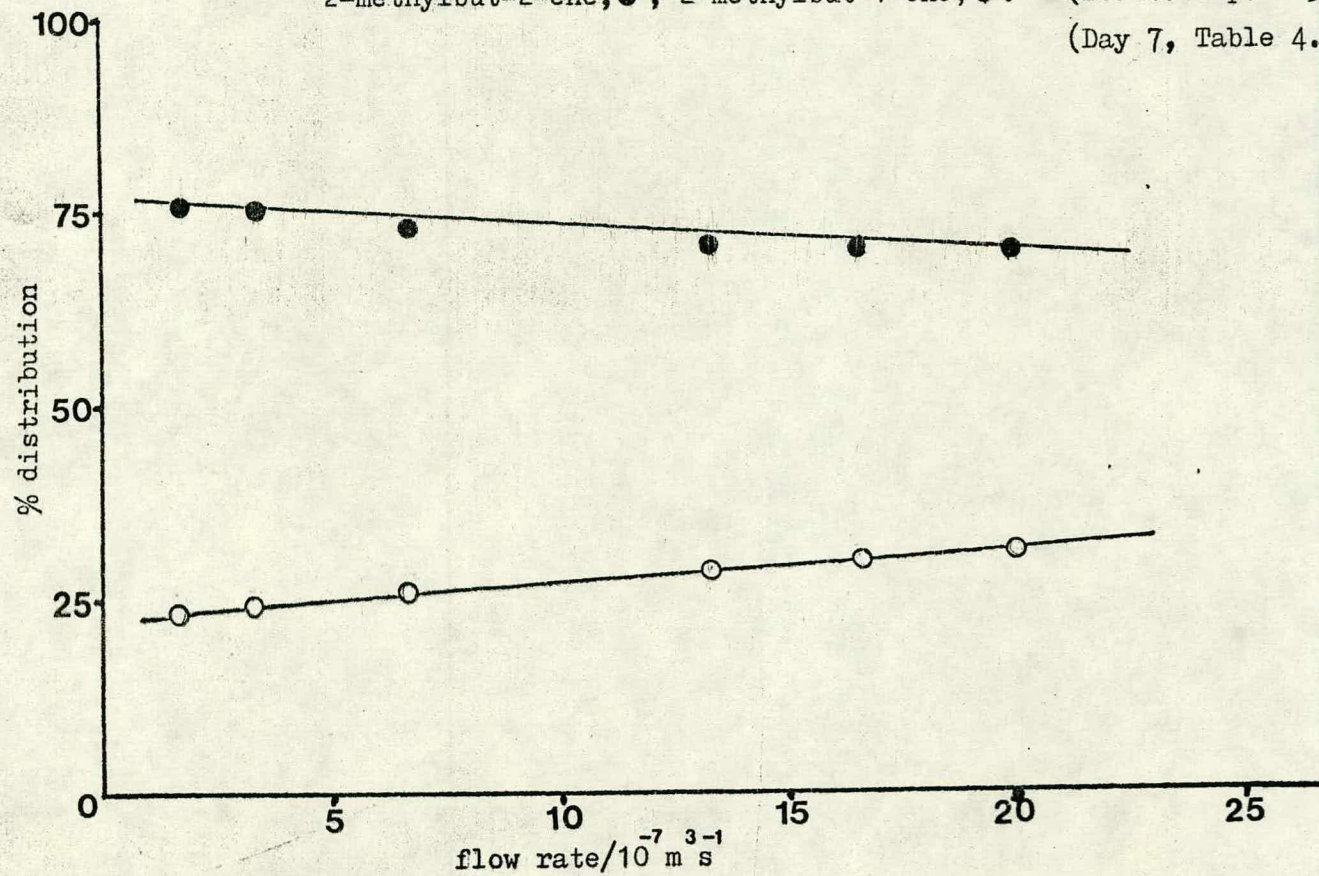


figure 4.27 repeat of the variation of % distribution of dehydration products of 2,2-dimethylpropan-1-ol decomposition with flow rate of carrier gas: 2-methylbut-2-ene, ●; 2-methylbut-1-ene, ○. (react. temp. = 534K) (Day 9, Table 4.8)

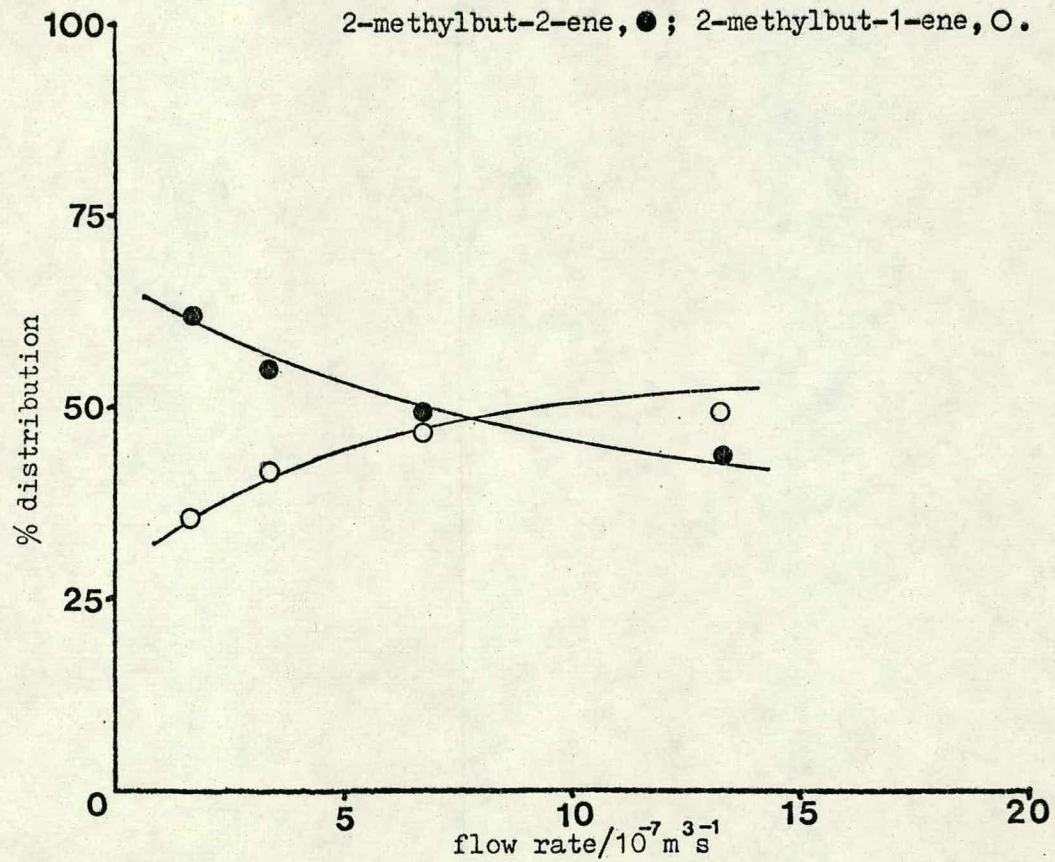


figure 4.28 repeat of the variation of % distribution of dehydration products of 2,2-dimethylpropan-1-ol decomposition with flow rate of carrier gas: 2-methylbut-2-ene, ●; 2-methylbut-1-ene, ○. (react.temp. = 534K) (Day 20, Table 4.8)

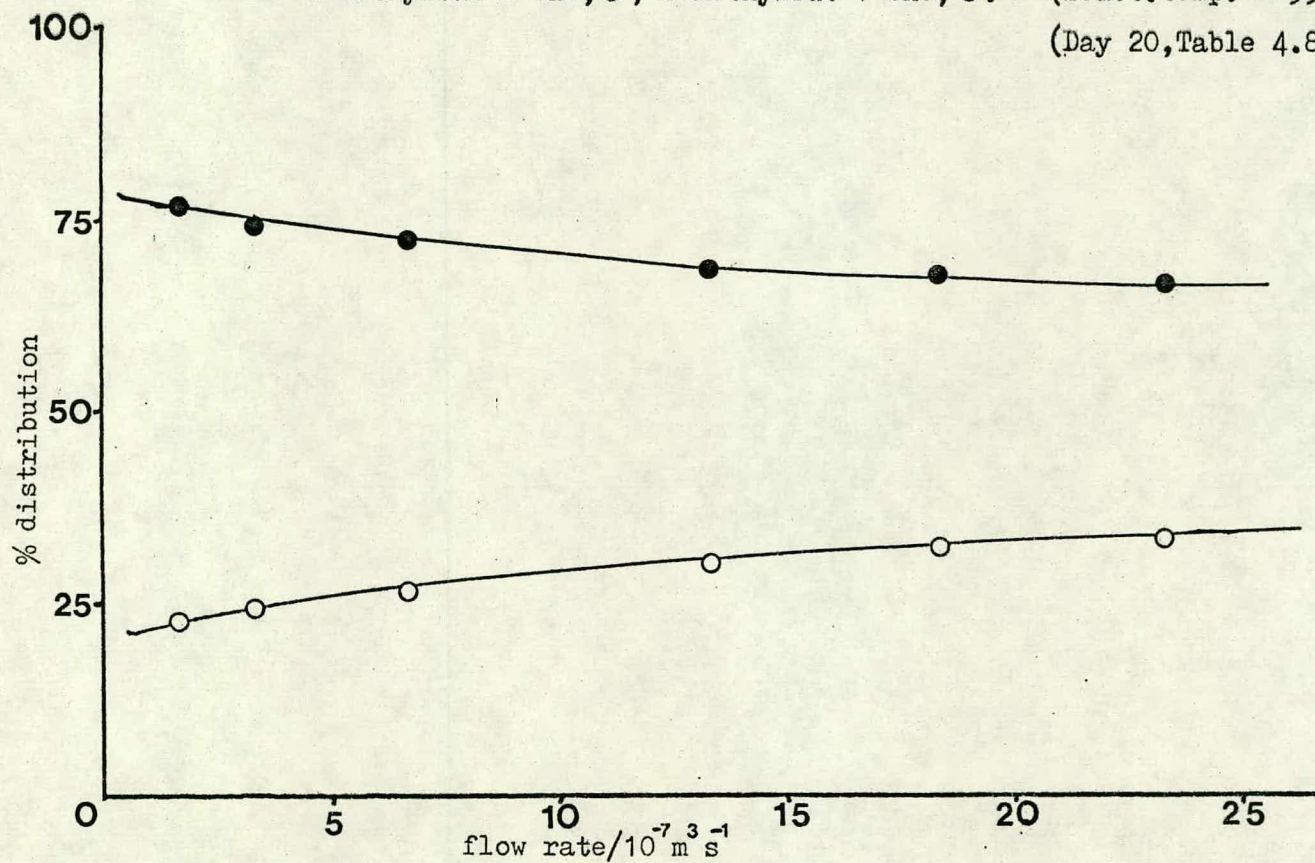
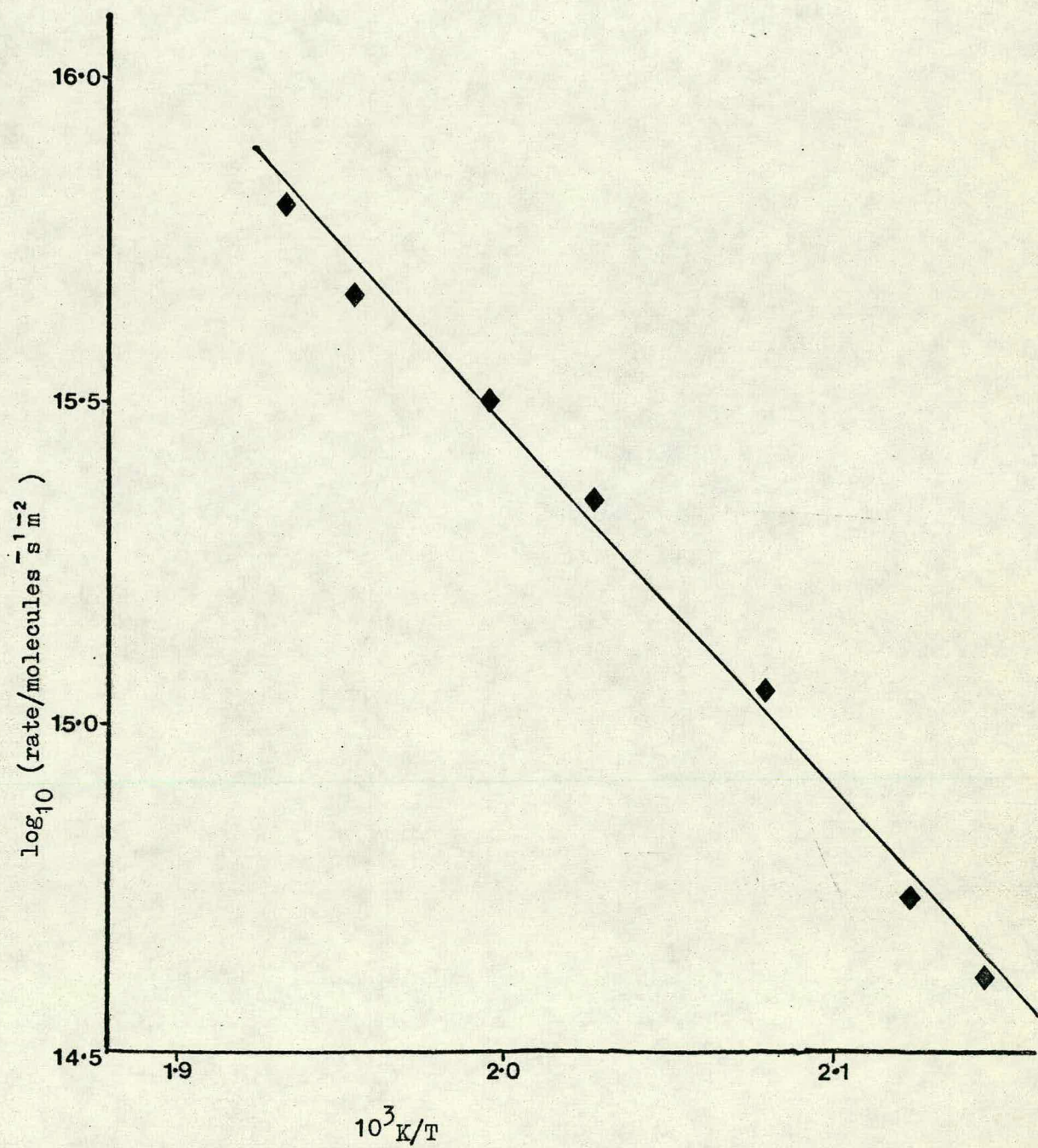


figure 4.29 Arrhenius plot for dehydration of pentan-1-ol over superactive rutile.

activation energy = 110kJmol^{-1} .



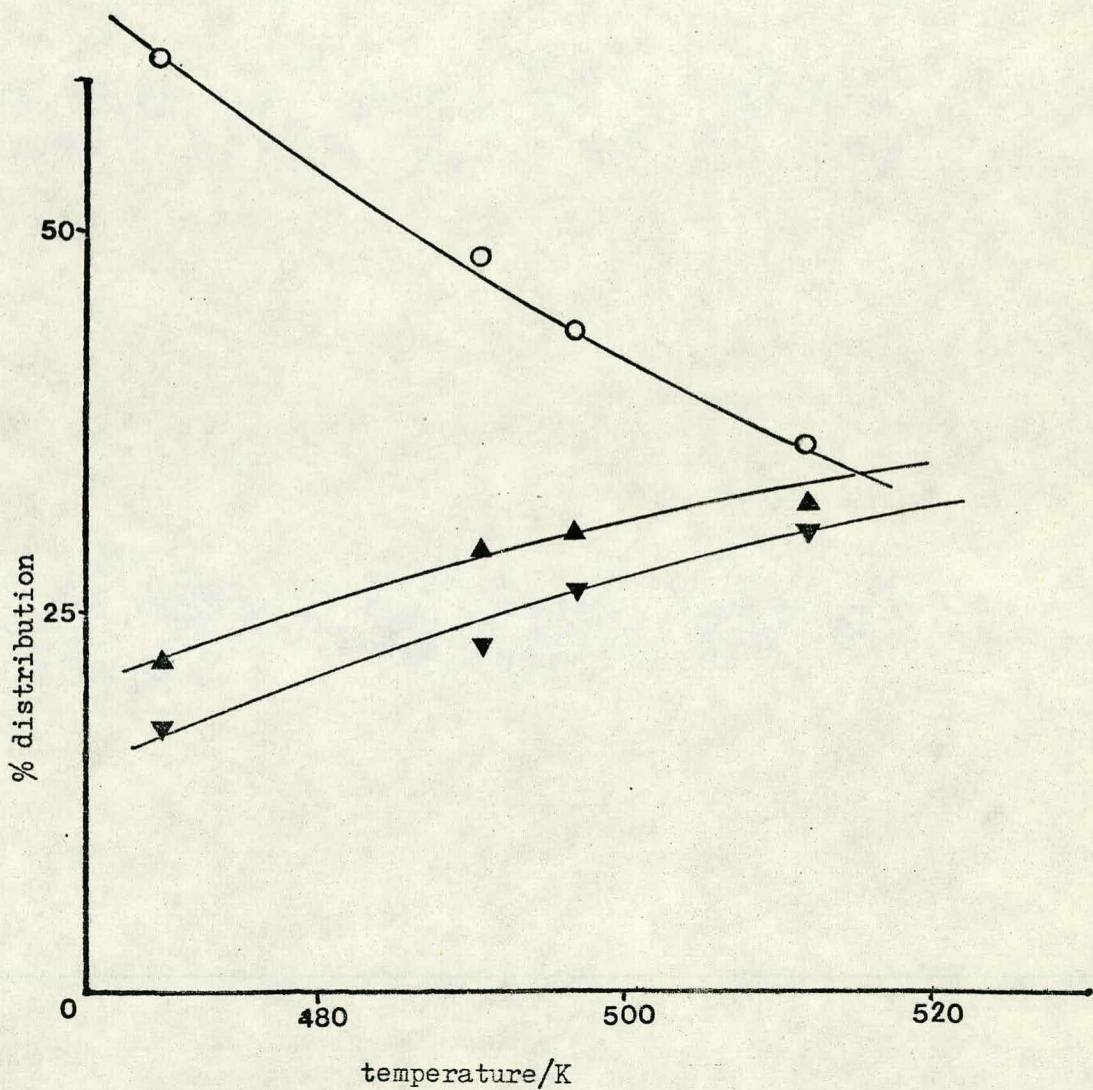
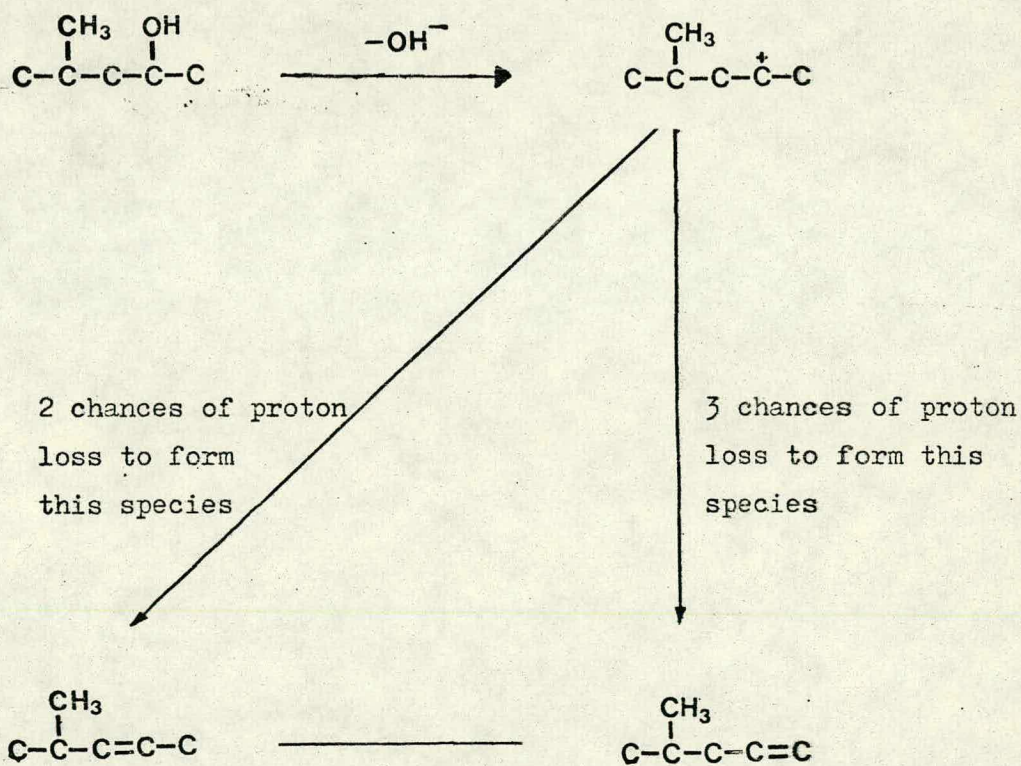


figure 4.30 decomposition of pentan-1-ol over superactive rutile:
 variation of product distribution with temperature:
 pent-1-ene, O; cis-pent-2-ene, \blacktriangle ; trans-pent-2-ene, \blacktriangledown .
 (no pentane was observed)
 (flow rate = $5 \times 10^{-7} \text{ m}^3 \text{ s}^{-1}$)

figure 4.31 decomposition of 4-methylpentan-2-ol .



statistical ratio 4-methylpent-2-ene/4-methylpent-1-ene
 = 2 / 3

figure 4.32 % distribution of the dehydration products from the decomposition of pentan-1-ol over rutile v total alkene production; pent-1-ene, \circ ; pentane, \blacksquare ; cis-pent-2-ene, \blacktriangle ; trans-pent-2-ene, \blacktriangledown ; unknown, \times .

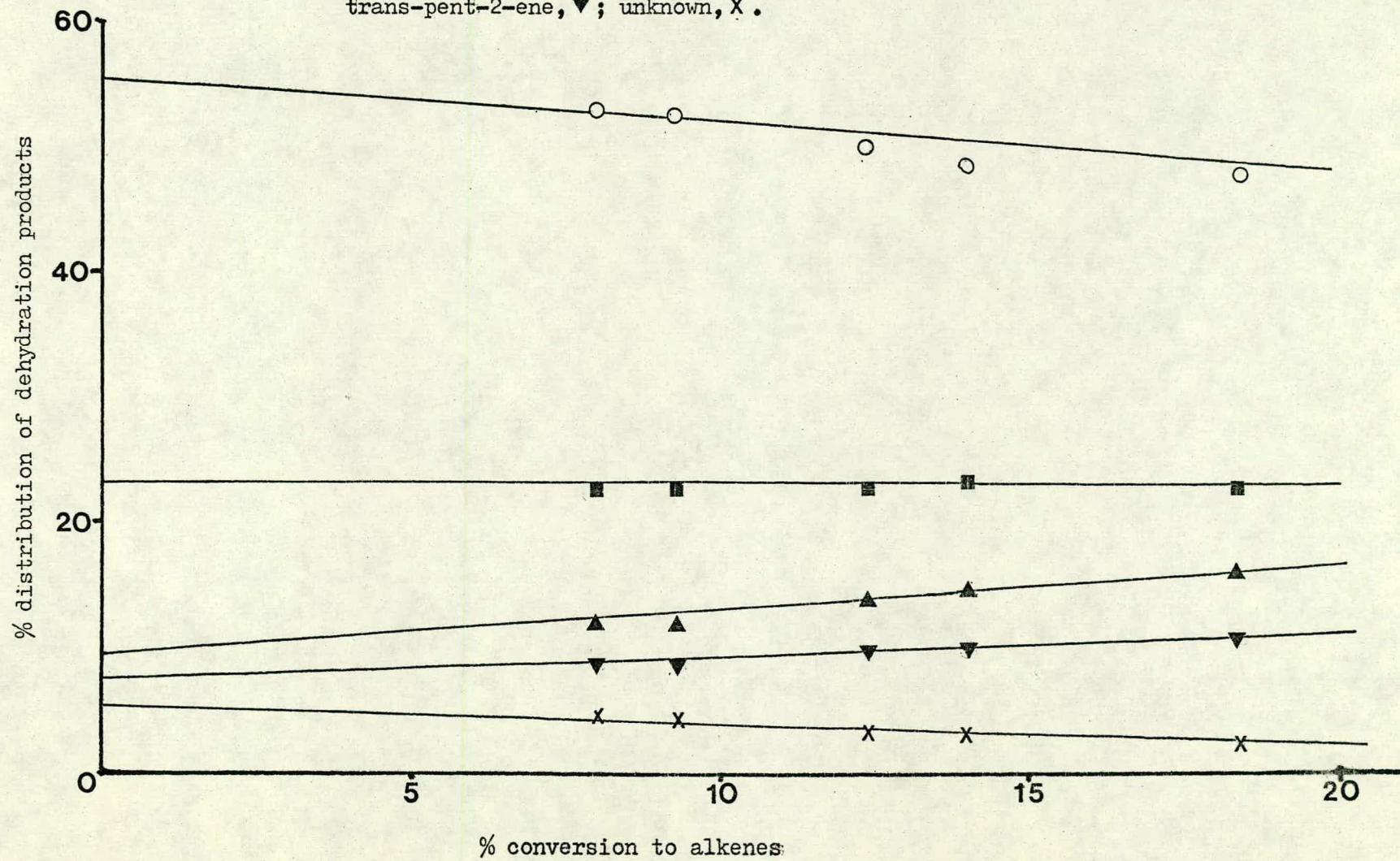


figure 4.33 % distribution of dehydration products of pentan-1-ol decomposition v flow rate⁻¹
pent-1-ene, O; pentane, ■; cis-pent-2-ene, ▲; trans-pent-2-ene, ▼; unknown, X.
(react. temp. = 549K)

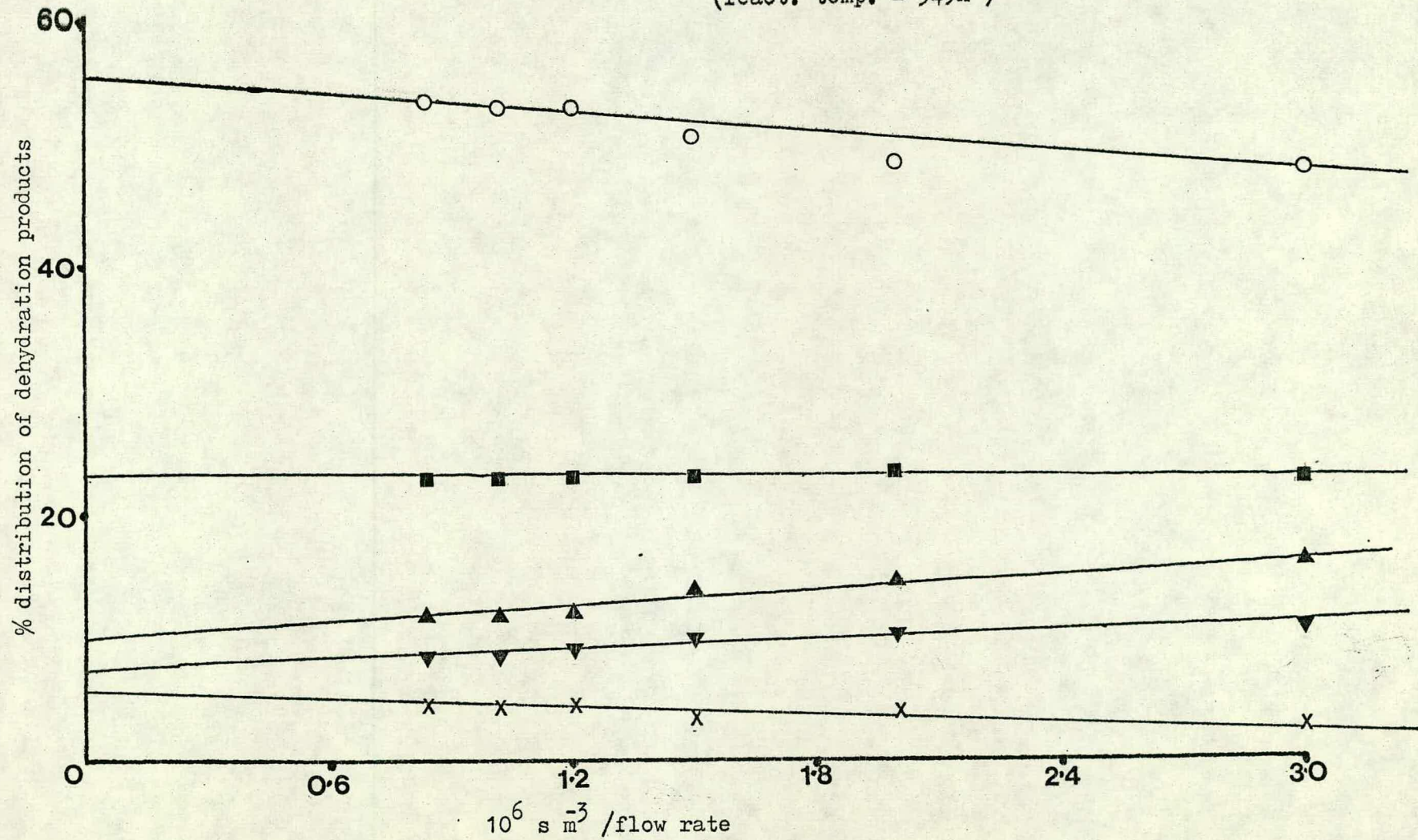
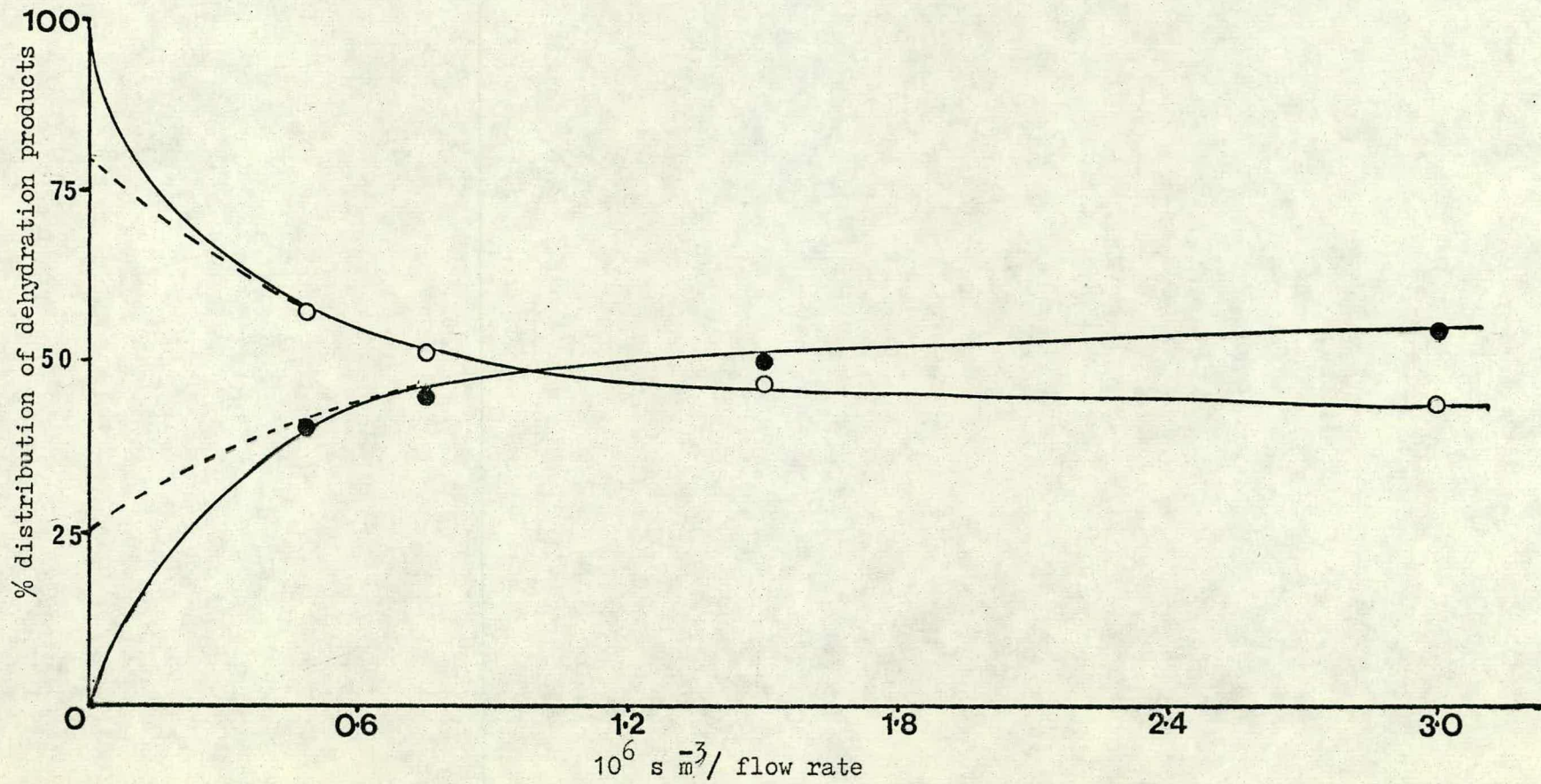


figure 4.34 % distribution of dehydration products of 2,2-dimethylpropan-1-ol decomposition
v flow rate⁻¹: 2-methylbut-2-ene, ●; 2-methylbut-1-ene, ○.



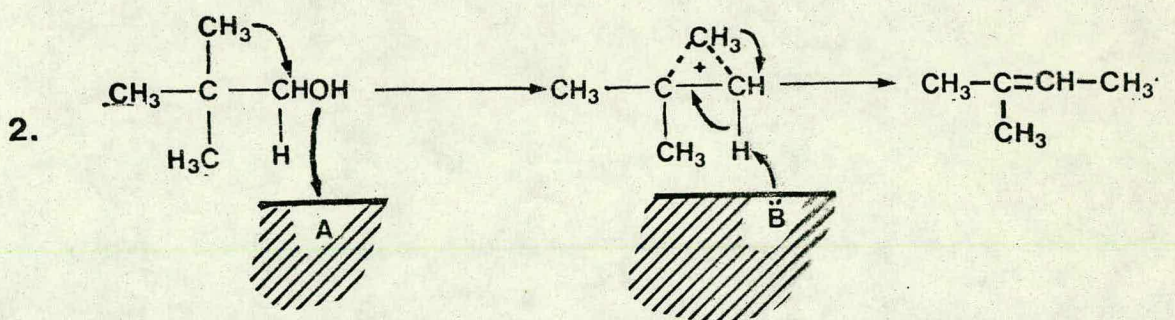
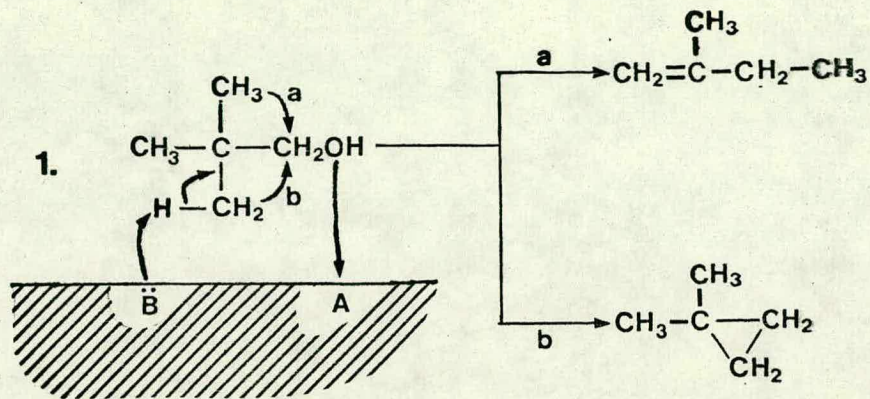


figure 4.36 catalytic decomposition of 2,2-dimethylpropan-1-ol
after Pines et al^{59 62}.

figure 4.37 % distribution of dehydration products of 2,2-dimethylpropan-1-ol decomposition over more active rutile v flow rate⁻¹:
2-methylbut-2-ene, ●; 2-methylbut-1-ene, ○.

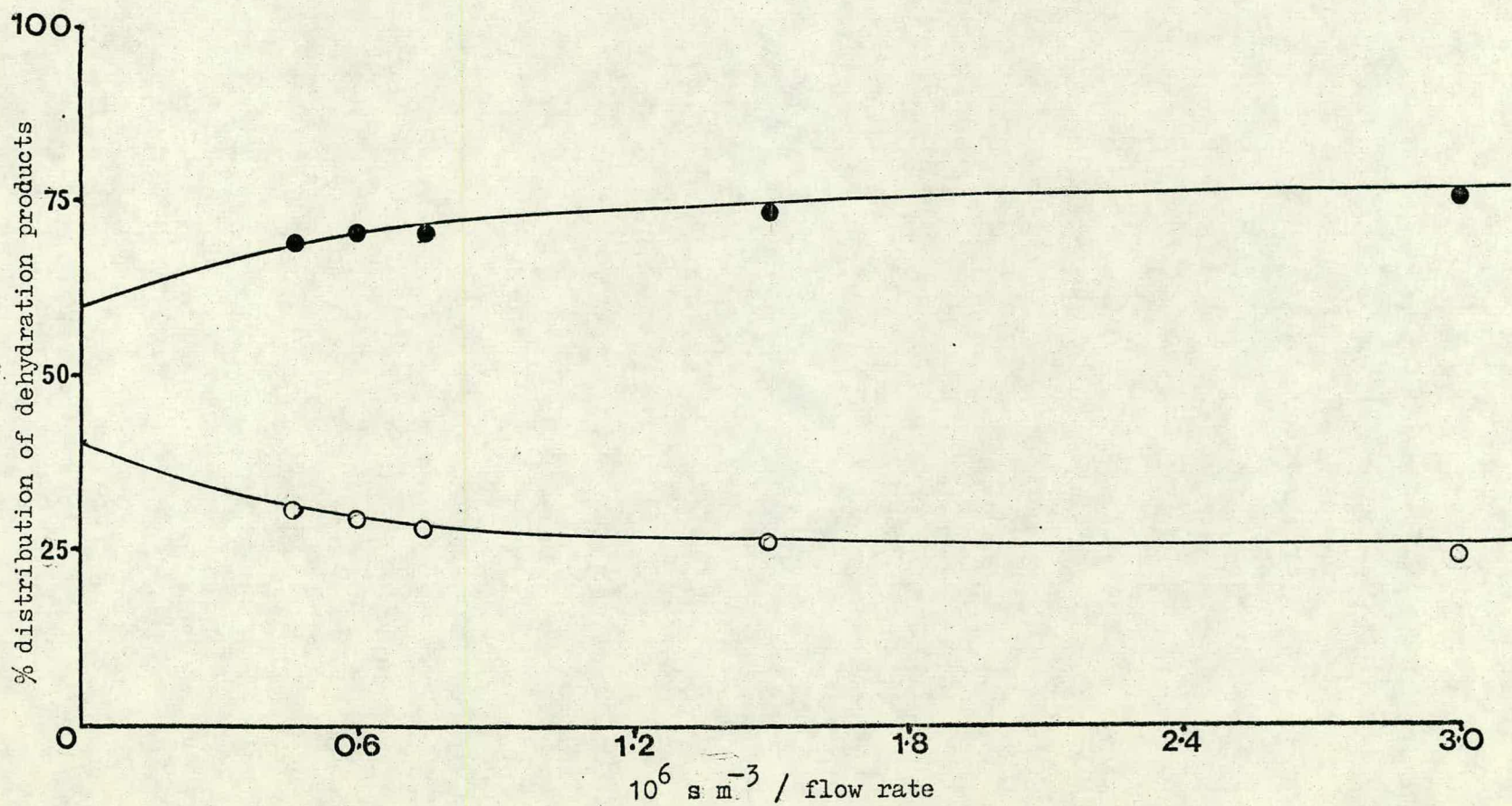
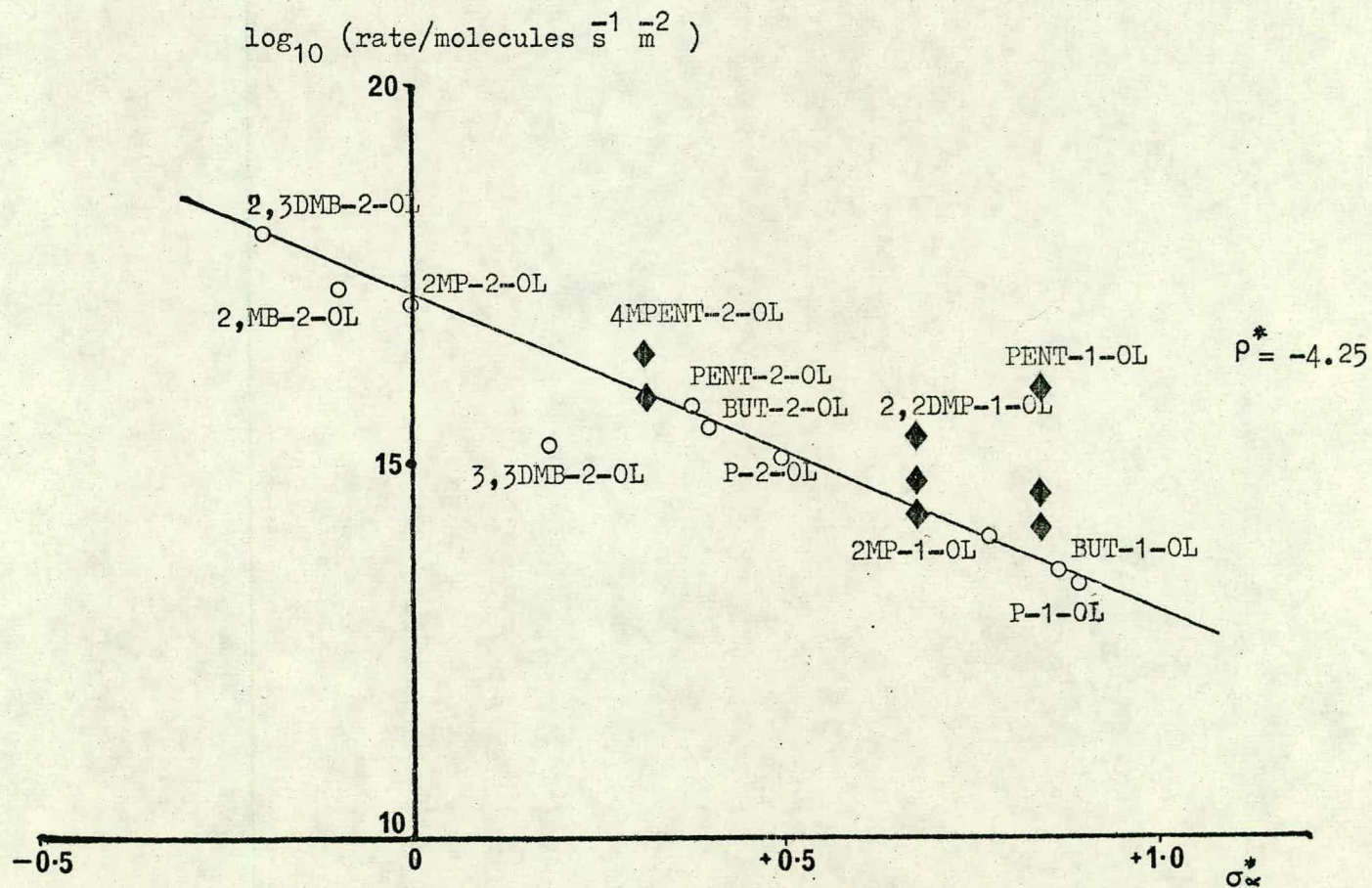


figure 4.38 correlation of rates of dehydration of alcohols over rutile at 523K in the co-ordinates of the Taft equation; previous work⁴⁵, o; alcohols examined in the present studies, ♦. (activation of catalyst samples with use is also indicated.)



CHAPTER 5

The Decomposition of Alcohols over Rutile (Static System)

5.1 Introduction

The increase in the activity towards dehydration of a rutile catalyst with repeated use as reported in Chapter 4 suggested that the existence of small amounts of impurities in the catalyst could profoundly affect the active sites. The purpose of the investigation in this chapter therefore was to determine the effect upon alcohol reactivity of a controlled exposure of rutile samples to certain molecules.

Previous work³⁷ has shown that the preadsorption of simple molecules such as H_2O , NH_3 and HCl onto rutile catalysts has a significant effect on the activity of the catalysts towards double bond migration reactions of alkenes. Using a static system, (vac-line I, Fig. 2.1) Brookes³⁷ found that preadsorption of water, ammonia, ethylene diamine, pyridine and hydrogen cyanide onto rutile had a marked poisoning effect on the rate of but-1-ene isomerisation and hydrogen chloride and chlorine preadsorption resulted in an enhancement of this rate. This led the author to conclude that the active site associated with double bond migration was a surface titanium ion which acted as a Lewis acid.

As alcohol dehydration is also thought to be an acid catalysed reaction, it was therefore considered appropriate to examine if similar experiments could lead to similar conclusions about the sites associated with

alcohol decomposition. The decompositions of propan-1-ol and 2-methylpropan-2-ol were selected for such a study.

The less complex reaction was the decomposition of 2-methylpropan-2-ol which is known⁴⁵ to occur under reaction conditions similar to those required for but-1-ene isomerisation. This would thus simplify any comparison with previous work on the controlled poisoning of rutile catalysts. The only decomposition products of 2-methylpropan-2-ol are those of dehydration i.e. 2-methylpropene and water, with no dehydrogenation being observed. To simplify comparison all experiments were undertaken at 427 K with 0.1 g catalyst.

Conversely, propan-1-ol decomposition only takes place at temperatures far higher than those required for but-1-ene isomerisation and with the formation of five major products. Poisoning studies were therefore undertaken in an attempt to (a) identify the sites associated with the formation of each of the products and (b) establish the reaction pathways by which such products might be formed. 590 ± 10 K was chosen as the reaction temperature range for the propan-1-ol experiments - with 0.1 g of catalyst again being used. Finally a short series of related reactions on rutile were attempted in order to gain more information about the propan-1-ol decomposition.

5.2 The Decomposition of 2-Methylpropan-2-ol

5.2.1 Introduction

Prior to the adsorption and poisoning studies, the decomposition of 2-methylpropan-2-ol over rutile at 427 ± 1 K was studied in the absence of any other species

and it was established that 2-methylpropene and water were the sole decomposition products of the reaction. Fig. 5.1 illustrates the course of the reaction over a period of 150 minutes and it is seen that initially the reaction follows zero order kinetics at a rate of 2.0×10^{-15} molecules $s^{-1} m^{-2}$. After approximately 50% of the decomposition has taken place, the rate of the decomposition begins to slow down thus giving the appearance of the reaction being first order with respect to the alcohol concentration. A log (% 2-methylpropan-2-ol) versus time plot for the reaction was found to be linear (Fig. 5.2) giving a rate constant for the reaction of $1.68 \pm 0.3 \times 10^{-4} s^{-1}$. As it was planned for the present studies to work at a constant reaction temperature, it was thus concluded that if the pretreatment of the catalyst resulted in an enhancement of the rate, a first order treatment of the results would be necessary whereas a zero order treatment may be more appropriate in conditions where poisoning resulted.

5.2.2 Water

Apart from the interest of this investigation in its own right, the effect of water upon alcohol decomposition reactions had particular importance since water is a product of the dehydration reaction and thus may interfere with the latter stages of such a reaction.

Pretreatment of rutile surfaces with quantities of water similar to those used by Brookes³⁷ to hinder but-1-ene/but-2-ene isomerisation produced the results illustrated in Fig. 5.3. A reasonably linear correlation of poisoning with

the amount of water preadsorbed was established, with a coverage of 2 water molecules nm^{-2} being required to produce a reduction of approximately 50% in the rate constant k .

The admission of larger quantities of water into the reaction system to produce an $\text{H}_2\text{O}/\text{alcohol}$ ratio $\approx 1.05/1$ led to a much greater poisoning of the reaction as illustrated in Figs. 5.4 and 5.5 with initial dropping to $\approx 0.53 \times 10^{15}$ molecules $\text{s}^{-1} \text{m}^{-2}$ and the first order rate constant (determined from the log (% 2-methylpropan-2-ol) versus time plot) being reduced to $0.26 \times 10^{-4} \text{ s}^{-1}$ from $1.68 \times 10^{-4} \text{ s}^{-1}$.

5.2.3 Ammonia

Ammonia is a Lewis base (pK_a 7.24) and at 427 K would be expected to adsorb onto any acidic sites on rutile. The experiments were of special interest therefore in order to test the suggestions by Halliday⁴⁵ that the mechanism of the dehydration of alcohols on rutile involves both acidic and basic surface sites. As Fig. 5.6 shows, the effect of ammonia preadsorption on the alcohol decomposition over rutile was similar in nature to that of water with increased coverage (in the range 0-2 molecules nm^{-2}) being directly related to a decrease in rate constant. Although, as with water, total poisoning of the reaction is not attained, the poisoning effect of ammonia seems to be more marked than that of water i.e. at a coverage of 2 ammonia molecules nm^{-2} the rate constant has been reduced by 70%. The poisoning effect of ammonia when

introduced into the reaction vessel simultaneously to the reactant (ratio $\text{NH}_3/\text{alcohol} \approx 1.10/1$) also seemed greater than that with water; the initial rate dropping to $0.34 \times 10^{15} \text{ molecules s}^{-1} \text{ m}^{-2}$ and the rate constant being reduced to $0.12 \times 10^{-4} \text{ s}^{-1}$ (Figs. 5.7 and 5.8).

5.2.4 Trimethylamine (T.M.A.)

The poisoning effect of ammonia upon the rate of dehydration of 2-methylpropan-1-ol just reported (section 5.2.3) was considerably less than that reported for but-1-ene isomerisation³⁷. Consequently it was felt that useful information could be collected from an examination of the effect of preadsorption of other bases. It was decided to focus attention upon species which were stronger than ammonia so pyridine (pKa 5.21) was excluded from such a study. With trimethylamine (pKa 9.81) the reduction in rate constant resulting from the preadsorption of T.M.A. is summarised in Fig. 5.9. At coverages in the range 0-2 molecules nm^{-2} , the poisoning was greater than that caused by water or ammonia. There is a danger of interaction between T.M.A. and stop-cock grease - attempts were made to minimise such interaction but the data regarding the preadsorption of T.M.A. on rutile are less quantitative than in previous sections.

To ensure maximum chemisorption of the base, excess T.M.A. was frozen into the reaction vessel and allowed to adsorb onto the rutile sample as the reaction system regained ambient temperature. At this point, excess T.M.A. was pumped from the system. The normal amount of alcohol was then introduced into the system.

This preadsorption treatment resulted in a reduction of the initial rate of the reaction to 0.23×10^{15} molecules $s^{-1} m^{-2}$ (see Fig. 5.10) compared to 2.0×10^{15} molecules $s^{-1} m^{-2}$. This was similar to the rate when 1.8 molecules of T.M.A. were known to have adsorbed onto the rutile surface (Fig. 5.9). The simultaneous admission of T.M.A. into the reaction system with the normal amount of alcohol (ratio approximately 1:1) completely poisoned the reaction.

5.2.5 Triethylamine (T.E.A.)

This molecule is a stronger Lewis base (pKa 10.7) than any of the previously studied molecules. As it was believed to be subject to the same problems as T.M.A. (interaction with stop-cock grease) only maximum preadsorption experiments were attempted as described in section 5.2.4. Poisoning by triethylamine seemed to be less than with T.M.A. with a reduction of the rate of decomposition of 2-methylpropan-2-ol to 1.49×10^{15} molecules $s^{-1} m^{-2}$, (Fig. 5.11). (Rate of unpoisoned decomposition 2.0×10^{15} molecules $s^{-1} m^{-2}$).

5.2.6 Hydrogen Chloride

The controlled preadsorption of HCl gas on rutile to produce coverages of between 0 and 2 molecules of HCl nm^{-2} led to a corresponding increase in the activity of the catalyst towards alcohol dehydration. The dramatic increase in the catalytic activity hindered accurate measurement of the kinetics of the reaction and since

at the reaction temperature under study of 427 K, complete decomposition of the alcohol took place within a short time, it was necessary to apply a first order treatment to all the reactions reported in this section. The variation of the rate constant of the reaction increased from $\approx 1.68 \times 10^{-4}$ to $\approx 33.3 \times 10^{-4} \text{ s}^{-1}$, with increasing coverage from 0 to 2 HCl molecules nm^{-2} as is seen in Fig. 5.12. Previous work³⁷ on HCl activated rutile reported the catalyst turning a pale pink colour after an alkene isomerisation. No such change in colouration was observed in the present series of experiments.

5.2.7 Chlorine

A detailed study of the effects of chlorine on the catalytic properties of rutile was not possible since it would have reacted with the mercury in the apparatus. However, by quickly using a manometer which was remote from the main part of the line, a quantity of chlorine gas was isolated into the dosing volume (Chapter 2) then frozen into the reaction vessel and allowed to adsorb onto the catalyst sample. The calculation of the adsorption of the Cl_2 molecules by this method corresponded to a coverage of 2 ± 0.5 molecules nm^{-2} . The rutile sample was activated by this treatment so that the dehydration of 2-methylpropan-2-ol proceeded with a rate constant of $\approx 17.3 \times 10^{-4} \text{ s}^{-1}$, a ten-fold increase in the rate of decomposition of this alcohol compared to untreated rutile samples.

5.3 The Reaction of Propan-1-ol over Rutile

5.3.1 Introduction

The decomposition of propan-1-ol over rutile was studied at ≈ 590 K on gas-line I (Fig. 2.1). Preliminary studies had shown⁴⁵ that the alcohol decomposes to form 5 products which had been assigned to certain peaks on a G.C. trace of the reaction mixture as follows:-

(see Table 2.4 for G.C. operating conditions)

No	Retention Time/s (approx.)	Identification
1	60	Propene
2	150	Propanal
3	240	Propan-1-ol
4	300	Hexene
5	360	Benzene
6	540	n-Propyl ether

The initial experiments in the studies described in this thesis, however, showed that the overall product mixture was more complex than described above.

Fig. 5.13 shows a typical G.C. trace of the reaction mixture for the decomposition of propan-1-ol at 586 K after 100 minutes and the total reaction mixture as identified by G.C. is summarised as follows:-

Component	Retention Time/s	Identity
1	36	Molecule of small carbon No < 3
2	48	Molecule of small carbon No < 3
3	60	Propene
4	84	Butene
5	150	Propanal
6	180	1-Chloropropane
7	240	Propan-1-ol
8	264	Hexene
9	330	Unknown
10	516	n-Propyl ether

Components 1, 2 and 4 of the reaction mixture are believed to be the result of the fragmentation of larger molecules and never contributed to more than 1% of the total and component 6, of similar low quantity is believed to be due to the reaction of the alcohol with chlorine impurities within the catalyst. The overall reaction at 586 K and 599 K is described in Figs. 5.14 and 5.15 respectively. The major dehydration product was propene with smaller but significant amounts of n-propyl ether also being produced. Dehydrogenation was also observed with the formation of propanal which after its formation in the first few minutes of the reaction remained an approximately constant fraction of the reaction mixture i.e. in the range 2-4%. First order plots of the overall decomposition of propan-1-ol

tended to deviate from linearity (Figs. 5.16 and 5.17) after a certain period of time indicating that poisoning of the catalyst may have been occurring during the latter stages of the reaction.

Products 8 and 9 were of interest in that they were both suspected to be C_6 species - and produced from the initial C_3 propan-1-ol reactant. Product 8 was identified by gas-chromatography to be a hexene although its exact identity could not be established. (Hex-1-ene, cis/trans-hex-2-ene, trans-hex-3-ene, methylpentenes and dimethylbutenes all had similar retention times using the Porapak S column). It would be expected that at such high temperatures, isomerisation of a hexene molecule would probably take place and thus a number of isomers of the formula C_6H_{12} would probably exist. Previous work⁴⁵ had led to the suggestion that component 9 of the reaction mixture was benzene; careful G.C. analysis of the reaction mixture in the present work was unable to confirm this assignment. G.C. analysis also excluded the following:- cyclohexene, 1,5-hexadiene, hexane, cyclohexane, methylcyclopentane, propionic acid, isopropyl ether, mesityl oxide, n-propyl isopropyl ether, propyl propionate and mesitylene.

Attempts to use a combined gas chromatograph mass spectrometer (G.C.M.S.) to establish the identity of this unknown with more certainty were largely unsuccessful as it was not possible to obtain a sufficient amount of the product to give a good and unequivocal mass spectrum. The mass spectrum of the compound did, however, reveal the existence of species with mass/charge ratios of 84, 69, 60

and 59 a.m.u. which strongly suggests that the carbon number of the species was larger than that of propan-1-ol. As the reaction proceeded, it was observed that the mass spectrum of the unknown changed with the emergence of species of mass/charge ratio 55, 56 and 57 a.m.u. accompanying the decline of those at 59 and 60 a.m.u. It seems reasonably certain, therefore, that the unknown species is some product of the coupling processes that take place over rutile although it is also clear that the major product of such processes is hexene.

5.3.2 The Effect of the Presence of Certain Species in the Reaction System on the Decomposition of Propan-1-ol over Rutile

5.3.2.1 Introduction

The study of the effect of preadsorbed molecules on the decomposition of propan-1-ol over rutile was only partially successful because at the high temperatures of ≈ 600 K necessary to obtain reaction rates that could be accurately measured, the preadsorbed species tended to desorb from the surface. Water is already known¹⁹ to desorb from the surface of rutile as it is heated and Fig. 5.18 also shows this to be the case with the rutile samples used in the present series of experiments. A sample of rutile containing water preadsorbed at room temperature (to a coverage of $0.188 \text{ H}_2\text{O molecule nm}^{-2}$) begins to lose this water as it is heated until at the reaction temperatures of ≈ 600 K necessary for propan-1-ol decomposition approximately $0.106 \text{ H}_2\text{O molecules nm}^{-2}$ remain.

The approximate coverage remaining on the rutile samples at the reaction temperatures appeared to be 0.2 ± 0.1 molecules nm^{-2} regardless of the magnitude of the initial coverage obtained at ambient temperatures. Previous studies³⁷ had suggested that ammonia, unlike water, would remain adsorbed on the rutile at the temperatures of ≈ 600 K required for propan-1-ol decomposition but in the present series of experiments this molecule was found to desorb on heating in a similar manner to water. It was also clear that significant desorption of pre-adsorbed hydrogen chloride also took place on heating to the necessary reaction temperatures. However, complete desorption of any preadsorbed species was never observed.

5.3.2.2 Water

Figs. 5.19 and 5.20 show the decomposition of propan-1-ol at 586 and 599 K respectively after prior adsorption of 0.2 ± 0.05 H_2O molecules nm^{-2} . It is apparent by comparison with Figs. 5.14 and 5.15 that the presence of the water molecules on the rutile surface has very little effect on the production of propanal, hexene or the unknown C_6 compound. The water pretreatment however does seem to have had an effect upon the formation of propene, the initial rate of production of the alkene increasing from $\approx 1.12 \times 10^{15}$ molecules $\text{s}^{-1} \text{m}^{-2}$ to $\approx 2.80 \times 10^{15}$ molecules $\text{s}^{-1} \text{m}^{-2}$ at 586 K and from 1.95×10^{15} molecules $\text{s}^{-1} \text{m}^{-2}$ to 5.71×10^{15} molecules $\text{s}^{-1} \text{m}^{-2}$ at 599 K. This effect was always observed when small quantities of water in the range 0-0.3 molecules nm^{-2} were preadsorbed

onto the rutile surface, although it was not possible to establish any clear or quantitative correlation. Plots of \log (% propan-1-ol) versus time, Figs. 5.21 and 5.22 show that after the preadsorption of water there was no deviation from linearity in the latter stages of the reaction unlike that previously observed (Figs. 5.16 and 5.17). Increasing the amount of water in the system by freezing in a mixture of water and alcohol (ratio H_2O /alcohol = 1.1/1) led to a further increase in the rate of alkene production at 599 K (7.67×10^{15} molecules $s^{-1} m^{-2}$ Fig. 5.23). Again no significant changes were observed in the production of the aldehyde or the C_6 compounds. During all the experiments where the catalyst samples have become more active for propene production, it was noted that when the amount of alcohol in the system has dropped to <5%, the n-propyl ether also begins to decompose; the rate of this decomposition matching that of the alcohol in the latter stages of the reaction.

Fig. 5.24 shows that admission of a large excess of water into the system along with the alcohol in the ratio water:alcohol > 10:1, completely poisons the production of the C_6 compounds and the amount of propanal increases throughout the reaction. The dehydration of the alcohol to propene is also poisoned, particularly in the latter stages of the reaction and no ether production could be detected.

5.3.2.3 Ammonia

As previously stated, ammonia also tended to desorb at the temperature of approximately 600 K required for

propan-1-ol decomposition although as was found with water, the desorption was not complete. Fig. 5.25 shows that preadsorption of approximately 0.4 ± 0.05 molecules nm^{-2} had a similar effect to that of water in that the catalyst appeared to become more active for the production of the alkene (2.84×10^{15} molecules $\text{s}^{-1} \text{m}^{-2}$) and there was less self-poisoning in the latter stages of the reaction. The preadsorption of NH_3 had little effect on the formation of the aldehyde or the C_6 compounds and the decomposition of the ether was again observed in the latter stages of the reaction. A large excess of ammonia admitted into the reaction vessel with the alcohol (in the ratio ammonia:alcohol=6:1) caused a reduction in the rate of the propene production from 2.80×10^{15} molecules $\text{s}^{-1} \text{m}^{-2}$ to 0.69×10^{15} molecules $\text{s}^{-1} \text{m}^{-2}$ at 586 K. It was also noted that the formation of the unknown C_6 compound was suppressed in this experiment although the amount of hexene was as normal, (Fig. 5.26), in the latter stages of the reaction.

5.3.2.4 Trimethylamine (T.M.A.)

In this experiment, trimethylamine was frozen into the reaction vessel, allowed to adsorb onto the rutile and when ambient temperature was reached, the excess T.M.A. was pumped off thus ensuring maximum preadsorption of T.M.A. onto the catalyst. Fig. 5.27 shows that unlike preadsorption of water or ammonia, the presence of small amounts of T.M.A. in the reaction system does not activate the catalyst for propene formation, but slightly lowers the initial rate of

production of the alkene to 0.85×10^{15} molecules $s^{-1} m^{-2}$ at 586 K. Fig. 5.27 also shows that the formation of the C_6 compounds was somewhat suppressed during the initial stages of the reaction.

5.3.2.5 Hydrogen Chloride

The partial desorption of hydrogen chloride at elevated temperatures from rutile surfaces occurred in a similar manner to that encountered with water and ammonia. The presence of small amounts (0.5 ± 0.1 molecules nm^{-2}) of hydrogen chloride on a rutile surface acted in a similar manner to water and ammonia in enhancing the rate of production of propene (3.12×10^{15} molecules $s^{-1} m^{-2}$ at 586 K) (Fig. 5.28). Again, the production of the aldehyde, the hexene and the C_6 unknown was not significantly affected and the ether decomposed in the latter stages of the reaction. In this case, however, an enhanced rate of n-chloropropane production was observed, reaching approximately 5% of the total reaction mixture after 40 minutes (compared to 0.05% in a "normal" experiment). This latter observation suggested the possibility that in these experiments, the presence of HCl may be altering the reaction pathway by promoting the formation of new intermediates during the reaction such as alkyl chlorides which might then rapidly decompose over rutile to form the alkene and HCl, i.e. the HCl might not simply alter the surface properties of the rutile samples.

The dehydration of aliphatic alcohols in the gas phase is known to be catalysed by hydrogen halides¹²⁴

and to test this, the normal amount of propan-1-ol was reacted with a similar quantity of HCl at the temperatures under study in the present series of experiments without the presence of rutile in the reaction system. Fig. 5.29 clearly shows that there is reaction at 600 K with the formation of propene, and also of 1-chloropropane and 2-chloropropane. A repeat of this experiment with the addition of the standard amount of rutile in the reaction vessel results in a very rapid decomposition of the alcohol to propene (too fast to be measured accurately). A reduction of the temperature to approximately 500 K allowed the reaction to be observed and it is seen (Fig. 5.30) that the normal propan-1-ol decomposition over rutile appears to have been replaced by the reaction of propan-1-ol with HCl to produce propene via the formation of 1-chloropropane and 2-chloropropane. As the observed reaction occurs at some 100 degrees lower than the gas phase process, it can be argued that the rutile is acting as a catalyst but possibly its action is not too dissimilar to that of acids such as H_2SO_4 when they promote the reaction of aqueous hydrogen halides with alcohols to form alkyl halides¹²⁵.

Thus although the presence of small amounts of halogenated species on a rutile surface probably only affects the intrinsic surface properties of a catalyst, in some catalytic studies, care must be taken to ensure that such species do not significantly alter the normal mechanisms of the reactions under study.

5.3.3 The Decomposition of Propan-1-ol: Related Studies

5.3.3.1 Introduction

The previous section revealed that the preadsorption and simultaneous admission of certain species on rutile catalysts do have some interesting effects upon its activity for propan-1-ol decomposition. However it was concluded that other approaches could perhaps also provide more information about this reaction; e.g. examining either variations in the reaction conditions or the reaction of related species at the temperatures required for propan-1-ol decomposition. The present section therefore describes the results of this final series of experiments which examined the nature of the decomposition of propan-1-ol over rutile.

5.3.3.2 The Reaction of Propanal

The addition of an excess of water to the reaction system as described in section 5.3.2.4 which resulted in the non-production of the C₆ coupling compounds and also allowed the formation of the propanal to continue throughout the reaction further strengthened previous suspicions that the aldehyde was the precursor to the formation of these coupling compounds. To confirm this, 0.4×10^{20} molecules of propanal were allowed to react over 0.1 g of rutile at 586 K. Fig. 5.31 shows the G.C. trace of the reaction mixture after 65 minutes and it reveals that the two C₆ compounds are indeed formed from propanal although the distribution was different to that seen previously i.e. now more unknown C₆ is produced with this reaction than hexene. Other products also appeared

in the reaction system with longer G.C. retention times which suggested that they might be compounds of even higher carbon number. As the reaction proceeded, all the components of the reaction mixture other than propene were eventually lost to the surface.

5.3.3.3 Reaction of Other Aldehydes and Ketones

As it was now established that the dehydrogenation product from the propan-1-ol decomposition was the precursor for the coupling compounds, it was considered that a brief investigation of the reaction of other carbonyl compounds over rutile could be of relevance; particularly when no coupling compounds are known to be formed from the decomposition of the alcohols corresponding to such compounds. The carbonyl compounds chosen for study were butanal, pentanal and 4-methylpentan-2-one and the amounts of catalyst and reactant employed were equal to those used during alcohol decomposition experiments.

The reaction of butanal over rutile at 523 K was found to result in the decarbonylation and fragmentation of the aldehyde and G.C. analysis of the reaction mixture after 50 minutes of reaction revealed the formation of ethene (4%), propene (8%), butene (4%) and butanol (18%). Approximately 15% of the total gas phase composition after 50 minutes reaction was of compounds with long retention times which could be reasonably assumed to be species of larger carbon number than the reacting molecules although no attempt was made towards their identification. The major reaction, however, was the loss of the aldehyde to the surface of the catalyst (12.8×10^{15} molecules $s^{-1} m^{-2}$)

and after the reaction it was clear that the catalyst surface was extensively coked. G.C. analysis of the decomposition of pentanal over rutile at 580 K revealed a similar product distribution to that obtained with butanal: ethene, propene, butene, pentene and traces of a compound with a larger retention time were observed. The main reaction at these temperatures was however the rapid loss of the reactant to the catalyst surface (12.20×10^{15} molecules $s^{-1} m^{-2}$) and considerable coking was again noted. 4-Methylpentan-2-one also reacted similarly over rutile at 600 K with the appearance of ethene, propene, butenes, pentenes and hexenes although in this case, there was no trace of any larger compounds. The loss of the ketone from the gas phase was again the main reaction (11.24×10^{15} molecules $s^{-1} m^{-2}$) and was accompanied by carbon deposition on the catalyst surface.

5.3.3.4 Excess Propan-1-ol

The effect of the addition of excess propan-1-ol into the reaction system (>10 times the normal amount) is similar to that obtained with excess H_2O i.e. non-appearance of the C_6 compounds and a steady increase in production of propanal throughout the reaction (Fig. 5.32). This fact was first observed when using the G.C.-M.S. to identify the unknown C_6 compound (section 5.3.1) and illustrates why attempts to increase the total production of the unknown by increasing the amount of starting material were unsuccessful. Increased production of the unknown may have facilitated its identification by mass spectrometry.

5.3.3.5 Propene

In order to be certain that propanal was indeed the only intermediate from propan-1-ol decomposition responsible for production of the coupling compounds, propene was allowed to react alone over a sample of rutile at 586 K. Although the reactions of alkenes over rutile have often been studied, the production of compounds of higher carbon number may not have been reported because of the inability of the G.C. columns used in such experiments to detect such compounds. Using the column filled with Porapak S however, which is that normally employed for alcohol decomposition studies, no significant reaction seemed to take place. Traces of ethene were detected but there were certainly no peaks on the G.C. trace which could be assigned to C₆ compounds. Addition of water to the system in order to simulate alcohol dehydration conditions more closely, caused no further reaction.

5.3.3.6 The Reaction of Alkyl Halides: Dehydrohalogenation

In order to complete the studies of the reaction of propan-1-ol over rutile in the presence of HCl, (section 5.3.2.5), 1-chloropropane and 2-chloropropane were both reacted over rutile at 425 K, approximately 150 K lower than the temperatures required for propan-1-ol decomposition. Apart from the difference in the required temperatures for the two reactions, the alkyl halide decomposition differs from that of the alcohols in that isomerisation of the starting materials takes place before the elimination reaction to propene and HCl goes to

completion; (Fig. 5.33). It was thought that as the dehydrohalogenation produces HCl, which is known to activate rutile catalysts, this reaction would perhaps be autocatalytic. However, Figs. 5.33 and 5.34 show that although the rapid initial decomposition may suggest some autocatalysis, the latter stages of the reaction appear to be poisoned and the temperature had to be raised for both reactants in order to promote further dehydrohalogenation. Noller and other workers¹¹³ have suggested that reduction of the rate of dehydrohalogenation as the reaction proceeds may be due to the reverse reaction taking place which is indicated in these experiments by the formation of the isomers of the reactants.

These experiments do show that in the reactions described in section 5.3.2.5, where propan-1-ol and HCl are both reacted over rutile at 500 K, rutile catalyses both the halogen substitution reaction and the subsequent decomposition of the alkyl halide to alkene + HCl.

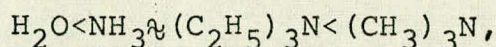
5.4 Discussion

5.4.1 2-Methylpropan-2-ol

The pretreatment of rutile with certain molecules has previously been found³⁷ to perturb the isomerisation of but-1-ene to cis/trans-butene. The reaction rate was retarded by some species (H_2O , HCN, NH_3 , ethylene diamine) and promoted by others e.g. HCl and Cl_2 .

The experiments described in this chapter show that such treatments cause rather similar perturbations on the rate of dehydration of 2-methylpropan-2-ol at 423 K.

The order of the inhibiting properties of the studied molecules being:-



whereas both HCl and Cl₂ were found to activate the catalyst for this reaction.

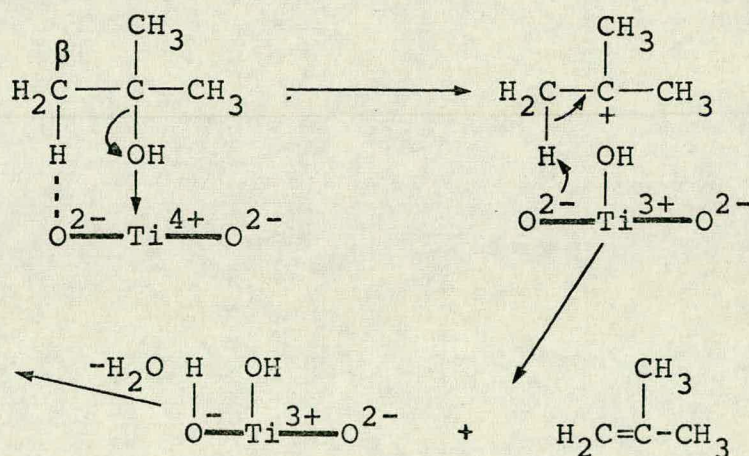
This approximately parallel decline in activity for the two reactions makes it attractive to postulate the catalytic centres for the dehydration of 2-methylpropan-2-ol are the same as those active for double bond migration reactions. Brookes³⁷ associated the sites for double bond migration with the exposed Ti⁴⁺ ions on the rutile surface as the catalyst was poisoned by nucleophilic molecules which could co-ordinate to such ions and therefore block the Lewis acid sites. The mechanism proposed by the author is described in Fig. 1.9 (Chapter 1).

The molecules water, ammonia and hydrogen chloride are known to adsorb both dissociatively and in a molecular fashion onto rutile surfaces. It is not entirely clear how the dissociative form of adsorption would affect the catalytic activity of rutile towards 2-methylpropan-2-ol dehydration. It may be that a dissociatively adsorbed molecule also blocks the catalytic sites. However trimethylamine, which readily poisons the dehydration is known to primarily adsorb on rutile by coordination to the titanium ion Lewis acid sites¹²⁶ and adsorption of HCl which enhances reactivity would be expected to activate the acidic sites on rutile. HCl is known to confer Brønsted²⁵ acidity to a rutile surface. The adsorption of chlorine, which cannot generate Brønsted

acid sites, activates the catalyst in a similar manner to HCl. It therefore seems rather likely that the enhanced activity reported in the relevant sections (5.2.6 and 5.2.7) was due not to Brønsted acidity but to an induction effect increasing the strength of the Lewis acid sites.

The sites associated with the dehydration of 2-methylpropan-2-ol are therefore believed to be Lewis acid Ti^{4+} ions. These probably operate in conjunction with O^{2-} ions acting as bases by removing the proton from the β -carbon atoms according to the scheme in Fig. 5.35 although the sensitivity of the reaction to the preadsorption of HCl and Cl_2 suggests that the cation is the more important of the two surface ions. The adsorption of HCl and Cl_2 probably shifts the reaction mechanism closer to a pure E1 elimination rather than the partial E2 described below.

Fig. 5.35



The fact that the inhibiting effect of the adsorption of bases onto rutile is lower for alcohol dehydration than for alkene isomerisation can be rationalised if the alcohols are regarded as stronger bases than alkenes and thus more capable of readily displacing the preadsorbed bases from the Lewis acid sites. If this were not the case, water formed during the dehydration reaction would poison the catalyst in the latter stages of the reaction and such behaviour is not observed with any 2-methylpropan-2-ol reactions. Adsorption studies by Day et al²⁸ suggested that ethanol rapidly displaces water from rutile surfaces at 298 K. Another explanation may be that a rutile surface may not be composed of acid sites which are all of equal strength and the preadsorption of nucleophilic species, especially at the lower levels of preadsorption, may only be blocking the stronger acid sites which are necessary for but-1-ene isomerisation but do not affect the weaker acid sites which may still be readily capable of catalysing alcohol dehydration. The general understanding of the sites associated with elimination reactions over oxides is not particularly well established and there is disagreement in the literature about this subject⁵¹.

Gentry, Rudham and Wagstaff¹⁰⁶, studying the decomposition of propan-2-ol over rutile at 473 K in a flow system reported that the presence of pyridine and tetracyanoethylene in the reactant stream poisoned the dehydration of this alcohol to propene. They thus concluded that the sites for the dehydration were the $Ti^{4+}O^{2-}$ Lewis acid/base pairs. They, however, considered

that the dehydration would be more likely to take place on the (100) and (101) faces of rutile than on the (110) face, since from spectroscopic^{11,12,22} and temperature-programmed-desorption studies¹⁹, at the reaction temperatures under study (473 K), the (110) face is covered with hydroxyl groups which, the authors implied, would block any active sites. The authors however seem to have neglected the shielding effect of the anions upon the accessibility of the titanium ion sites. Infra-red spectroscopic studies and an examination of a scale-model of a rutile surface (Fig. 5.36) based on the ionic radii of the titanium and oxide species have allowed Speakman¹²⁶ to conclude that only the (110) plane includes titanium ion Lewis acid sites which are accessible for the adsorption of certain organic bases. An examination of this model and also molecular models of trimethylamine and triethylamine showed that adsorption of trimethylamine was only possible on the Lewis acid sites on the (110) plane and that no Lewis acid sites on the (100) and (101) planes were accessible for trimethylamine adsorption due to steric hindrance from neighbouring oxide ions. This explained why the infra-red spectrum of trimethylamine adsorbed on rutile which had been outgassed at 473 K displayed a sharp band at 1490 cm^{-1} which indicated adsorption of trimethylamine on Lewis acid sites which were all of the one type i.e. those on the (110) plane. Spectroscopic studies also showed that with triethylamine, a stronger base than trimethylamine, there was no detectable adsorption onto the rutile. Inspection of the model revealed that this

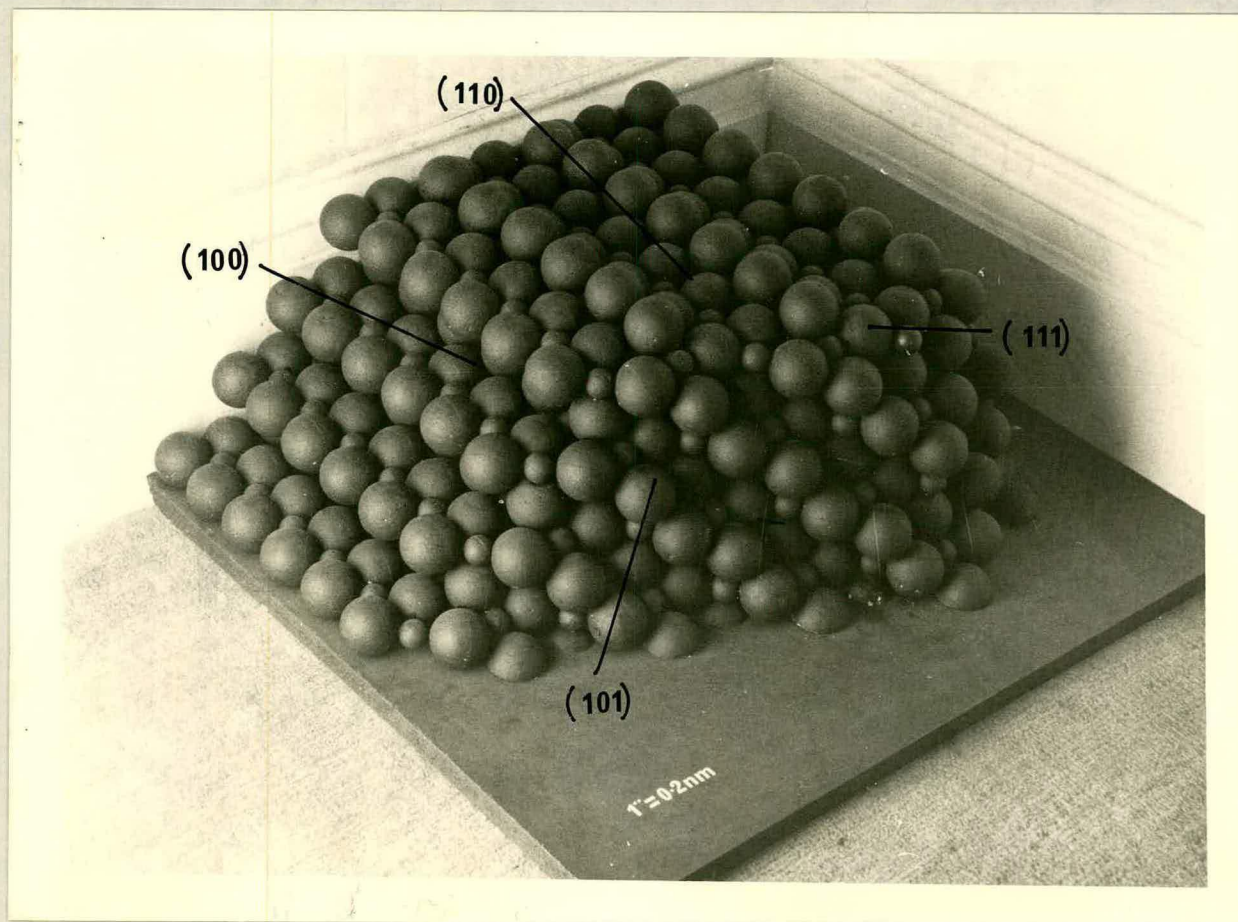


figure 5.36 the surface of rutile after Speakman¹²⁶ showing the various crystal planes; the small balls represent titanium ions and the large balls oxide ions.

was because no surface titanium ions are accessible for the adsorption of a triethylamine molecule. A paper by Krubek et al¹²⁷ describes similar results for amine adsorption on γ -alumina where steric hindrance during adsorption was considered to be the reason for the amount of adsorbed amines on γ -alumina decreasing in the order

ethylamine > diethylamine > triethylamine

The results described in section 5.2.4 suggest that as preadsorption of trimethylamine readily poisons the dehydration of 2-methylpropan-2-ol, the active plane for this reaction is the (110) plane and not the (100) or (101) planes where trimethylamine is not readily adsorbed. This is further substantiated by the fact that the adsorption of triethylamine, a stronger base, had a lesser poisoning effect than trimethylamine. The model structure already referred to would indeed predict very little triethylamine adsorption. The rate of dehydration is reduced after triethylamine pretreatment which suggests that there is some adsorption, and the ideal model structure is certainly likely to be significantly different to the real catalyst sample. In any case, it is clear that the accessibility of surface catalytic sites is probably as important as their acid/base strength when certain catalytic reactions are under consideration.

5.4.2 Propan-1-ol

The decomposition of propan-1-ol differed from that of 2-methylpropan-2-ol in that the former is overall

more complex with five major (not including H₂O) and four minor products being formed during the reaction. The poisoning studies did not increase the understanding of the surface chemistry of the decomposition of propan-1-ol to the extent as had been hoped and even tended to suggest further complications. The significant desorption of the preadsorbed species at the elevated temperatures (\approx 590 K) required for the reaction precluded any quantitative estimate of the sites involved with the various surface reactions, and did not help to identify the nature of such sites.

In contrast to the 2-methylpropan-2-ol results, preadsorption of the appropriate species did not affect the formation of any of the products of the propan-1-ol decomposition in a similar manner to that reported by Brookes³⁷ for alkene isomerisation reactions. This made it difficult to reconcile the results of the poisoning experiments with the view that all the surface reactions could be described in terms of the Lewis acid/base properties of the rutile surface. In particular, the poisoning studies did not produce a clearer insight into the mechanism of the formation of the coupling compounds, the reaction which was initially thought to be the most interesting aspect of the decomposition; especially if, indeed, benzene had been formed as had been previously reported⁴⁵. The preadsorption of water, ammonia and hydrogen chloride did, however, interfere with the dehydration of propan-1-ol in an unexpected manner.

5.4.2.1 Dehydration

The major reaction during the decomposition of propan-1-ol over rutile was always the dehydration to propene and as described in section 5.3.2, the preadsorption of small amounts (0-0.2 molecules nm^{-2}) of water, ammonia and hydrogen chloride all tended to confer on rutile greater activity for this reaction. These results were the converse of those observed when the reaction under study was the dehydration of 2-methylpropan-2-ol or the isomerisation of but-1-ene³⁷. Adsorption of trimethylamine, on the other hand, acted as a poison for this reaction (section 5.3.2.4).

The necessity of surface water or hydroxyl groups for oxide catalysts to be active for dehydration has often been suggested⁵¹ to explain certain experimental results obtained in this field. Brey and Krieger⁵⁶, basing their conclusions on earlier work by Eucher and co-workers^{70,71,128} suggested the existence of an optimum surface water content for the dehydration of ethanol to ethene over γ -alumina after observing a consistent increase in activity with use of certain catalyst preparations. Pines and Haag⁶⁰ came to a similar conclusion about surface water content when examining the isomerisation of cyclohexene over alumina as did Munro and Horn¹²⁹ when examining the dehydration of ethanol to diethyl ether over alumina. A number of authors have pointed out that results in this field are often contradictory, especially when oxide catalysts are under consideration.

There is more general agreement on this topic when zeolites have been used as catalysts. The promoting action of water in cracking reactions on Y-type zeolites has been discussed by Romanovskii et al¹³⁰ and recently Jacobs et al¹³¹ reported that the addition of small amounts of water into the reactant stream of a flow system had a favourable effect upon the initial dehydrating ability of alkali cation-exchanged X and Y zeolites. Results reported by Gryaznova¹³² and co-workers showed that when butanols were dehydrated over type X and Y zeolites, water formed during the reaction was adsorbed by the zeolite which caused an increase in its activity. On NaNiY zeolite, for example, water adsorption was responsible for a four-fold increase in catalytic activity.

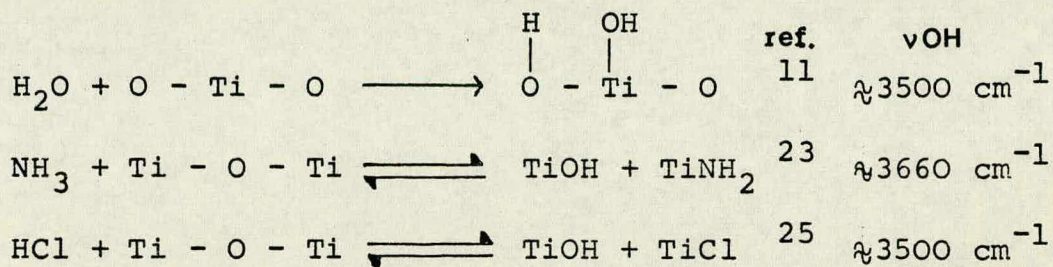
The increased activity of a catalyst towards acid site catalysed reactions with water adsorption immediately suggests the active presence of protonic (Brønsted) acid sites on the catalyst surface and such sites have often been considered to be a source of activity for alcohol dehydration reactions on zeolites^{113,133} and to a lesser extent on oxides⁵¹.

The desirability of an optimum water or hydroxyl content on oxide catalyst surfaces has often been postulated^{51,56} but, until recently, very little evidence has been presented to show that oxide catalysts possess active Brønsted acid sites. Pines and Haag⁶⁰ in 1960, concluded from studies using organic indicators that Brønsted acid sites on alumina, if present at all, are of very low acid strength. Peri and Hannan¹³⁴, also

working with alumina, found that hydroxyl groups on alumina could exchange hydrogen easily, but at a rate significantly lower than the rate of isomerisation of but-1-ene. This observation led the authors to question if the hydroxyl groups were the active isomerisation sites. Recent work by John¹³⁵ and other workers, which will be referred to in Chapter 6, has clearly indicated the existence of Brønsted acid sites on alumina, especially when water is "added back" onto the alumina.

With respect to titanium dioxide there are reports in the literature suggesting the presence of Brønsted acid sites on anatase^{21,42}, but on the rutile form there is no clear evidence from either spectroscopic^{21,22,23,24,126} or catalytic^{37,45} studies for the existence of such sites. Deuterium exchange reactions between D₂O and other species have however often been reported over rutile and Boehm³⁴ reported at the Discussions of the Faraday Society (1971) that hydroxyl species on a number of oxides, including rutile, are amphoteric in character, approximately half being acidic and half being basic. His interpretations were based on a range of experimental data, including adsorption measurements, but his conclusions were not entirely accepted in the general discussions that followed the presentation of the paper¹³⁶. Parfitt and co-workers²⁵ have also reported that the adsorption of hydrogen chloride gas on rutile leads to surface species which act as Brønsted acid sites in the presence of adsorbed ammonia or pyridine.

Several authors^{37,45,106} have thus tended to discount the participation of Brønsted acids in catalytic reactions on rutile, particularly alcohol dehydration. The results described in this chapter however, strongly suggest their participation in the dehydration of propan-1-ol to propene. The unexpectedly similar results with H₂O, NH₃ and HCl may not be so surprising when considered in the light of dissociative adsorption which has been reported to occur over rutile with such species, with the formation of hydroxyl groups as shown below^{11,23,25}. It is interesting to note that with the preadsorption of trimethylamine, which is not known to adsorb in a dissociative manner, no enhancement of the dehydrating activity of rutile was observed.



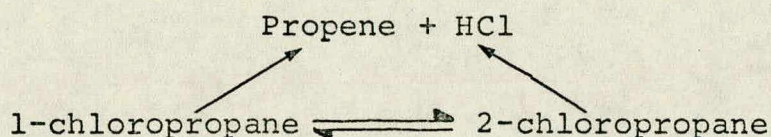
All the above dissociative adsorptions produce those hydroxyl species which, according to Boehm³⁴, are most likely to be acidic, as they are formed from the combination of a proton and a lattice oxygen species. According to the model of Speakman¹²⁶, the adsorption of organic bases, e.g. pyridine, trimethylamine or triethylamine, onto such hydroxyl groups would be subject to strong steric hindrance and the author thus concluded that this may well be the reason why infrared spectroscopic techniques do not reveal Brønsted acid

sites on rutile. Those hydroxyl groups which are accessible are of basic character and thus would not be expected to react with other bases.

In the experiments using an excess of water or ammonia in the reaction system with the alcohol, a decrease in the activity of rutile towards dehydration was observed. During these experiments therefore the surface hydroxyl content of the rutile must have been in excess of the optimum and similar observations have been reported by Brey and Krieger⁵⁶ for the dehydration of ethanol over alumina and by Pines and Haag⁶⁰ for the isomerisation of cyclohexene over alumina. The inhibiting effect of the excess water or ammonia may have been due to the co-ordinate adsorption of these species onto bare Lewis acid Ti^{4+} ion sites but since the presence of Brønsted acid sites has been indicated the interference may have been due to water or ammonia molecules blocking the active hydroxyl groups via hydrogen bonding. The possibility thus exists that the interference was due to physical adsorption of the poisoning species with the formation of multi-layers and this form of adsorption has no relevance to the identification of the catalytic sites. Although physical adsorption is not considered likely at the temperature ranges under study (≈ 600 K), infra-red spectroscopic studies by Jackson and Parfitt¹⁴ have shown that rutile can retain physically adsorbed water molecules at temperatures up to 573 K.

The presence of excess HCl in the system completely changed the characteristics of the propan-1-ol

decomposition reaction and altered the role of the rutile to that of a catalyst for the formation of chloropropane and then for the dehydrohalogenation of the alkyl halide to propene and HCl. Since dehydrohalogenation, like dehydration, is an elimination reaction, it is worth considering it at this point. Other than the lower temperatures required for dehydrohalogenation of an alkyl halide, it differed from the dehydration of the alcohol in that considerable isomerisation of the starting material was observed i.e.



These results support the ideas of Noller and Kladnig¹¹³. As a C-Cl bond is more polar than a C-O bond, it is more easily broken and therefore elimination occurs both at a lower temperature and has more E1 character than dehydration which results in a longer lifetime for the carbonium ion intermediates. This increases the likelihood of isomerisation of the starting material. As previously stated, the reaction may be autocatalytic because the HCl produced during the reaction confers increased acidity to the rutile. The situation is perhaps even more complex in that there is also the possibility of HCl production resulting in an increase of the polarity of the rutile catalyst which consequently causes the reaction to shift towards an E1 elimination as the reaction proceeds. The fact that in the latter stages the reaction tended to

slow down indicates that excess HCl hinders the reaction.

5.4.2.2 Dehydrogenation and the formation of C₆ compounds

As was previously suspected (Chapter 4), the absence of any similarity between the effects of H₂O, NH₃, HCl and the organic bases on the dehydration and the dehydrogenation reactions indicates that the active sites involved with the two reactions are not the same. The poisoning studies also revealed that the sites active for dehydrogenation on rutile are not likely to be acid/base pairs. Such sites have been suggested by Kibby and Hall⁷² and Jacobs and Uytterhoeven⁷⁵ to be present on zeolite catalysts (see Fig. 3.7).

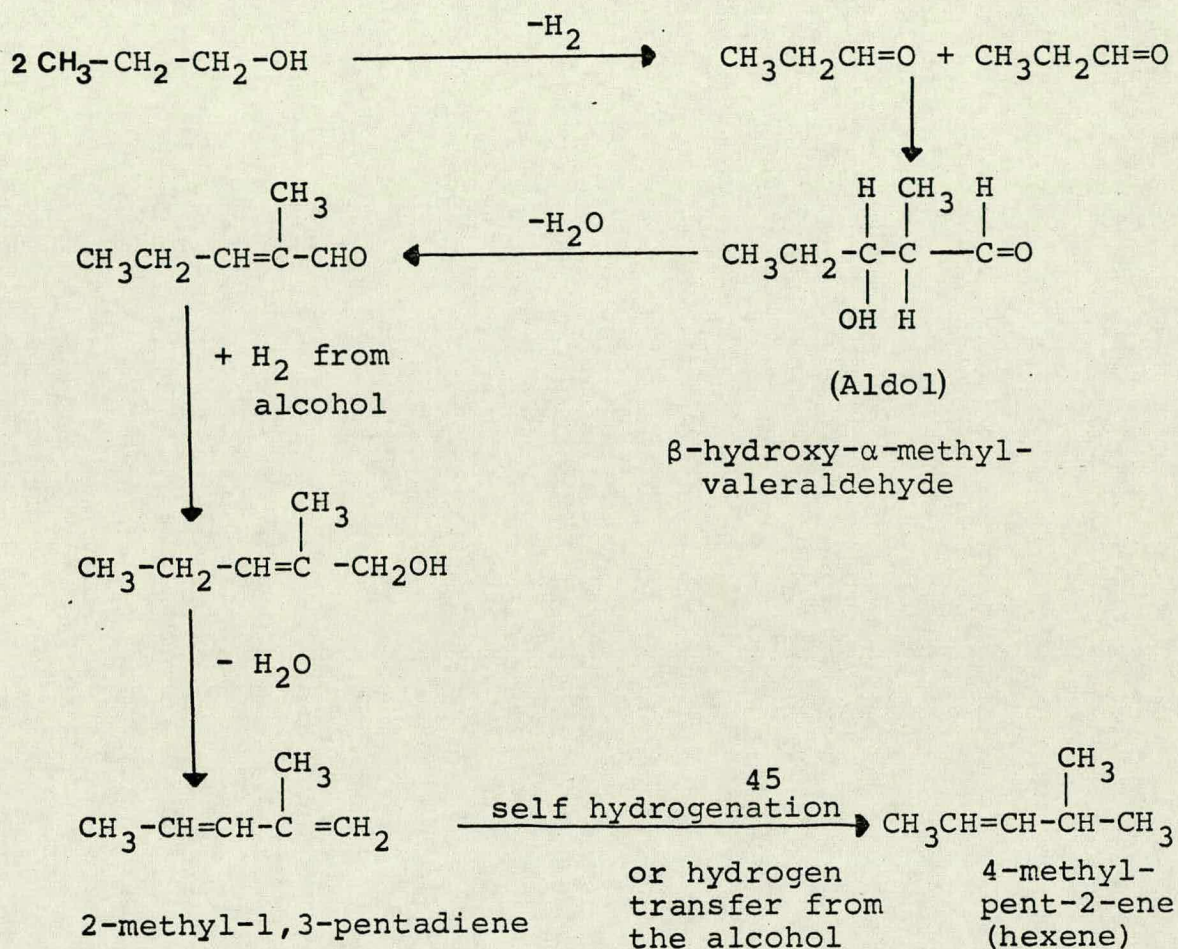
Very little information was obtained from the poisoning studies, therefore, concerning the dehydrogenation of the alcohol to the aldehyde.

The results do confirm that the aldehyde plays an important role during the coupling reaction. The experiment when propene alone was reacted over rutile showed that this compound was not involved in the coupling reaction. The experiments which resulted in an inhibition of the formation of the coupling compounds were accompanied by an increase in the production of propanal and the reaction of this aldehyde alone over rutile also resulted in the formation of the coupling compounds.

The reaction of carbonyl group-containing compounds to form species of higher carbon number is known as an aldol condensation, is well documented in the chemical literature¹³⁷ and, in the field of organic

chemistry, is known to be promoted by the influence of dilute acid or dilute base. The condensation of aldehydes and ketone is also known to be promoted by heterogeneous catalysts. Nondek¹³⁸ has recently discussed the liquid phase alumina catalysed aldol condensation of cyclohexanone and work by Fujii¹³⁹ and later Kemball³⁶ described the condensation of acetone over titanium dioxide to form mesityl oxide, mesitylene and other high molecular weight compounds. Ipattief and Haensel¹⁴⁰ concluded from a study of the formation of higher ketones from a mixture of alcohols and ketones on Cu-ZnO-Al₂O₃ and other catalysts that only those catalysts which had both dehydration and dehydrogenation properties could effect condensation. They also concluded that the formation of 4-methylpentan-2-one from a mixture of propan-2-ol and acetone was initiated by the condensation of two molecules of acetone. The alcohol thus served two functions being (a) a source of acetone and (b) a source of hydrogen which participated in later stages of the reaction. The formation of hexenes from propan-1-ol by the catalytic action of rutile could proceed in a similar manner with the initial dehydrogenation of the alcohol being followed by the condensation of two molecules of propanal e.g.

Fig. 5.37

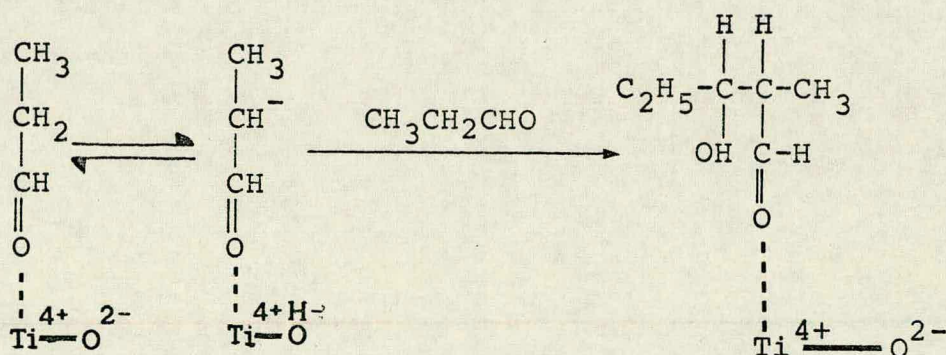


Clearly the role of the catalyst in the above scheme is rather complex and the above is probably only one of a number of possible reaction schemes based on the initial condensation of two aldehyde molecules. The unknown compound on the G.C. trace could thus be any of a number of the possible intermediates as described in the above or similar schemes. The high temperatures required for propan-1-ol decomposition probably generate the high activity of rutile towards both dehydration and dehydrogenation and this may explain why coupling reactions are not observed during the decomposition of propan-2-ol over rutile which occurs at the lower temperature of 530 ± 20 K ⁴⁵.

The fact that the coupling reaction is poisoned by the presence of excess water, ammonia, trimethylamine or alcohol in the reaction system suggests that the sites involved in the initial condensation may be the same as those involved with the dehydration of the alcohol to propene; i.e. the acid site.

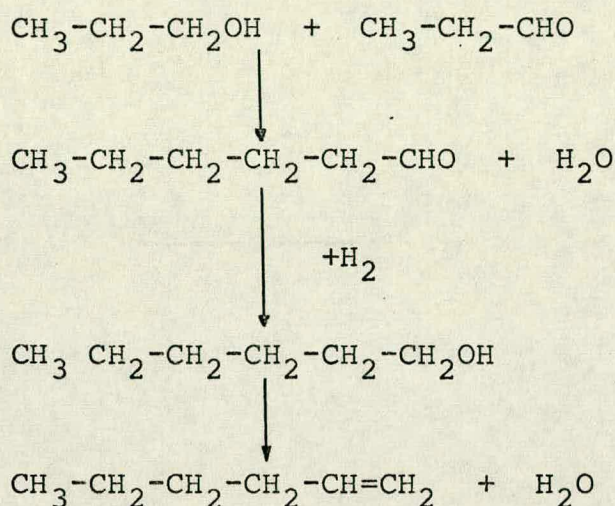
This is in agreement with the results of Griffith and Rochester³³ who concluded from I.R. studies that the formation of mesityl oxide from acetone occurred on rutile via the rapid adsorption of acetone onto the Lewis acid Ti^{4+} ion sites followed by a slow reaction involving a second acetone molecule. Thus the initial condensation of propanal to the aldol may proceed as follows:-

Fig. 5.38



Another mechanism has been proposed for coupling reactions over heterogeneous catalysts which involves an intermolecular dehydration between an alcohol and a carbonyl group containing compound and therefore the formation of hexene from propan-1-ol could proceed as follows:-

Fig. 5.39



This mechanism has been proposed by Kawamoto¹⁴¹ for the condensation of propan-2-ol over copper catalysts and by Davis¹⁴² and Venuto for a similar condensation over Pt/Al₂O₃, Rh/Al₂O₃ and Pd/Al₂O₃ catalysts.

This mechanism is not considered likely during propan-1-ol decomposition over rutile however as G.C. analysis did not reveal the formation of hexanol during the reaction. The mechanism also requires reactive hydrogen atoms which although present on the methyl group of an acetone molecule due to their position adjacent to the carbonyl group, are not present on propanal.

5.4.3 Conclusion

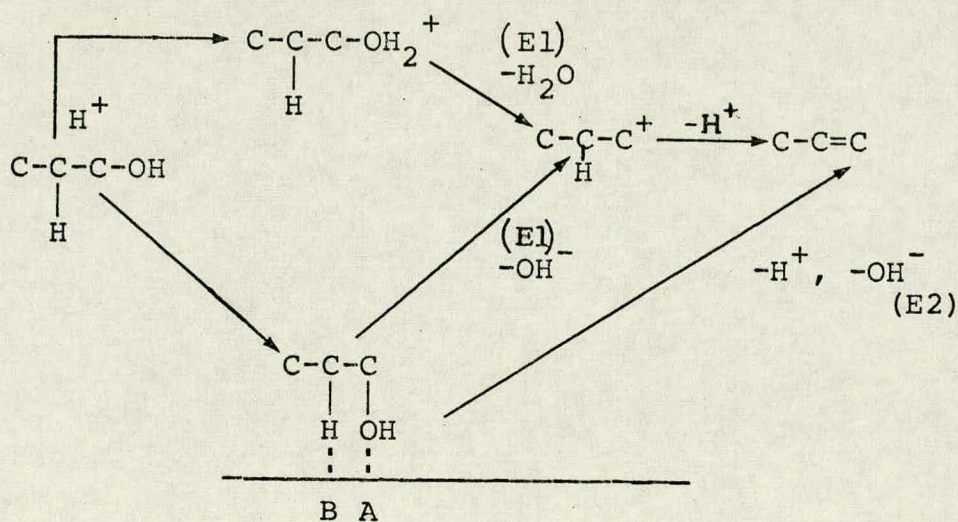
The results described in this chapter show that the action of rutile catalysts during the decomposition of alcohols is highly complex, particularly when high reaction temperatures are necessary. The effect of simultaneous or prior adsorption of certain species on rutile on the decomposition of 2-methylpropan-2-ol at

423 K shows a similarity to previous work on but-1-ene isomerisation. Thus it can be concluded that similar sites are operating during the two reactions, i.e. the Lewis acid coordinately unsaturated Ti^{4+} surface sites with the possible co-participation of the basic O^{2-} ions. The studies with the larger organic bases also indicate that the catalytic centres are situated, although not necessarily exclusively, on the (110) plane of the rutile surface.

The role of the rutile catalyst during the decomposition of propan-1-ol is more complex as there are a large number of factors which have to be taken into consideration in order to obtain a complete understanding of the reaction system e.g. the relative strength of adsorption of the various components in the reaction mixture and their ability to displace each other from the catalyst surface, the extent of hydration or hydroxylation of a rutile surface during a reaction or the effect of the loss of material from the gas phase to the catalyst surface. The applicability of certain experimental results described in the chemical literature to the reaction systems discussed in this chapter must also be treated with caution. The acid/base strength of compounds is normally determined in aqueous media at ambient temperature¹⁴³ and infra-red surface studies of catalysts are also normally carried out at room temperature. Results in the literature also suggest that the actual properties are strongly dependent on the exact mode of preparation of the rutile catalysts.

The high temperature of 590 K associated with the decomposition of propan-1-ol may offer an explanation for the differences in the effects of the preadsorbed species on the reactions of 2-methylpropan-2-ol and propan-1-ol. The differences encountered suggest the development of Brønsted acidity at the elevated temperatures required for propan-1-ol decomposition. As stated in section 5.4.2, there are no reports in the literature of evidence from adsorption and infra-red spectroscopic studies for the existence of Brønsted acid sites on rutile, even after prior adsorption of water to the surface. The acidity of hydroxyl groups on rutile may however increase with temperature as has been shown to occur with some forms of zeolite¹⁴⁴. Infra-red studies have indicated that alumina does not develop protonic acidity at elevated temperatures¹⁴⁵. The careful study of sensitive catalytic reactions on alumina however has shown the opposite to be the case¹³⁵. The main conclusion therefore is that the latter approach should be employed in catalytic studies on rutile and the results of such studies are described in Chapter 6. Thus although rutile may not, indeed, possess intrinsic Brønsted acid sites, and consequently such sites may not play a role in reactions such as alkene isomerisation³⁷ or butadiene self-hydrogenation, the fact that the dehydration of an alcohol probably involves the formation of hydroxyl groups on a rutile surface implies that Brønsted sites may develop and become important during such reactions; particularly when such reactions occur at high temperatures.

The outgassing procedure described in Chapter 2 will result in very few hydroxyl groups remaining on a rutile surface¹⁴⁶ therefore the Lewis acid/base sites must initially be active for propan-1-ol dehydration and so a situation probably exists with rutile which is similar to that envisaged by Yamaguchi¹⁴⁷. He studied the dehydration of alcohols on a series of polar catalysts (not rutile) and concluded that both Brønsted and Lewis acid sites were active and proposed a reaction path as follows.



A : Lewis acid site

B : Lewis base site

figure 5.1 decomposition of 2-methylpropan-2-ol over rutile at 427K:

% composition v time: 2-methylpropan-2-ol, \blacktriangle ; 2-methylpropene, \circ .

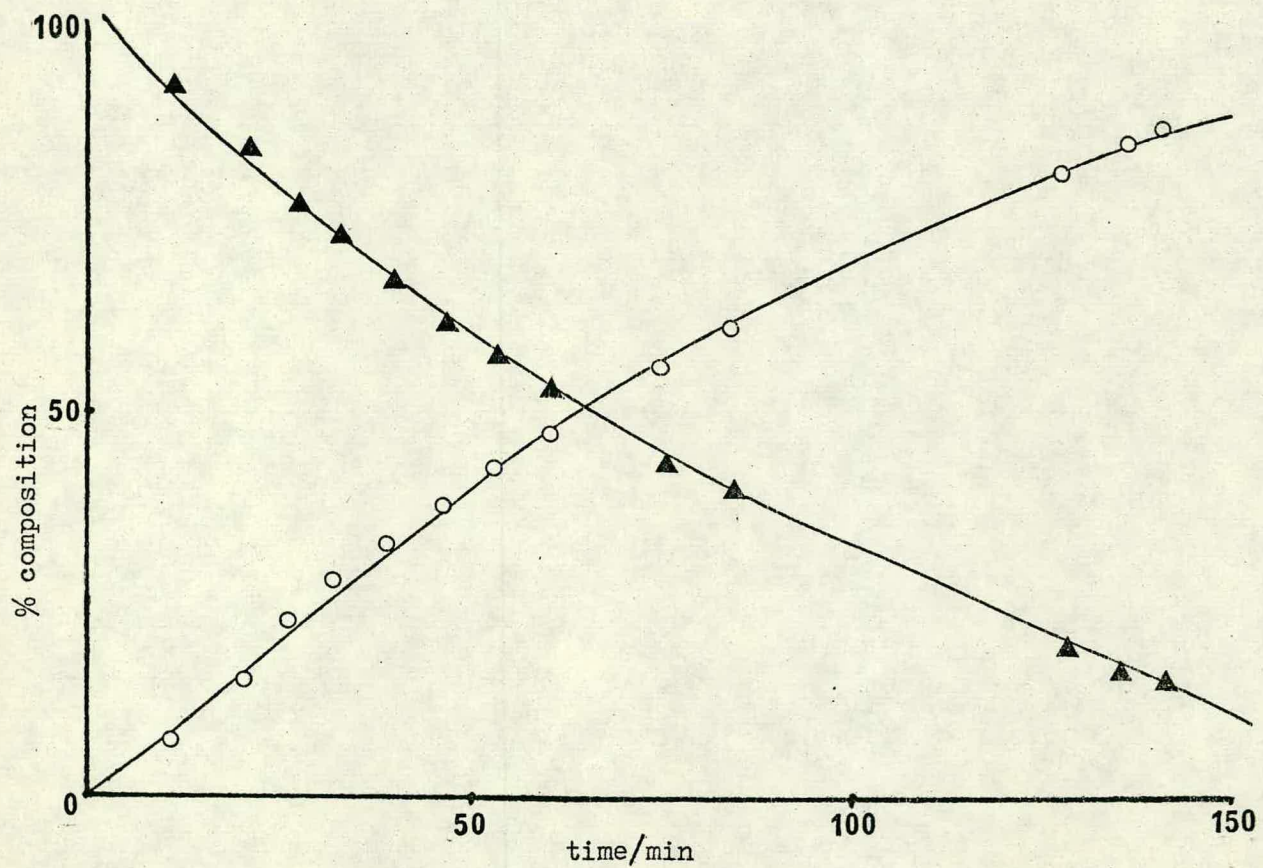


figure 5.2 decomposition of 2-methylpropan-2-ol at 427K:

$\log_{10}(\text{2-methylpropan-2-ol}) \text{ v time}$

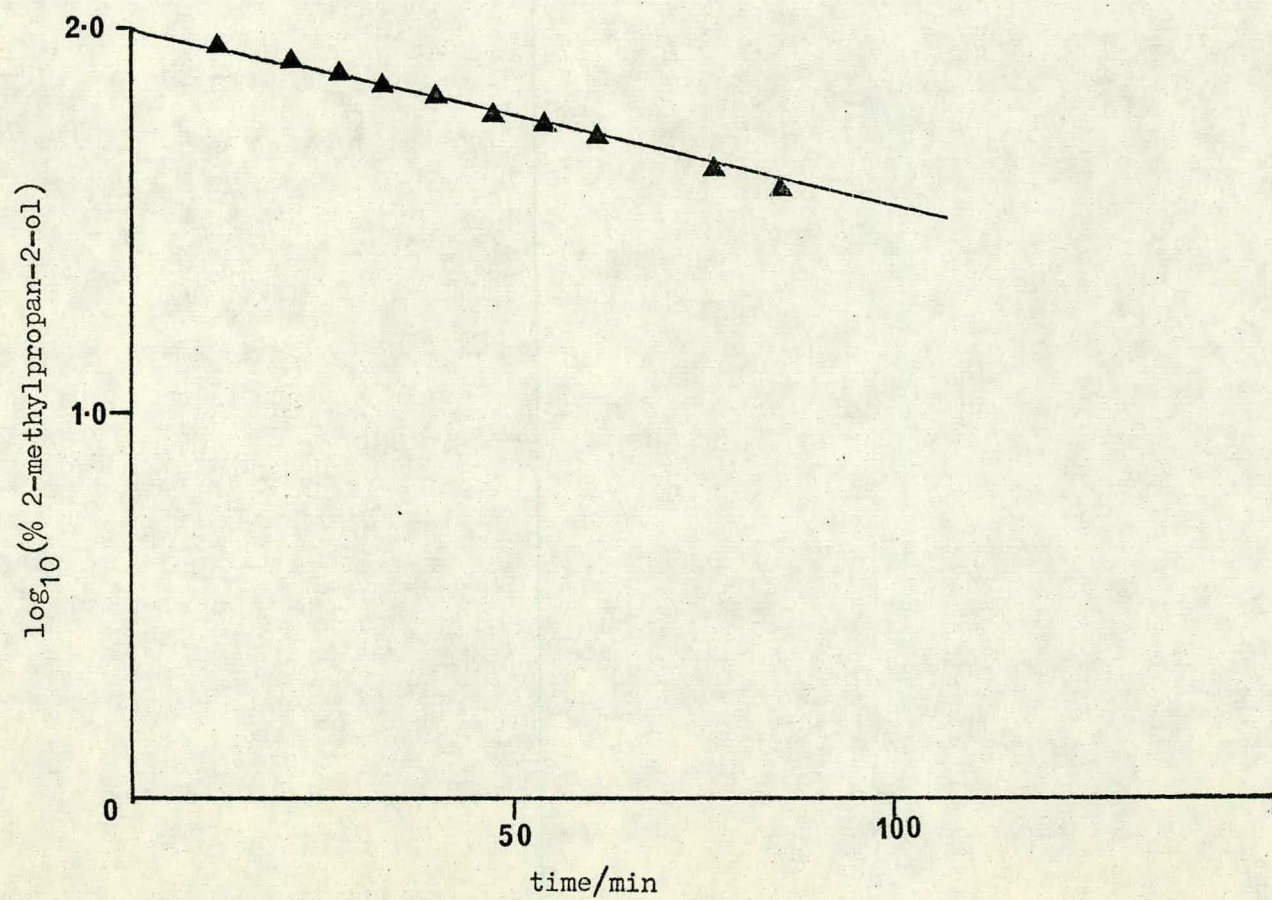


figure 5.3 poisoning of the dehydration of 2-methylpropan-2-ol on rutile at 427K
by water molecules adsorbed at the reaction temperature .

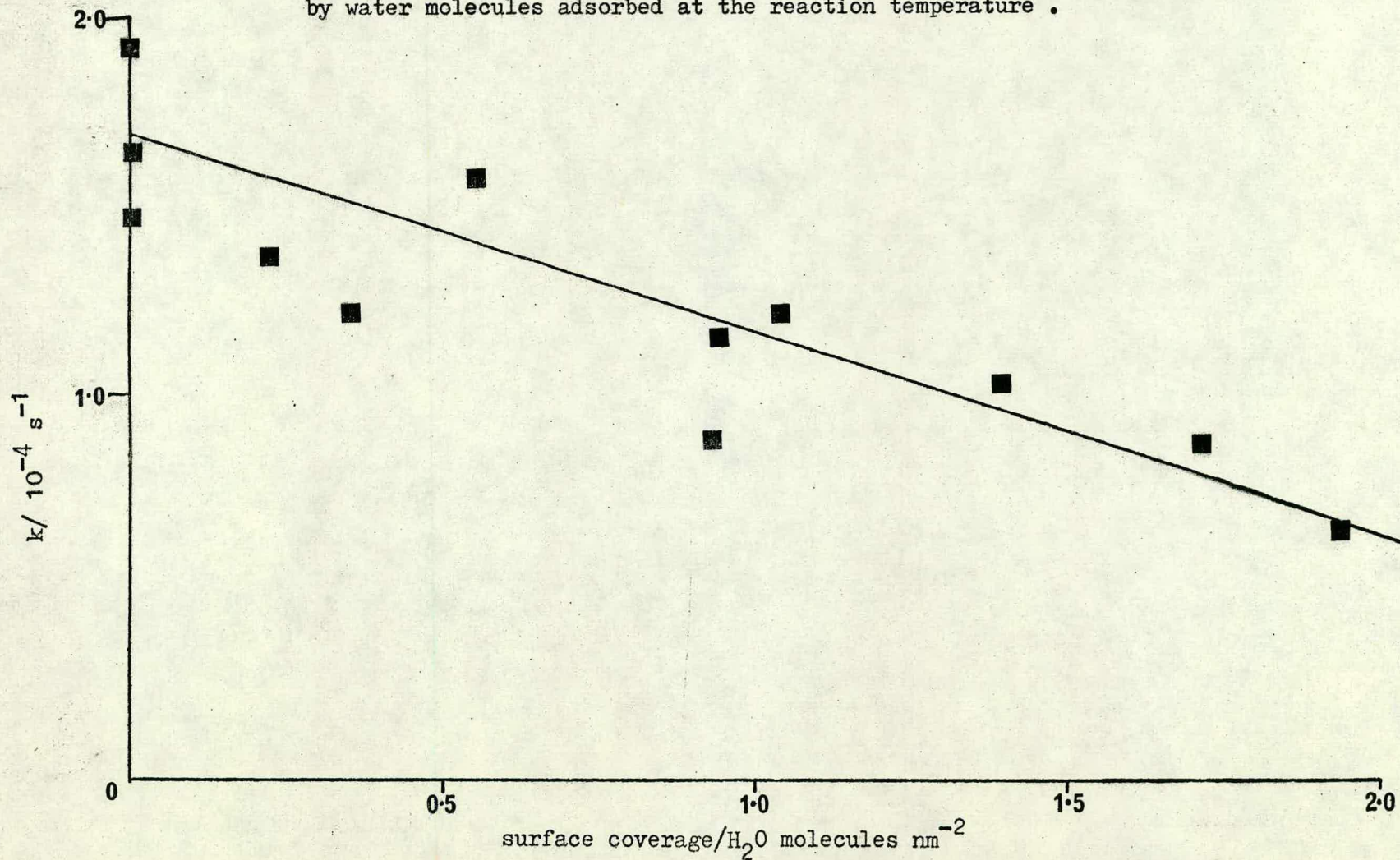


figure 5.4

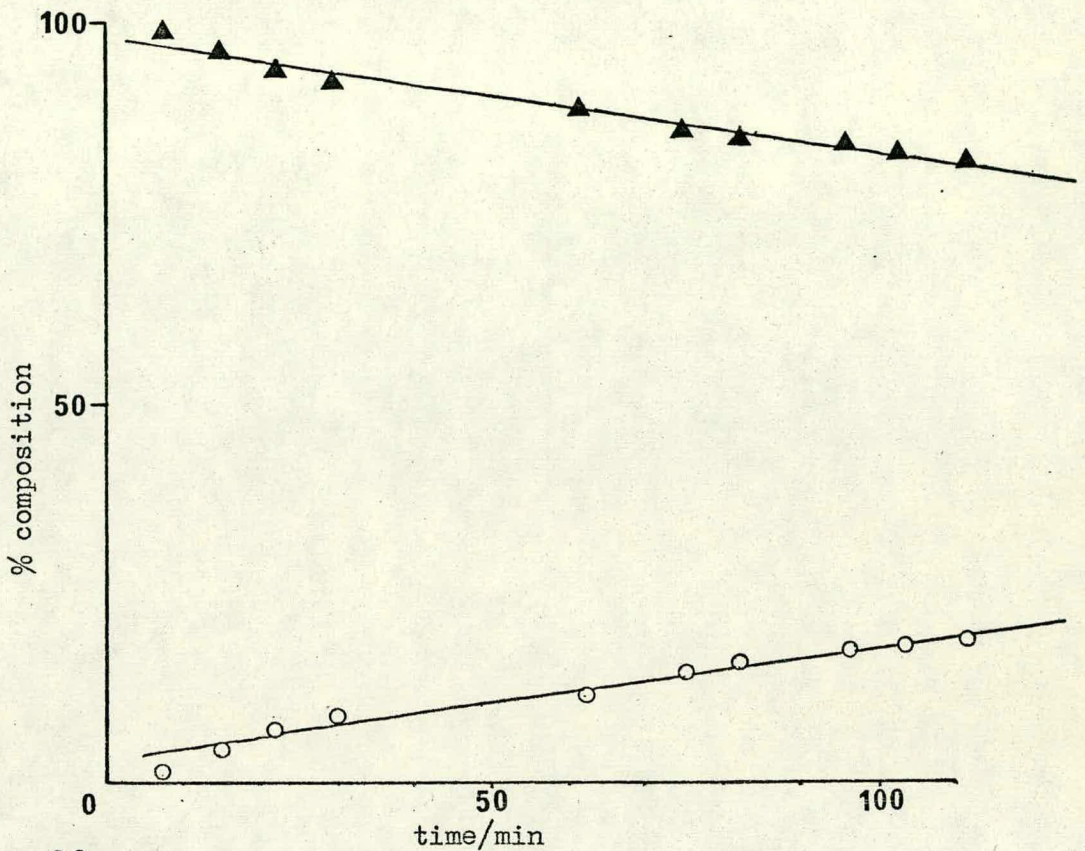
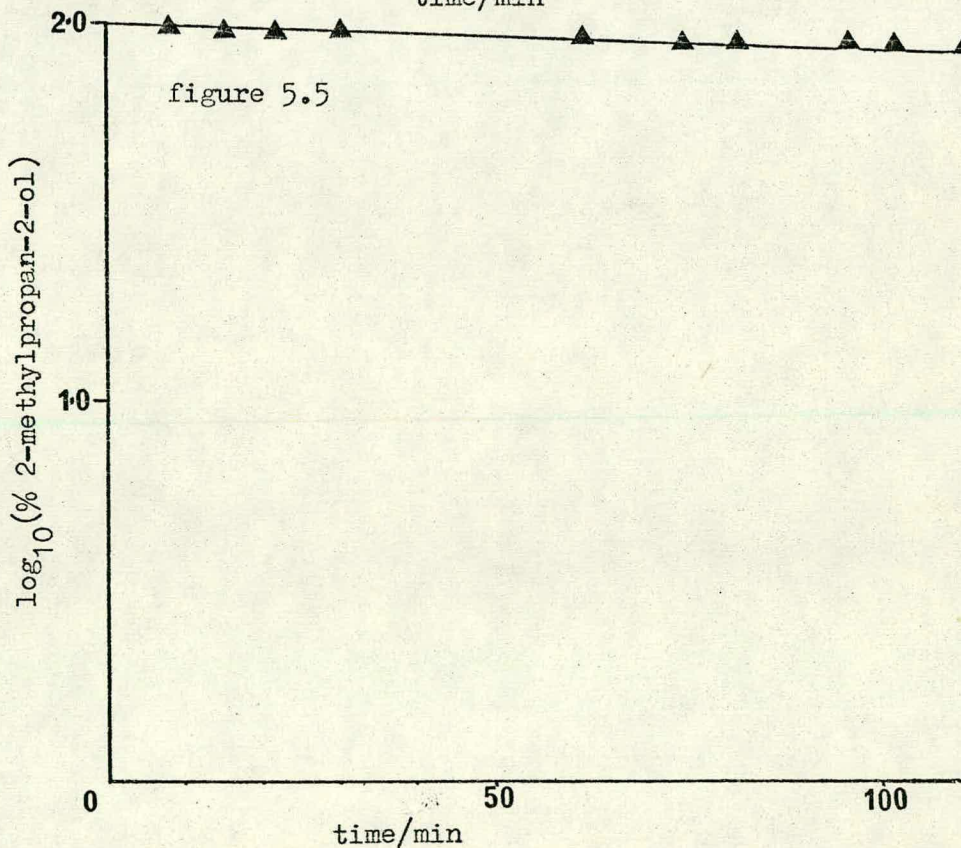


figure 5.5



poisoning of the dehydration of 2-methylpropan-2-ol on rutile at 427K by water molecules admitted to the reaction system simultaneously with the alcohol: 2-methylpropan-2-ol, ▲; 2-methylpropene, ○.
figure 5.4 % composition \checkmark time
figure 5.5 $\log_{10}(\% \text{ 2-methylpropan-2-ol}) \checkmark$ time

figure 5.6 poisoning of the dehydration of 2-methylpropan-2-ol on rutile at 427K
by ammonia molecules adsorbed at the reaction temperature.

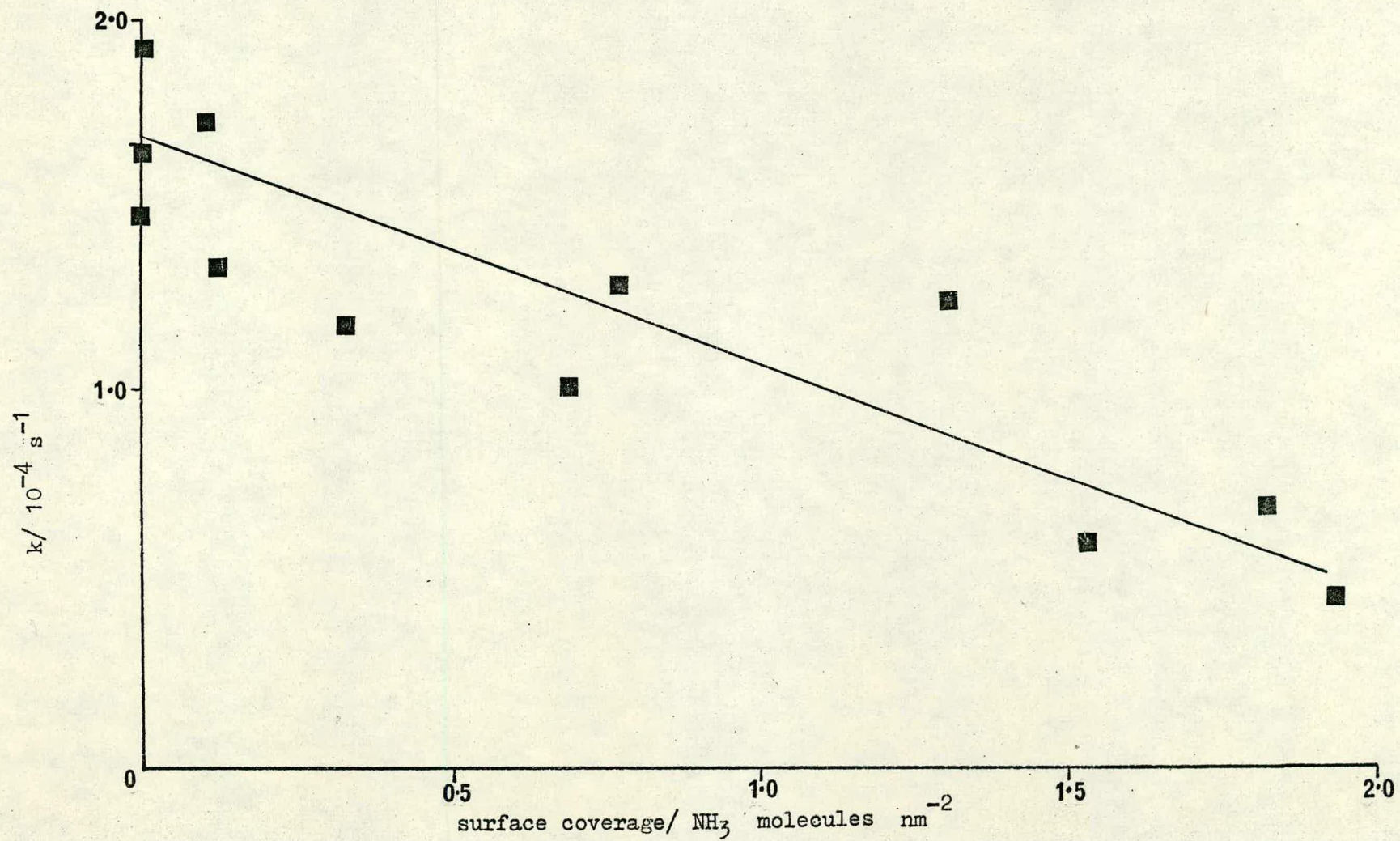


figure 5.7

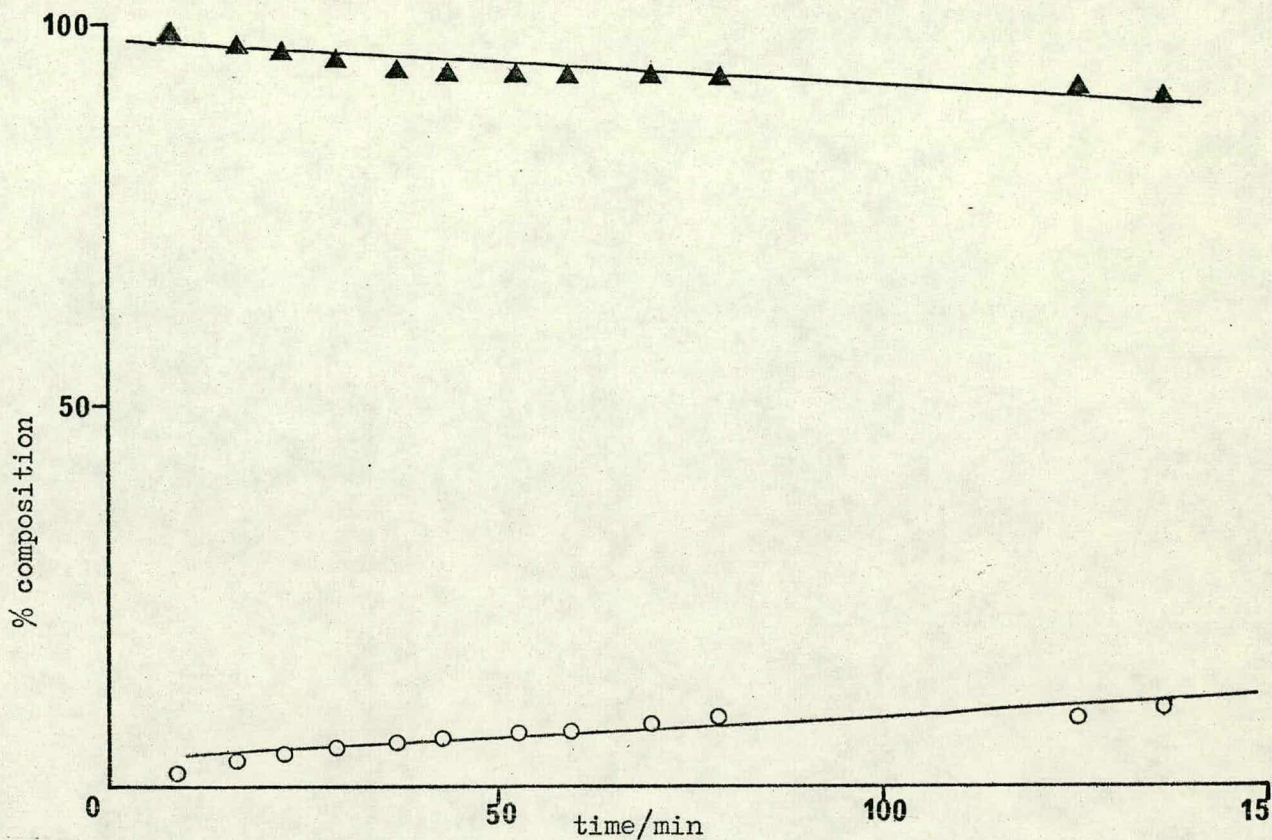
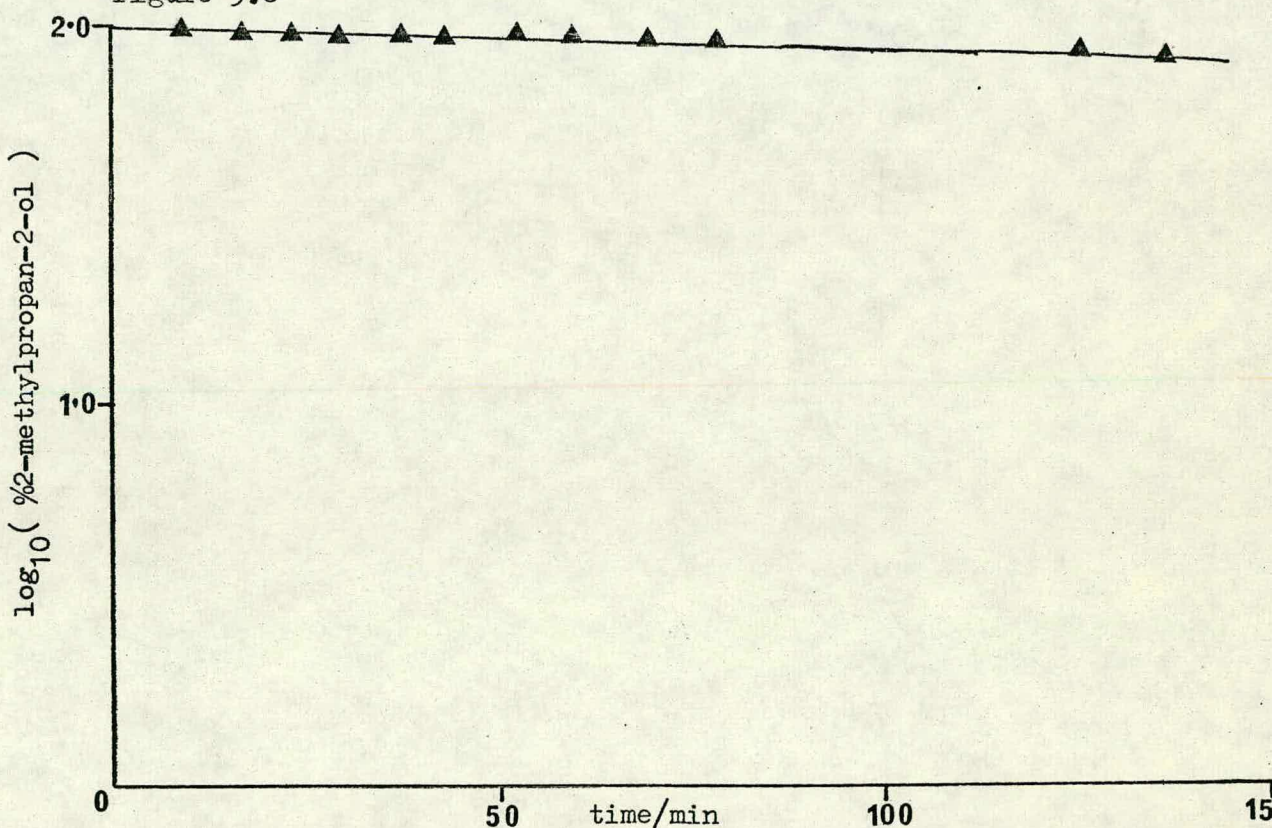


figure 5.8



poisoning of the dehydration of 2-methylpropan-2-ol on rutilite at 427K by ammonia molecules admitted to the reaction system simultaneously with the alcohol: 2-methylpropan-2-ol, ▲; 2-methylpropene, ○.

figure 5.7 % composition v time

figure 5.8 $\log_{10}(\% \text{ 2-methylpropan-2-ol})$ v time

figure 5.9 poisoning of the dehydration of 2-methylpropan-2-ol over rutile at 427K by trimethylamine molecules adsorbed at the reaction temperature.

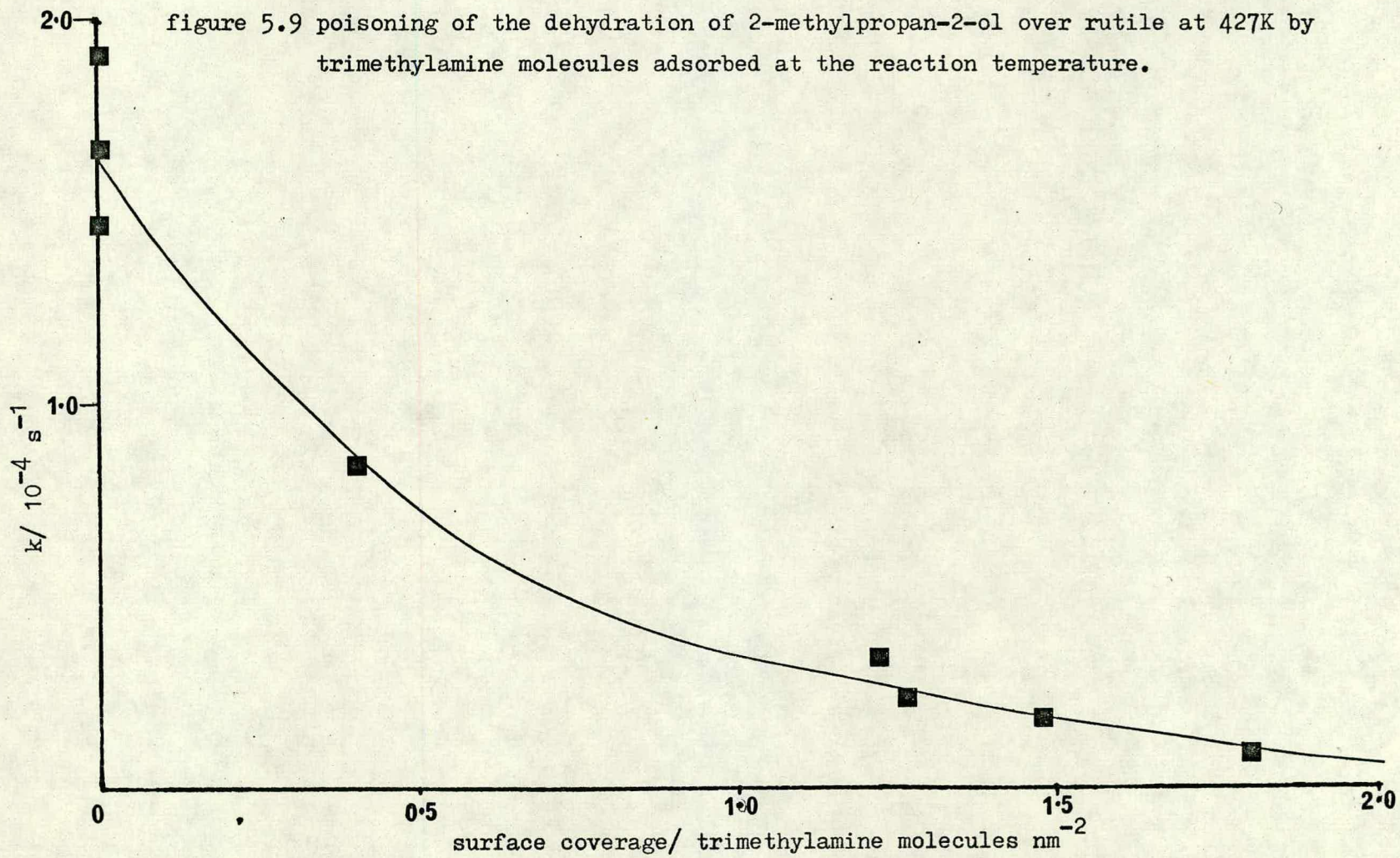


figure 5.10 dehydration of 2-methylpropan-2-ol over rutile at 427K in the presence of trimethylamine as described in section 5.2.4:

2-methylpropan-2-ol, \blacktriangle ; 2-methylpropene, \circ .

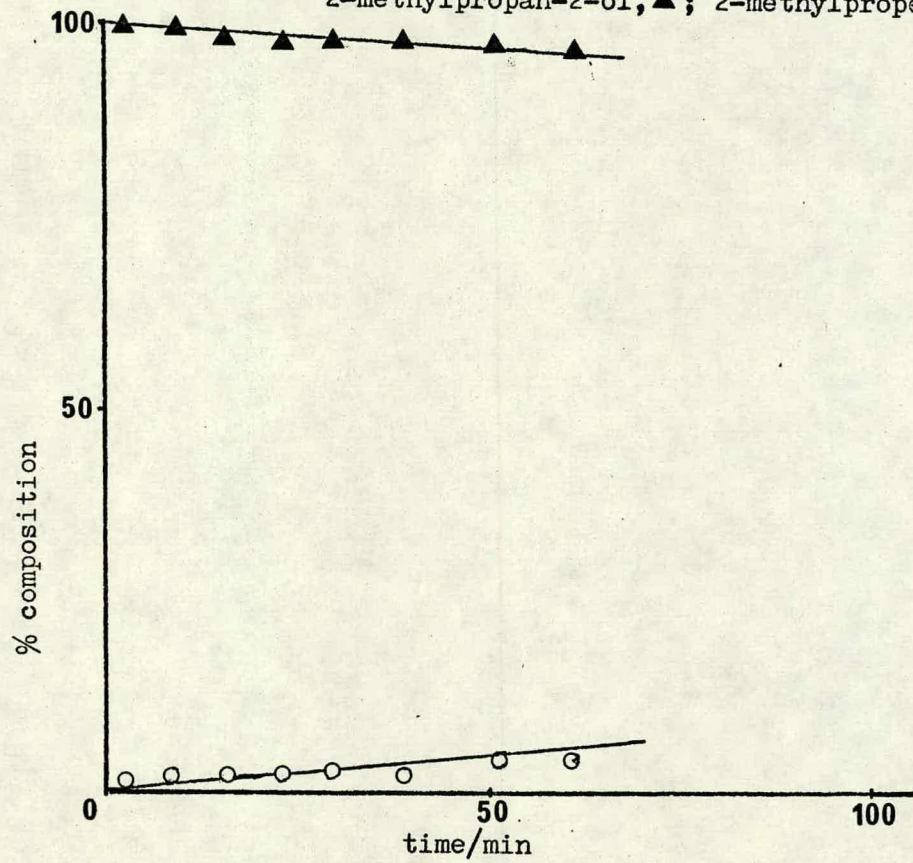


figure 5.11 dehydration of 2-methylpropan-2-ol over rutile at 427K in the presence of triethylamine as described in section 5.2.5:
2-methylpropan-2-ol, \blacktriangle ; 2-methylpropene, \circ .

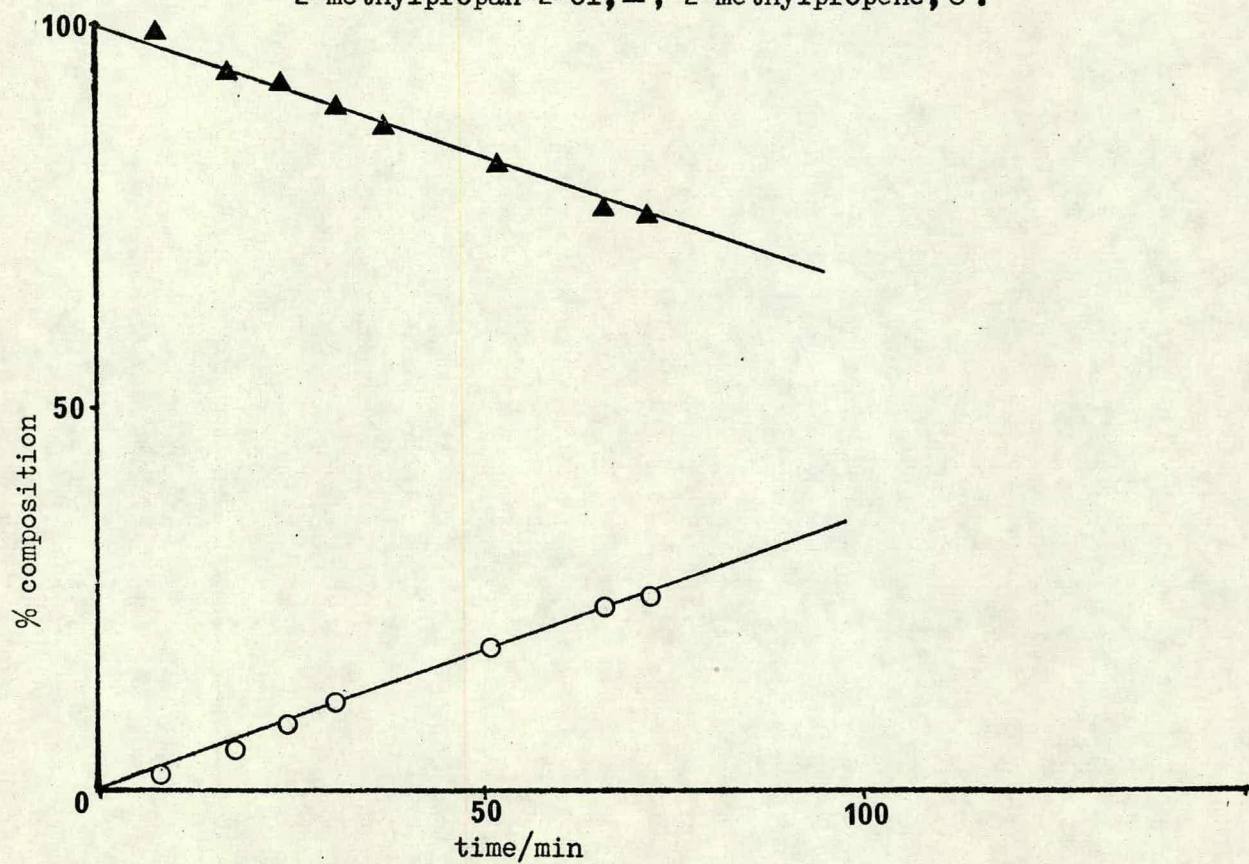
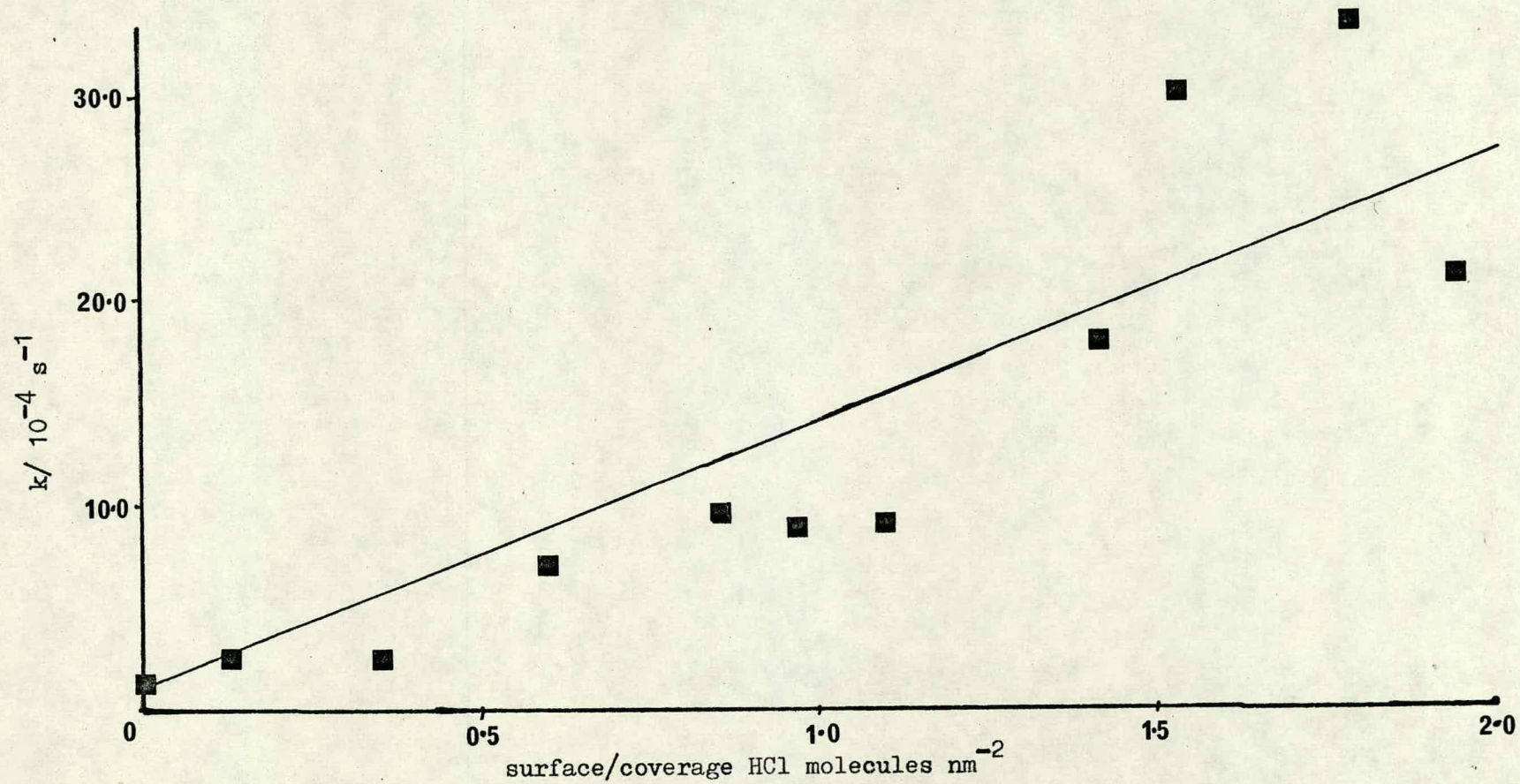


figure 5.12 activation of the dehydration of 2-methylpropan-2-ol over rutile at 427K by hydrogen chloride molecules pre-adsorbed at the reaction temperature .



- 1,2 ?
- 3 propene
- 4 butene
- 5 propanal
- 6 1-chloropropane
- 7 propan-1-ol
- 8 hexene
- 9 ?
- 10 n-propyl ether

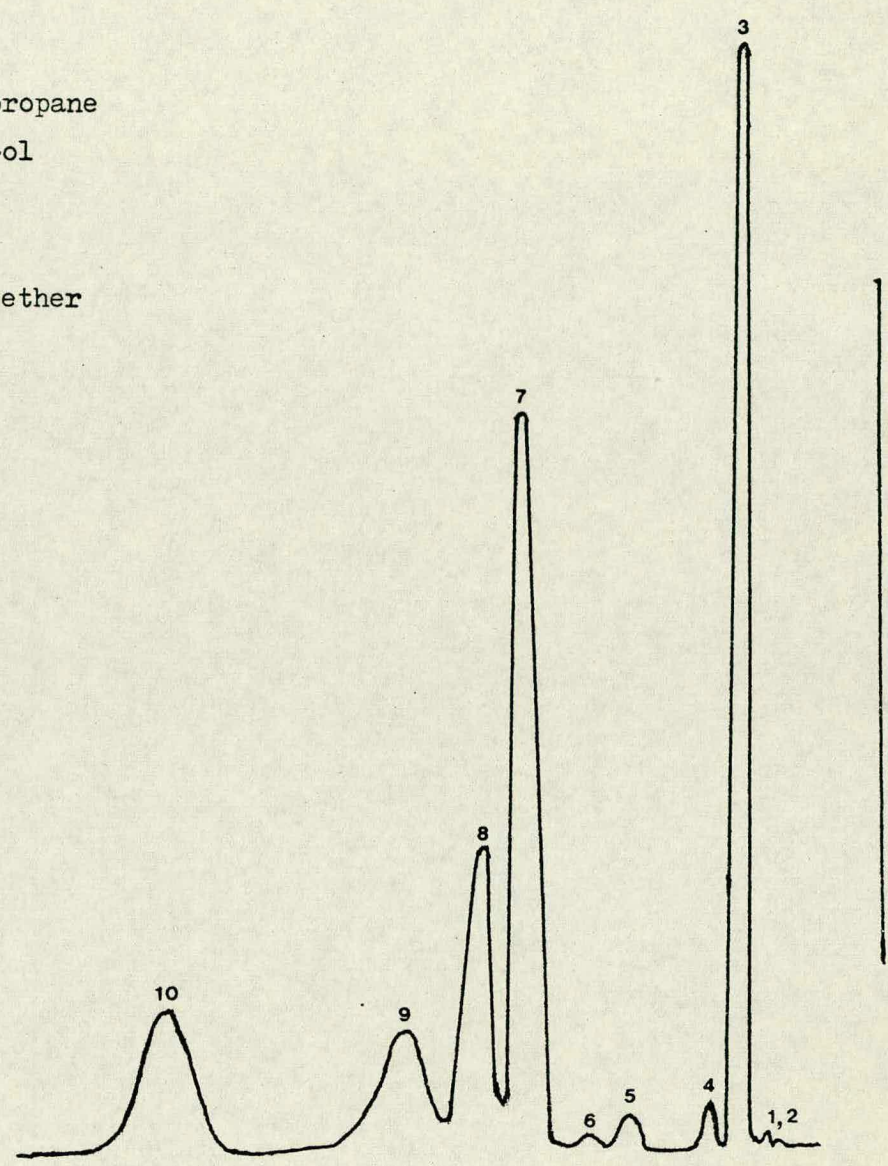


figure 5.13 G.C. trace of the decomposition of propan-1-ol.

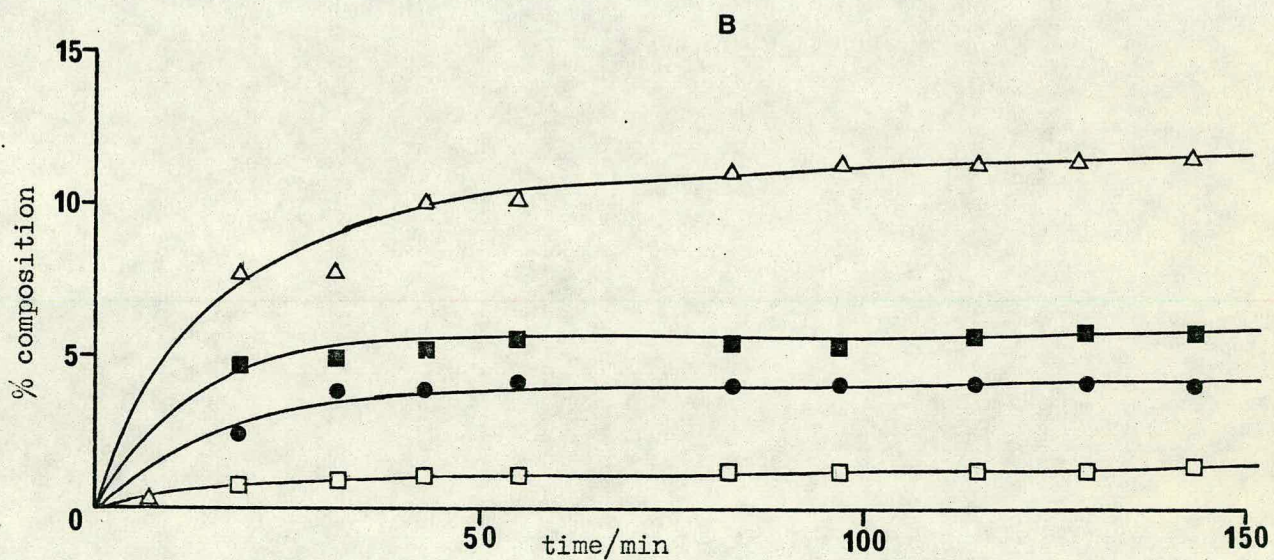
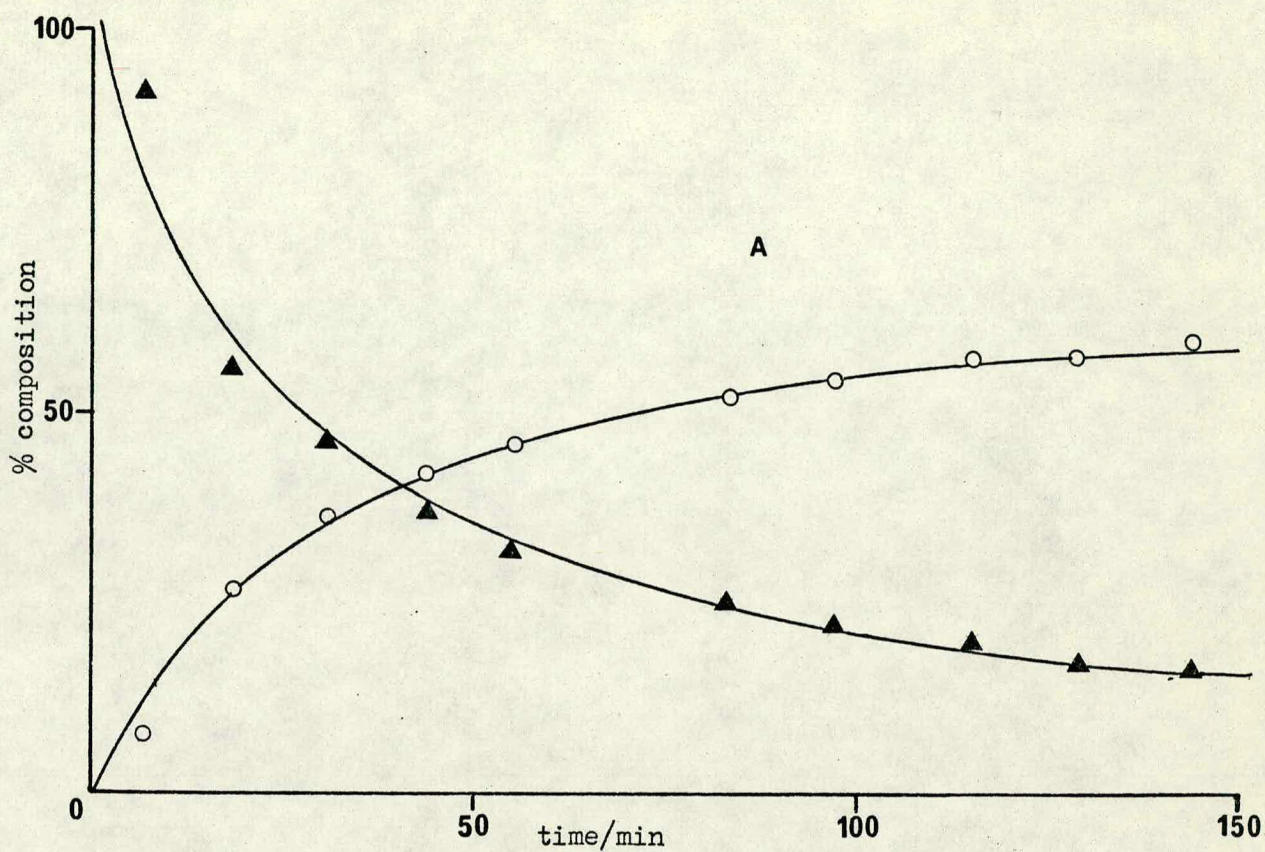


figure 5.14 decomposition of propan-1-ol over rutile at 586K:

A propan-1-ol, ▲; propene, ○.

B hexene, Δ; unknown, ■; n-propyl ether, ●; propanal, □.

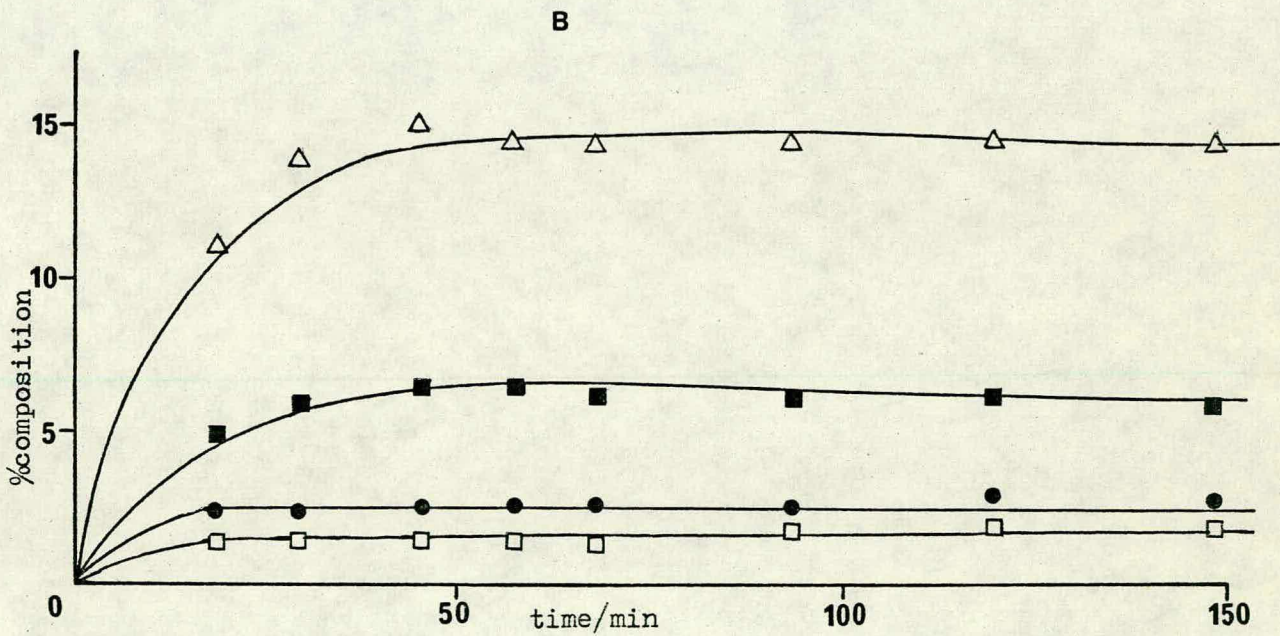
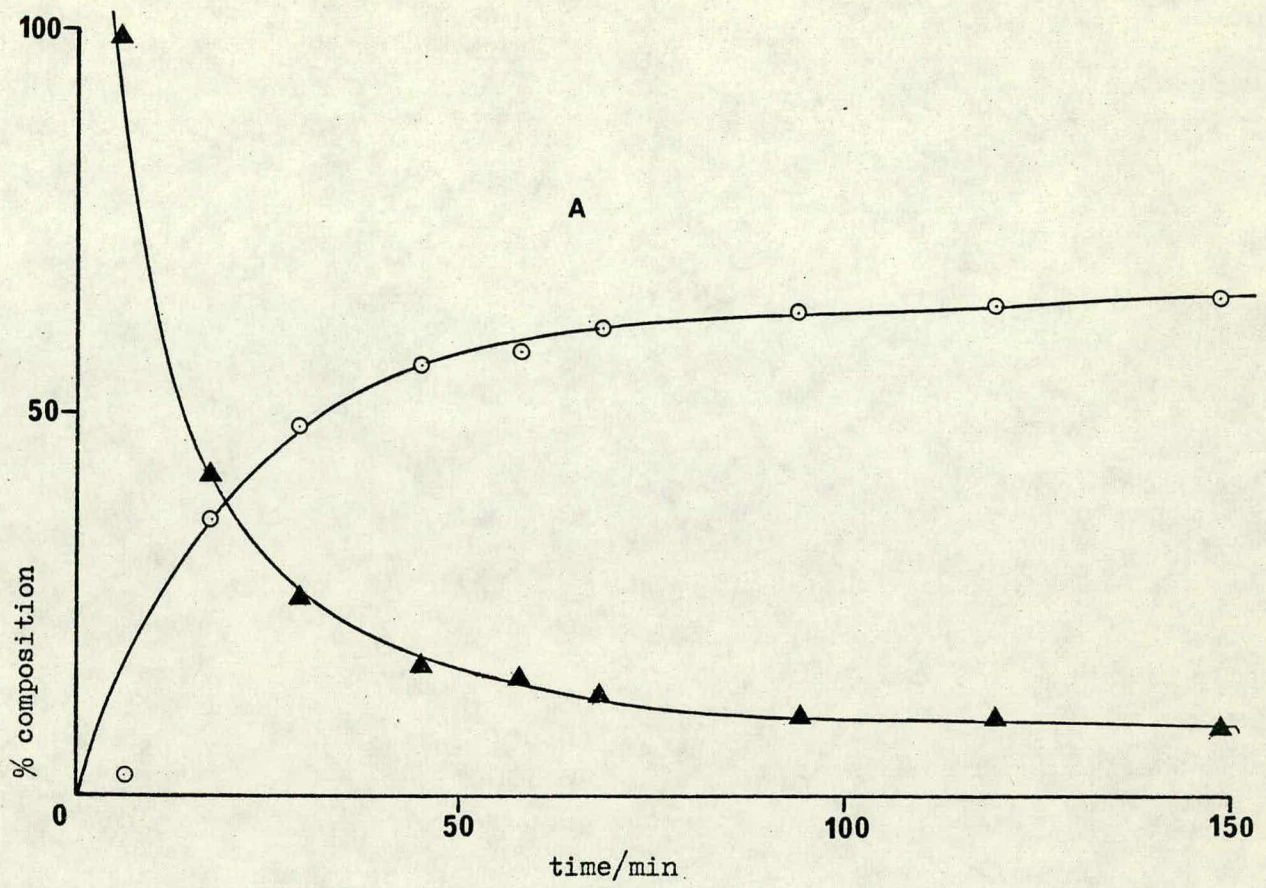


figure 5.15 decomposition of propan-1-ol over rutile at 599K:

A propan-1-ol, ▲; propene, ○.

B hexene, △; unknown, ■; n-propyl ether, ●; propanal, □.

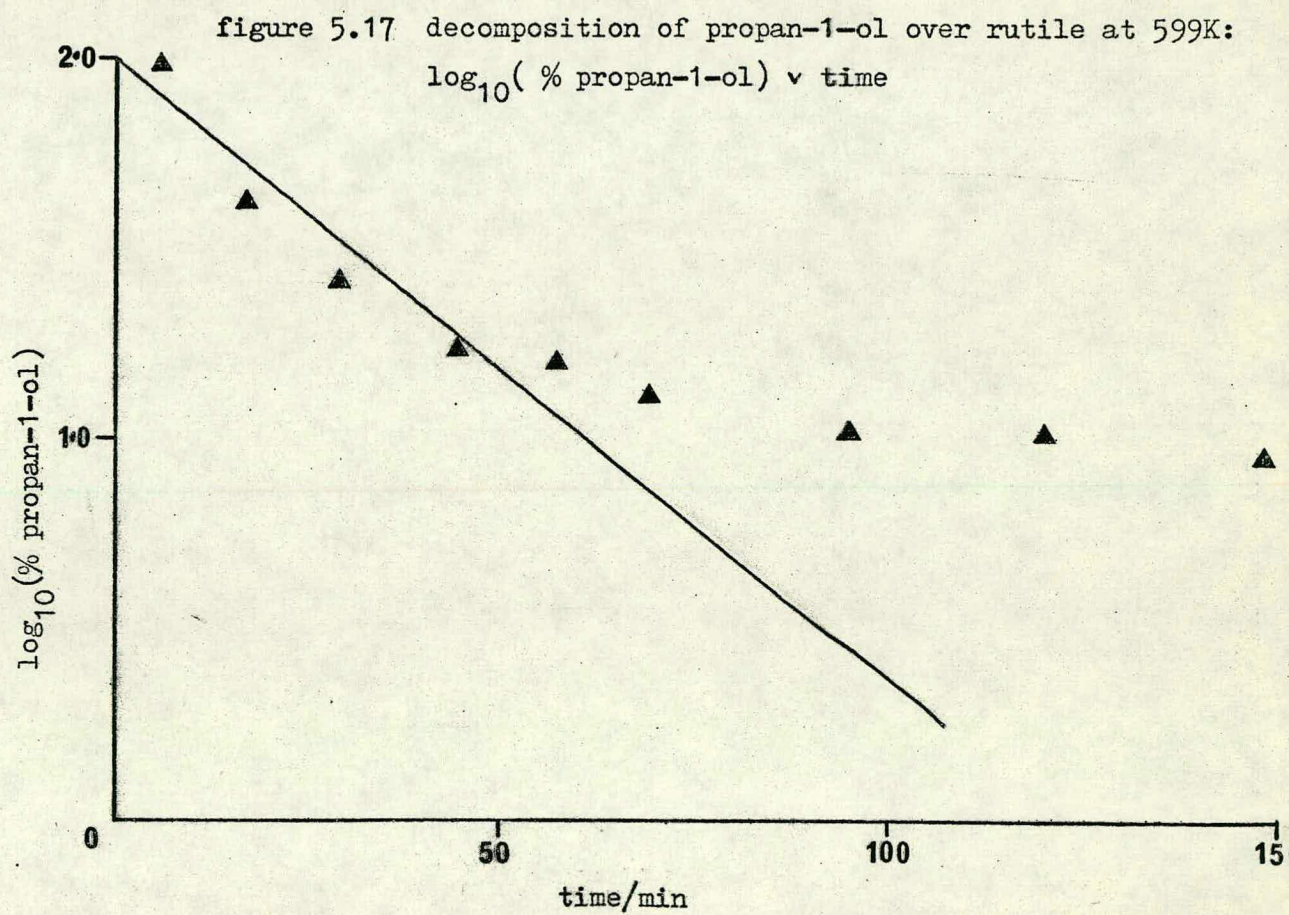
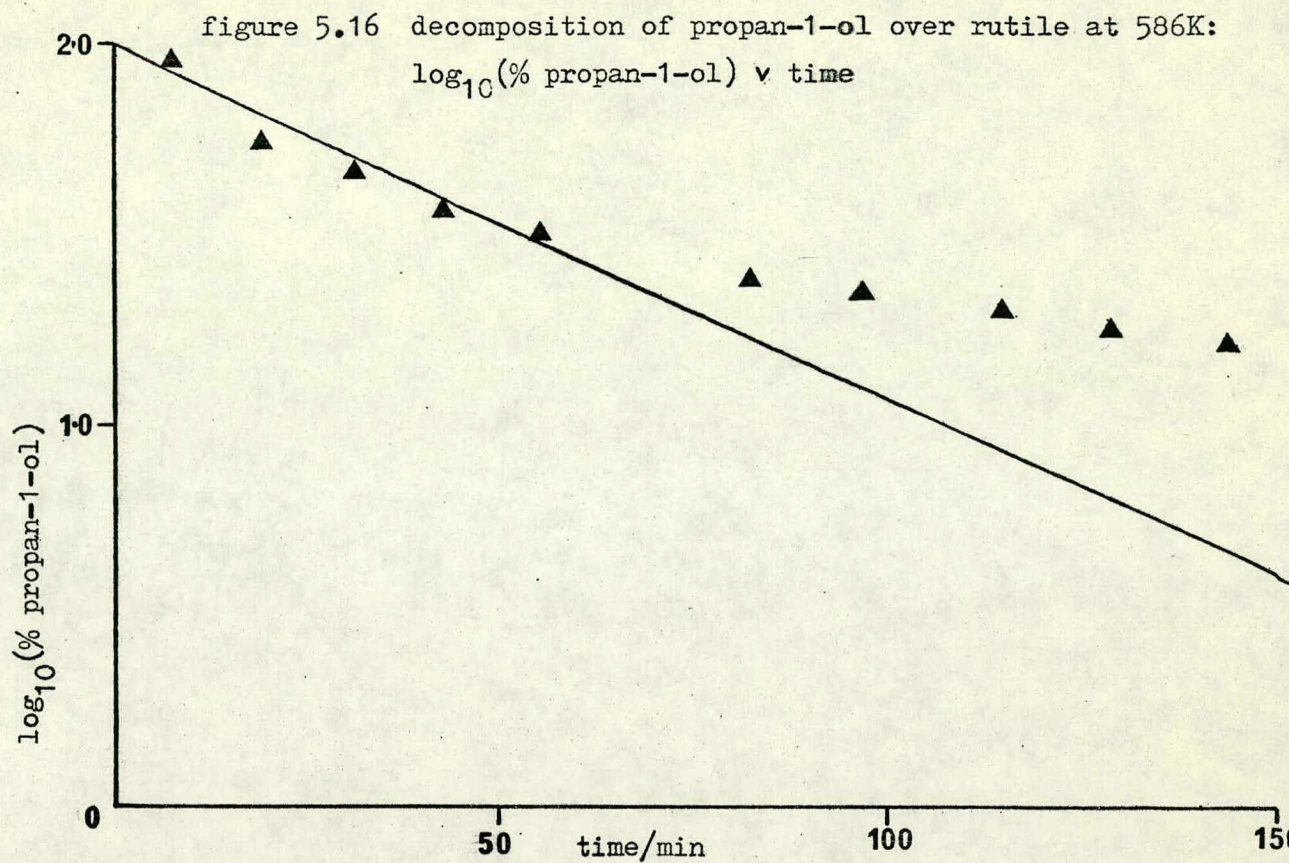
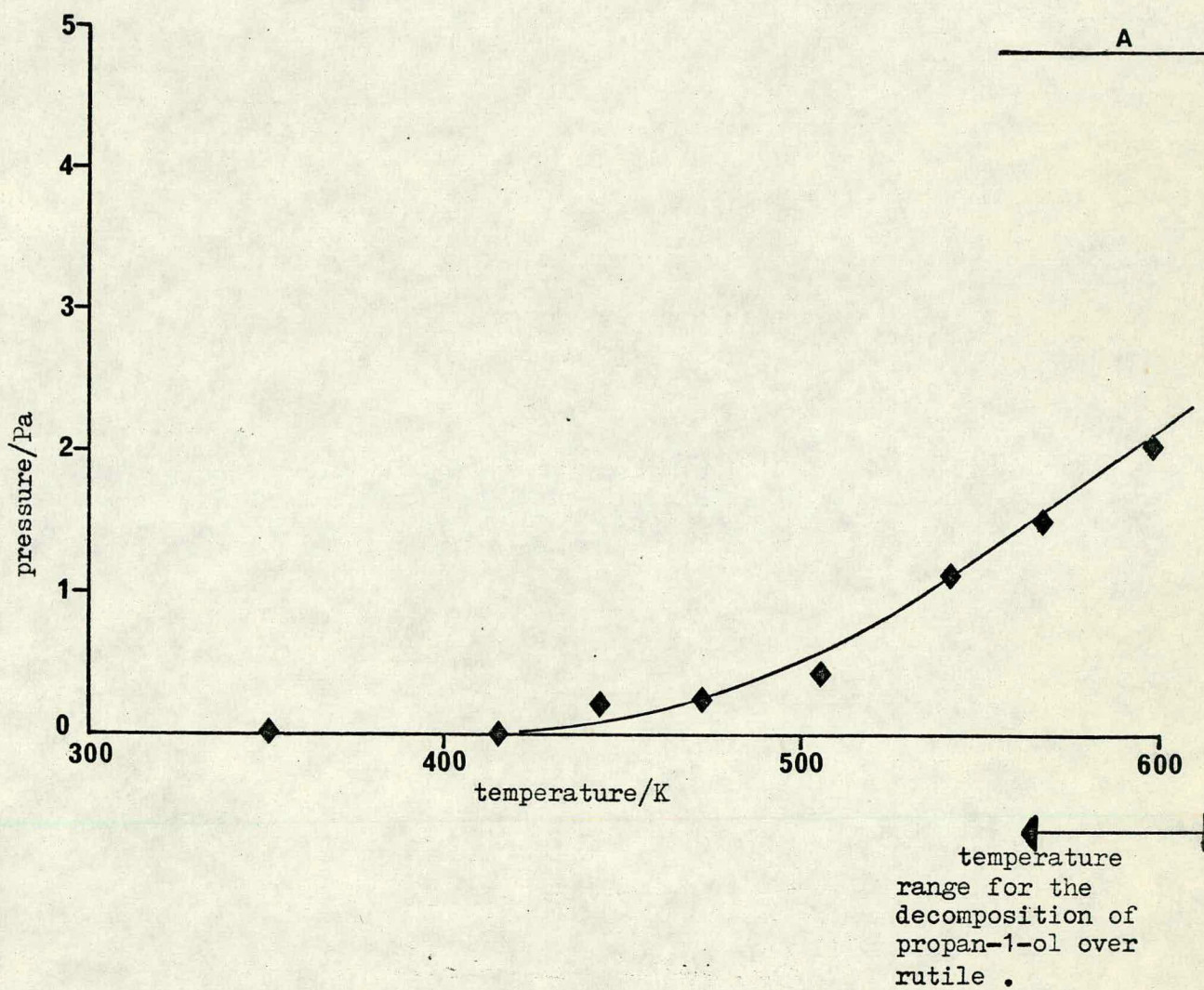


figure 5.18 desorption of pre-adsorbed H_2O with temperature:
 H_2O vapour pressure \downarrow temperature



A: pressure of total H_2O in reaction system when no rutile is present .

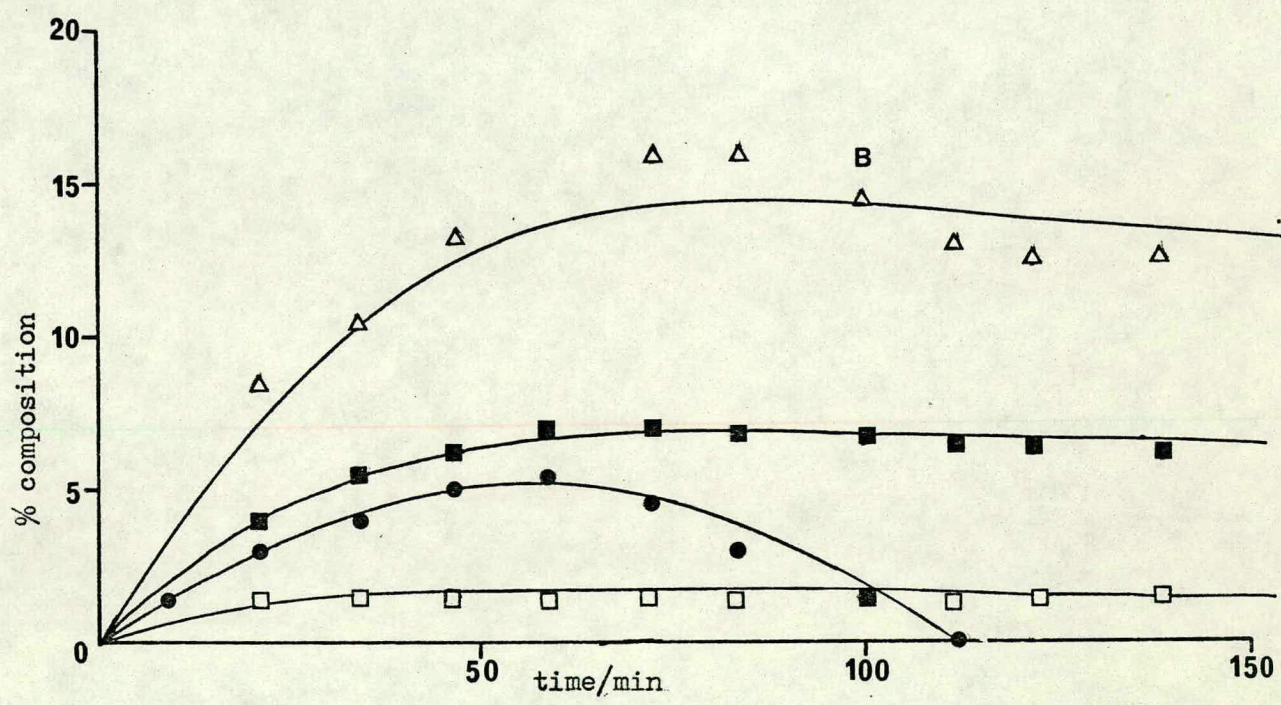
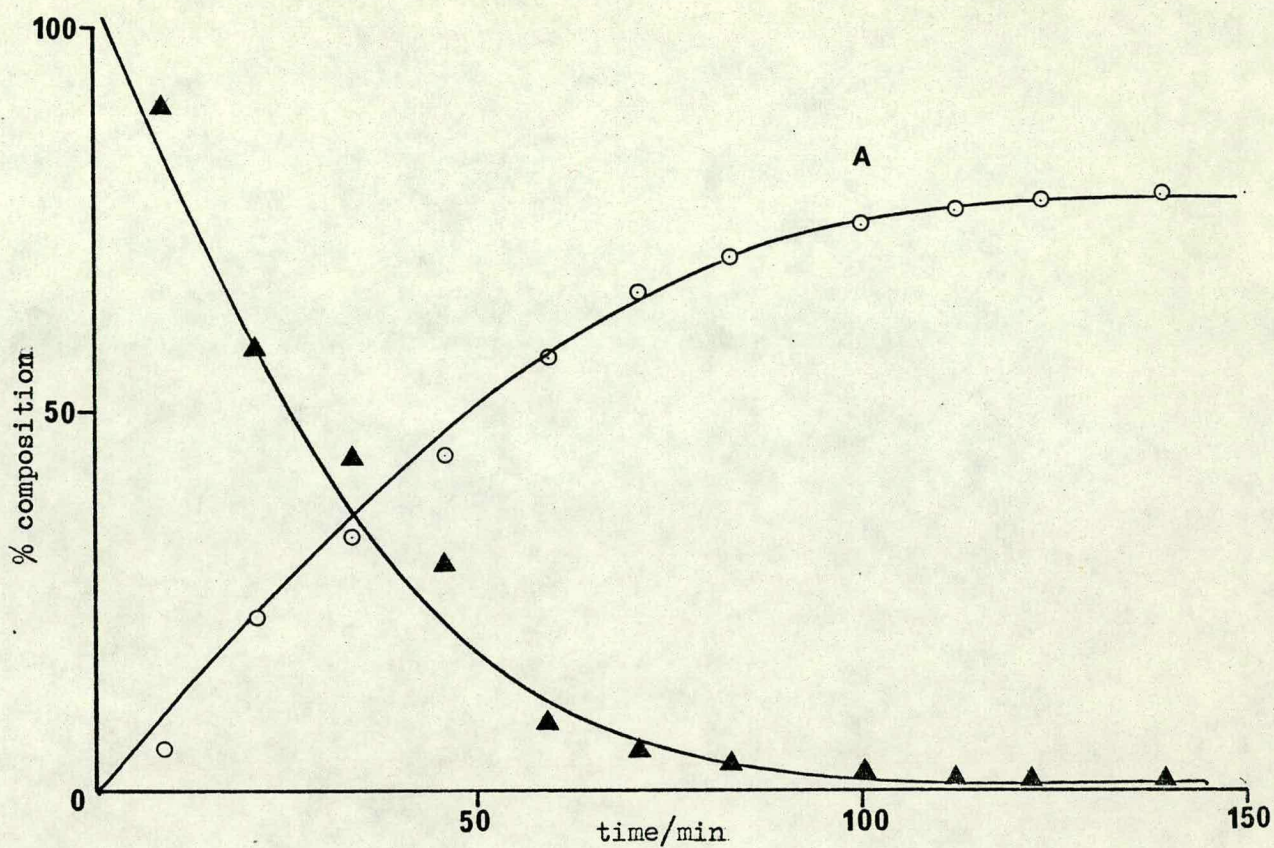


figure 5.19 decomposition of propan-1-ol at 586K after pre-adsorption of water; water coverage $\approx 0.189 \text{ H}_2\text{O molecules nm}^{-2}$:
 A: propan-1-ol, ▲; propene, ○.
 B: hexene, Δ; unknown, ■; n-propyl ether, ●; propanal, □.

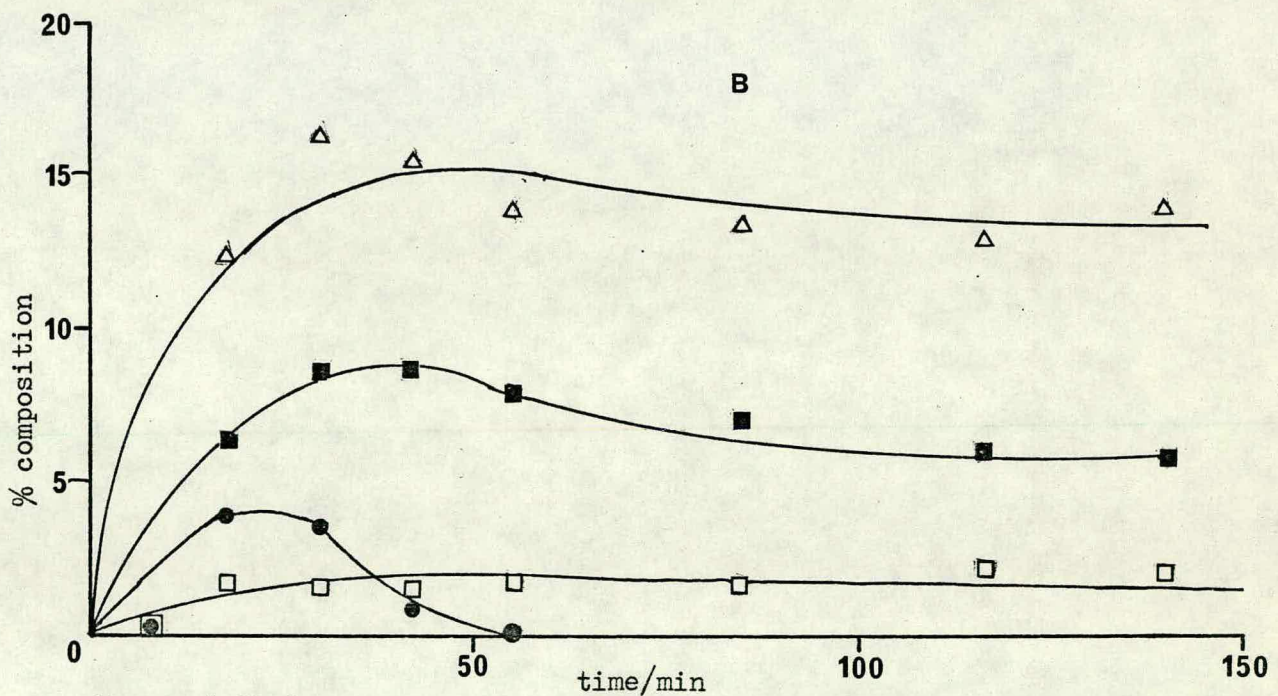
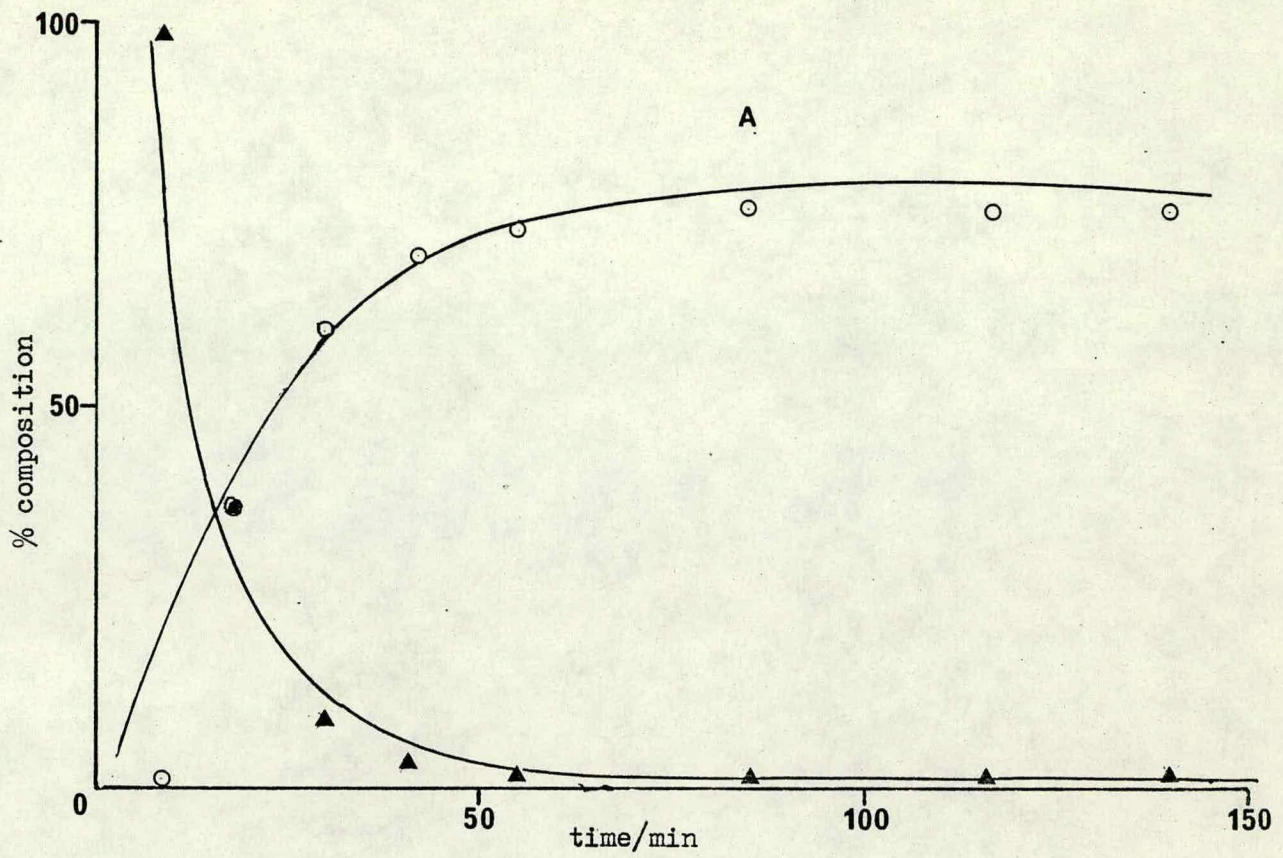


figure 5.20 decomposition of propan-1-ol over rutile at 599K after

pre-adsorption of water:

water coverage $\approx 0.154 \text{ H}_2\text{O molecules nm}^{-2}$:

A: propan-1-ol, ▲; propene, ○.

B: hexene, Δ; unknown, ■; n-propyl ether, ●; propanal, □.

figure 5.21 decomposition of propan-1-ol over rutile at 586K
after pre-adsorption of water: water coverage ≈ 0.186 H₂O
molecules nm⁻² : $\log_{10}(\% \text{ propan-1-ol}) \downarrow \text{time}$.

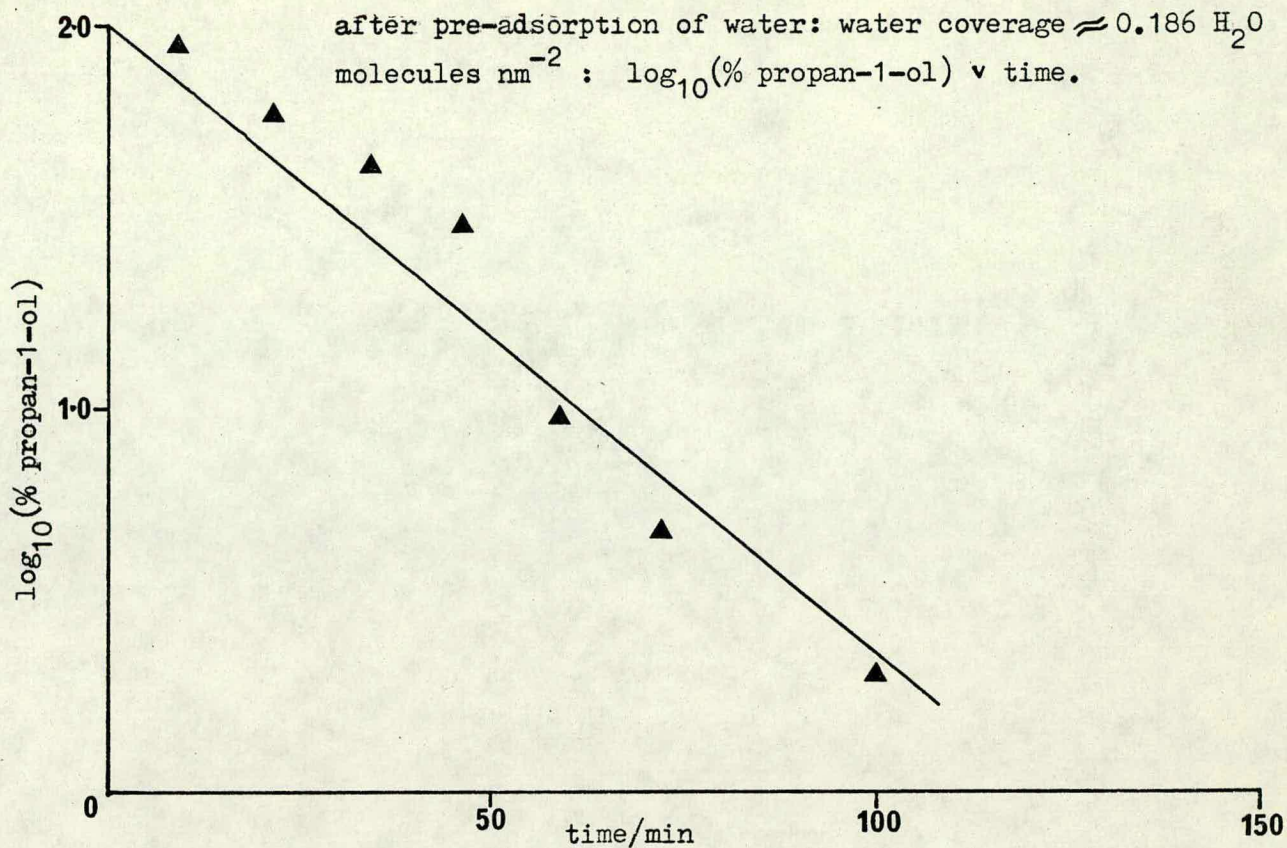
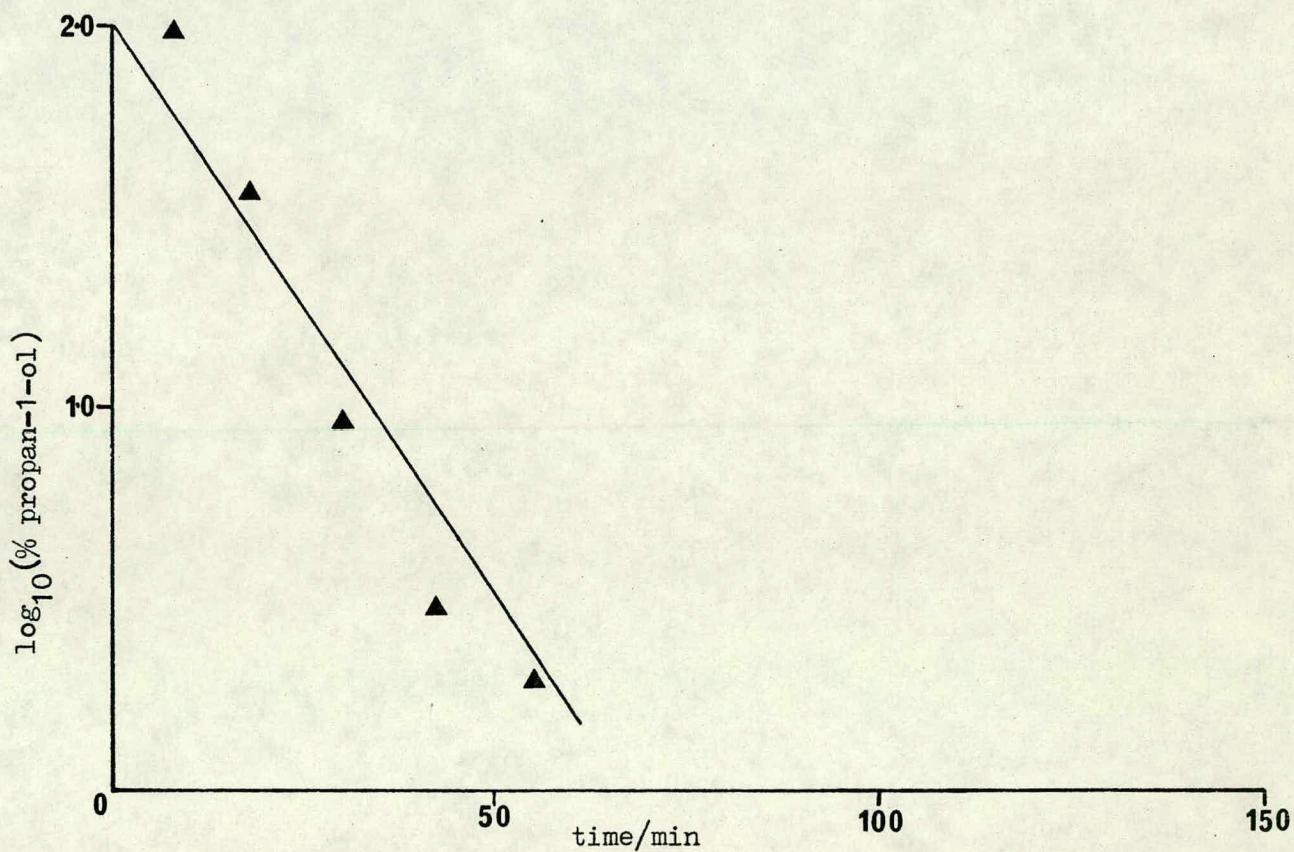


figure 5.22 as figure 5.21 except at 599K



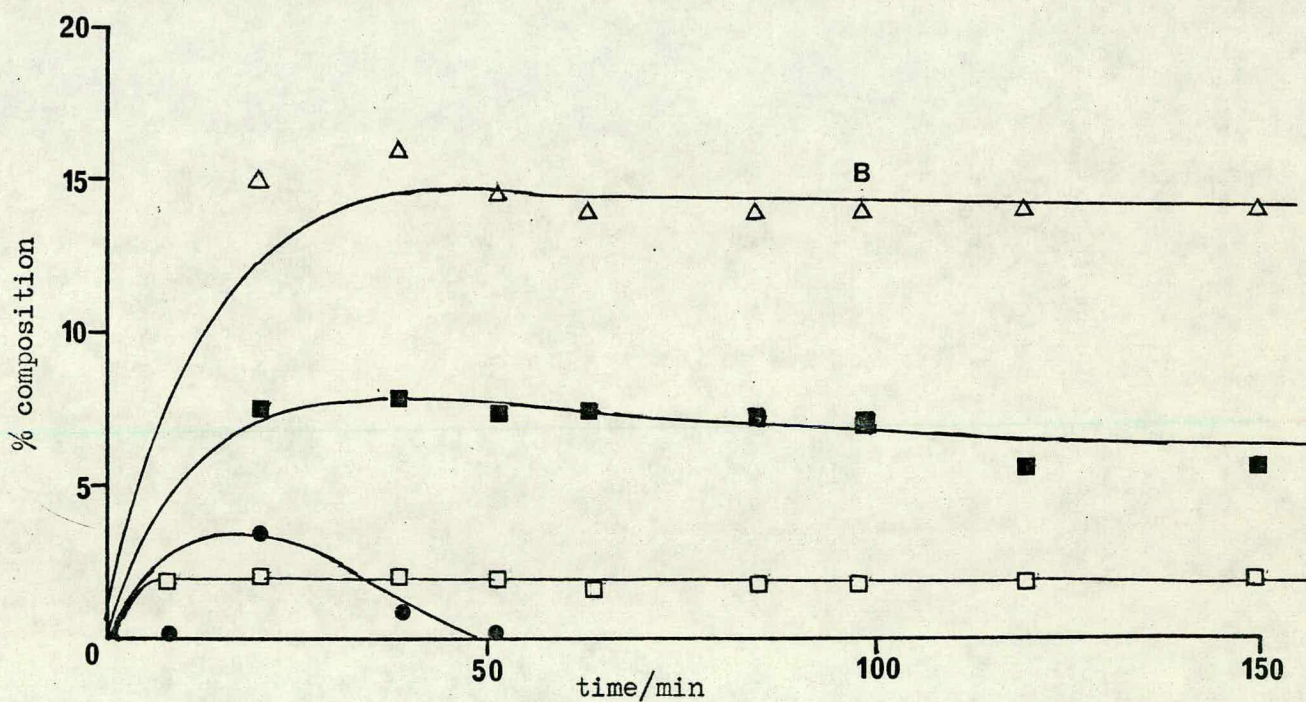
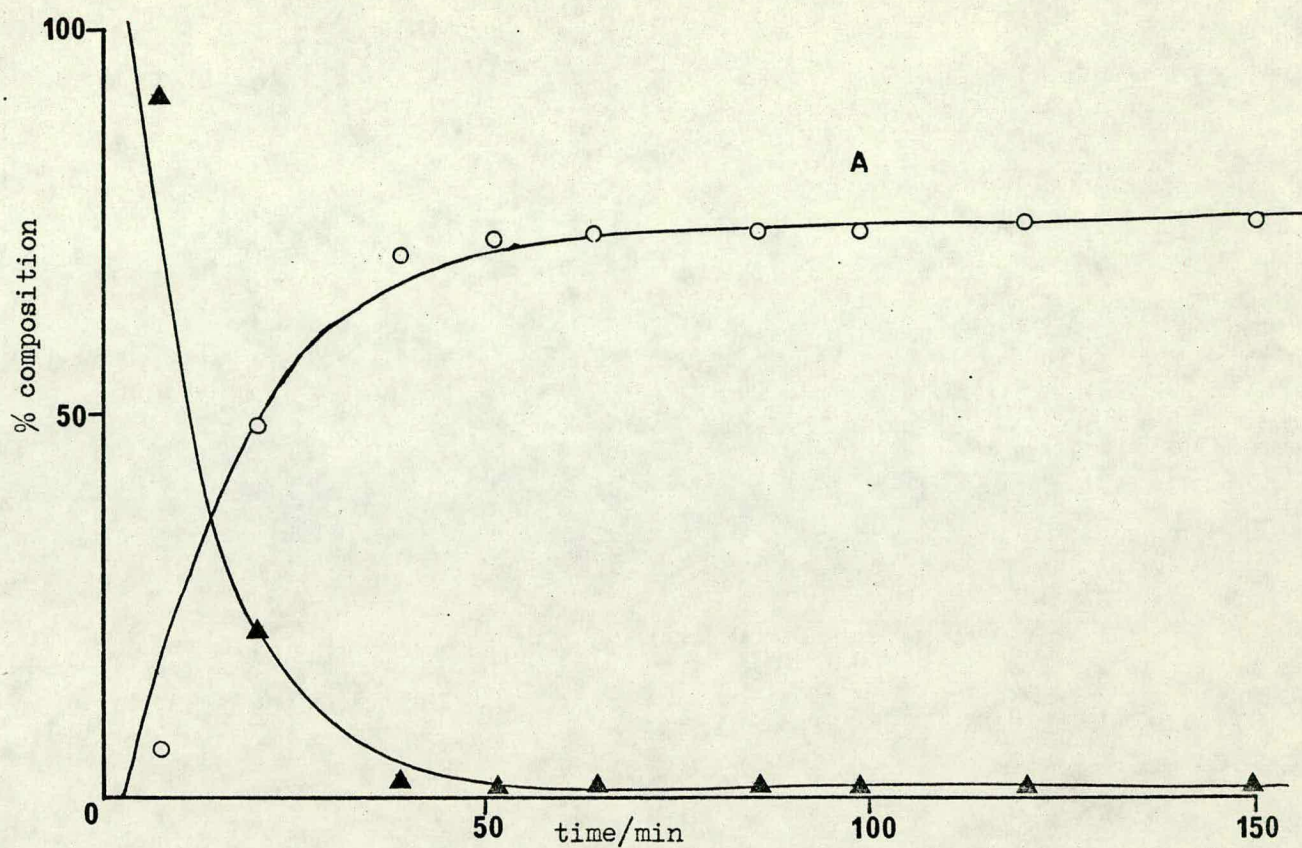


figure 5.23 decomposition of propan-1-ol over rutile at 599K in the presence of water ; initial ratio $H_2O/propan-1-ol \approx 1.142/1$.

A: propan-1-ol, ▲; propene, ○.

B: hexene, △; unknown, ■; n-propyl ether, ●; propanal, □.

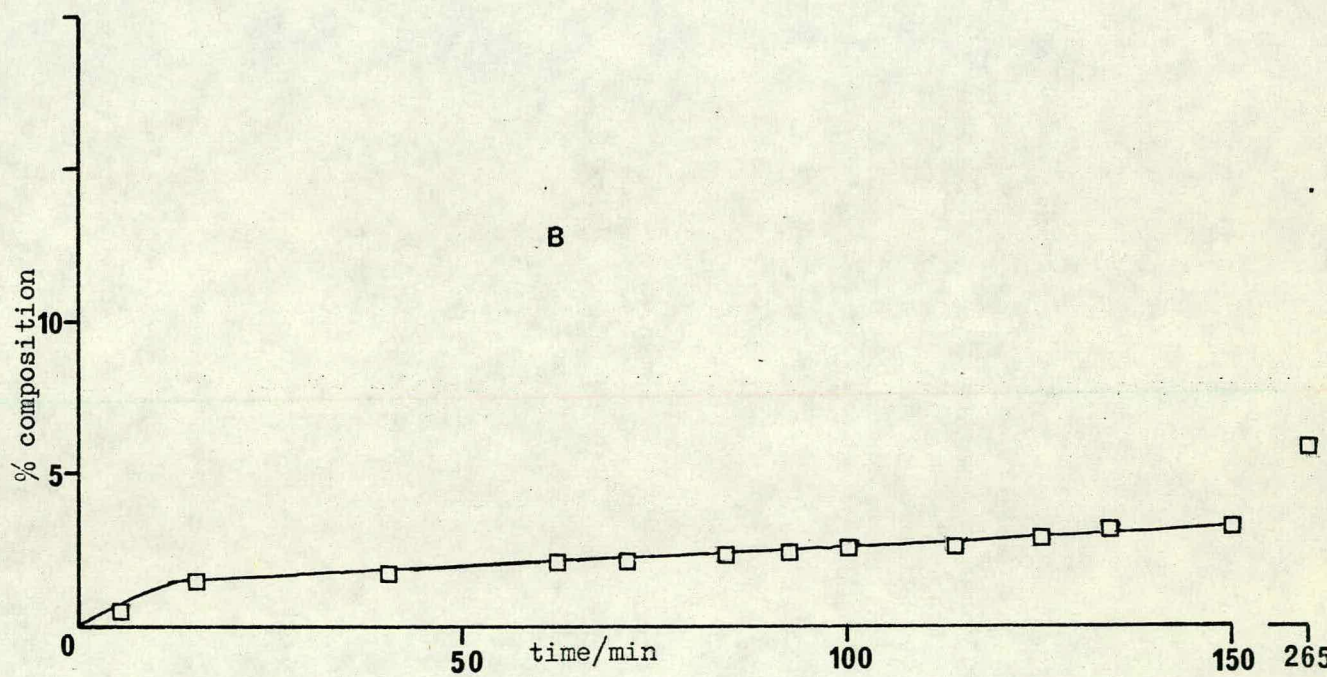
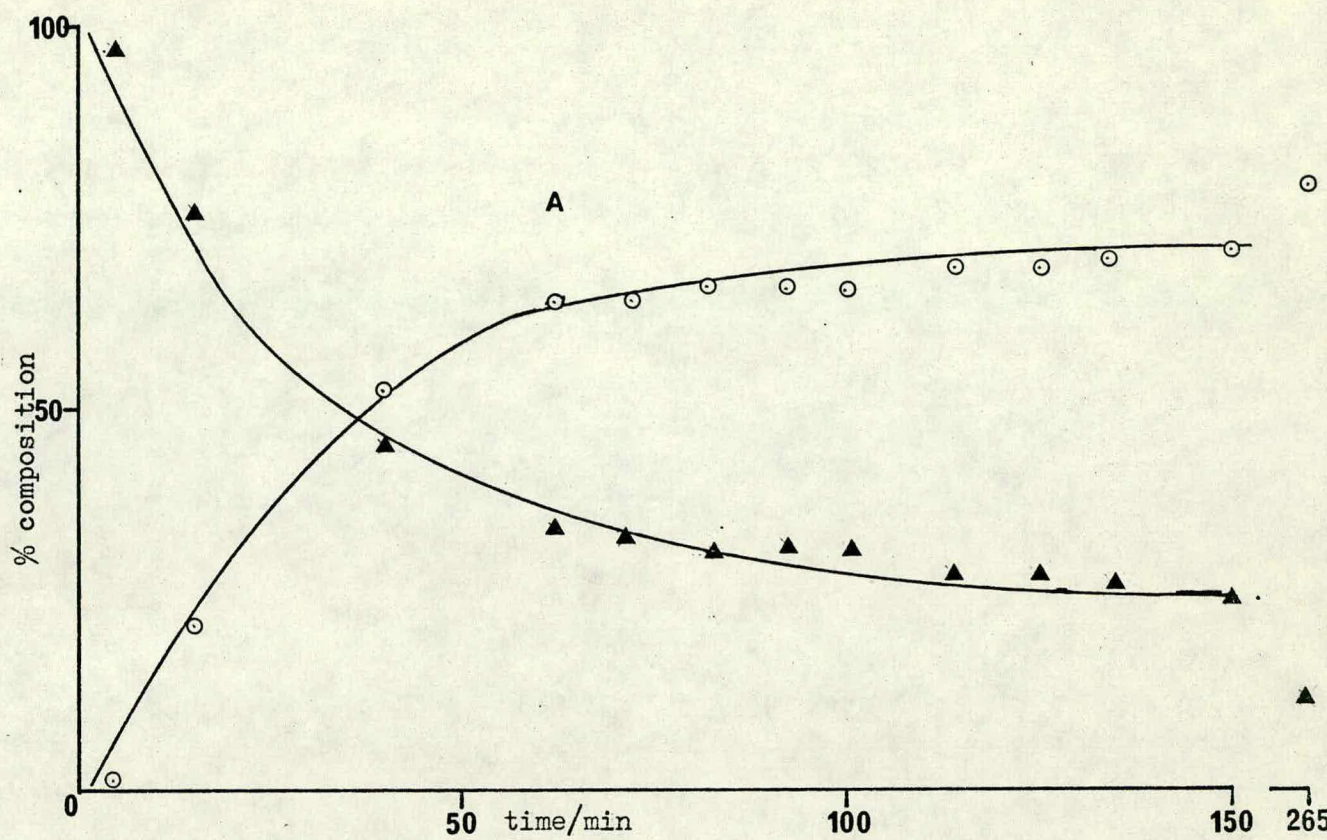


figure 5.24 decomposition of propan-1-ol over rutile at 599K in the presence of water; initial ratio $H_2O/propan-1-ol \approx 10/1$.

A: propan-1-ol, ▲; propene, ○.

B: propanal, □.

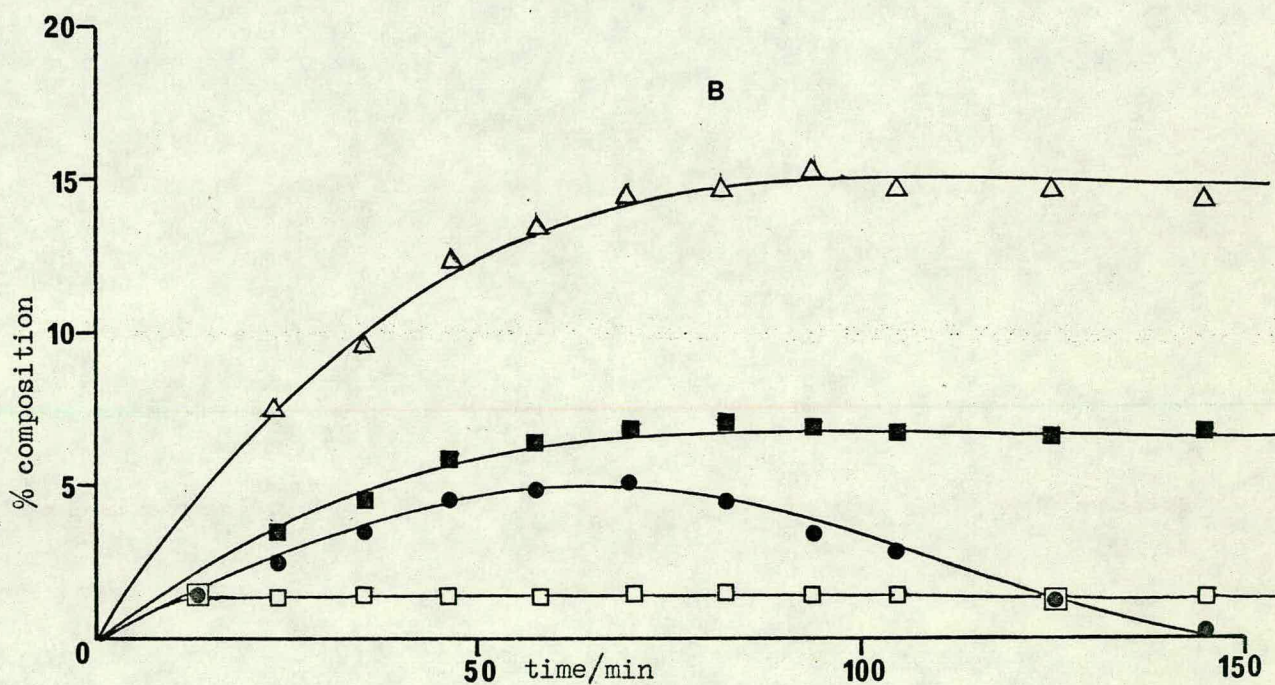
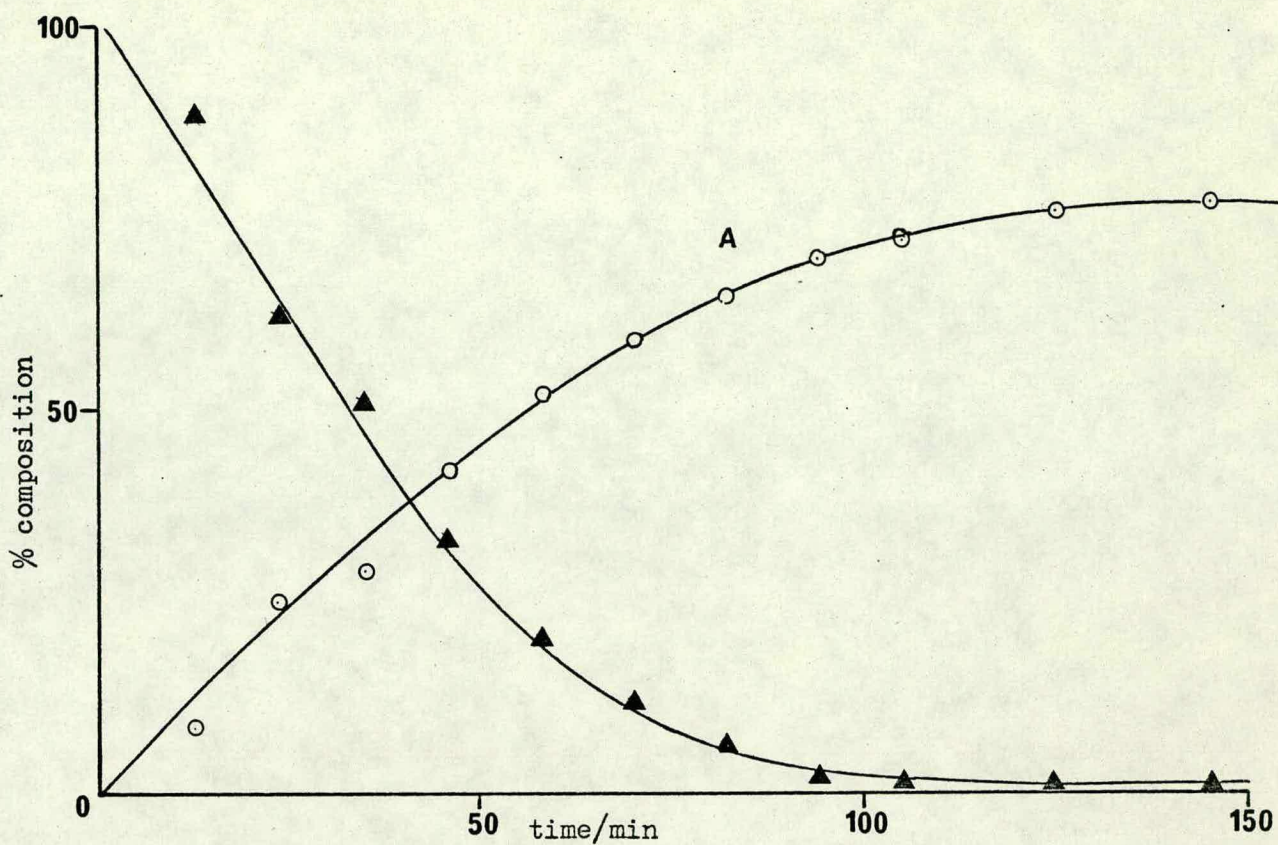


figure 5.25 decomposition of propan-1-ol over rutile at 586K after pre-adsorption of ammonia: ammonia coverage $\approx 0.49 \text{ NH}_3$ molecules nm^{-2} .

A: propan-1-ol, ▲; propene, ○.

B: hexene, △; unknown, ■; n-propyl ether, ●; propanal, □.

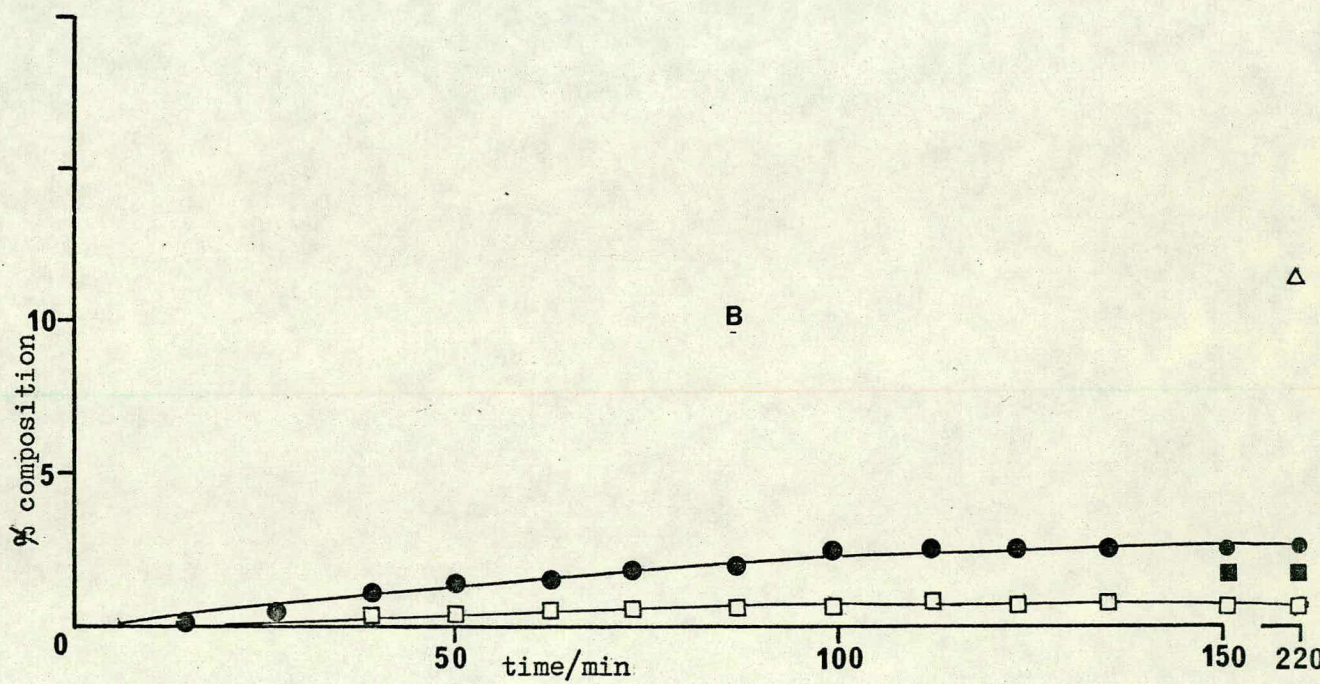
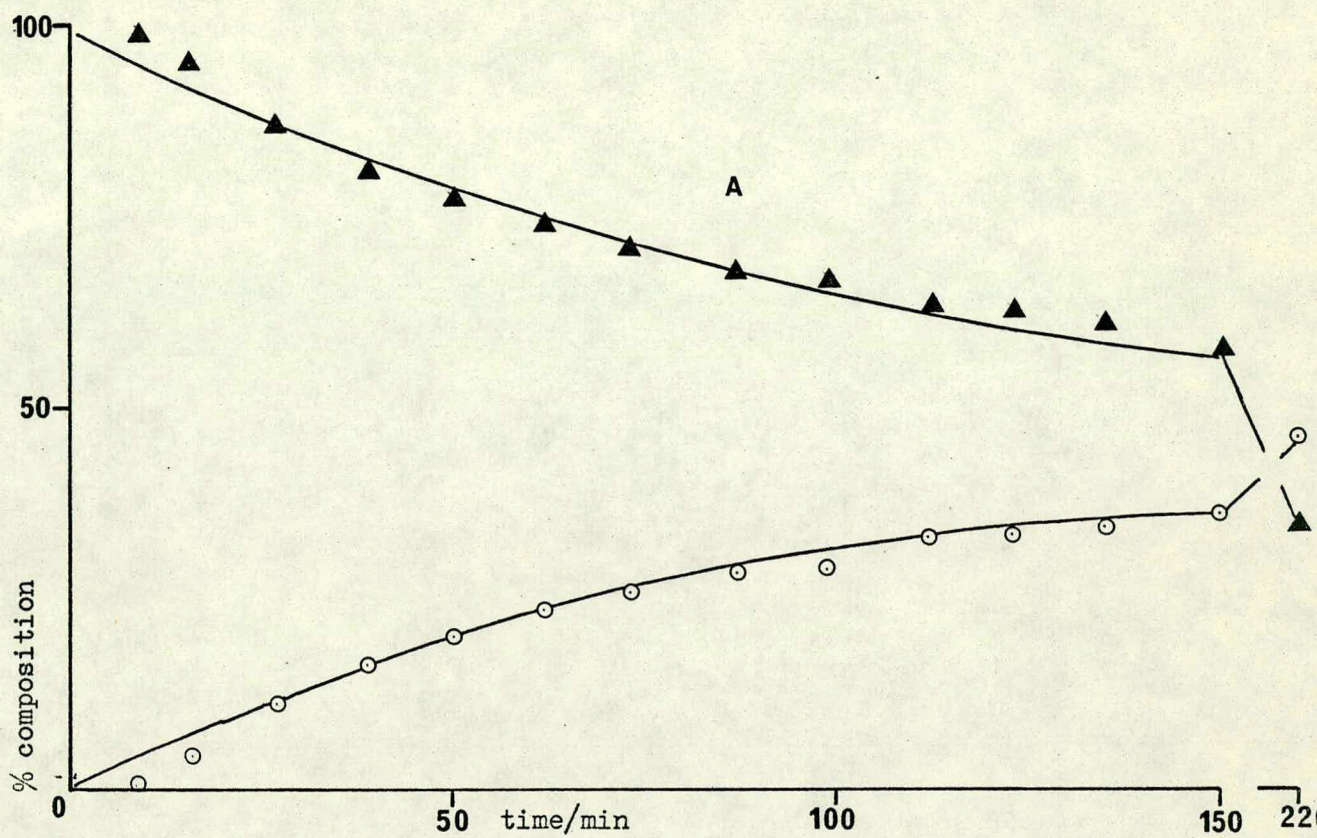


figure 5.26 decomposition of propan-1-ol over rutile at 586K in the presence of excess ammonia; ratio $\text{NH}_3/\text{propan-1-ol} \approx 6.1/1$.
 A: propan-1-ol, ▲; propene, ○.
 B: hexene, Δ; unknown, ■; n-propyl ether, ●; propanal, □.

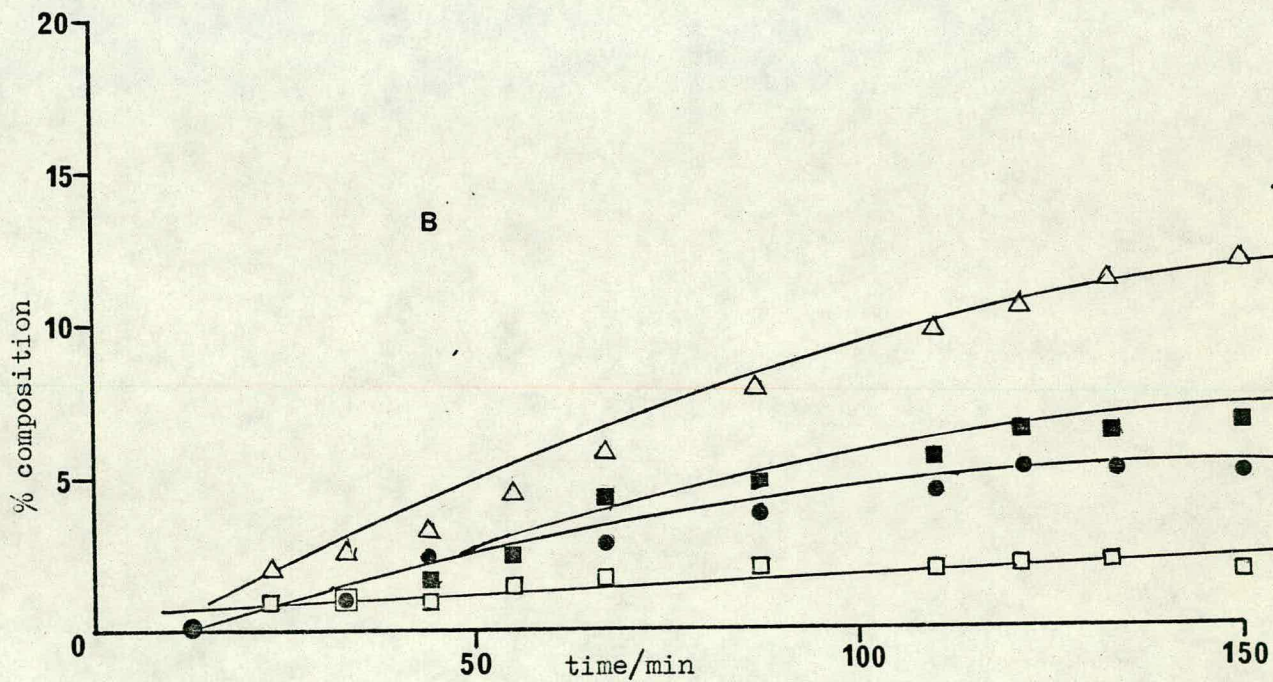
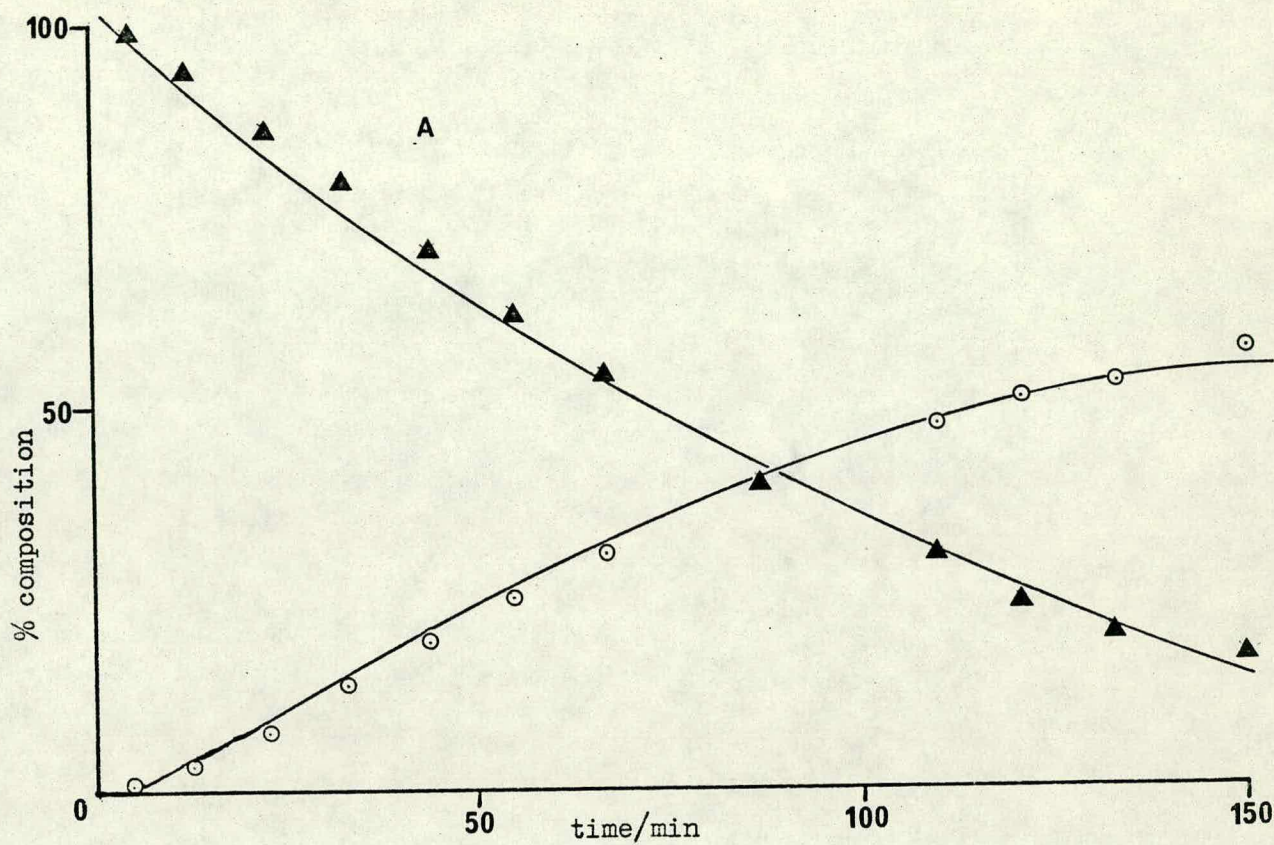


figure 5.27 decomposition of propan-1-ol over rutile at 586K after prior adsorption of trimethylamine as described in section 5.3.2.4.

A:propan-1-ol,▲; propene, ○ .

B:hexene,△; unknown,■; n-propyl ether,●; propanal,□ .

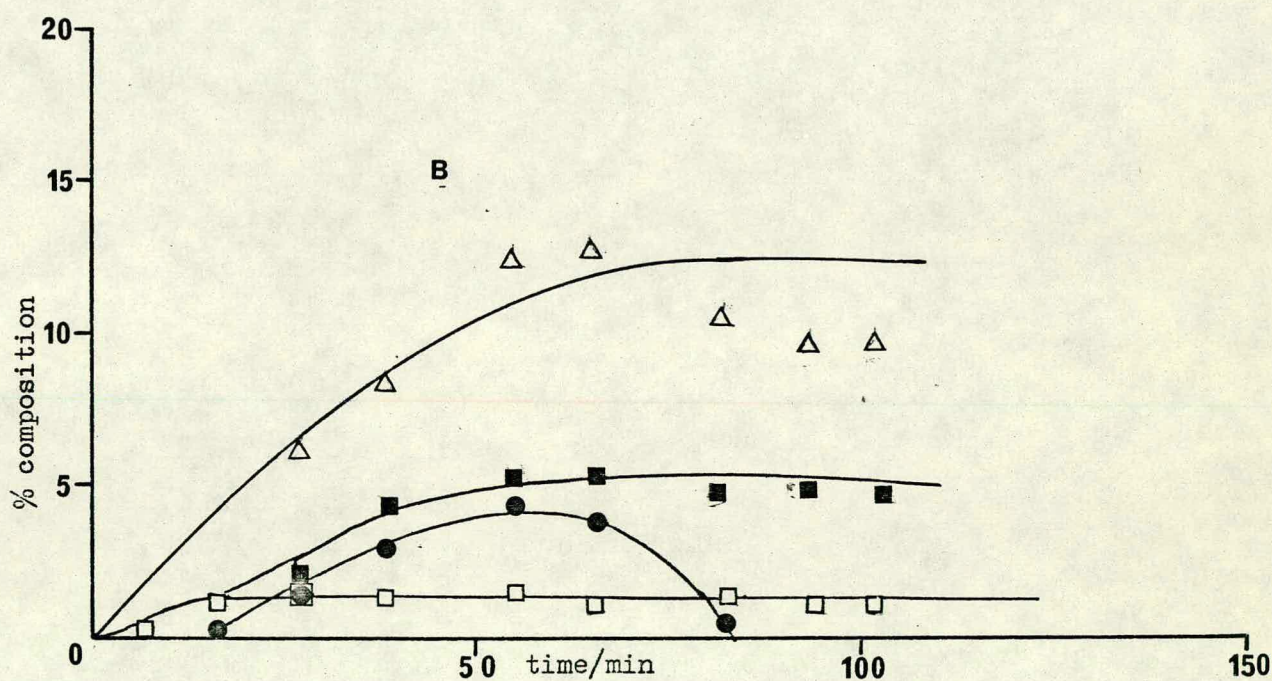
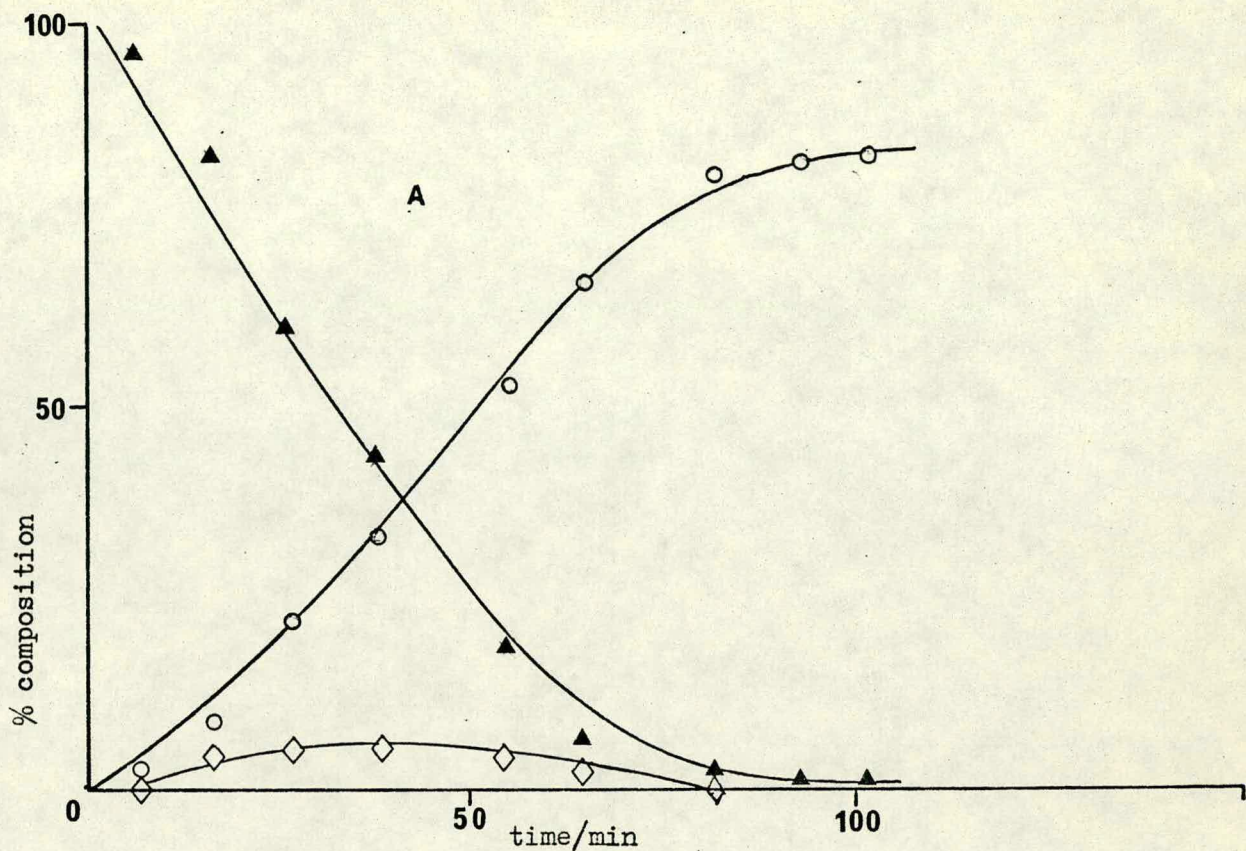


figure 5.28 decomposition of propan-1-ol over rutile at 586K after pre-adsorption of HCl: HCl coverage ≈ 0.68 HCl molecules nm^{-2} .

A: propan-1-ol, \blacktriangle ; propene, \circ ; n-chloropropane, \diamond .

B: hexene, \triangle ; unknown, \blacksquare ; n-propyl ether, \bullet ; propanal, \square .

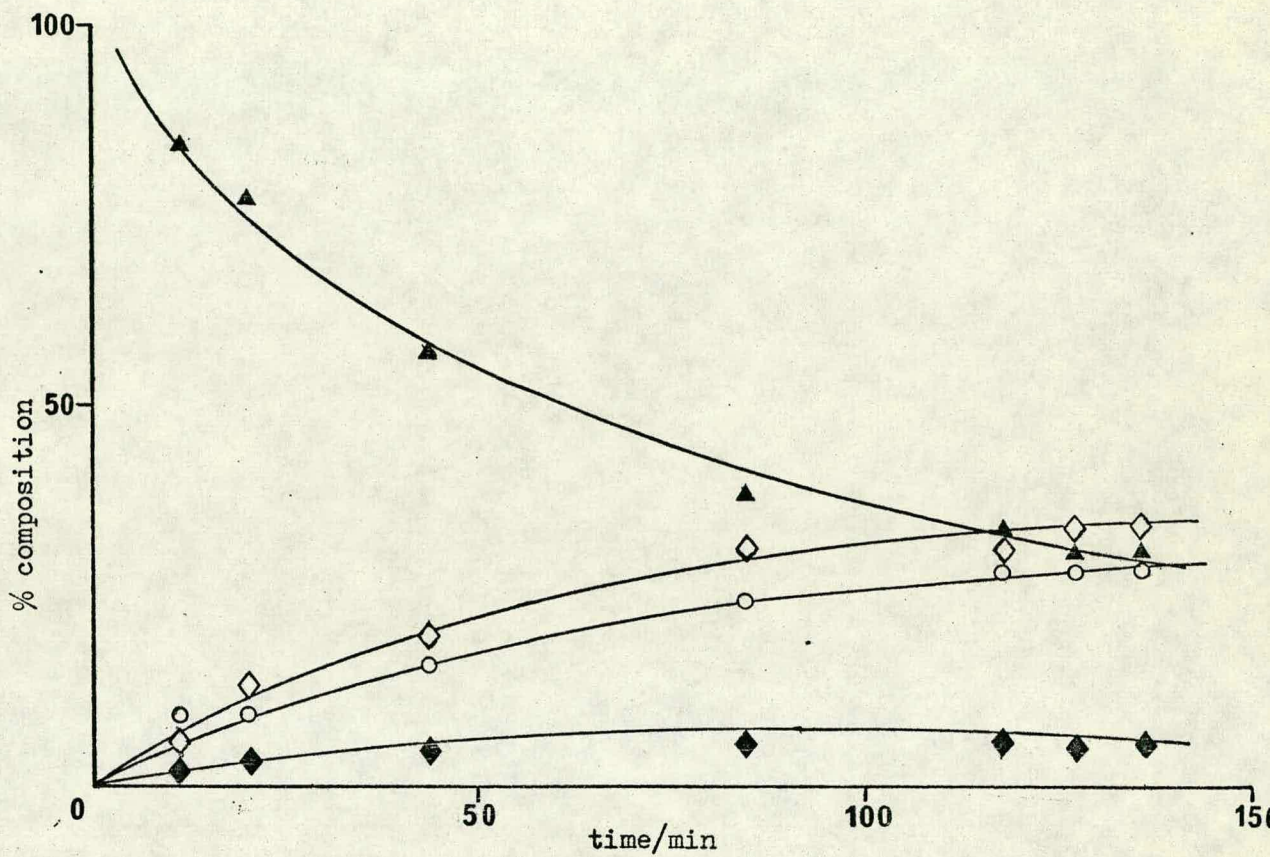


figure 5.29 decomposition of propan-1-ol at 600K in the presence of HCl; (no rutile present):
 propan-1-ol, ▲; propene, ○; 1-chloropropane, ◇;
 2-chloropropane, ◆.

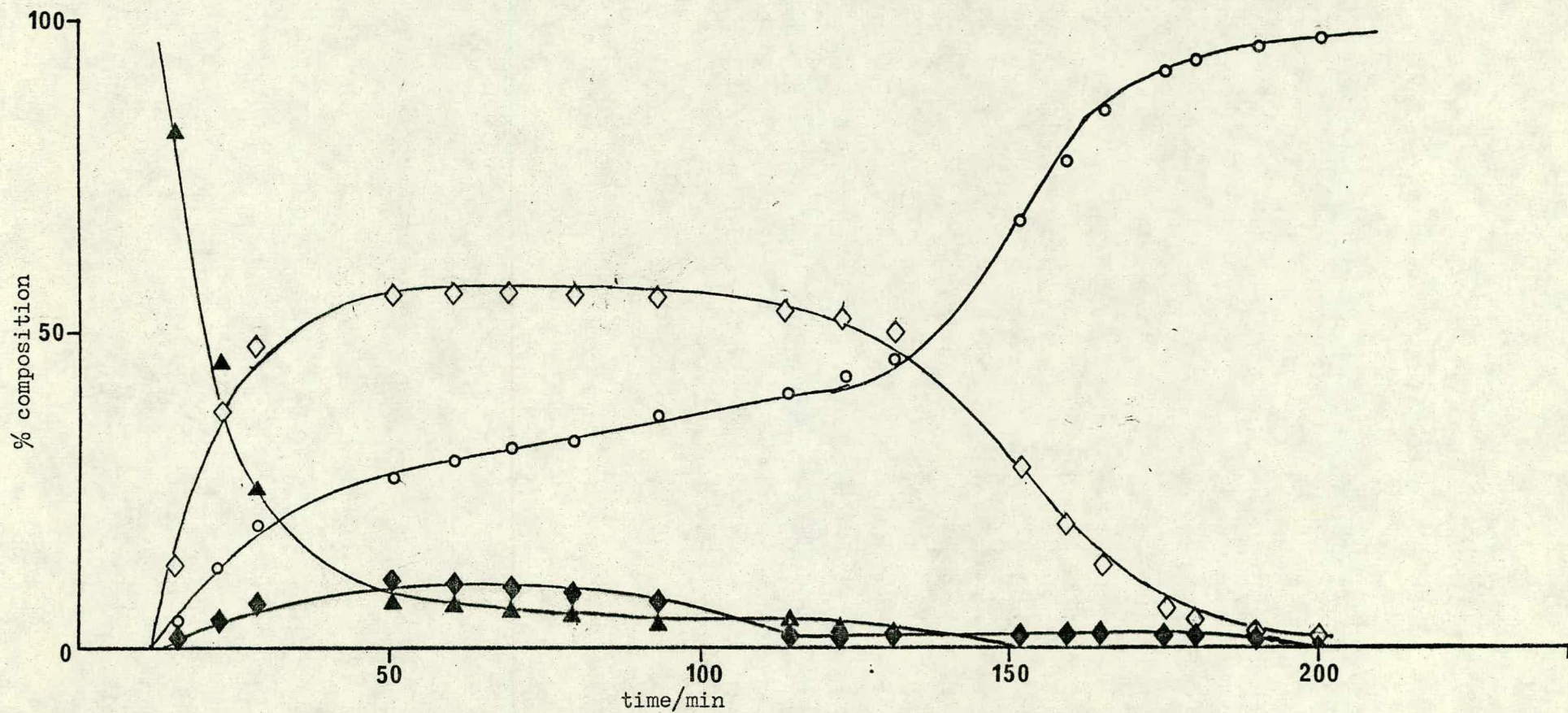


figure 5.30 decomposition of propan-1-ol over rutilite at 502K in the presence of HCl:

initial ratio HCl/propan-1-ol $\approx 1.72/1$:

propan-1-ol, ▲; propene, ○; 1-chloropropane, ◇; 2-chloropropane, ◆.

- 1,2 ?
- 3 propene
- 4 butene
- 5 propanal
- 6 hexene
- 7 ?
- 8 ?
- 9 ?
- 10 ?

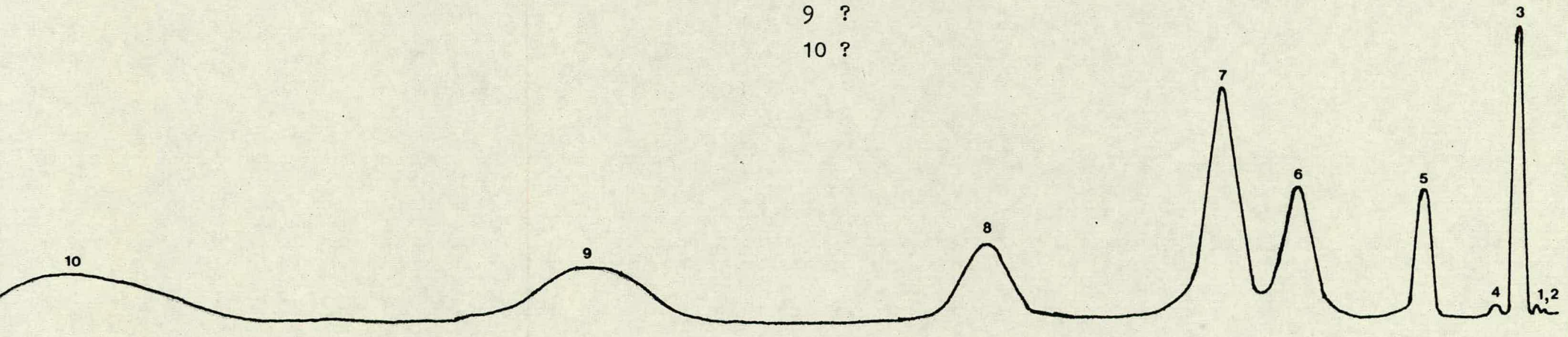


figure 5.31 G.C. trace of the decomposition of propanal over rutile.

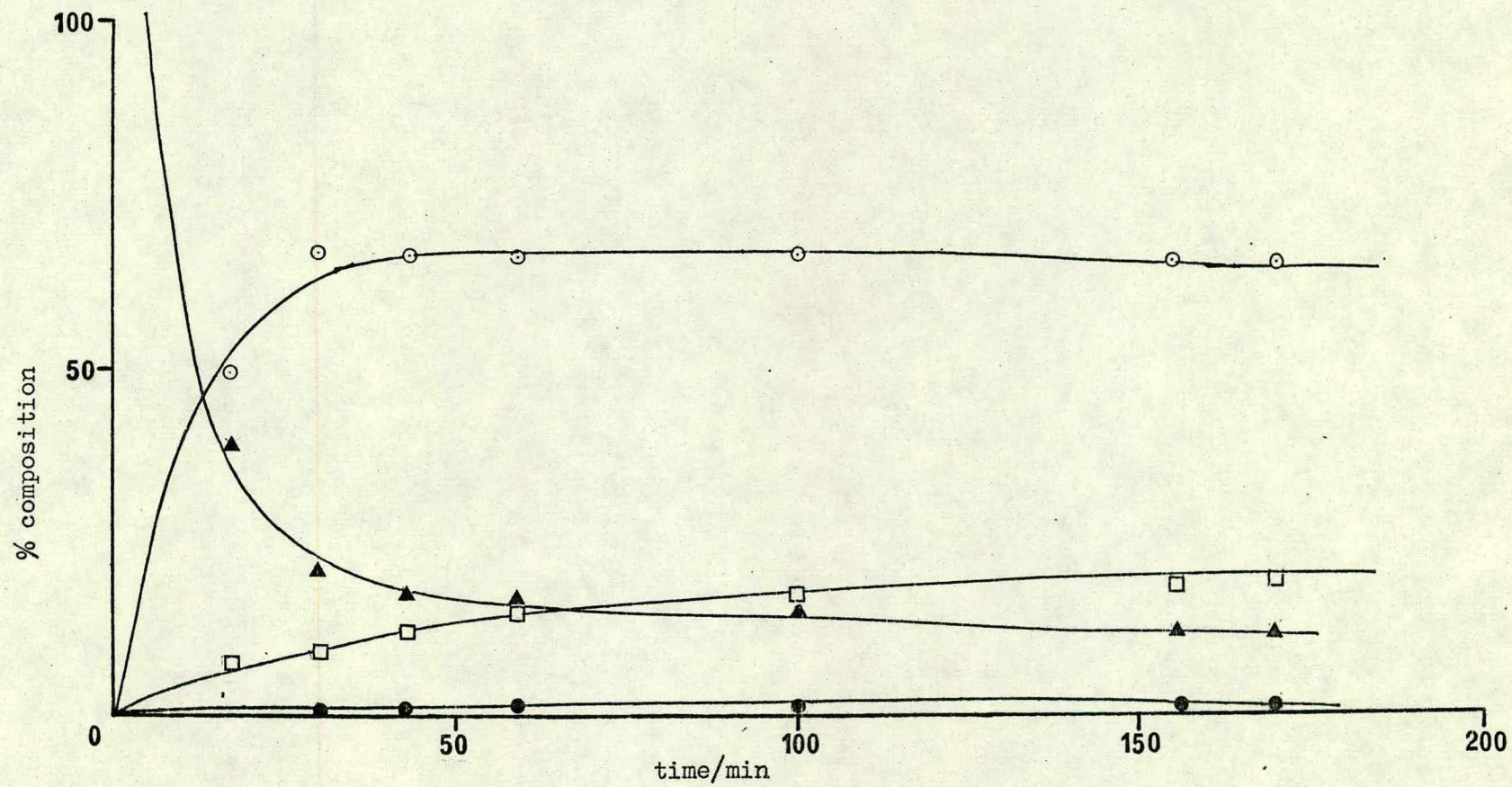


figure 5.32 decomposition of excess propan-1-ol over rutile at 599K:
 propan-1-ol, ▲; propene, O; n-propyl ether, ●; propanal, □.

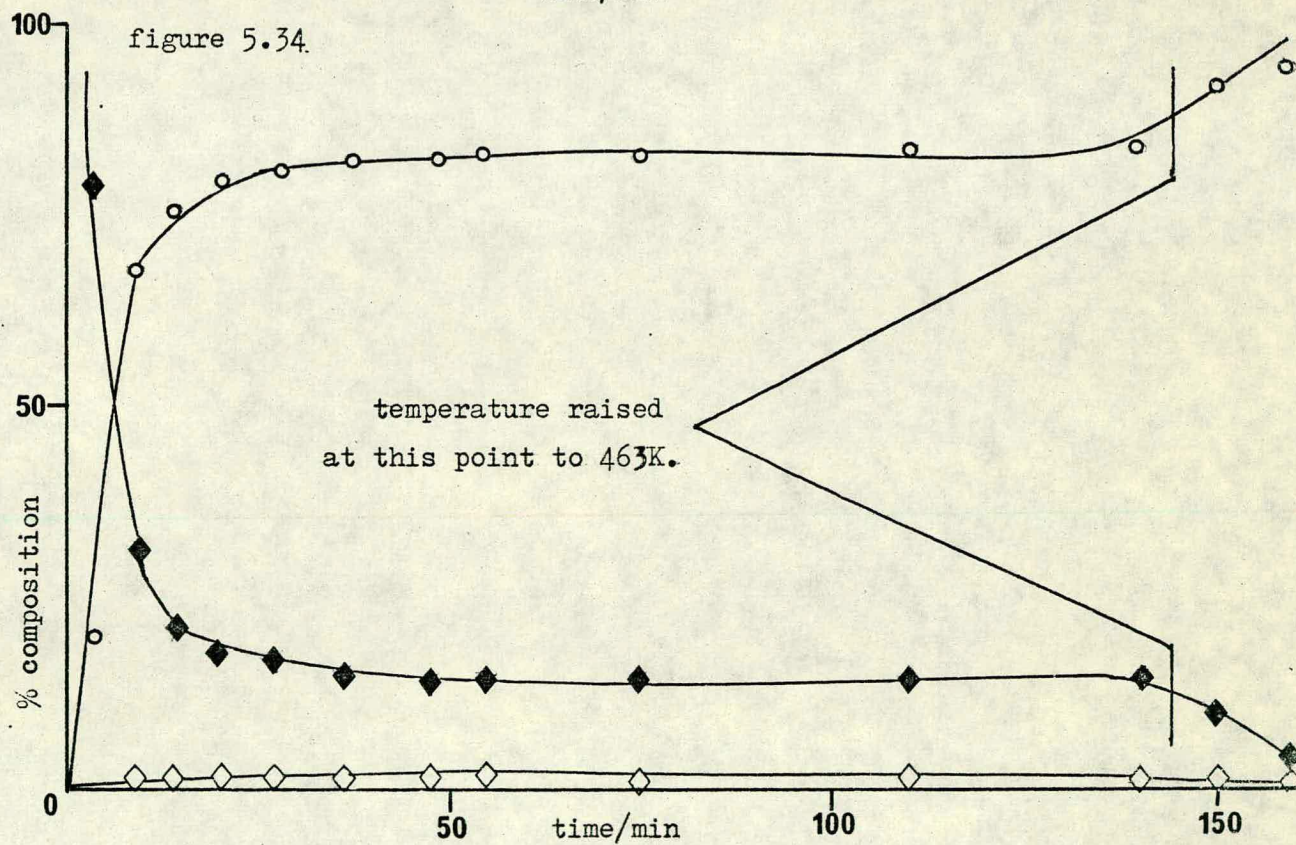
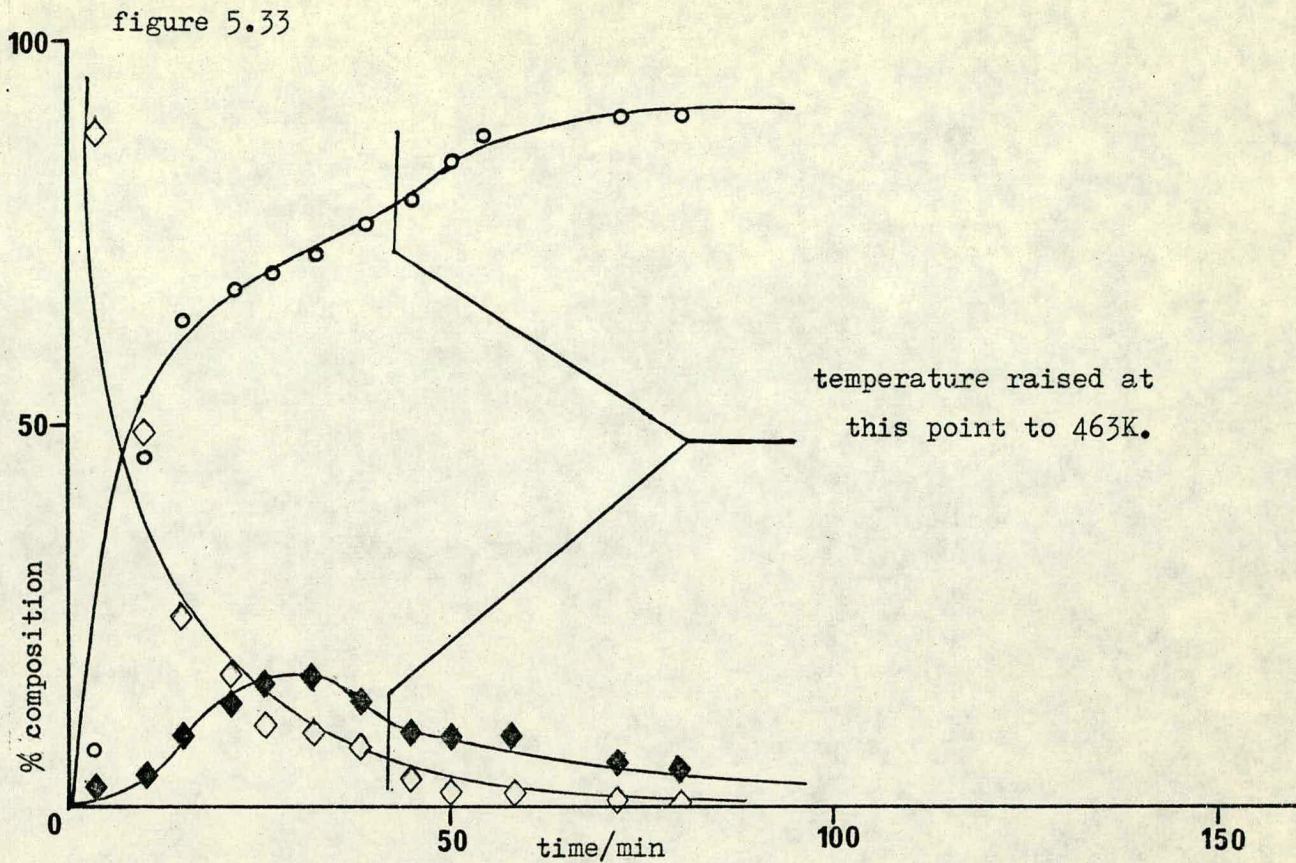


figure 5.33 decomposition of 1-chloropropane at 425K.

figure 5.34 decomposition of 2-chloropropane at 425K.

1-chloropropane, \diamond ; 2-chloropropane, \blacklozenge ; propene, o.

CHAPTER 6

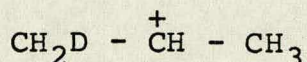
The Development of Brønsted Acidity on Rutile

6.1 Introduction

As described in Table 4.10, a comparison of the alkene product distribution from the dehydration of pentan-1-ol over rutile at ≈ 500 K with that observed from the isomerisation of pent-1-ene at slightly lower reaction temperatures has suggested that the dehydration reaction may interfere with any subsequent isomerisation of the initial products. Also, as described in Chapter 5, treatment of rutile with water tended to poison the comparatively low temperature (≈ 423 K) dehydration of 2-methylpropan-2-ol whereas similar treatment resulted in enhanced reactivity of the catalyst for the dehydration of propan-1-ol which takes place at higher temperatures (≈ 600 K). A possible explanation for these results might be the development of active Brønsted acid sites on rutile after treatment of the catalyst with water or alcohol. As previously stated however, (pages 166-169) such sites have rarely been considered active during rutile catalysed reactions. A careful study of catalysed double bond migration reactions has recently shown that, under certain conditions, Brønsted acid sites are active on alumina¹³⁵. It was therefore considered desirable to make use of this approach in the present studies with rutile.

In the absence of water or alcohol, research has indicated that n-butenes and propene isomerise over rutile at ≈ 430 K, predominantly by an intramolecular dissociative

mechanism⁴⁴, at rates of $\sim 1 \times 10^{15}$ molecules $s^{-1} m^{-2}$. The intermediates were believed to be π -allylic in character and were not formed via Brønsted acid sites^{44,148}, (see Fig. 6.2). (Although carbanionic allylic intermediates have been considered^{36,44,148}, poisoning studies and work with branched alkenes have suggested that positively charged intermediates are more likely^{37,118}). Hughes et al¹⁴⁹ reported that the exchange of [²H₀] propene with D₂ and/or D₂O occurs at similar rates to the above but requires temperatures of approximately 570 K. A microwave examination of the products revealed that the deuteriopropenes produced had deuterium randomly distributed over the 5 terminal positions. This, however, did not necessarily imply that a water-treated rutile surface possesses Brønsted acid sites because although such a distribution is characteristic of the formation of carbonium ion intermediates i.e.



this is only the case if the supply of the deuterium is not rate-determining for the exchange reaction. If it is rate-determining, the above distribution can also be produced via the formation of other intermediates followed by rapid double bond shift on the catalyst surface⁴⁴.

John et al¹⁵⁰ have envisaged the double bond shift reaction of alkenes as occurring by one of three mechanisms i.e. associative, dissociative or concerted. The specifically labelled propene, CD₂=CH-CH₃, may be used as a model alkene for investigation of this reaction;

each mechanism redistributes the labelling deuterium atoms around the molecule in a characteristic manner.

In the associative mechanism, Fig. 6.1, a carbonium ion is produced by addition of a proton or a deuteron from the surface. If a protonated carbonium intermediate is formed, this can then lose a proton to either regenerate the reactant or form the species $\text{CH}_2=\text{CH}-\text{CHD}_2$ as a primary product. Alternatively, it can lose D^+ to give $\text{CDH}=\text{CH}-\text{CH}_3$ which provides D^+ on the surface for the "start" of the reaction. This D^+ can interact with the reactant forming $\text{CD}_3-\text{CH}=\text{CH}_2$ as the only $[\text{}^2\text{H}_3]$ propene present initially. When the surface is pretreated with D_2O , as in the experiments reported here, the formation of $\text{CD}_3-\text{CH}=\text{CH}_2$ will predominate if isomerisation proceeds via a carbonium ion mechanism.

Fig. 6.2 illustrates the dissociative mechanism in which electronic charges are omitted for generality. The reactant may dissociate to form a π -allylic species $\overline{\text{CD}}_2-\overline{\text{CH}}-\overline{\text{CH}}_2$. If the original hydrocarbon is the only source of deuterium, this intermediate can only pick up hydrogen from the surface to regenerate the reactant or produce $\text{CHD}_2-\text{CH}=\text{CH}_2$ as the product. This $[\text{}^2\text{H}_2]$ propene can lose deuterium to the surface in a subsequent reaction to produce $\overline{\text{CDH}}-\overline{\text{CH}}-\overline{\text{CH}}_2$ which, following the gain of hydrogen, results in the formation of $\text{CHD}=\text{CH}-\text{CH}_3$ and $\text{CH}_2=\text{CH}-\text{CH}_2\text{D}$. Addition of a surface deuteron to the original π -allylic species $\overline{\text{CD}}_2-\overline{\text{CH}}-\overline{\text{CH}}_2$ will give rise to $\text{CDH}_2-\text{CH}=\text{CD}_2$ and $\text{CD}_3-\text{CH}=\text{CH}_2$ in equal amounts. If, as in the present series of experiments deuterium is available from another source, the production of the two $[\text{}^2\text{H}_3]$

propenes will be enhanced if the isomerisation proceeds via a dissociative intermolecular mechanism. To summarise, the main distinction between the associative and dissociative mechanisms is that $\text{CD}_3\text{-CH=CH}_2$ is the only $[\text{}^2\text{H}_3]$ propene produced if carbonium ion intermediates are formed whereas $[\text{}^2\text{H}_3]$ propene can take the forms $\text{CDH}_2\text{-CH=CD}_2$ or $\text{CD}_3\text{-CH=CH}_2$ if the dissociative mechanism is operating. This is the case whether deuterons from D_2O or protons from H_2O or alcohol are available for donation into a reacting species.

A concerted mechanism, Fig. 6.3, must also be considered as a mechanism for double bond shift of $\text{CD}_2\text{=CH-CH}_3$. It can be seen that this involves the simultaneous loss of hydrogen from the methyl group with hydrogen gain at the methylenic carbon. The products with this mechanism are similar to those from a carbonium ion mechanism and other criteria have to be considered in order to distinguish between the two.

6.2 Results and Discussion

The source and pretreatment of the rutile were as reported in Chapter 2. Samples of 1 g were used with approximately 1×10^{20} molecules of alkene and a similar amount of D_2O or pentan-1-ol as appropriate. The reaction was followed by mass spectrometry to a predetermined point, at which time a gas phase sample was removed for subsequent microwave analysis. The experimental details and the results are summarised in Table 6.1. Fig. 6.4 and the results of experiments 1 and 2 provide clear evidence that in the presence of water (D_2O), exchange of propene

Table 6.1 % Analyses ^(a) of deuteriopropenes and deuterio-2-methylpropenes produced over rutile

Experiment	1	2	3	4 (ref. 121)	5
Reactants	$\text{CD}_2=\text{CH}-\text{CH}_3$ + D_2O ^(c)	$\text{CD}_2=\text{CH}-\text{CH}_3$ + D_2O ^(d)	$\text{CD}_2=\text{CH}-\text{CH}_3$ + pentan-1-ol ^(e)	$\text{CD}_2\text{C}(\text{CH}_3)_2$ ^(f)	$\text{CH}_2=\text{C}(\text{CH}_3)_2$ + D_2O ^(c)
Reaction Temperature/K	523	523	553	283	390
$\text{CD}_2=\text{CR}-\text{CH}_3$ ^(b)	87.6 (96)	68.8 (89)	46.0 (57)	12.6 (17)	-
$\text{CHD}_2-\text{CR}-\text{CH}_2$	3.6 (4)	8.4 (11)	33.6 (46)	34.9 (47)	-
$\text{CH}_2\text{D}-\text{CR}=\text{CH}_2$	0	0	5.8 (34)	6.0 (54)	24.9 (73)
$\text{CH}_3-\text{CR}=\text{CHD}$	1.0 (100)	2.1 (100)	11.1 (66)	5.0 (45)	9.2 (27)
$\text{CD}_2=\text{CR}-\text{CH}_2\text{D}$	1.0 (13)	3.3 (16)	0.4 (17)	-	-
$\text{CD}_3-\text{CR}=\text{CH}_2$	6.8 (87)	17.4 (84)	2.0 (83)	-	-

Table 6.1 continued

Table 6.1 continued

- (a) numbers in brackets are normalised distributions of [$^2\text{H}_i$]-species for various i .
- (b) R is either H (propene) or CH_3 (2-methylpropene).
- (c) reactants both added at 283 K and warmed to reaction temperature.
- (d) D_2O added initially at ≈ 700 K prior to cooling to 283 K and admitting $\text{CD}_2=\text{CH}-\text{CH}_3$.
- (e) pentan-1-ol admitted initially at 550 K and partially dehydrated for 20 minutes prior to cooling to 283 K and admitting $\text{CD}_2=\text{CH}-\text{CH}_3$.
- (f) also contained 26.9% $\text{CHD}=\text{C}(\text{CH}_3)\text{CH}_2\text{D}$ (and $\text{CH}_2=\text{C}(\text{CH}_2\text{D})_2$) with 11.7% unknown [$^2\text{H}_3$]-species.

with D and double bond shift occurred at essentially the same rate i.e. the reaction is termed "clean" and deuterium exchange does not occur other than during isomerisation. Furthermore, the highly selective production of $\text{CD}_3\text{-CH=CH}_2$ at ≈ 520 K is strongly indicative of classical carbonium ion intermediates reacting on Brønsted acid centres produced with D^+ from D_2O , irrespective of whether water (D_2O) was initially added at 300 K or 700 K.

Similarly, exposure of rutile to $\text{CD}_2\text{=CH-CH}_3$ and pentan-1-ol at 298 K with subsequent heating to ≈ 550 K revealed that the alcohol alone was sufficient to poison the previously postulated^{37,44,118,148} intramolecular (π -allylic) reaction of propene at ≈ 450 K. No reaction of the [$^2\text{H}_2$] propene was observed on the mass spectrum until the system was warmed to 553 K at which temperature gas chromatographic analysis revealed that dehydration of the alcohol was taking place. The microwave studies confirmed that in the presence of pentan-1-ol and its dehydration products, propene reacts on Brønsted acid centres which initially contain H^+ leading to the selective production of CDH=CH-CH_3 , $\text{CH}_2\text{=CH-CHD}_2$ and, more importantly, $\text{CD}_3\text{-CH=CH}_2$ as the sole [$^2\text{H}_3$] product. It is not fully clear, however, whether protons were provided directly from the alcohol or from the water dehydration products, or from both sources.

In the absence of water, the labelled 2-methylpropene $\text{CD}_2\text{=C(CH}_3)_2$ has been found to undergo intramolecular double bond migration at a rate of 1×10^{15}

molecules $\text{s}^{-1} \text{m}^{-2}$ at 283 K (experiment 4¹²¹). Experiments with $\text{CD}_2=\text{C}(\text{CH}_3)_2$ and $\text{CH}_2=\text{C}(\text{CH}_3)_2$ have shown that in the presence of D_2O , a temperature of approximately 390 K is necessary for the two alkenes to react (Figs. 6.5 and 6.6). The two alkenes now react in an intermolecular fashion at similar rates and the ratio, $\text{CH}_2=\text{C}(\text{CH}_3)\text{CH}_2\text{D}$: $\text{CHD}=\text{C}(\text{CH}_3)_2$ was $2.7 \pm 0.3:1$ in the reaction of $\text{CH}_2=\text{C}(\text{CH}_3)_2 + \text{D}_2\text{O}$ (experiment 5). These observations confirm directly that 2-methylpropene reacts on rutile in the presence of D_2O via the carbonium ion intermediate, $(\text{CH}_3)_2\overset{+}{\text{C}}-\text{CH}_2\text{D}$; random loss of H^+ gives the above [²H₁] product ratio whereas a π -allylic intermediate would give only $\text{CH}_2=\text{C}(\text{CH}_3)\text{CH}_2\text{D}$ (Fig. 6.7). Thus, reaction through a tertiary carbonium ion (from 2-methylpropene) occurs at similar rates to that through a secondary ion (from propene) in the presence of the same quantity of water, but at approximately 160 K lower in agreement with its greater stability. (The greater activity of 2-methylpropene over propene also suggests a greater likelihood of an associative rather than a concerted mechanism).

It is clear, therefore, that the reaction of alkenes on rutile in the presence of water or alcohol occurs by a different mechanism (carbonium ions on Brønsted acid centres) to that found previously in the absence of water (allylic intermediates on Lewis acid centres^{37,118}). Studies of alkene isomerisation in the absence of water or alcohol should not therefore be used to describe such reactions in their presence. Also, when it is considered that alcohols are generally thought of as stronger bases than alkenes, it

is not unreasonable to conclude that Brønsted acid sites may be active on the surface of rutile catalysts during alcohol dehydration as described in Chapter 5. The higher temperatures required for double bond migration to occur with Brønsted as opposed to Lewis acid sites confirms that the Brønsted acidity of a rutile surface is a function of reaction temperature as was also suggested in Chapter 5. The main conclusion from the results in this chapter is that the use of sensitive catalytic reactions as a probe to catalyst characterisation can be more useful than inferences from indirect techniques such as infra-red spectroscopy. This conclusion was also reached by John¹³⁵ et al who carried out similar studies with water pretreated alumina.

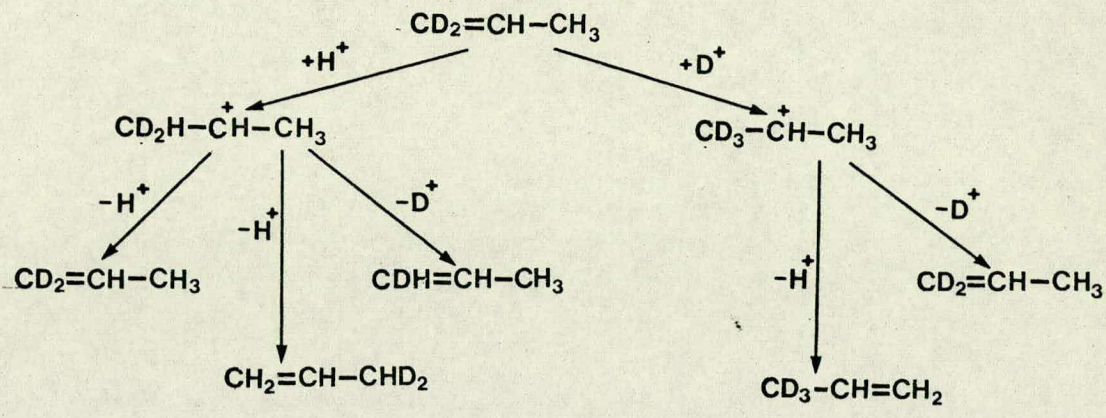


figure 6.1 associative mechanism for the double bond migration of $\text{CD}_2=\text{CH}-\text{CH}_3$.

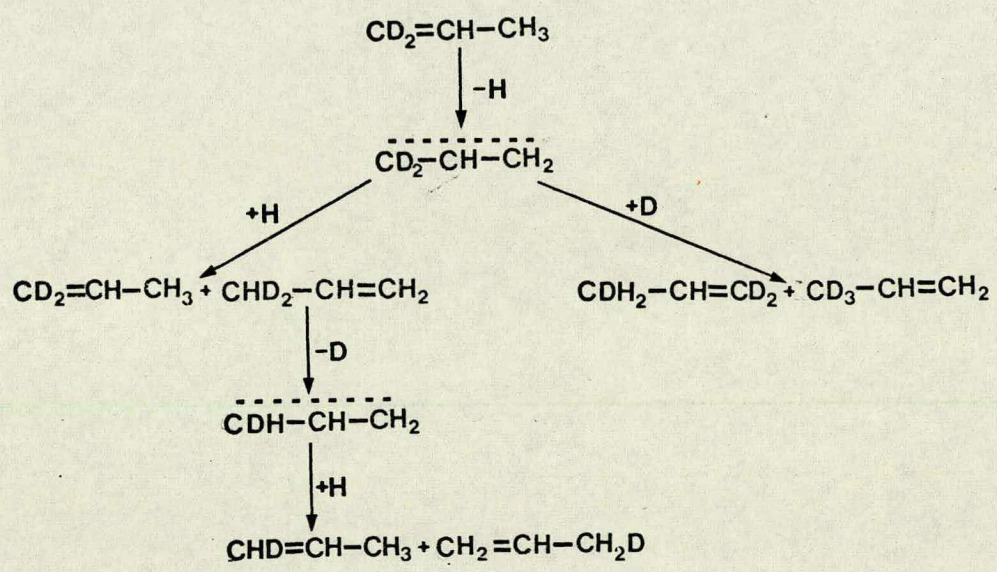


figure 6.2 dissociative mechanism for the double bond migration of $\text{CD}_2=\text{CH}-\text{CH}_3$.

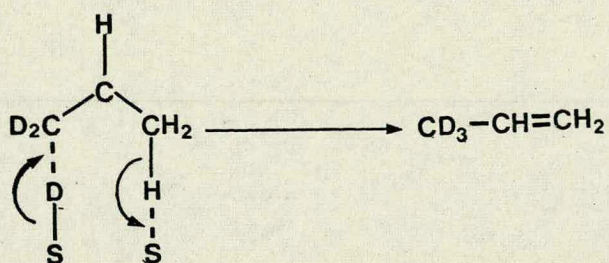
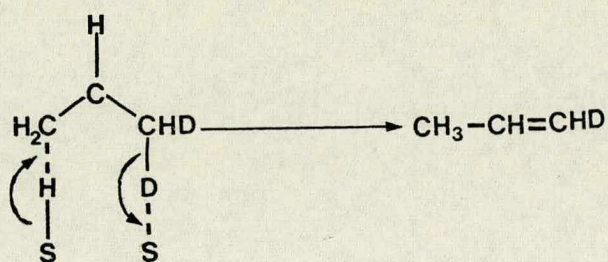
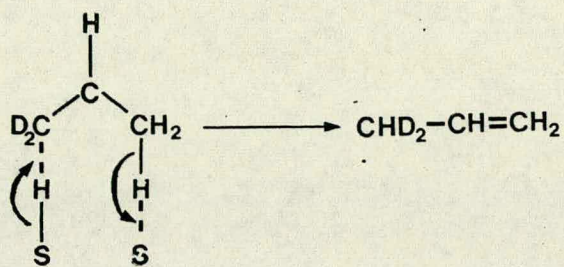


figure 6.3 concerted mechanism for the double bond shift
of $\text{CD}_2=\text{CH}-\text{CH}_3$.

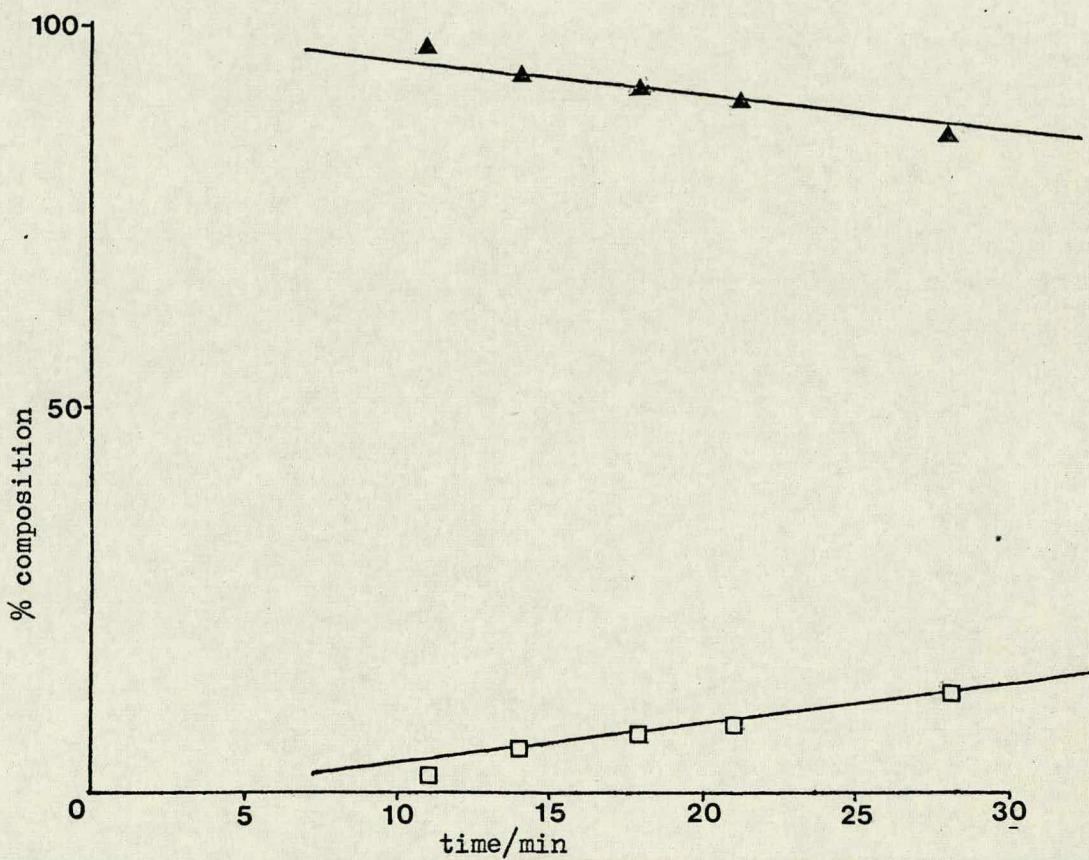


figure 6.4 conversion of $[^2\text{H}_2]$ propene to $[^2\text{H}_3]$ propene at 523K over D_2O pretreated rutile; $[^2\text{H}_2]$ propene, ▲; $[^2\text{H}_3]$ propene, □.

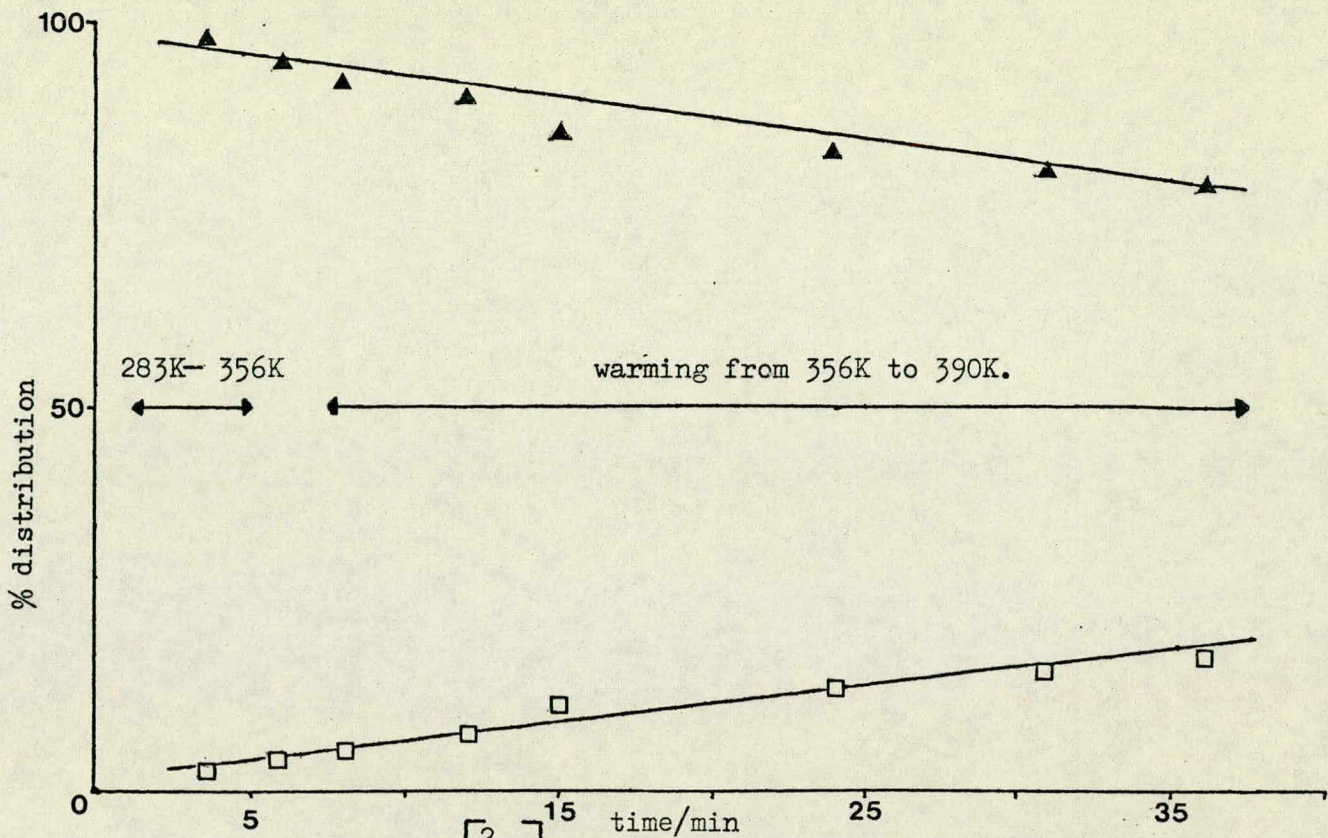


figure 6.5 exchange of $[^2\text{H}_2]$ 2-methylpropene with D_2O on raising the temperature from 283K to 390K; $[^2\text{H}_2]$ 2-methylpropene, ▲; $[^2\text{H}_3]$ 2-methylpropene, □.

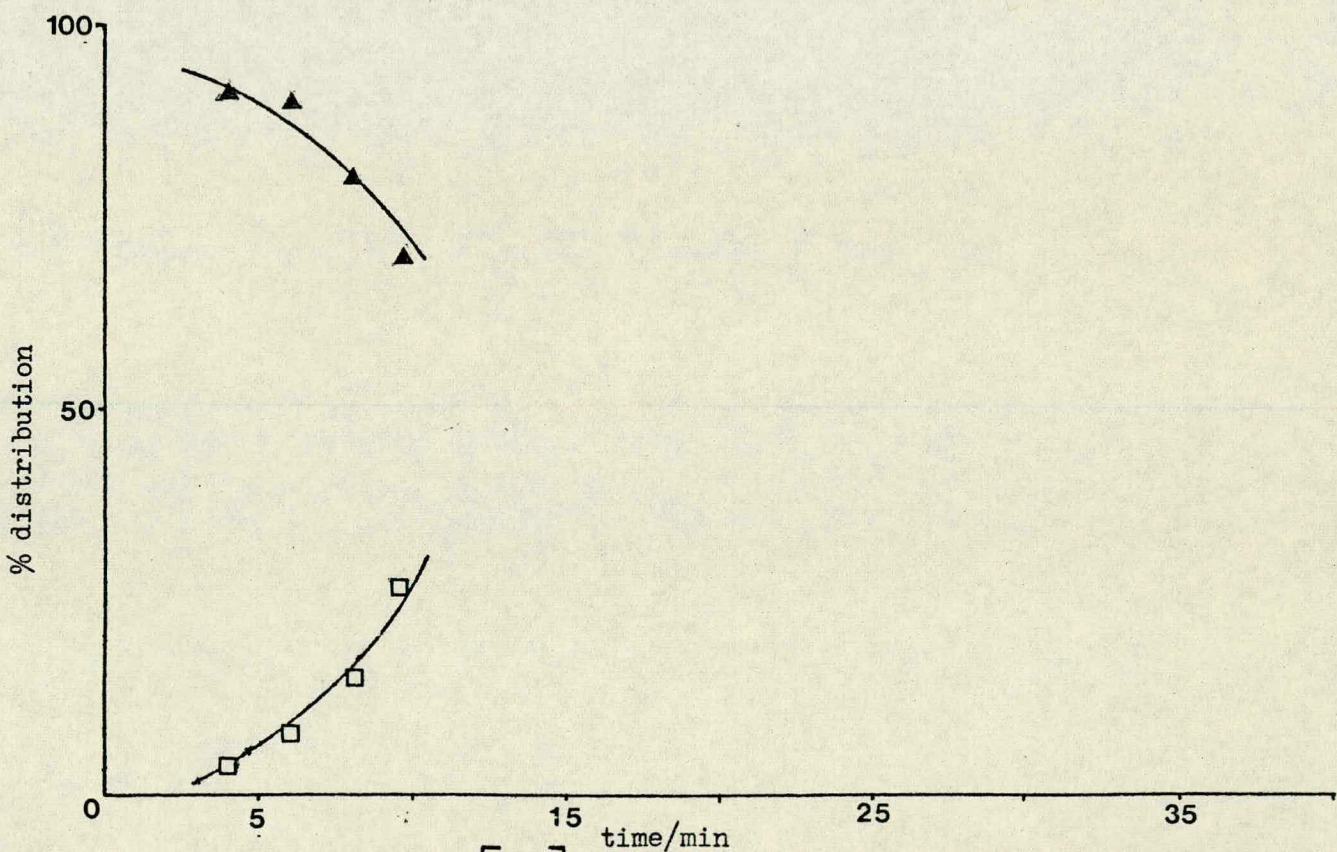
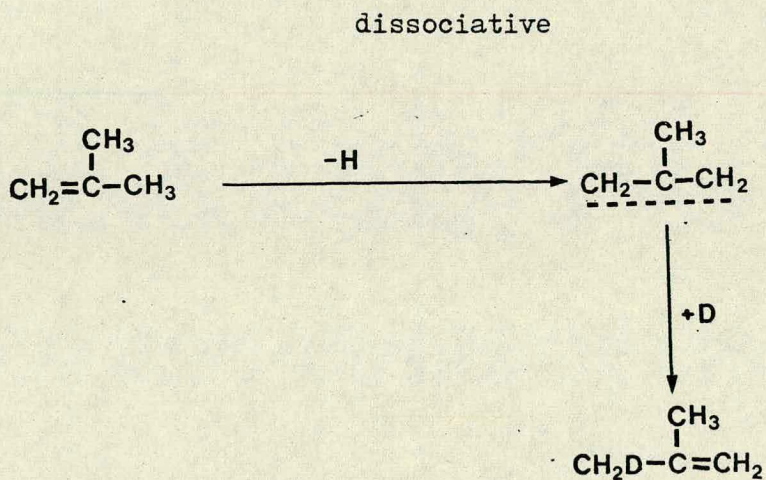
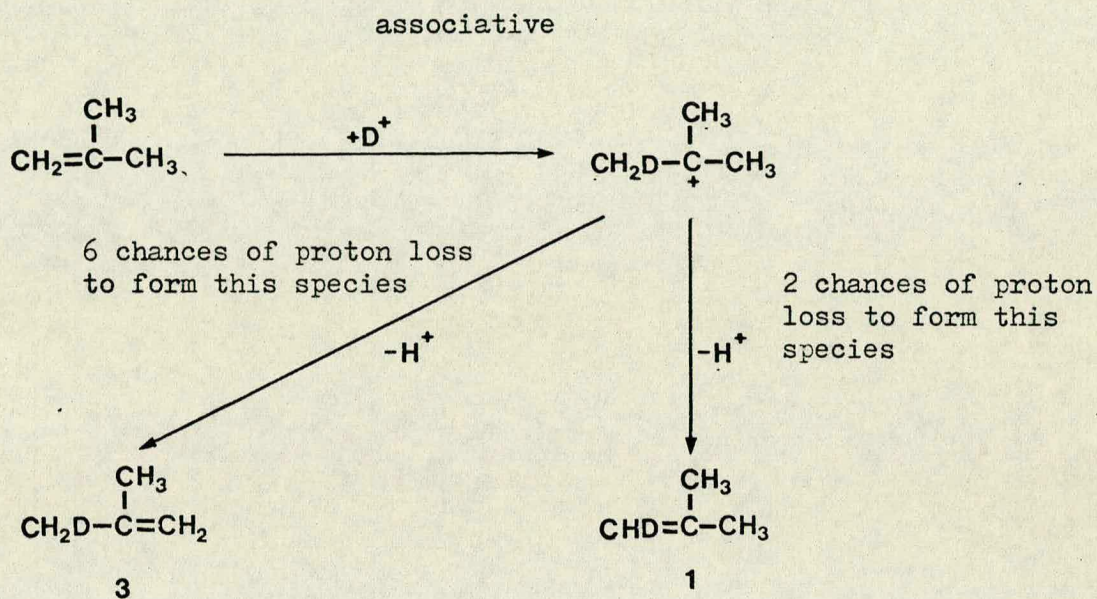


figure 6.6 exchange of $[^2\text{H}_0]$ 2-methylpropene with D_2O at 390K; $[^2\text{H}_0]$ 2-methylpropene, ▲; $[^2\text{H}_1]$ 2-methylpropene, □.

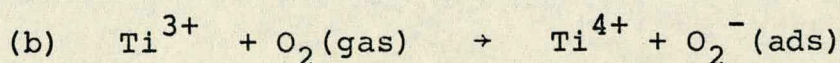
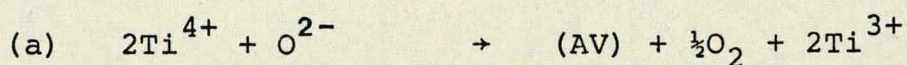
figure 6.7 associative and dissociative exchange of D_2O with $CH_2=C(CH_3)_2$.



CHAPTER 7The Influence of the Mode of Catalyst Pretreatment on the Dehydration/Dehydrogenation Properties of Rutile7.1 Introduction

Some recent studies over rutile¹⁰⁶ and other metal oxides¹⁵¹ have suggested that the active centres responsible for the dehydration of an alcohol are not those responsible for dehydrogenation. Work reported in Chapters 4 and 5 of this thesis has also indicated this to be the case. (Those treatments which altered the activity of rutile towards dehydration did not have a similar effect on the activity of the catalyst towards dehydrogenation). It has also become apparent that those alcohols which require dehydration temperatures between 523 and 600 K show greater activity for dehydrogenation than those alcohols which are dehydrated over rutile at lower temperatures indicating that the centres for dehydrogenation may be generated at higher temperatures.

E.S.R. experiments have shown^{152,153,154} (i) that the reduction of TiO₂ (anatase and rutile) at temperatures between 573 and 773 K under vacuum or in the presence of CO or H₂ creates surface Ti³⁺ ions (equation a) and (ii) that oxygen adsorbs onto this partially reduced rutile surface in a largely ionic form as an O₂⁻ radical (equation b).



(AV = anionic vacancy)

It was considered, therefore, that there might be a connection between dehydrogenation and the production of Ti^{3+} ions and/or O_2^- ions and that alteration of the normal pre-experimental pretreatment of the catalyst may provide information about the dehydrogenation reaction.

As discussed in section 3.4, the selectivity of an oxide catalyst for alcohol decomposition via dehydration or dehydrogenation has been found by Davis et al⁸⁶⁻⁹⁰ to be heavily dependent on the pretreatment of the catalyst, whether in O_2 or H_2 , but the authors were unable to draw conclusions which they considered were applicable to oxide catalysts in general.

7.2 Experimental

The reaction chosen for study was the decomposition of propan-2-ol because it was known from previous reports^{45,106,151} that it reacts to produce mainly propene and small amounts of acetone. Previous reports had also indicated that the situation would not be complicated by the production of ethers or other large organic molecules as was found with the decomposition of propan-1-ol (section 5.3). The experiments were carried out in a static system, gas-line I, using a 1 metre column of Porapak S at 453 K in a Perkin-Elmer F.I.D. FII Gas-Chromatograph for analytical determinations. Fresh samples of 0.1 g of catalyst were used in each experiment with

approximately 0.4×10^{20} molecules of reactant.

The following forms of pretreatment, labelled A, B and C were employed:-

- (A) This was the normal oxygen pretreatment, as described in section 2.4.1.1, which produces a clean, white, rutile surface composed essentially of Ti^{4+} and O^{2-} ions.
- (B) In this pretreatment, the catalyst was heated overnight at 723 K under a vacuum of approximately 10^{-3} Pa in order to enrich the rutile surface with Ti^{3+} ions. This treatment changes the rutile surface to a dull grey colour.
- (C) After heating under vacuum as in (B), pretreatment C involves cooling the catalyst to the appropriate reaction temperature and then exposing it to ≈ 8 kPa of oxygen for 30 seconds after which the excess oxygen is pumped away for 20 seconds. This is a similar procedure to that described by Gravelle et al¹⁵³ which, it was reported, generated surface O_2^- ions. During this procedure the rutile samples remained grey and did not take on a white colour.

After each of these treatments the reactant vapour was expanded into the reaction vessel. The experiments carried out were as follows:-

Table 7.1

<u>Experiment</u>	<u>Pretreatment</u>	<u>Reactant</u>	<u>Temp/K</u>
1	A	propan-2-ol	523
2	B	propan-2-ol	523
3	C	propan-2-ol	523
4	A	acetone	523
5	C	acetone	523
6	A	propene	573
7	C	propene	573
8	A	2-methylpropan-2-ol	425
9	C	2-methylpropan-2-ol	425

7.3 Results and Discussion

In all the experiments, only gas-phase analysis was possible and no information concerning reactants lost to the surface was obtained.

The effect of pretreatment A in experiment 1 is shown in Fig. 7.1. This shows that the main reaction is the conversion of the alcohol to alkene (90% in 45 minutes) and subsidiary formation of small amounts of acetone (4% in 45 minutes).

The effect of pretreatment B in experiment 2 (Fig. 7.2) shows that the reaction of propan-2-ol over partially reduced rutile is, within experimental error, identical to that obtained from pretreatment A outlined above. This suggests that the active centres responsible for dehydrogenation are not markedly affected by partial reduction. If anything, ketone

production appears to decrease rather than increase following partial reduction. Small traces (0.5%) of di,isopropyl ether were also observed during this experiment.

Figs. 7.3, 7.4 and 7.5 illustrate that oxygen admitted into the reaction system using pretreatment C in experiment 3 results in the marked activation of the catalyst towards the production of acetone. Figs. 7.3 and 7.4 also show that after the majority of the alcohol has decomposed, the ketone itself begins to decompose. Fig. 7.5 also reveals that during this experiment, substantial amounts of two compounds with longer G.C. retention times were observed but they remain unidentified. One of the compounds has a retention time similar to that of propan-1-ol and the larger retention time of the other suggests that a coupling process may have taken place. Substantial amounts of butene were also produced. Pure samples of the following were examined by gas chromatography in an attempt to identify the unknown compounds but with negative results:- di-isopropyl ether, mesitylene, mesityl oxide, 4-methyl-pentene, hex-1-ene and allyl alcohol.

Figs. 7.6 and 7.7 show the results of experiments 4 and 5 which were to monitor the products obtained when the ketone begins to decompose as in experiment 3 and also to see if the increased production of ketone in experiment 3 was responsible for the unidentified products. Figs. 7.6 and 7.7 do not accurately reflect the total situation as they show only the changes in the % composition of the

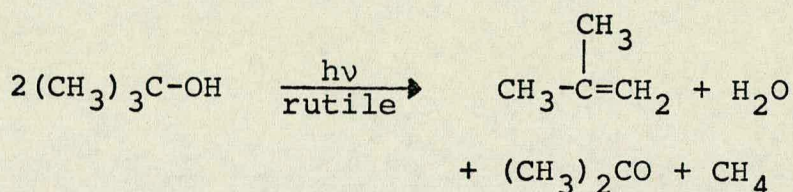
gas phase. The main reaction was predominantly the loss of reactant to the surface, as reflected by the G.C. peak areas (80% in 40 minutes). They do reveal that the production of butene, propene and ethene is probably due to the decomposition of acetone. However with neither of the differently pretreated rutile samples was there any trace of the long retention time products obtained in experiment 3. This suggests that for their production, a rather complicated surface situation may be necessary requiring the presence of Ti^{4+} and Ti^{3+} ions, O^{2-} and O_2^- ions, H_2O , alcohol, alkene, acetone and hydroxyl groups.

Experiments 6 and 7 were carried out in order to ascertain whether any propene produced by the dehydration of the alcohol could subsequently react to form acetone via an oxidation process. The catalysed oxidation of alkenes by gas phase oxygen is a well established process¹⁵⁵. Yoshida et al^{156,157} have reported that oxygen adsorbed on partially reduced $V_2O_5-SiO_2$ catalysts in the form of O_2^- radicals are the active species for the oxidation of propene to propanal. However, in both experiments 6 and 7, no reaction was observed which indicates that the acetone formed in experiments 1 and 3 was certainly not derived from propene alone.

In experiment 8, 2-methylpropan-2-ol was allowed to decompose over normally pretreated rutile and the results of this experiment have been reported in Chapter 5. (The only reaction which takes place is a dehydration to form 2-methylpropene and water and no other products are observed). Experiment 9 involving

pretreatment C, however, resulted in the formation of small amounts of acetone which increased as the reaction proceeded as in Fig. 7.8.

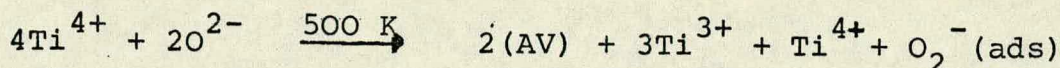
The results of experiment 9 can be compared with work carried out by Cunningham and Meriaudeau¹⁵⁸ who examined the interaction of butyl alcohols with flash-illuminated rutile surfaces and found that the products of such an interaction with 2-methylpropan-2-ol as a reactant were as follows:-



When the authors tested the reaction of 2-methylpropan-1-ol, the only product was 2-methylpropanal, no alkene being produced. A little, but not all, of the acetone from 2-methylpropan-2-ol could be attributed to the subsequent oxidation of 2-methylpropene but no information was obtained concerning the identity of the sites connected with the formation of either the bulk of the acetone from 2-methylpropan-2-ol or the 2-methylpropanal from 2-methylpropan-1-ol. The similarity of the results however suggests that there may be a connection between the results of Cunningham et al¹⁵⁸ and the results of experiment 9 described here; the major difference being that the flash-illuminated reactions are predominantly active for the production of aldehydes and ketones whereas the pretreatments employed here result mainly in the catalyst being active for dehydration. In the present

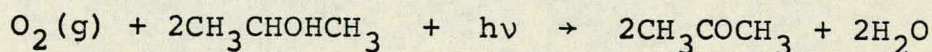
experiments there was no evidence of any methane but the gas-chromatographic technique would not readily detect methane. Overall, the results following pretreatment C suggest that the same sites may be involved with both the production of acetone from propan-2-ol and of acetone from 2-methylpropan-2-ol.

It is interesting now to speculate about the nature of the active sites in the dehydrogenation of an alcohol over rutile. The result of experiment 3, in which the increased production of acetone from propan-2-ol followed the enrichment of the rutile surface with O_2^- ions, makes it attractive to postulate that such species are the active sites during alcohol dehydr^{ogenation}~~ation~~ reactions over rutile. If such O_2^- sites are consumed during a reaction however, by definition the reaction is not genuinely catalytic. Calculations show that if a surface density of Ti^{3+} ions of approximately 7 nm^{-2} is considered (using data of Munuera and Stone¹⁹ and also considering that all the Ti^{4+} surface ions are reduced to Ti^{3+} ions) 1.75×10^{19} O_2^- ions could be formed on the surface after pretreatment C. This is approximately 44% of the total number of reactant molecules which is similar to the amount of acetone produced in experiment 3. Nevertheless, such considerations do not necessarily rule out O_2^- ions as being the active sites for dehydrogenation when a normally pretreated catalyst is used, as in experiment 1, as such sites may be produced by partial degradation of the rutile surface when reaction temperatures in excess of 500 K are employed:-



(AV = anionic vacancy)

The initial burst of activity for dehydrogenation when the flow system is employed (Figs. 4.1 and 4.21) is characteristic of processes that involve lattice oxygen and, as discussed in section 3.6, Kemball et al¹⁰⁴ have considered the incorporation of lattice oxygen into the final products formed during the decomposition of alcohols over anatase. Although experiments 6 and 7 rule out the formation of acetone via the oxidation of propene, another reaction during which O_2^- species could be consumed is one in which the formation of water, as opposed to hydrogen, accompanies the formation of the ketone. Bickley and co-workers¹⁵⁹ concluded that O_2^- ions were the active sites on rutile during the photocatalytic oxidation of propan-2-ol and the overall reaction was envisaged as follows:-



Similarly, Hasegawa et al¹⁶⁰ have proposed from E.S.R. studies that O_2^- species are active during the dehydrogenation of propan-2-ol over MnO_2 .

As discussed in section 5.4.2.2, the dehydrogenation of alcohols via an acid/base mechanism similar to that proposed by Kibby and Hall⁷² (Fig. 3.7) is not considered likely over rutile.

As another alternative to an oxidative dehydrogenation, propan-2-ol could perhaps decompose to form acetone and

hydrogen via a radical mechanism by virtue of the fact that O_2^- ions are radical species.

Halliday⁴⁵ concluded from studies of the dehydrogenation of alkanes over rutile that at high temperatures, similar to those required for alcohol dehydrogenation, the catalytic properties of rutile resemble those of a metal in that homolytic splitting of chemical bonds takes place to form neutral radical species. (Halliday⁴⁵, however, believed that Ti^{3+} ions were the active sites involved with this reaction (Fig. 1.11). Experiment 2 of the present study indicates that such sites alone are not the sites involved with the dehydrogenation of alcohols). The ability to promote the dehydrogenation as opposed to the dehydration of alcohols is a noted characteristic of metal catalysts and therefore it is concluded that the homolytic fission of chemical bonds may also be occurring during the dehydrogenation of alcohols over rutile as reported in this thesis. Fig. 7.9 shows a possible reaction scheme using O_2^- radical anions as the active sites. This conclusion is further strengthened when the dehydrogenation of alcohols in the flow system (as reported in Chapter 4) is compared with H_2 - D_2 exchange over rutile as reported by Lake and Kemball⁴³. H_2 - D_2 exchange almost certainly proceeds via the homolytic fission of chemical bonds and, like dehydrogenation, requires temperatures in excess of 473 K. Also, the activation energy for the reaction was reported to be approximately 80 kJ mol^{-1} which is similar to that for the dehydrogenation of pentan-1-ol and 4-methylpentan-2-ol. Thus the rate determining step in both processes could be similar, perhaps involving the associative desorption of H_2 .

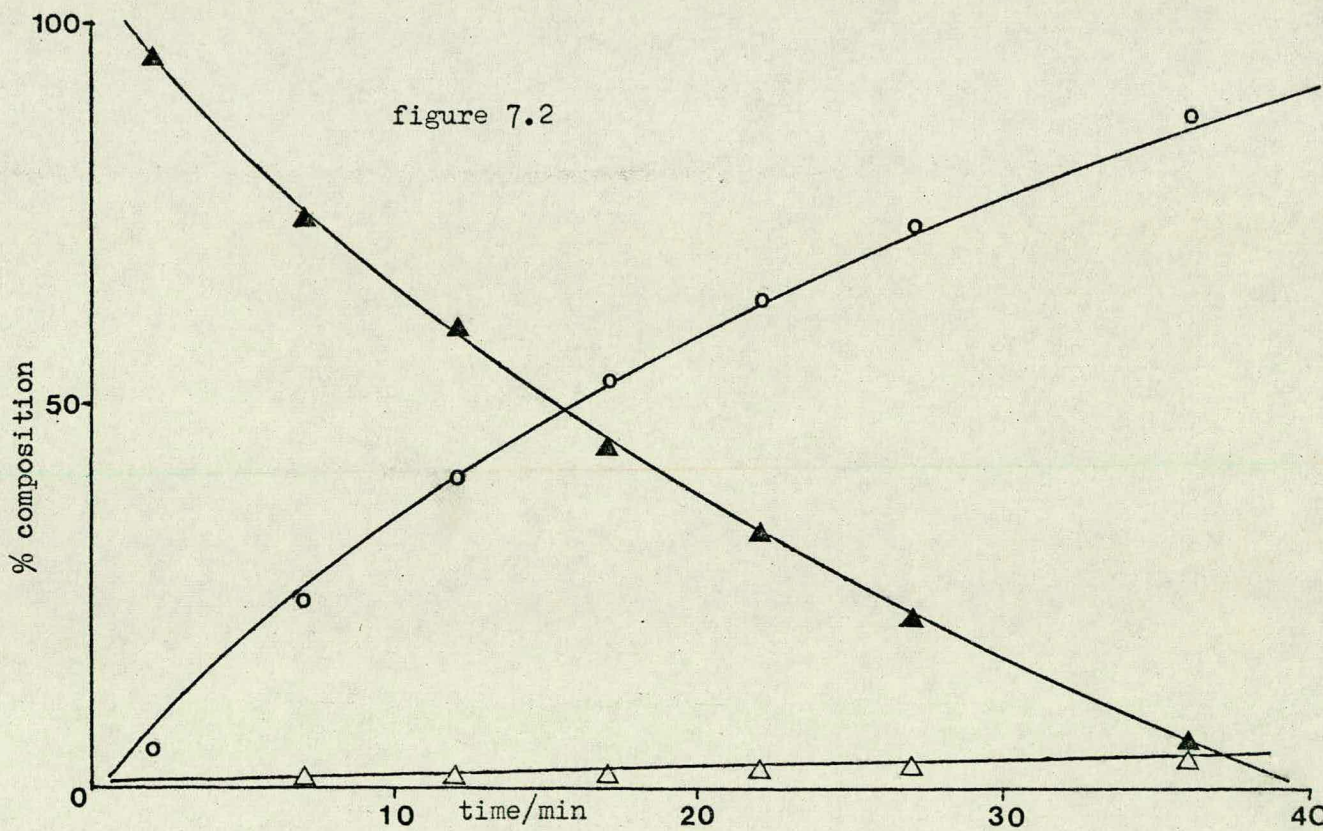
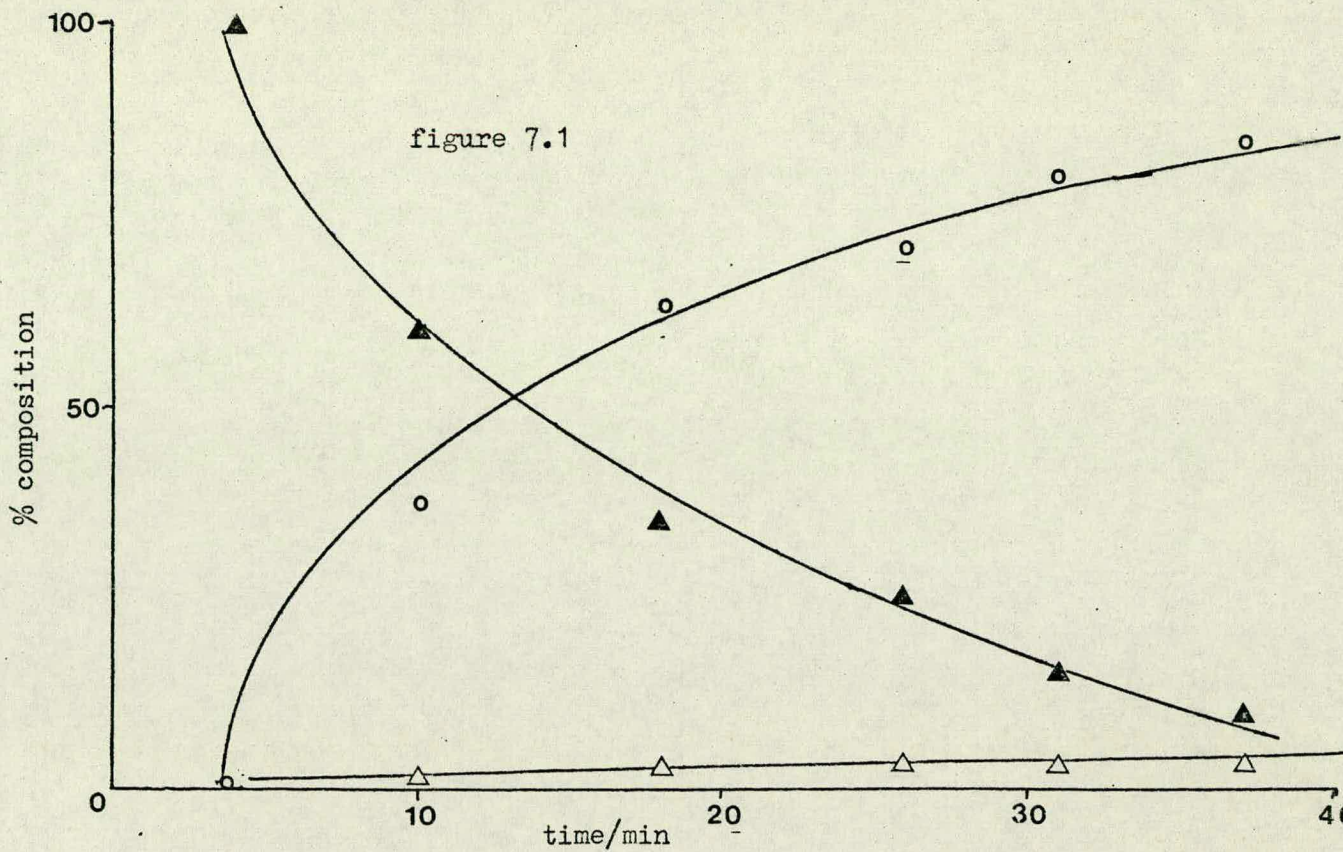


figure 7.1 decomposition of propan-2-ol over rutile at 523K after pretreatment A;

figure 7.2 decomposition of propan-2-ol over rutile at 523K after pretreatment B;

propan-2-ol,▲; propene,○; acetone,△.

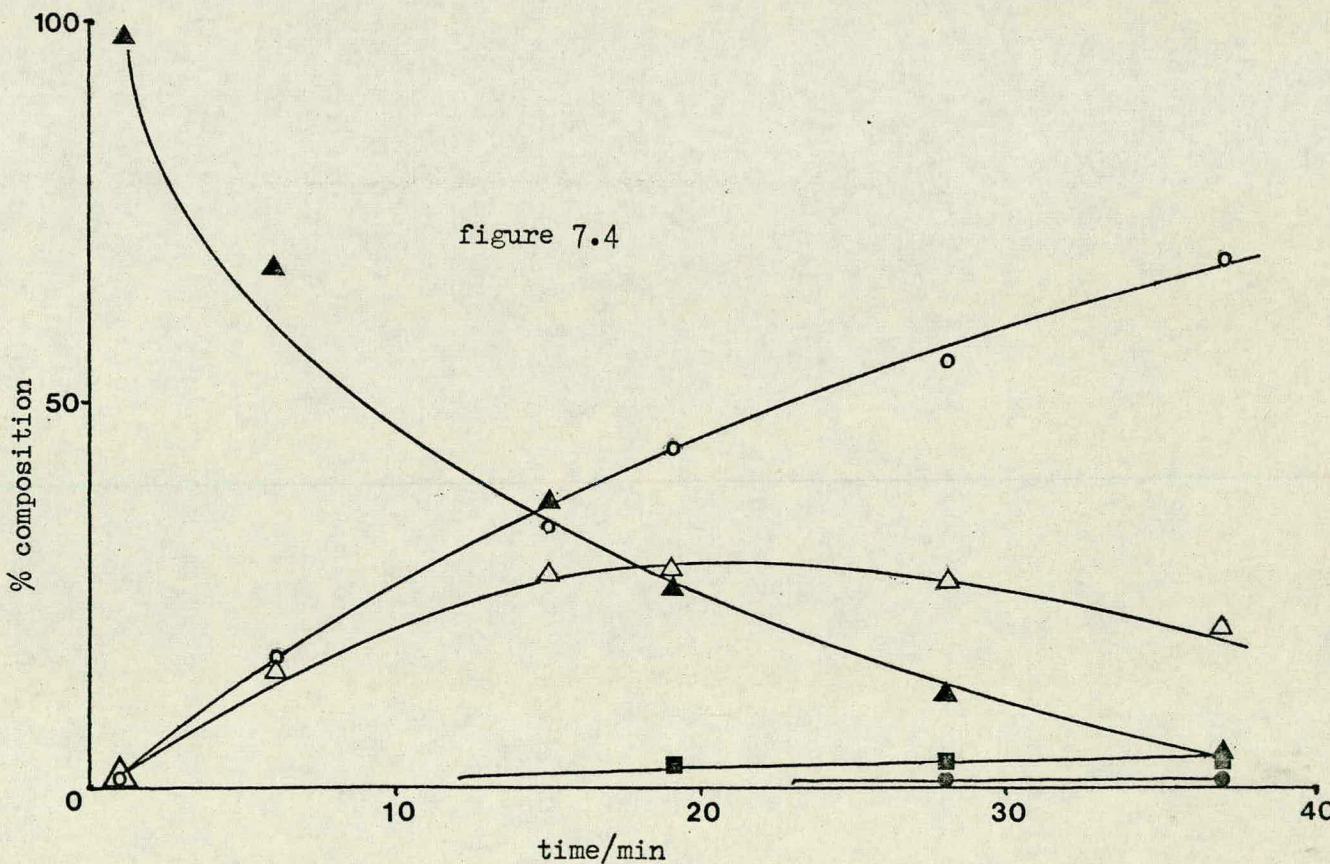
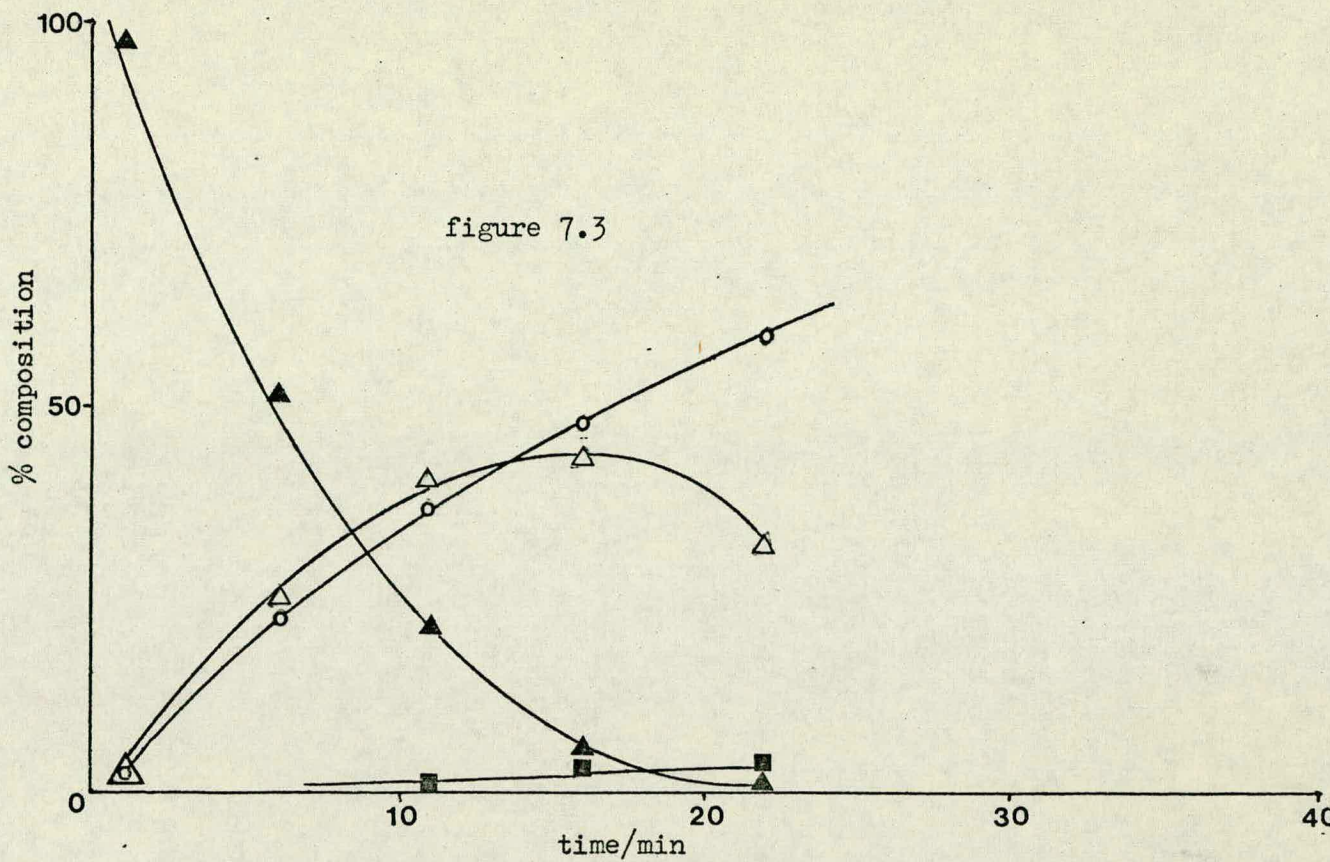


figure 7.3 decomposition of propan-2-ol over rutile at 533K after pretreatment C:

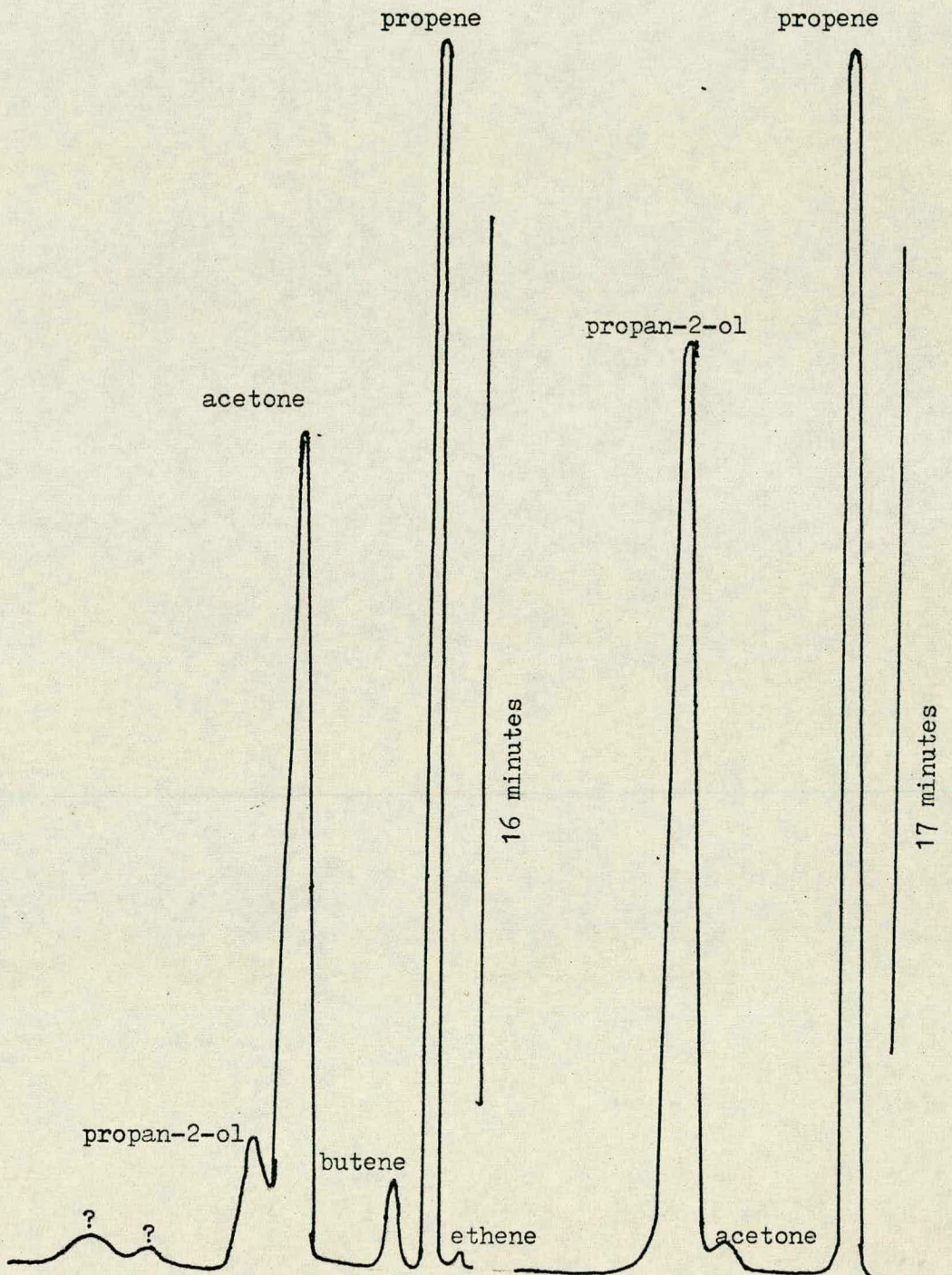
figure 7.4 decomposition of propan-2-ol over rutile at 523K after pretreatment C:

propan-2-ol, ▲; propene, ○; acetone, △; unknown, ■; butene, ●.

figure 7.5 G.C. traces of decomposition of propan-2-ol over rutilite after pretreatments A and C.

experiment 3 pretreatment C

experiment 1 pretreatment A



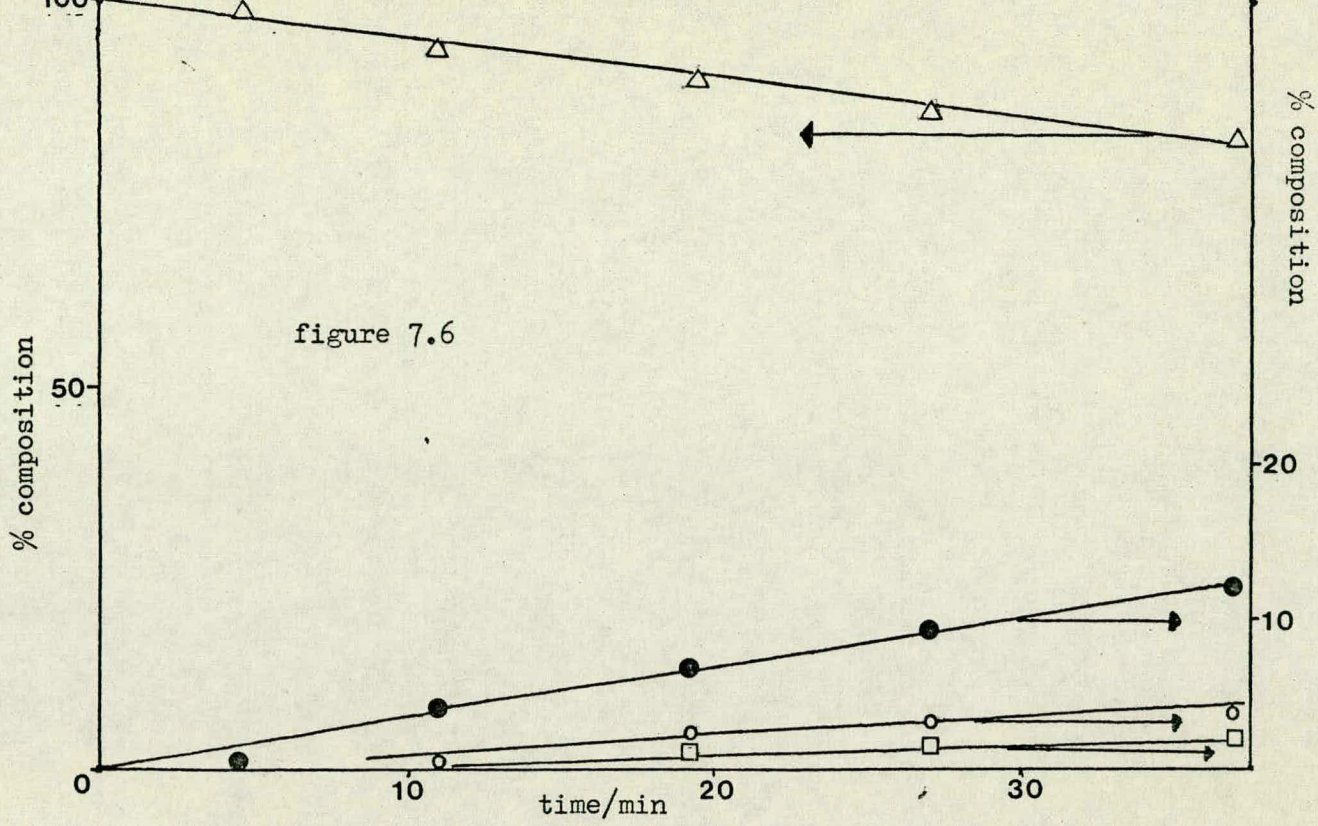


figure 7.6

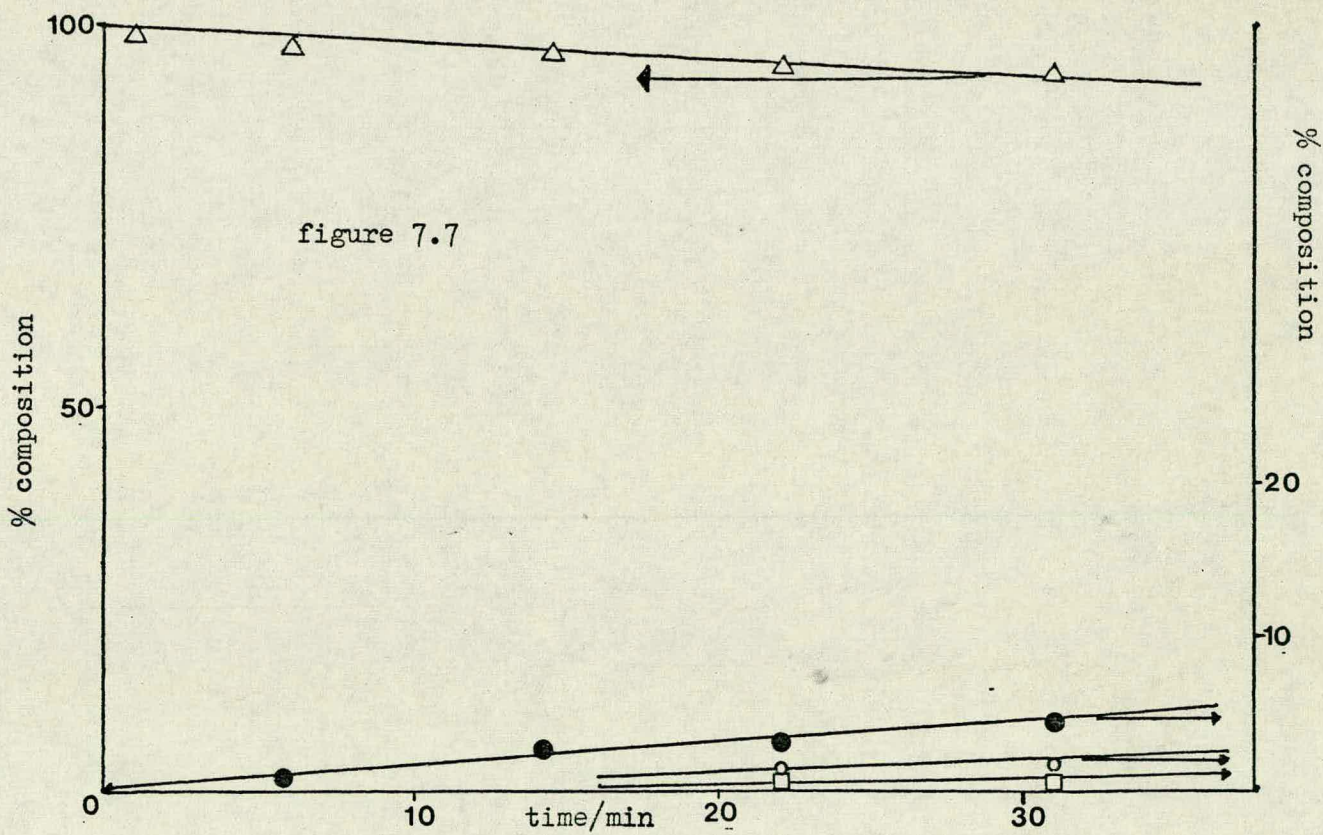


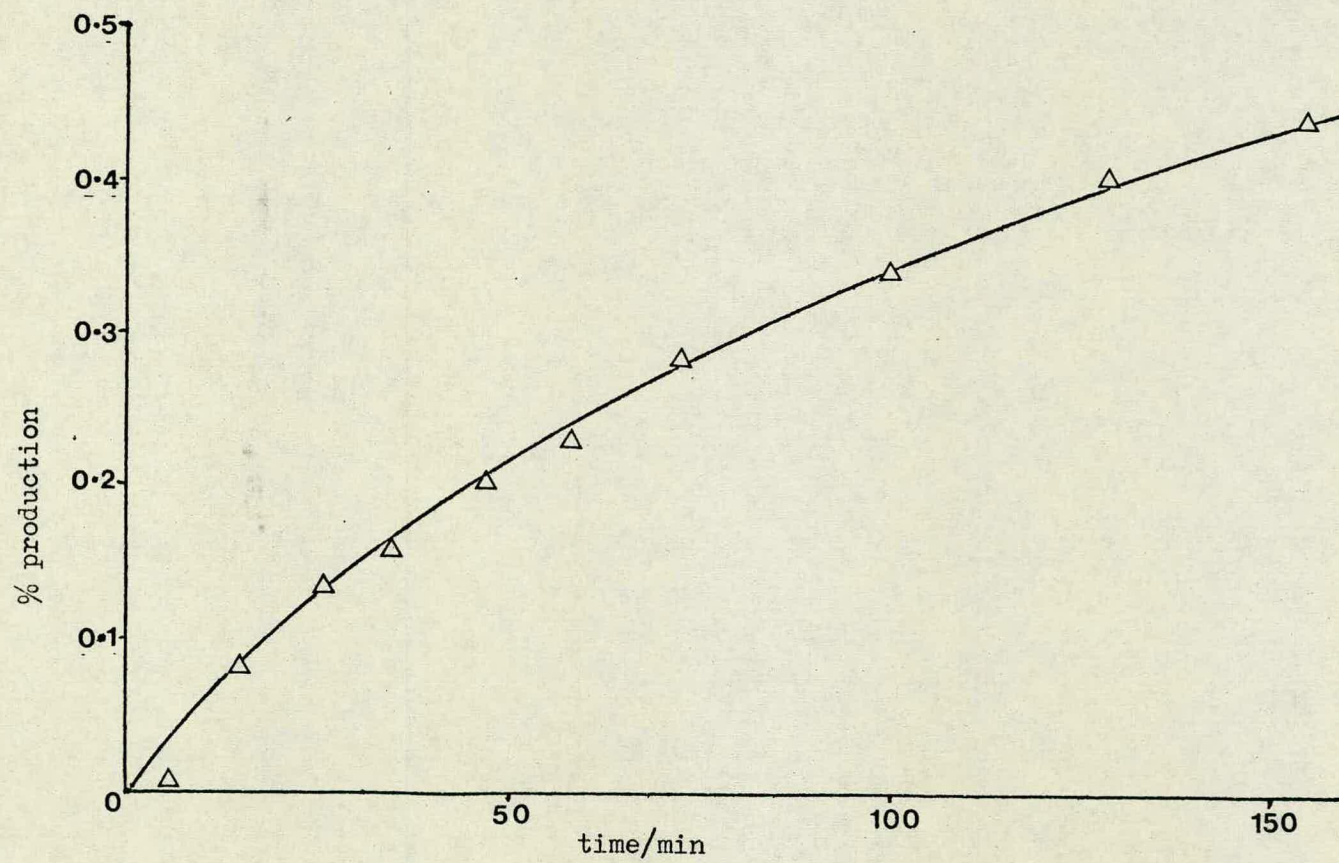
figure 7.7

figure 7.6 decomposition of acetone over rutile at 523K after pretreatment A:

figure 7.7 decomposition of acetone over rutile at 523K after pretreatment C:

acetone, Δ ; butene, \bullet ; propene, \circ ; ethene, \square .

figure 7.8 production of acetone from the decomposition of 2-methylpropan-2-ol over rutile after pretreatment C.



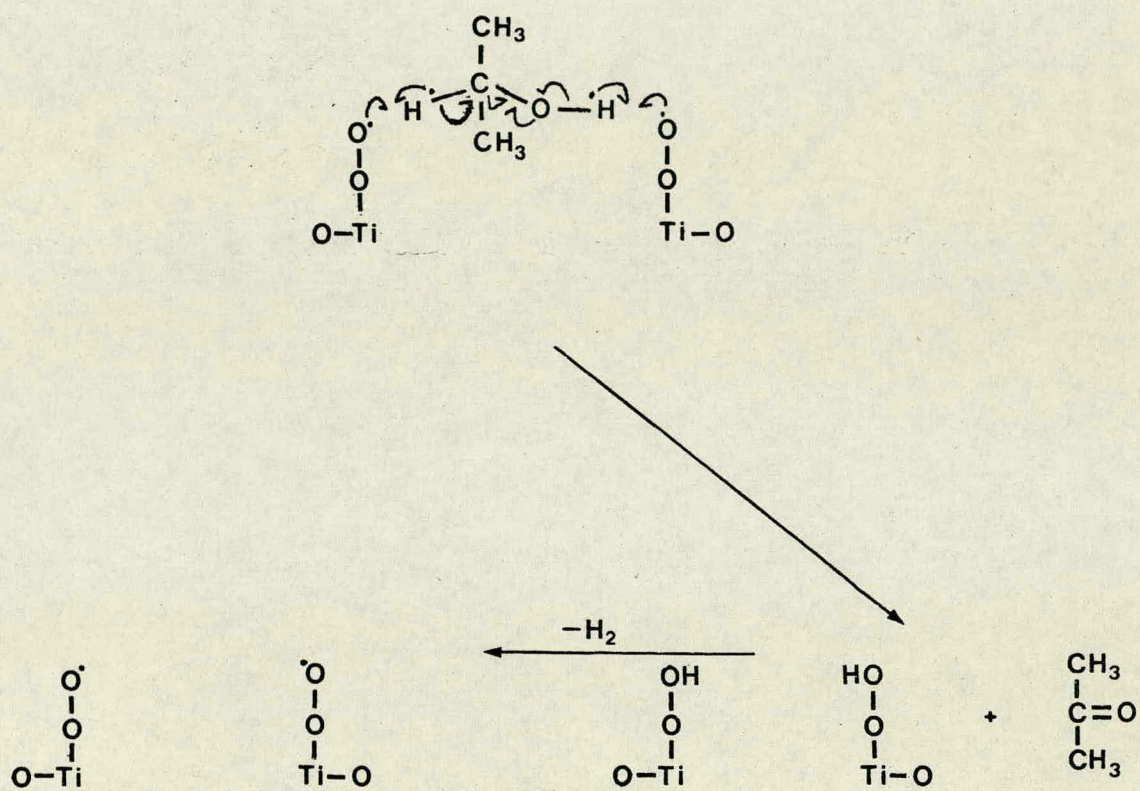


figure 7.9 reaction mechanism of the dehydrogenation of propan-2-ol over rutile via radical species.

References

1. S.F.S. Chun, K.D. Pang, J.A. Cutts and J.M. Ajello, *Nature*, 274, 875 (1978).
2. F.A. Grant, *Rev. Modern Physics*, 31, 646 (1959).
3. A. Von Hippel, J. Kalnajs and W.B. Westphal, *J. Phys. Chem. Solids*, 23, 779 (1962).
4. A.F. Wells, *Structural Inorganic Chemistry*; Oxford University Press 1975.
5. N.B. Hannay and C.P. Smythe, *J. Am. Chem. Soc.*, 68, 171 (1946).
6. H.P. Boehm, *Adv. Cat.*, 16, 179 (1966).
7. I. Carrizosa, G. Munuera and S. Castanar, *J. Cat.*, 49, 265 (1977).
8. M. Che, C. Naccache and B. Imelik, *J. Cat.*, 24, 328 (1972).
9. Rutley's "Elements of Minerology", ed. H.H. Read, published by George Allen and Unwin Ltd., London (1962).
10. J. Speakman, Teesside Polytechnic, private communication.
11. P. Jones and S.A. Hockey, *Trans. Faraday Soc.*, 67, 2679 (1971).
12. P. Jones and S.A. Hockey, *J.C.S. Faraday I*, 68, 907 (1972).
13. K.E. Lewis and G.D. Parfitt, *Trans. Faraday Soc.*, 62, 204 (1966).
14. P. Jackson and G.D. Parfitt, *Trans Faraday Soc.*, 67, 2469 (1971).
15. M. Primet, P. Pichat and M. Mathieu, *J. Phys. Chem.*, 75, 1216 (1971).

16. D.M. Griffiths and C.H. Rochester, *J.C.S. Faraday I*, 73, 1510 (1977).
17. J.B. Peri, *J. Phys. Chem.*, 69, 220 (1965).
18. M.J. Jaycock and J.C.R. Waldsay, *J.C.S. Faraday I*, 70, 1501 (1974).
19. G. Munuera and F.S. Stone, *Disc. Faraday Soc.*, 52, 205 (1971).
20. E.P. Parry, *J. Cat.*, 2, 371 (1963).
21. M. Primet, P. Pichat and M. Mathieu, *J. Phys. Chem.*, 75, 1221 (1971).
22. P. Jones and J.A. Hockey, *Trans. Faraday Soc.*, 67, 2669 (1971).
23. G.D. Parfitt, J. Ramsbotham and C.H. Rochester, *Trans. Faraday Soc.*, 67, 841 (1971).
24. G.D. Parfitt, J. Ramsbotham and C.H. Rochester, *Trans. Faraday Soc.*, 67, 1500 (1971).
25. G.D. Parfitt, J. Ramsbotham and C.H. Rochester, *Trans. Faraday Soc.*, 67, 3100 (1971).
26. M. Primet, J. Bisset, M.V. Mathieu and M. Prettre, *J. Phys. Chem.*, 74, 2868 (1970).
27. Yu.M. Shchekochikhin, V.N. Filimonov, N.P. Keier and A.N. Terenin, *Kinet. Katal.*, 5, 113 (1964).
Chem. Abs. 60: 12788h.
28. R.E. Day, G.D. Parfitt and J. Peacock, *Disc. Faraday Soc.*, 52, 215 (1971).
29. P. Jackson and G.D. Parfitt, *J.C.S. Faraday I*, 68, 896 (1972).
30. P. Jackson and G.D. Parfitt, *J.C.S. Faraday I*, 68, 1443 (1972).

31. D.M. Griffiths and C.H. Rochester, J.C.S. Faraday I, 73, 1988 (1977).
32. D.M. Griffiths and C.H. Rochester, J.C.S. Faraday I, 73, 1913 (1977).
33. D.M. Griffiths and C.H. Rochester, J.C.S. Faraday Trans. I, 74, 403 (1978).
34. H.P. Boehm, Disc. Faraday Soc., 52, 264 (1971).
35. I.R. Shannon, Ph.D. Thesis, Edinburgh University, (1969).
36. I.R. Shannon, I.J.S. Lake and C. Kemball, Trans. Faraday Soc., 67, 2760 (1971).
37. B.I. Brookes, Ph.D. Thesis, Edinburgh University, (1972).
38. W.O. Haag and H. Pines, J. Am. Chem. Soc., 82, 387 (1960).
39. S. Bank, S. Schriesheim and C.A. Rowe, J. Am. Chem. Soc., 87, 3244 (1965).
40. H. Hattori, M. Itoh and K. Tanabe, J. Cat., 38, 172 (1975).
41. H. Hattori, M. Itoh and K. Tanabe, J. Cat., 41, 46 (1976).
42. J.L. Lemberston, G. Perot and M. Guisnet, J.C.S. Chem. Comm., 883 (1977).
43. I.J.S. Lake and C. Kemball, Trans. Faraday Soc., 63, 2535 (1967).
44. C. Kemball, Annals of the New York Academy of Sciences, 213, 90-109 (1973).
45. M.M. Halliday, Ph.D. Thesis, Edinburgh University, (1975).
46. M.M. Halliday, C. Kemball and H.F. Leach, J.C.S. Faraday I, 70, 1743 (1974).

47. M.M. Halliday, C. Kemball, H.F. Leach and M.S. Scurrall, Proc. 6th International Congr. Catalysis, London, 1976, The Chemical Society, Vol. 1, pp 283-289.
48. B.W. Moller, Ph.D. Thesis, Edinburgh University, (1974).
49. T.R.C. Tables, Volume II, Thermodynamical Research Center Data Project, Texas A&M University, 1974.
50. K.G. Denbigh and J.C.R. Turner, "Chemical Reactor Theory", 2nd ed., Cambridge Univ. Press (1971).
51. H. Knozinger, "The Dehydration of Alcohols" in "Chemistry of the Hydroxyl Group" Part 2, Chapter 12, page 641, ed., S. Patai, Interscience Publishers, (1971).
52. G.C. Bond, "Catalysis by Metals", Academic Press Inc., London (1962).
53. a. E.D. Hughes and C.K. Ingold, J. Chem. Soc., 2038 (1948). *ibid*, 2043 (1948).
b. E.D. Hughes and C.K. Ingold, Trans Faraday Soc., 37, 657 (1941), and references cited therein.
54. W.I. Ipatiew, Ber. Deutsch. Chem. Gesellschaft, 35, 1047 (1902); *ibid*, 35, 1057 (1902); *ibid*, 36, 1990 (1903); *ibid*, 36, 2003 (1903); *ibid*, 37, 2986 (1904).
55. F.C. Whitmore, J. Am. Chem. Soc., 54, 3274 (1932), and subsequent papers.
56. W.S. Brey, Jr., and K.A. Krieger, J. Am. Chem. Soc., 71, 3637 (1949).
57. J.G.M. Bremner, Research, 1, 281 (1948).
58. A.L. Henne and A.H. Matuszak, J. Am. Chem. Soc., 66, 1649 (1944).

59. H. Pines and J. Manassen, *Adv. Cat.*, 16, 49 (1966).
60. H. Pines and W.O. Haag, *J. Am. Chem. Soc.*, 82,
2471 (1960).
61. H. Pines and C.N. Pillai, *J. Am. Chem. Soc.*, 82,
2401 (1960).
62. C.N. Pillai and H. Pines, *J. Am. Chem. Soc.*, 83,
3274 (1961).
63. L. Beranek, M. Kraus, K. Kochloefl and V. Bazant,
Collect. Czech. Chem. Commun., 25, 2513 (1960).
64. M. Misono, Y. Saito and Y. Yoneda, *Proc. III
Inter. Congr. Catalysis. Amsterdam, (1964),
North-Holland Publ. Comp., Amsterdam, (1965), p.408.*
65. H. Pines and W.O. Haag, *J. Am. Chem. Soc.*, 83, 2847
(1961).
66. F.F. Roca, A. Nohl, L. de Mourges and Y. Trambouze,
Compte. Rend., 266, 1123 (1968).
67. H. Knozinger, H. Buhl and E. Röss, *J. Cat.*, 12, 121
(1968).
68. J.R. Jain and C.N. Pillai, *J. Cat.*, 9, 322 (1967).
69. D.V. Krylov, "Catalysis by Non-metals", Academic
Press, New York (1970).
70. A. Eucken, *Naturwissenschaften*, 36, 48 (1949).
71. E. Wicke, *Z. Electrochem.*, 53, 279 (1949).
72. C.W. Kibby and W.K. Hall, *J. Cat.*, 29, 144 (1973).
73. C.W. Kibby and W.K. Hall, *J. Cat.*, 31, 65 (1973).
74. Y. Noto, K. Fukuda, T. Onishi and K. Tamaru,
Trans. Faraday Soc., 63, 3081 (1967).
75. P.A. Jacobs and J.B. Uytterhoeven, *J. Cat.*, 50,
109 (1977).

76. C.F. Heylen, P.A. Jacobs and J.B. Uytterhoeven, *J. Cat.*, 43, 99 (1976).
77. L. Nondek and J. Sedlacek, *J. Cat.*, 40, 34 (1975).
78. P. Sabatier, "La Catalyse en Chimie Organique"; Paris et Liegh (1913): Translated to English as "Catalysis in Organic Chemistry" Leipzig (1927).
79. K. Hauffe, *Adv. Cat.*, 7, 213 (1955).
80. F.F. Vol'kenshtein, "The Electronic Theory of Catalysis on Semiconductors". Macmillan Co., New York, 1963.
81. a. I. Batta, S. Borcsok, F. Solymosi and Z.G. Szabo, *Proc. III Inter. Congr. Catalysis, Amsterdam*, (1964), North-Holland Publ. Comp., Amsterdam, (1965), p.1340.
b. Z.G. Szabo, *J. Cat.*, 6, 458 (1966).
82. L. Pauling, "The Nature of the Chemical Bond"; 3rd edition. Cornell University Press, Ithaca, New York, (1960).
83. H. Niiyama and E. Echigoya, *Bull. Chem. Soc. Jap.*, 44, 1739 (1971).
84. G.M. Schwab and E. Schwab-Agallidis, *J. Am. Chem. Soc.*, 71, 1806 (1949).
85. B.M.W. Trapnell, *Adv. Cat.*, 3, 1 (1951).
86. B.H. Davis and W.S. Brey, Jr., *J. Cat.*, 25, 81 (1972).
87. B.H. Davis, *J. Cat.*, 26, 348 (1972).
88. B.H. Davis, *J. Cat.*, 52, 176 (1978).
89. B.H. Davis, *J. Cat.*, to be published.
90. B.H. Davis, *Colloid and Interface Science*, (Proc. Int. Conf.) 50th, III, 115 (1976).

91. L.P. Hammett, J. Am. Chem. Soc., 59, 96 (1937).
92. R.W. Taft, J. Am. Chem. Soc., 75, 4231 (1953).
93. P.R. Well, Chem. Rev., 67, 171 (1963).
94. J.E. Leffler and E. Grunwald, "Rates and Equilibrium of Organic Reactions", Wiley New York (1963).
95. J. Shorter, "Correlation Analysis in Organic Chemistry", Clarendon Press. Oxford (1973).
96. M. Kraus, Adv. Cat., 17, 75 (1967).
97. M. Boudart, J. Am. Chem. Soc., 74, 3556 (1952).
98. M. Kraus, K. Kochloefl, L.B. eranek and V. Bazant, Proc. III Inter. Congr. Catalysis, Amsterdam, 577 (1964).
99. I. Carrizosa and G. Munuera, J. Cat., 49, 189 (1977).
100. K. Kochloefl, M. Kraus and V. Bazant, Proc. IV Inter. Congr. Catalysis, Moscow, 2, 490 (1968).
101. J.M. Criado, Proceedings, 4th Ibero-American Symposium on Catalysis, Mexico (1974).
102. C.J. Engelder, J. Phys. Chem., 21, 679 (1917).
103. W.A. Rudisill and C.J. Engelder, J. Phys. Chem., 30, 106 (1926).
104. a. D.J. Wheeler, P.W. Darby and C. Kemball, J. Chem. Soc., p.332 (1960).
b. D.J. Wheeler and C. Kemball, J. Chem. Soc., p. 1840 (1960).
105. I.S. Sazanova, N.P. Keier, T.P. Khokhlova and I.L. Mikhailova, Kinet. I. Katal., 11, 447 (1970). (Kinetics and Catalysis, 11, 371 (1970)).
106. S.J. Gentry, R. Rudham and K.P. Wagstaff, J.C.S. Faraday Trans. I, 71, 657 (1975).

107. I. Carrizosa and G. Munuera, *J. Cat.*, 49, 265 (1977).
108. J.E. Kilpatrick, E.J. Prosen, K.S. Pitzer and F.D. Rossini, *J. Res. Nat. Bur. Stand.*, 36, 559 (1946).
109. B.H. Davis, *J. Cat.*, 55, 158 (1978).
110. H. Pines and W.O. Haag, *J. Am. Chem. Soc.*, 82, 2488 (1960).
111. B.H. Davis, *J. Org. Chem.*, 37, 1240 (1972).
112. H. Knozinger, H. Buhl and K. Kochloefl, *J. Cat.*, 24, 57 (1972).
113. H. Noller and W. Kladnig, *Catal. Rev. - Sci. Eng.*, 13 (2), 149-207 (1976).
114. F.C. Whitmore, *J. Am. Chem. Soc.*, 54, 3431 (1932).
115. K. Kochloefl and H. Knozinger, *Proc. V. Inter. Congr. Catalysis, (Miami), 1972* 83 1171.
116. V.H.J. De Beer, C. Bevelander, T.H.M. Van Sint Fiet, P.G.A.J. Werter and C.H. Amberg, *J. Cat.*, 43, 68 (1976).
117. H. Pines and C.N. Pillai, *J. Am. Chem. Soc.*, 83, 3270 (1961).
118. C.S. John, University of Edinburgh, private communication.
119. D.N. Furlong and G.D. Parfitt, *J. Colloid Interface Sci.*, 65, 548 (1978).
120. K. Shibata, T. Kiyoura and K. Tanabe, *J. Res. Inst. Catalysis, Hokkaido Univ.*, 18, 189 (1970).
121. C.S. John, C. Kemball, L.V.F. Kennedy and J.K. Tyler, unpublished results.

122. I.I. Zakharycheva, G.V. Isagulyants and A.A. Balandin, *Izvest. Akad. Nauk, S.S.S.R. Otdel Khim. Nauk* 179-180 (1963) (Chem Abs 58:12401a).
123. S.A. Ballard, H.D. Finch and D.E. Winkler, *Adv. Cat.*, 9, 754 (1957).
124. A. Maccoll and V.R. Stimson, *Proc. Chem. Soc.*, 80 (1958) and subsequent papers.
125. R.T. Morrison and R.N. Boyd, *Organic Chemistry*. Allyn and Bacon, Inc. (1971) page 524.
126. J. Speakman, Ph.D. Thesis, Teesside Polytechnic (1978).
127. J. Koubek, J. Volf and J. Pasek, *J. Cat.*, 38, 385 (1975)
128. A. Eucken and E. Wicke, *Naturwissenschaften*, 32, 161 (1944).
129. L.A. Munro and W.R. Horn, *Canadian J. Res.*, 12, 707 (1935).
130. S.T. Ho, B.V. Romanovskii and K.V. Topchieva, *Dokl. Akad. Nauk. S.S.S.R.* 168, (5) 1114 (1966). Chem Abs 65 134936.
131. P.A. Jacobs, M. Tielen and J.W. Uytterhoeven, *J. Cat.*, 50, 98 (1977).
132. Z.V. Gryaznova, M.M. Ermilova, G.V. Tsitsishvili, T.G. Andronikashvili and A. Yu. Krupennikova, *Kinet. I. Katal.*, 10, 1336 (1969) (*Kinetics and Catalysis*, 10, 1099 (1969)).
133. R. Rudham and A. Stockwell, *Catalysis, Specialist Periodical Report*, 1, 87 (1977) published by The Chemical Society; and references cited therein.

134. J.B. Peri and R.B. Hannan, *J. Phys. Chem.*, 64, 1526 (1960).
135. C.S. John, A. Tada and L.V.F. Kennedy, *J.C.S. Faraday I*, 74, 498 (1978).
136. General Discussion, *Disc. Faraday Soc.*, 52, 276 (1971).
137. J. March, *Advanced Organic Chemistry*. McGraw and Hill Book Company (1968) page 692.
138. L. Nondek, *J. Res. Inst. Catalysis, Hokkaido Univ.*, 27, 7 (1979).
139. R. Fujii, *J. Chem. Soc. Japan, Pure Chem. Sect.*, 69, 151 (1948).
140. V.N. Ipattief and V. Haensel, *J. Org. Chem.*, 7, 189 (1942).
141. K. Kawamoto, *Bull. Chem. Soc. Japan*, 34, 161 (1961).
142. B.H. Davis and P.B. Venuto, *J. Cat.*, 13, 100 (1969).
143. Reference 137, page 217.
144. J.W. Ward, *J. Cat.*, 11, 259 (1968).
145. H. Knozinger and C.P. Kaerlein, *J. Cat.*, 25, 436 (1972).
146. G.D. Parfitt, *Prog. Surf. Memb. Sci.*, 11, 181 (1976).
147. T. Yamaguchi and K. Tanabe, *Bull. Chem. Soc. Japan*, 47, 424 (1974).
148. C.S. John, C. Kemball, R. Dickinson and J.K. Tyler, *J.C.S. Faraday I*, 72, 1782 (1976).
149. B.T. Hughes, C. Kemball and J.K. Tyler, *J.C.S. Faraday I*, 71, 1285 (1975).
150. C.S. John, C.E. Marsden and R. Dickinson, *J.C.S. Faraday I*, 72, 2923 (1976).

151. J. Jambor and L. Beranek, Collect. Czech. Chem. Commun., 40, 1374 (1975).
152. C. Naccache, P. Meriaudeau, M. Che and A.J. Tench, Trans. Faraday Soc., 67, 506 (1971).
153. P.C. Gravelle, F. Juillet, P. Meriaudeau and S.J. Teichner, Disc. Faraday Soc., 52, 140 (1971).
154. R.D. Iyengar and M. Codell, Adv. Colloid Interface Sci., 3, 365 (1972).
155. G.C. Bond, Heterogeneous Catalysis: principles and applications, Clarendon Press. Oxford. (1974).
156. S. Yoshida, T. Matsuzaki, S. Ishida and K. Tarama, Proc. V. Int. Cong. Catalysis, (Miami Beach), 2, 1049 (1972).
157. S. Yoshida, T. Matsuzaki, T. Kashiwazaki, K. Mori and K. Tarama, Bull. Chem. Soc. Japan, 47, 1564 (1974).
158. J. Cunningham and P. Meriaudeau, J.C.S. Faraday I, 72, 1499 (1976).
159. R.I. Bickley, G. Munuera and F.S. Stone, J. Cat., 31, 398 (1973)
160. S. Hasegawa, K. Yasuda, T. Mase and T. Kawaguchi, J. Cat., 46, 125 (1977).

Brønsted Acidity of Rutile Developed During Alcohol Dehydration as Shown by Simultaneous Alkene Isomerization: Microwave Spectroscopic Analyses

By GORDON G. FERRIER, CHRISTOPHER S. JOHN,*† and H. FRANK LEACH

(Department of Chemistry, University of Edinburgh, West Mains Road, Edinburgh EH9 3JJ)

and LOIS V. F. KENNEDY and J. KELVIN TYLER

(Chemistry Department, University of Glasgow, Glasgow G12 8QQ)

Reprinted from

**Journal of The Chemical Society
Chemical Communications
1978**

The Chemical Society, Burlington House, London W1V 0BN

Brønsted Acidity of Rutile Developed During Alcohol Dehydration as Shown by Simultaneous Alkene Isomerization: Microwave Spectroscopic Analyses

By GORDON G. FERRIER, CHRISTOPHER S. JOHN,*† and H. FRANK LEACH

(Department of Chemistry, University of Edinburgh, West Mains Road, Edinburgh EH9 3JJ)

and LOIS V. F. KENNEDY and J. KELVIN TYLER

(Chemistry Department, University of Glasgow, Glasgow G12 8QQ)

Summary Microwave spectroscopic analyses of deuterio-propenes produced from $\text{CD}_2=\text{CH}-\text{CH}_3$, and of deuterioisobutenes from $\text{CD}_2=\text{C}(\text{CH}_3)_2$, indicate conclusively that on rutile in the presence of water and/or alcohol carbonium ion intermediates are involved in alkene isomerization; in contrast, comparison of rates of reaction of $\text{CD}_2=\text{CH}-\text{CH}_3$ and $\text{CD}_2=\text{C}(\text{CH}_3)_2$ implies that π -allylic species with partial carbonium ion character are the intermediates in isomerization in the absence of water or alcohol.

SOME recent studies of reactions of primary alcohols over rutile (TiO_2) indicated that dehydration (to alkene and water) occurred at *ca.* 550 K. It became desirable to establish if the product alkenes could isomerize under the reaction conditions or whether the primary product distribution was sensibly preserved.

Recently the reaction of $\text{CD}_2=\text{CH}-\text{CH}_3$ with D_2O was successfully employed to demonstrate the Brønsted acid nature of alumina at *ca.* 470 K.⁵ The present work was undertaken to establish if a similar reaction mechanism was operative for labelled propene over TiO_2 at *ca.* 570 K in the presence of D_2O or pentan-1-ol, *i.e.*, to investigate if the reaction proceeded by a different route in the presence of such species. Additionally the reaction of a selectively labelled isobutene, $\text{CD}_2=\text{C}(\text{CH}_3)_2$, with water was examined to provide further information of the Brønsted acid nature of the rutile surface.

The source and pretreatment of the rutile were as previously reported.³ Samples of 1 g were used with *ca.* 1×10^{20} molecules of alkene and a similar amount of D_2O or pentan-1-ol as appropriate. Reaction was followed by mass spectrometry to the desired extent, at which time a gas phase sample was removed for subsequent microwave analysis.² The experimental details and results are summarised in the Table.

TABLE. Percentage analyses^a of deuteriopropenes and deuterioisobutenes produced over TiO_2

Experiment no. Reactants	1 $\text{CD}_2=\text{CH}-\text{CH}_3 + \text{D}_2\text{O}^c$	2 $\text{CD}_2=\text{CH}-\text{CH}_3 + \text{D}_2\text{O}^d$	3 $\text{CD}_2=\text{CH}-\text{CH}_3$ + Pentan-1-ol ^e	4 $\text{CD}_2=\text{C}(\text{CH}_3)_2^f$	5 $\text{CH}_2=\text{C}(\text{CH}_3)_2 + \text{D}_2\text{O}^e$
Reaction temperature/K	523	523	553	283	390
$\text{CD}_2=\text{CR}-\text{CH}_3^b$	87.6(96)	68.8(89)	46.0(57)	12.6(17)	—
$\text{CHD}_2-\text{CR}=\text{CH}_2$	3.6(4)	8.4(11)	33.6(46)	34.9(47)	—
$\text{CH}_2\text{D}-\text{CR}=\text{CH}_2$	0	0	5.8(34)	6.0(54)	24.9(73)
$\text{CH}_3-\text{CR}=\text{CHD}$	1.0(100)	2.1(100)	11.1(66)	5.0(45)	9.2(27)
$\text{CD}_3-\text{CR}-\text{CH}_2\text{D}$	1.0(13)	3.3(16)	0.4(17)	—	—
$\text{CD}_3-\text{CR}=\text{CH}_2$	6.8(87)	17.4(84)	2.0(83)	—	—

^a Numbers in parentheses are normalised distributions of [$^2\text{H}_1$]-species for various i. ^b R is either H (propene) or CH_3 (isobutene). ^c Reactants both added at 283 K and warmed to reaction temperature. ^d D_2O added initially at *ca.* 700 K prior to cooling to 283 K and admitting $\text{CD}_2=\text{CH}-\text{CH}_3$. ^e Pentan-1-ol added initially at 550 K and partially dehydrated for 20 min prior to cooling to 283 K and admitting $\text{CD}_2=\text{CH}-\text{CH}_3$. ^f Also contained 26.9% $\text{CHD}=\text{C}(\text{CH}_3)\text{CH}_2\text{D}$ [and $\text{CH}_2=\text{C}(\text{CH}_2\text{D})_2$] with 11.7% unknown [$^2\text{H}_3$]-species.

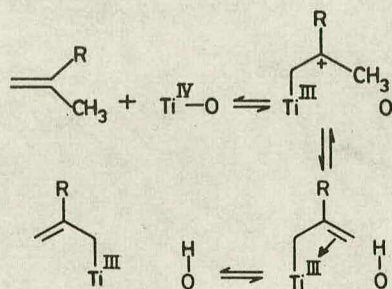
It is known that in the absence of alcohol or water, n-butenes¹ and propene² isomerize over TiO_2 at rates of *ca.* 1×10^{15} molecule $\text{m}^{-2} \text{s}^{-1}$ at 430 K, with the reaction of propene (as $\text{CD}_2=\text{CH}-\text{CH}_3$) being predominantly intramolecular and involving π -allylic species. However, Hughes *et al.*³ reported that the exchange of propene, with D_2 or D_2O , achieved such a rate only at *ca.* 570 K, and the deuteriopropenes produced had D randomly distributed over the five terminal positions. Such a distribution is characteristic of carbonium ion intermediates if the supply of D is not rate determining for the exchange reaction. With D_2 as the source, the supply of D was indeed shown to be rate determining but this was somewhat uncertain with D_2O . The exchange reaction of isobutene over rutile at 530 K has been reported⁴ as some thirty times faster with D_2O than with D_2 which suggests that water can indeed induce a carbonium ion reaction.

Experiments 1 and 2 provide clear evidence that in the presence of water (D_2O) exchange of propene with D and double bond migration (DBM) occurred at essentially the same rate. Furthermore, the highly selective production of $\text{CD}_3-\text{CH}=\text{CH}_2$ at *ca.* 520 K is strongly indicative⁵ of classical carbonium ion intermediates reacting on Brønsted acid centres produced with D^+ from D_2O , irrespective of whether water was initially added at 300 or 700 K.

Exposure of TiO_2 to $\text{CD}_2=\text{CH}-\text{CH}_3$ and pentan-1-ol at 298 K, with subsequent warming to *ca.* 550 K, showed that alcohol alone was sufficient to poison the (π -allylic) reaction of propene at *ca.* 450 K as dehydration products were only detectable by g.l.c. at *ca.* 550 K. Experiment 3 confirms that in the presence of pentan-1-ol and its dehydration products, propene reacts on Brønsted acid centres which initially contain H^+ leading to the selective production of $\text{CHD}=\text{CH}-\text{CH}_3$, $\text{CHD}_2-\text{CH}=\text{CH}_2$, and $\text{CD}_3-\text{CH}=\text{CH}_2$.

† Present address: Dr. C. S. John, Koninklijke/Shell-Laboratorium, Amsterdam, Badhuisweg 3, Postbus 3003, Amsterdam-Noord, The Netherlands.

Compound $\text{CD}_2=\text{C}(\text{CH}_3)_2$ reacted on TiO_2 at a rate of *ca.* 1×10^{15} molecule $\text{m}^{-2} \text{s}^{-1}$ at 283 K (experiment 4); 450 K was needed for similar reaction of $\text{CD}_2=\text{CH}-\text{CH}_3$.² Microwave analysis of deuterioisobutenes produced⁶ indicates that predominantly intramolecular DBM occurred; $\text{CHD}=\text{C}(\text{CH}_3)\text{CH}_2\text{D}$ was produced from $\text{CH}_2=\text{C}(\text{CH}_3)\text{CHD}_2$ in preference to $[\text{H}_1]$ -species. In previous work on D_2 exchange with both propene and isobutene, therefore, the rate of supply of D from D_2 was rate determining. In addition, substitution of H on C(2) in propene for CH_3 , to give isobutene, confers greatly enhanced reactivity which, with the intramolecular nature of the reaction, implies the involvement of allylic species with carbonium ion character, in contradiction to the conclusion of π -allylic carbanions reached⁷ on the more subjective basis of product distribution in butene isomerization. Such species might be formed⁸ on the Lewis acid centres of rutile as shown in the Scheme.



SCHEME. Schematic representation of the active site for alkene isomerization over rutile.

Intermolecular reaction of either $\text{CD}_2=\text{C}(\text{CH}_3)_2$ or $\text{CH}_2=\text{C}(\text{CH}_3)_2$ with D_2O occurred at very similar rates at 390 K. The ratio, $\text{CH}_2=\text{C}(\text{CH}_3)\text{CH}_2\text{D}:\text{CHD}=\text{C}(\text{CH}_3)_2$ was $2.7 \pm 0.3:1$ in the latter case (experiment 5) whereas DBM in the former was predominantly intermolecular and occurred at sensibly the same rate as exchange. These observations confirm directly that isobutene reacts on TiO_2 in the presence of D_2O through the carbonium ion intermediate, $(\text{CH}_3)_2\text{C}^+-\text{CH}_2\text{D}$; random loss of H^+ gives the above $[\text{H}_1]$ product ratio whereas a π -allylic intermediate would give only $\text{CH}_2=\text{C}(\text{CH}_3)\text{CH}_2\text{D}$. Thus, reaction through a tertiary carbonium ion (from isobutene) occurs at similar rates to that through a secondary ion (from propenes) in the presence of the same quantity of water, but at 160 K lower in agreement with its greater stability.

It is clear, therefore, that reaction of both propene and isobutene on TiO_2 in presence of water or alcohol occurs by a different mechanism (carbonium ions on Brønsted centres) to that found previously (π -allyls) in their absence. Studies of alkene isomerization in the absence of water or alcohol cannot therefore be used to describe such reactions in their presence, a conclusion also reached with water on alumina⁵ which should probably, therefore, be regarded as of general validity for metal oxide catalysts.

L.V.F.K. and G.G.F. thank the S.R.C. and Tioxide International, respectively, for financial support.

(Received, 19th June 1978; Com. 642.)

¹ C. Kemball, *Ann. New York Acad. Sci.*, 1973, **213**, 90.

² C. S. John, C. Kemball, R. Dickinson, and J. K. Tyler, *J.C.S. Faraday I*, 1976, **72**, 1782.

³ B. T. Hughes, C. Kemball, and J. K. Tyler, *J.C.S. Faraday I*, 1975, **71**, 1285.

⁴ M. M. Halliday, C. Kemball, H. F. Leach, and M. S. Scurrrell, Proc. 6th International Congr. Catalysis, London, 1976, The Chemical Society, Vol. 1 pp. 283-289.

⁵ C. S. John, A. Tada, and L. V. F. Kennedy, *J.C.S. Faraday I*, 1978, **74**, 498.

⁶ C. S. John, C. Kemball, L. V. F. Kennedy, and J. K. Tyler, unpublished results.

⁷ I. R. Shannon, I. J. S. Lake, and C. Kemball, *Trans. Faraday Soc.*, 1971, **67**, 2760.

⁸ B. I. Brookes, Ph.D. Thesis, Edinburgh University, 1972.